

Rothamsted Repository Download

F - Theses

Audley, M. 2016. *Understanding the role of gibberellin signalling in wheat anther development during heat stress*. F - Theses Plant Sciences

The output can be accessed at:

<https://repository.rothamsted.ac.uk/item/95xyv/understanding-the-role-of-gibberellin-signalling-in-wheat-anther-development-during-heat-stress>.

© 1 September 2016, Please contact library@rothamsted.ac.uk for copyright queries.

**UNDERSTANDING THE ROLE OF GIBBERELLIN SIGNALLING IN
WHEAT ANTHOR DEVELOPMENT DURING HEAT STRESS**

MATTHEW AUDLEY, MSc.

**Thesis submitted to The University of Nottingham for the degree of Doctor
of Philosophy**

SEPTEMBER 2016

ABSTRACT

High temperature (HT) stress during wheat male reproductive development causes irreversible damage to the anther tapetum layer and the developing microspores it supports, resulting in reduced yield. With the frequency of pre-flowering temperature stress events likely to increase, a better understanding of the effects of high temperature stress on anther developmental regulation is required. Gibberellin (GA) signalling has been shown to regulate tapetum programmed cell death (PCD) and pollen coat formation via the transcription factor (TF) *GAMYB*. This project aimed to investigate the function of two putative GA-signalling components in wheat anther development and characterise the global hormonal and transcriptional anther responses to HT.

RNAi and TILLING mutants for *TaGAMYB* and a putative orthologue of a rice tapetum PCD component, *TabHLH141*, revealed that both are required for male fertility. *Tagamyb* mutants displayed stunted anther development with irregular tapetum vacuolisation and reduced pollen viability. An interaction between RHT-D1 and *TabHLH141* suggests that GA may mediate anther development through regulation of DELLA-TF interactions.

Having characterised and developed a non-destructive staging method for wheat anther development, RNA-Seq and global hormone analysis was used to investigate the response to HT stress around pollen mother cell meiosis. Significant changes in expression of tapetum metabolism and PCD annotated transcripts and anther GA, auxin and jasmonate concentrations indicates that hormonal regulation of HT-responsive transcription may contribute to defective anther development.

The work in this project demonstrates that advanced functional genomics techniques can now be applied to the dissection of complex signalling pathways in hexaploid wheat.

ACKNOWLEDGEMENTS

My sincerest thanks must firstly go to Steve, Peter and Andy for their fantastic supervision throughout this project. They have patiently supported my learning and progress towards becoming a competent scientist and I have enjoyed working with them immensely. Each of them has helped me steer this project in the right direction.

Likewise, Zoe Wilson and her group at Nottingham have provided a great deal of support throughout and special mention must go to Carus for his help in harvesting anthers at all hours over a couple of days. José has also provided lots of advice on overcoming some of the particular difficulties of working on cereal reproduction. This work was completed with support from the BBSRC Doctoral Training Partnership between Rothamsted Research and The University of Nottingham.

The bioinformatics work in chapter 5 could not have been done without the hard work of Asier Gonzalez who went above and beyond to help me complete what turned out to be a huge undertaking. It is only thanks to his skill and persistence in solving the many problems we faced that some interesting analysis could be carried out.

I would also like to thank the many people that have made Rothamsted such a great place to study. Within the GA-group, Aakriti, George and Dave have provided not only support in the lab but also friendship and good company. Till and Simon have also been a constant source of good humour and conversation at lunchtime and coffee breaks as well as practical advice from their wealth of experience.

I also want to thank my family. My mother, Paula, for always encouraging me and taking a genuine interest in my project. My brother, Joe, for all the evenings after work watching Liverpool games in the pubs of Harpenden. My parents-in-law, Jane and John for their support.

And finally to my wife, Jennifer, who has been my rock throughout.

Contents

| | |
|---|------|
| ABSTRACT | ii |
| ACKNOWLEDGEMENTS..... | iii |
| List of Figures | viii |
| List of Tables | xi |
| List of Abbreviations | xii |
| CHAPTER 1: GIBBERELLIN SIGNALLING DURING MALE REPRODUCTIVE DEVELOPMENT IN WHEAT AND THE IMPACT OF HIGH TEMPERATURE STRESS..... | 1 |
| 1.1. Wheat production, food security and climate change | 1 |
| 1.1.1. The impact of high temperature stress on wheat production | 3 |
| 1.2. Anther and pollen cell morphology and development..... | 6 |
| 1.2.1. Pollen development..... | 6 |
| 1.2.2. The role of the tapetum in pollen development | 8 |
| 1.3. Genetic regulation of pollen development..... | 9 |
| 1.3.1. Floral organ identity and differentiation | 10 |
| 1.3.2. Genetic regulation of pollen and tapetum development..... | 11 |
| 1.4. Gibberellin signalling in anther development | 11 |
| 1.4.1. <i>GAMYB</i> is a GA-responsive transcription factor crucial for anther development..... | 21 |
| 1.4.2. GA-dependent regulation of <i>GAMYB</i> | 23 |
| 1.4.3. <i>GAMYB</i> regulates secretory functions and PCD | 24 |
| 1.4.4. GA controls multiple aspects of male reproductive development..... | 26 |
| 1.5. Anther hormonal signalling responses to HT-stress..... | 28 |
| 1.5.1. GA-signalling in anther HT-responses..... | 29 |
| 1.5.2. Other hormone signalling pathways in anther HT-responses | 31 |
| 1.6. Aims and objectives | 32 |
| CHAPTER 2: GENERAL MATERIALS AND METHODS..... | 34 |
| 2.1. Plant Material and Growing Conditions | 34 |
| 2.2. Molecular biology | 34 |
| 2.2.1 DNA Extraction..... | 34 |
| 2.2.2 Polymerase Chain Reaction | 35 |
| 2.2.3 Agarose Gel Electrophoresis..... | 36 |
| 2.2.4 Extraction and Purification of PCR Products from Agarose Gel | 37 |
| 2.2.5 Primer Design..... | 37 |

| | |
|---|-----------|
| 2.2.6 PCR Product Sequencing..... | 38 |
| 2.2.7 DNA Cloning and Modification | 38 |
| 2.2.8. Bacterial strains used..... | 39 |
| 2.2.9. E-coli transformation | 40 |
| 2.2.10. Yeast strains used | 41 |
| 2.2.11. Gateway cloning for yeast expression..... | 41 |
| 2.2.12. Restriction enzyme digests | 42 |
| 2.3. Quantitative reverse-transcription PCR..... | 42 |
| 2.3.1 Extraction of RNA..... | 42 |
| 2.3.2. cDNA Synthesis | 43 |
| 2.3.3. Quantitative Reverse-Transcription PCR | 43 |
| 2.3.4. Data Analysis..... | 44 |
| 2.4. Generation of transgenic plants | 45 |
| 2.4.1. Cloning of wheat RNAi vectors | 45 |
| 2.4.2. Transformation of wheat by biolistics | 46 |
| 2.4.3. TaqMan Zygosity Assay..... | 46 |
| 2.5. Breeding of TILLING mutants | 48 |
| 2.5.1. Plant Breeding..... | 48 |
| 2.5.2. Embryo Rescue | 48 |
| 2.6. Histology | 49 |
| 2.6.1 Fixation of Tissue | 49 |
| 2.6.2 Sectioning, Staining and Visualisation of Samples..... | 49 |
| 2.6.3 Alexander Pollen Viability Staining | 50 |
| CHAPTER 3: NON-DESTRUCTIVE STAGING OF MALE REPRODUCTIVE DEVELOPMENT IN WHEAT | 52 |
| 3.1. Introduction | 52 |
| 3.1.1. External development | 54 |
| 3.1.2. Development of the wheat anther and pollen | 57 |
| 3.1.3. Existing non-destructive reproductive development staging methods | 61 |
| 3.2. Materials and Methods | 64 |
| 3.2.1. Growing conditions..... | 64 |
| 3.2.2. Material collection and measurement | 64 |
| 3.2.3. Histological analysis of anther development..... | 64 |
| 3.3. Results..... | 65 |

| | |
|--|-----|
| 3.3.1. Identification of wheat anther development stages | 65 |
| 3.3.2 Flag leaf sheath length can be used to stage wheat anther development | 69 |
| 3.4. Discussion | 77 |
| CHAPTER 4: INVESTIGATING THE ROLES OF TaGAMYB AND TabHLH141 IN GA-MEDIATED WHEAT ANTHER DEVELOPMENT..... | 80 |
| 4.1. INTRODUCTION..... | 80 |
| 4.1.1. <i>GAMYB</i> | 80 |
| 4.1.2. <i>bHLH141</i> | 81 |
| 4.1.3. Reverse genetic approaches to characterising wheat anther gene function | 82 |
| 4.2. MATERIALS AND METHODS..... | 85 |
| 4.3. RESULTS | 85 |
| 4.3.1. Identification of TaGAMYB and TabHLH141 orthologues | 85 |
| 4.3.2. <i>Tagamyb-RNAi</i> and <i>Tabhlh141-RNAi</i> plants are male sterile | 92 |
| 4.3.3. <i>Tagamyb</i> lines generated by TILLING are male sterile..... | 101 |
| 4.3.4. TabHLH141 interacts with RHT-1..... | 108 |
| 4.4. DISCUSSION | 110 |
| 4.4.1. The role of <i>TaGAMYB</i> in wheat male fertility | 112 |
| 4.4.2. The role of <i>TabHLH141</i> in wheat male fertility | 117 |
| 4.4.3. Regulation of TabHLH141 by RHT-1..... | 118 |
| CHAPTER 5: THE TRANSCRIPTIONAL AND HORMONAL RESPONSE TO HT IN WHEAT ANTHERS..... | 121 |
| 5.1. Introduction | 121 |
| 5.2. Materials and methods..... | 124 |
| 5.2.1 RNA-Seq plant material | 124 |
| 5.2.2. Sequencing of total mRNA..... | 125 |
| 5.2.3. Quality control and pre-processing of short reads..... | 125 |
| 5.2.4. Mapping to a whole genome reference and counting | 126 |
| 5.2.5. Mapping to a transcriptome reference and counting | 128 |
| 5.2.6. Identifying differentially expressed transcripts | 128 |
| 5.2.7. Assigning gene annotations and GO terms | 130 |
| 5.2.8. Global hormone quantification plant material..... | 130 |
| 5.2.9. Extraction and quantification of GAs..... | 132 |
| 5.2.10. Extraction and quantification of all other hormones | 132 |
| 5.3. Results..... | 132 |

| | |
|---|-----|
| 5.3.1 The impact of HT on wheat anther development | 132 |
| 5.3.2 Hierarchical clustering of total expressed transcripts | 134 |
| 5.3.3. Transcriptional regulation of anther development | 136 |
| 5.3.4. Transcriptome profiling using a cDNA reference | 142 |
| 5.3.5. The impact of HT on expression of GA-signalling and biosynthesis genes. | 145 |
| 5.3.6. Quantification of anther endogenous hormone levels in response to HT | 149 |
| 5.4. Discussion | 156 |
| 5.4.1. Acceleration of the tapetum development programme | 158 |
| 5.4.2. Modulation of the anther hormone profiles in response to HT | 162 |
| CHAPTER 6: GENERAL DISCUSSION | 168 |
| 6.1. Project Summary | 168 |
| 6.2. Limitations of studying anther development in wheat | 168 |
| 6.3. GA-signalling and the wheat tapetum | 169 |
| 6.4. HT-stress elicits hormonal and transcriptional responses..... | 173 |
| REFERENCES..... | 177 |
| ANNEX I..... | 199 |
| ANNEX II..... | 200 |
| ANNEX III..... | 202 |

List of Figures

| | |
|--|----|
| Figure 1.1. Wheat grain yields 1855-2010 at Broadbalk long term experiment, Rothamsted Research, UK..... | 2 |
| Figure 1.2. Typical progression of pollen development in angiosperms..... | 7 |
| Figure 1.3. The ABCE model of floral organ identity determination..... | 10 |
| Figure 1.4. Anther development genetic regulatory network in <i>Arabidopsis</i> and rice..... | 12 |
| Figure 1.5 Proposed GA-signalling pathway regulating tapetum PCD in rice... | 15 |
| Figure 1.6. The Gibberellin biosynthesis pathway..... | 17 |
| Figure 1.7. The Gibberellin signalling pathway..... | 18 |
| Figure 1.8. Transcriptional regulation by DELLAs..... | 20 |
| Figure 1.9. Cross sections of rice <i>gamyb-2</i> mutant and wild type anthers during young microspore, vacuolated microspore and mature pollen development stages..... | 22 |
| Figure 1.10. Hormonal regulation of anther HT-defects..... | 28 |
| Figure 3.1. Growth stages of wheat based on external morphological development..... | 55 |
| Figure 3.2. Defining morphological features of wheat (var. Cadenza) according to Zadocks scale..... | 56 |
| Figure 3.3. Staging of wheat anther development in wheat..... | 68 |
| Figure 3.4. Extension of the flag leaf sheath during booting stages..... | 71 |
| Figure 3.5. Development of the immature wheat ear..... | 72 |
| Figure 3.6. Logistic model of relationship between wheat anther developmental stage and flag leaf sheath length in the spring variety Cadenza..... | 74 |
| Figure 3.7. Microscopic analysis of wheat pollen development during FLS extension..... | 76 |

| | |
|--|-----|
| Figure 4.1. Protein alignments of putative a) <i>TaGAMYB</i> and b) <i>TabHLH141</i> sequences predicted from sequence isolated from IWGSC CSS..... | 87 |
| Figure 4.2. Phylogenetic trees for <i>TaGAMYB</i> and <i>TabHLH141</i> | 89 |
| Figure 4.3. Quantification of (a) <i>TaGAMYB</i> and (b) <i>TabHLH141</i> expression during wheat anther development..... | 91 |
| Figure 4.4. Schematic showing selection of RNAi trigger sequences for <i>TaGAMYB</i> and <i>TabHLH141</i> | 93 |
| Figure 4.5. Zygosity of T ₂ <i>gamyb-RNAi</i> plants..... | 95 |
| Figure 4.6. Phenotypic characterisation of <i>gamyb-RNAi 1</i> , -2 and Null lines..... | 97 |
| Figure 4.7. Increase magnification of <i>gamyb-RNAi 1</i> and Null tapetum..... | 98 |
| Figure 4.8. Phenotypic characterisation of <i>bhlh141-RNAi 2</i> and Null lines..... | 99 |
| Figure 4.9. Quantification of target transcript relative abundance in RNAi and Null lines..... | 100 |
| Figure 4.10. Schematic representation of SNP positions in <i>TaGAMYB</i> homoeologues..... | 10 |
| 2 | |
| Figure 4.11. Visualisation of exon-capture reads to <i>TaGAMYB</i> reference sequence..... | 103 |
| Figure 4.12. Sequencing alignment of TILLInG mutants..... | 104 |
| Figure 4.13. Abnormal anther development in <i>Tagamyb</i> plants..... | 106 |
| Figure 4.14. Thin section of <i>Tagamyb</i> anthers at different stages of development..... | 107 |

| | |
|--|-----|
| Figure 4.15. Interaction between RHT-D1-GRAS and TabHLH141..... | 110 |
| Figure. 4.16. Putative tapetum PCD GA-signalling pathway..... | 119 |
| Figure 5.1. Experimental time course structure of RNA-Seq experiment..... | 125 |
| Figure 5.2. Treatment and interaction effects on an example transcript..... | 129 |
| Figure 5.3. The effect of HT on anther development and morphology..... | 133 |
| Figure 5.4. Cluster dendrogram for all differentially expressed genes..... | 134 |
| Figure 5.5. MDS plot of RNA-seq samples mapped to IWGSC whole genome reference..... | 135 |
| Figure 5.6. MDS plot of whole genome aligned expressed genes in two biological replicates of T ₃ control and HT samples..... | 137 |
| Figure 5.7. Top 50 most abundant GO-terms amongst DEGs at 24 h HT treatment..... | 140 |
| Figure 5.8. Top 50 most frequently represented GO-terms in 24 h DEGs list using TGACv1 transcriptome reference..... | 145 |
| Figure 5.9. Mean effective counts of GA-signalling and biosynthesis genes..... | 147 |
| Figure 5.10. Hormone concentrations (pmol/g) in anthers at two development stages (10 cm or 15 cm FLS length) under control an HT conditions..... | 151 |
| Figure 5.11. The 13-hydroxylated and non-13-hydroxylated GA-biosynthesis pathway..... | 153 |
| Figure 5.12. Quantification of gibberellins in anthers at two development stages (10 cm or 15 cm FLS length) under control an HT conditions..... | 154 |
| Figure 6.1. Proposed model of anther developmental regulation by GA..... | 172 |

List of Tables

| | |
|--|-----|
| Table 2.1. PCR primers, oligonucleotide sequences, predicted melting temperatures and experimental purpose..... | 38 |
| Table 2.2. Plasmids and their respective selection methods used for cloning and transformation in this project..... | 39 |
| Table 3.1. Description of wheat anther and pollen development..... | 59 |
| Table 3.2. Non-destructive anther staging method in barley..... | 63 |
| Table 3.3. Description of wheat anther development stages as shown in Figure 3.3..... | 69 |
| Table 3.4. Predicted anther development stages based on logistic staging model for user defined flag leaf sheath lengths..... | 75 |
| Table 4.1. Gene identification labels in reference genome assemblies..... | 90 |
| Table 5.1. Top 20 DEGs in anther tissue after 24 h exposure to HT..... | 138 |
| Table 5.2. Selected GO-terms extracted from Fisher’s Exact Test output..... | 141 |
| Table 5.3. Top 20 most significant DEGs at 24 h HT..... | 143 |

List of Abbreviations

| | |
|-------|--|
| ABA | Abscisic Acid |
| AD | Activation Domain |
| ANOVA | Analysis of Variance |
| bHLH | Basic Helix-loop-helix |
| BLAST | Basic Local Alignment Search Tool |
| BP | Bicellular Pollen |
| bp | Base Pair |
| BR | Brassinosteroid |
| cDNA | Complementary DNA |
| CE | Controlled environment |
| cm | Centimetre |
| Co-IP | Co-Immunoprecipitation |
| DBD | DNA-Binding Domain |
| DEG | Differentially Expressed Gene |
| EMS | Ethyl methanesulfonate |
| FDR | False discovery Rate |
| FLS | Flag Leaf Sheath |
| GA | Gibberellin |
| GARE | Gibberellin Responsive Element |
| GC-MS | Gas Chromatography Mass spectrometry |
| GGPP | trans-geranylgeranyl diphosphate |
| GO | Gene Ontology |
| GS | Growth Stage |
| HPLC | High Performance Liquid Chromatography |
| IAA | Indole 3-Acetic Acid |
| IWGSC | International Wheat Genome Sequencing Consortium |
| JA | Jasmonic Acid |
| LC-MS | Liquid Chromatography Mass Spectrometry |
| LFE | Last Flag Extension |
| LSD | Least Significant Difference |
| MDS | Multidimensional Scaling |
| ML | Middle Layer |
| ml | Millilitre |
| mm | Millimetre |
| mM | Millimolar |
| MP | Mature Pollen |
| ng | Nanogram |
| PAR | Photosynthetically Active Radiation |
| PCD | Programmed Cell Death |
| PCR | Polymerase Chain Reaction |
| pg | Picogram |
| PMC | Pollen Mother Cell |
| PPL | Primary Parietal Layer |
| RNAi | RNA Interference |

| | |
|---------|--|
| RNA | Ribonucleic Acid |
| RNA-Seq | RNA-Sequencing |
| ROS | Reactive Oxygen Species |
| SNP | Single Nucleotide Polymorphism |
| SPL | Secondary Parietal Layer |
| TF | Transcription Factor |
| TILLInG | Targeted Induced Legions in Genome |
| TP | Tricellular Pollen |
| TUNEL | Terminal deoxynucleotidyl transferase (TdT) dUTP Nick-End Labelling |
| VP | Vacuolated Pollen |
| YM | Young Microspore |
| HT | High Temperature |
| μg | Microgram |
| μl | Microlitre |
| μm | Micrometre |
| μM | Micromolar |

CHAPTER 1: GIBBERELLIN SIGNALLING DURING MALE REPRODUCTIVE DEVELOPMENT IN WHEAT AND THE IMPACT OF HIGH TEMPERATURE STRESS

1.1. Wheat production, food security and climate change

Wheat (*Triticum aestivum*) is one of the world's most important plants, with over 600 million tonnes harvested annually, it contributes 19% of global dietary energy and even holds significance in human cultures and religions around the world (Shewry, 2009; Ray *et al.*, 2013). Modern bread wheat is an allohexaploid ($2n = 6x = 42$, AABBDD), the result of a spontaneous hybridisation between the tetraploid wheat *T. turgidum* ($2n = 4x = 28$, AABB) and goat grass *Aegilops tauschii* ($2n = 2x = 14$, DD) around 10,000 years ago in the near-eastern region often referred to as the fertile crescent (McFadden and Sears, 1946; Simons *et al.*, 2006; Shewry, 2009). Selection for domestication traits such as a non-shattering and free threshing ears, which reduced loss of grains and labour required to harvest them, further separated cultivated hexaploid wheat from its wild relatives as cultivation spread across central Asia and Europe, (Salamini *et al.*, 2002). Hexaploid bread wheat has now come to dominate agriculture in temperate regions due to its high yields, nutritional and culinary value and genetic diversity which allows its adaptation to a range of environments and changing cultivation practices (Shewry, 2009). During the mid-20th century, dramatic advances in the way in which wheat is bred and cultivated led to unprecedented yield improvement. This remarkable acceleration in the rate of wheat yield gains can be traced in the Broadbalk long-term wheat experiment at Rothamsted Research. Started by Sir John Bennett Lawes in 1843 as a means to demonstrate the effectiveness of his commercial fertiliser, the experiment records annual wheat yield data across a range of treatments and is thought to be the oldest continuous field experiment in the world (Fig. 1.1).

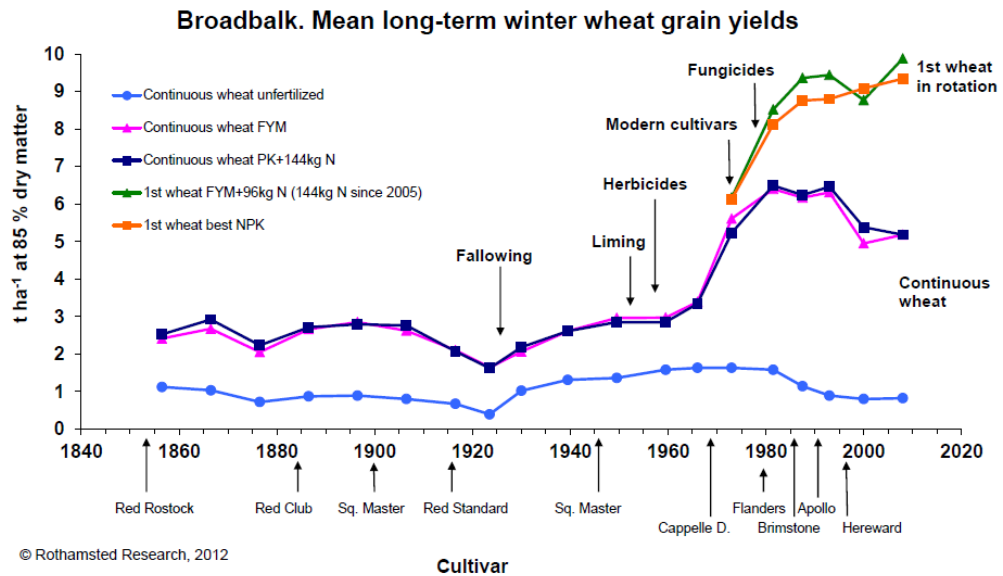


Figure 1.1. Wheat grain yields 1855-2010 at Broadbalk long term experiment, Rothamsted Research, UK. Lines show mean average grain yields ($t\ ha^{-1}$) under either continuous or 1st in rotation cultivation with farm yard manure (FYM) or synthetic fertiliser (NPK) fertilisation. Additional labels denote introduction of improved cultivar and/or agronomic practice (used with permission from Rothamsted Research).

The post-war period from 1945 onwards marks an important shift in the approaches taken to augmenting wheat yields in a period which became known as the “green revolution” (Evenson and Gollin, 2003). Multiple factors contributed to the green revolution ranging from advances in mechanisation and synthetic chemistry to socio-economic transitions but arguably the most important change to occur was the integration of improved understanding of plant physiology and genetics with breeding approaches.

One such wheat breeding programme led by Dr. Norman Borlaug at the Centro Internacional de Mejoramiento de Maíz y Trigo (CIMMYT) in Mexico produced a semi-dwarf varieties using a novel Japanese cultivar; Norin 10 (Hedden, 2003). The restricted stem elongation trait of this variety made it resistant to lodging, meaning that increased quantities of nitrogenous fertiliser could be applied resulting in increased partitioning of assimilate to grain rather than vegetative biomass (Flintham *et al.*, 1997). The introduction of dwarfing genes contributed to an increase in average wheat yields from just over $5\ t\ ha^{-1}$ to

nearly 10 t ha⁻¹ (Fig. 1.1.). The introduction of these high yielding varieties at a time of rapid population expansion is credited with preventing a billion people from suffering malnourishment and preventing hundreds of millions of hectares from being converted to agricultural use (Evenson and Gollin, 2003; Stevenson *et al.*, 2013). For this achievement Dr. Borlaug was awarded the Nobel Peace Prize in 1970.

Since then however, average farm yields have closed on the genetic potential maximum of many crops including wheat (Cassman, 1999). Therefore, providing any further yield gains in regions in which yield improvements have plateaued without inflicting significant environmental damage requires an unprecedented intensification of plant breeding, agronomy, ecology and environmental science research.

1.1.1. The impact of high temperature stress on wheat production

The world's population is anticipated to reach 9 billion around the year 2050. This increase in people will place significant pressure on the global agricultural system and at the same time place limitations upon the land, resources and acceptable level of environmental impact available to agriculture (Godfray *et al.*, 2010). Crop production alone needs to have doubled from current levels by this point to meet projected demand, however, if current rates of improvement are maintained wheat yields will only be 38% of that required (Ray *et al.*, 2013). Further confounding efforts to increase wheat yields is the negative consequences of global climate change for crop production. Climate change models suggest that rising average temperatures are already slowing yield gains in most wheat growing regions and that for every 1 °C increase in temperature further losses of 6% of global production can be expected (Asseng *et al.*, 2014). Development of mitigation strategies aimed at reducing future yield losses requires a comprehensive understanding of physiological responses of wheat to the abiotic stresses expected to accompany various climate change scenarios. By understanding the impact of stress on vulnerable processes and periods of development, desirable traits for breeding of stress

tolerant varieties and stress avoidance alterations to cultivation practices can be developed.

Yield penalties are associated with chronic temperature stress throughout the growing period and heat shock events which coincide with reproductive development and grain filling (Farooq *et al.*, 2011; Cossani & Reynolds, 2012). High temperature (HT) stress during grain filling reduces plant photosynthetic capacity which also reduces assimilate available for grain filling, grain quality, metabolic capacity to partition assimilate to grain and can induce grain abortion (Cossani & Reynolds, 2012; Hays *et al.*, 2007; Ortiz *et al.*, 2008). Furthermore, the phenological effect of increased temperature is to accelerate developmental rate and therefore post-anthesis HT stress shortens the grain filling period resulting in reduced grain weight (Ferris *et al.*, 1998). Grain filling generally coincides with the hottest part of the growing season (Gourdji *et al.*, 2013), therefore, it has been suggested that modification of wheat phenology to shift completion of grain filling to avoid peak daily maximum temperatures and terminal drought combined with further genetic improvement for heat tolerance is the best route to yield stability in warmer climates (Gouache *et al.*, 2012; Sadras & Monzon, 2006; Sadras *et al.*, 2007; Semenov *et al.*, 2014).

Short periods of HT stress overlapping pre-anthesis and early reproductive development are known to have a negative impact on reproductive development in flowering plants, including cereal crops such as wheat, rice and barley (Saini and Aspinall, 1982; Saini *et al.*, 1984; Sakata *et al.*, 2000; Barnabas *et al.*, 2008; Endo *et al.*, 2009; Oshino *et al.*, 2011). Male reproductive development in particular is highly sensitive to fluctuation in temperature at various stages of anther and pollen development, pollen release and pollen tube growth (Saini and Aspinall, 1982; Saini *et al.*, 1983; Giorno *et al.*, 2013; Müller and Rieu, 2016). Saini and Aspinall (1982) demonstrated that early anther development in wheat can be severely impaired by brief induction of HT stress. Exposure to 1 day at 30 °C or 3 days at 30 °C / 20 °C day/night around meiosis of the pollen mother cells in wheat

reduced grain set by 23.75 and 34.9% respectively due to a loss of pollen fertility (Saini and Aspinall, 1982). As wheat is a predominately self-fertilising plant (De Vries, 1971) any reduction in either male or female fertility will negatively affect fecundity.

The tapetum, an internal anther cell layer responsible for critical processes in pollen development, has been shown to be highly sensitive to abiotic stress in many species including cereals such as rice and wheat (Saini *et al.*, 1984; Oshino *et al.*, 2007; Parish *et al.*, 2013). Developing anthers are major sinks for assimilate and protecting their development and ability to maintain carbohydrate supply via the tapetum is crucial to ensuring fertility under abiotic stress conditions (Ji *et al.*, 2010). Furthermore, the tapetum also has a vital role in the formation of the pollen exine which is critical for its attachment and recognition by the style (Mizelle *et al.*, 1989; Shi *et al.*, 2015). Extremes of temperature during critical periods of tapetum activity have been shown to reduce its ability to transfer carbohydrates to developing pollen cells and disrupts tapetum cell lifecycle leading to reduced fertility (Parish *et al.*, 2013). Hormonal signaling pathways exert a strong influence on normal tapetum function (Plackett *et al.*, 2011; Zhang and Yang, 2014) and changes to function and structure under HT stress (Sakata *et al.*, 2010; Ji *et al.*, 2011; Higashitani, 2013). However, our understanding of the precise regulatory mechanisms which control the function of the tapetum remain limited.

Climate change models predict that more frequent, extreme HT events coinciding with periods of early wheat reproductive development will become a significant source of yield loss over the next 30 years (Semenov and Shewry, 2011). The vulnerability of the tapetum under these conditions will make a significant contribution to these losses if a means of reinforcing tapetum cells against HT stress cannot be found. Unlike terminal HT and drought stress, sporadic and unpredictable periods of extreme temperature cannot simply be avoided by altering phenology. It is therefore timely that the mechanisms underlying the anther response to HT is better understood in order to begin identifying the breeding traits required to produce HT-tolerant cultivars.

1.2. Anther and pollen cell morphology and development

The male reproductive gamete, pollen, is manufactured in floral organs called anthers. This begins with the formation of stamen primordia by the sporophyte and the differentiation of specialised anther tissues which support the development of sporophytic cells followed by meiosis to form gametophytes and the eventual release of mature haploid pollen (Ma, 2005). This is a developmentally complex process which requires the coordination of cellular processes such as division, differentiation and cell death which result in observable cytological changes which are broadly conserved across flowering species but have mostly been studied in model species *Arabidopsis*, barley and rice (Ma, 2005; Wilson and Zhang, 2009; Gómez and Wilson, 2012). Some attention has been given to characterisation of wheat anther and pollen development in the context of abiotic stress response, development of male sterile hybrid breeding varieties and hybridisation agents (De Vries, 1971; Saini *et al.*, 1984; Ji *et al.*, 2010). In rice and barley, male reproductive development spanning from anther primordia differentiation to dehiscence has been morphologically characterised and divided into discrete stages based on distinctive cytological features (Wilson and Zhang, 2009; Gómez and Wilson, 2012) which can be considered broadly analogous to the pollen development process in wheat although some differences may occur.

1.2.1. Pollen development

Pollen development is the process of producing haploid reproductive gametes with adequate nutrient reserves and outer protective coating to ensure fertilisation (Fig. 1.2.). After the formation of the stamen primordia, mitotic division of archesporial cells give rise to the four cell layers of the anther. Initially a primary sporogenous and a primary parietal layer are formed. These cells undergo further divisions to form pollen mother cells (PMCs) and the somatic layers of the anther wall (endothecium, middle layer and tapetum) all of which is surrounded by an outer epidermis (Wilson and Zhang, 2009, Zhang

and Yang, 2014). PMCs divide by meiosis to form tetrads of haploid microspore cells surrounded by a callose wall. Free microspores are released from the tetrads into the anther locule after degeneration of the callose envelope. During the second phase of pollen development the newly released gametophytes undergo two rounds of mitosis to form two sperm cells which will complete the fertilisation of the ovary and endosperm, begin to form a vegetative cell which maintains pollen cell function (McCormick, 1993). Coinciding with mitosis is the vacuolation of pollen cells and the initiation of carbohydrate accumulation during which pollen cells begin to take on their familiar spherical form and appear filled (Mizelle *et al.*, 1989).

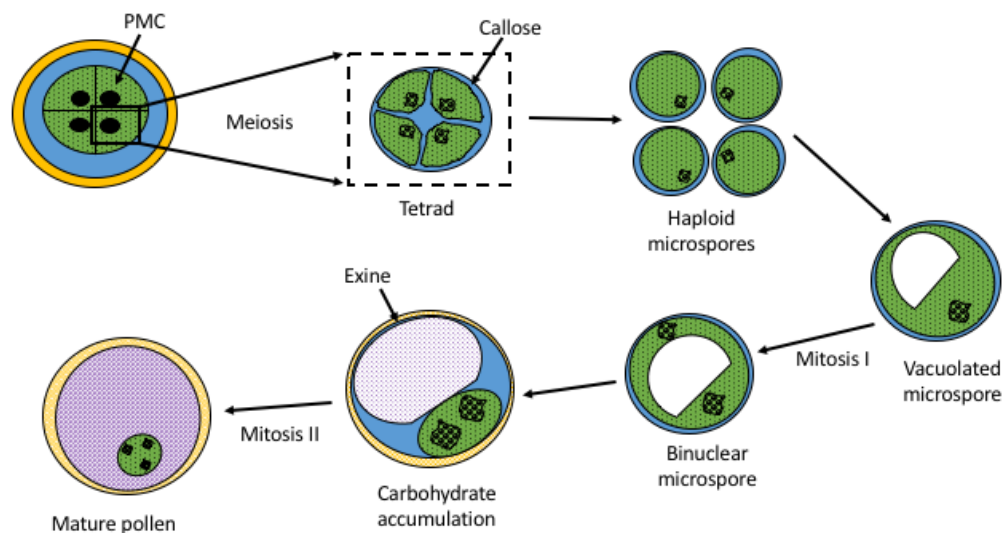


Figure 1.2. Typical progression of pollen development in angiosperms. *Haploid microspores are released into the anther locule in tetrads after meiosis of PMCs. Young microspores then undergo mitosis, accumulate carbohydrates and pollen coat formation before they are released as mature pollen cells* (adapted from McCormick, 1993).

Upon completion of PMC meiosis, the process of pollen wall synthesis begins. The pollen wall is formed of two layers, the inner intine and the outer exine comprised mostly of pectocellose and sporopollenin respectively (Mizelle *et al.*, 1989; McCormick, 1993). The sporopollenin forms a species-specific

pattern as it is laid down on the exine which is determined by the sporophyte and is required for cell-cell recognition during fertilisation (McCormick, 1993; Ma, 2005). In the later stages of pollen development once the pollen coat has formed, the swelling of the pollen cells coincides with degradation of anther wall tissues leading to dehiscence, the splitting of the anther theca which releases pollen into the environment (Matsui *et al.*, 1999).

1.2.2. The role of the tapetum in pollen development

The events leading up to the release of mature, viable pollen cells from the anther are dependent upon the prior competence of the tapetum. The tapetum is a layer of cells lining the anther locule which provide microspores with nutrients, enzymes required for their release from meiotic tetrad callose envelopes and later the molecular components of the pollen exine wall are provided by the secretory tapetum layer (Parish and Li, 2010, Plackett *et al.*, 2011, Liu and Fan, 2013, Plackett *et al.*, 2013, Lui *et al.*, 2014). Beyond its nutritive and structural support function (Ma, 2005) the tapetum has been shown to have a crucial role in developmental signalling required to support post-meiotic pollen processes such as mitosis (Ma, 2005; Yang *et al.*, 2007; Xu *et al.*, 2010; Plackett *et al.*, 2014).

During pollen mitotic division and exine wall formation the tapetum layer undergoes programmed cell death (PCD), releasing further components essential to pollen formation (Parish and Li, 2010, Lui and Fan, 2013). The timing and execution of tapetum PCD is a highly regulated process which depends on a complex and poorly understood signalling network which if interrupted results in male sterility (Aya *et al.*, 2009, Parish and Li, 2010, Nui *et al.*, 2013, Min *et al.*, 2013). Wheat tapetum cells are highly metabolically active at PMC meiosis with plastids and the cytosol becoming dense and the initiation of vacuole formation (Mizelle *et al.*, 1989). At some point during this period, an as of yet poorly understood signal is received which commences tapetum PCD. As tapetum cell walls degrade, lipidal Pro-Ubisch bodies collect on the locule surface on which sporopollenin accumulates although it is not clear exactly

what role orbicular Ubisch bodies play in delivery of these vital pollen wall components (Mizelle *et al.*, 1989; Parish and Li, 2010). Tapetum cells then disintegrate as the pollen cells swell during their vacuolation phase giving the appearance that the tapetal cells are collapsing under the pressure. Tapetum cells have completely degraded by the time pollen cells enter the second round of mitosis (Zhang *et al.*, 2011).

Tapetum PCD is apoptotic-like, occurring rapidly and characterised by cellular collapse, remobilisation of components and detectable DNA fragmentation (Varnier *et al.*, 2005; Parish and Li, 2010). Synchronisation of tapetum PCD with pollen development is crucial for male fertility. Abiotic stress disrupts this developmental programme by modifying complex hormone and secondary signals signalling cascades which regulate the activity of PCD executing enzymes (Parish *et al.*, 2013).

1.3. Genetic regulation of pollen development

Anther and pollen development involves a number of complex developmental steps, beginning with stamen meristem specification and ending with the release of viable pollen cells. During these processes tens of thousands of unique transcripts are expressed in anther and gametophytic cells (Guo and Liu, 2012). Many of the most important genes which regulate anther and pollen development have been identified in model species such as rice and *Arabidopsis* for which considerable genetic and genomic resources are available (Gómez *et al.*, 2015). Pollen development in both species involves similar stages and the analysis of male sterile mutants of orthologous genes in both species reveal that the underlying genetic regulatory mechanism is highly conserved (Wilson and Zhang, 2009; Gómez *et al.*, 2015). The challenge now is to translate this knowledge into more genetically complex, non-model crop species such as wheat to allow the dissection of agronomically important traits such as heat stress tolerance.

1.3.1. Floral organ identity and differentiation

Molecular studies have identified a suite of genes and their specific temporal and spatial expression profiles which form the ABCE model of floral organ identity specification including the male reproductive organ, the stamen. Floral organs (sepals, petals, stamen and gynoecium) are each confined to within one of four concentric whorls where the localised, overlapping expression of specific ABCE genes determines the organ identity in each whorl (Chandler, 2011). Reduced or ectopic expression of ABCE genes result in the interchangeable conversion of organ identities (Goto *et al.*, 2001). The A function genes determining sepal and petal identity are *APETALA1 (AP1)* and *APETALA2 (AP2)*, B function gene *APETALA3 (AP3)/PISTILATA* determine petal and stamen identity, C function gene *AGAMOUS (AG)* determines stamen and carpel development whilst E function genes *SEPALLATA1, -2, -3* and *-4* are required for all functions (Ma, 2005). Therefore, the B and C functions are required for the determination of stamen identity in the floral meristem (Fig. 1.3.).

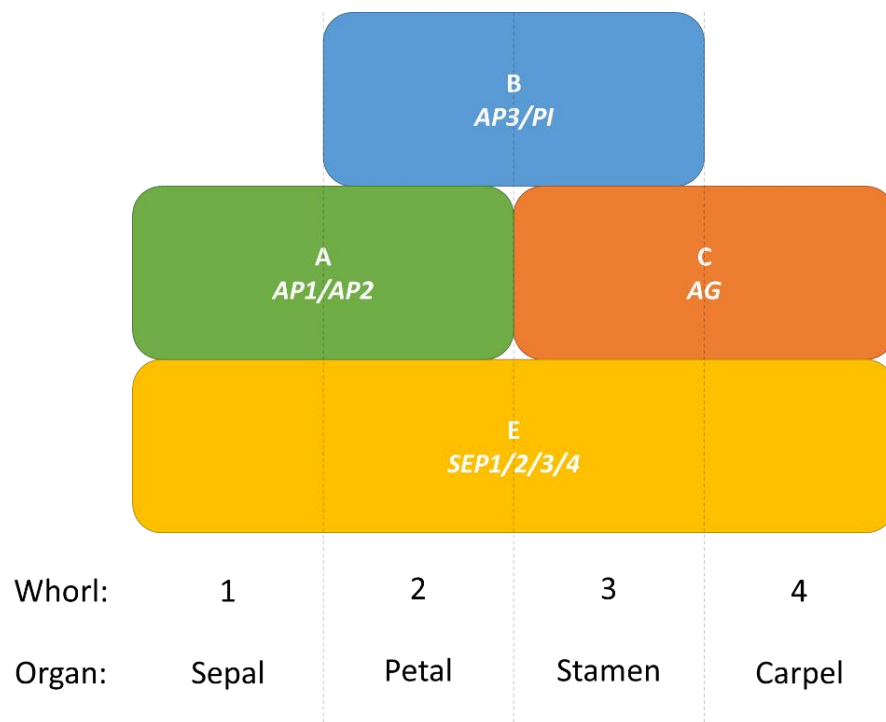


Figure 1.3. The ABCE model of floral organ identity determination. *Whorl-specific expression of floral-homeotic family genes determines organ differentiation on the floral meristem. Determination of stamen identity arises from combined gene-family expression; A+E = sepals, A+B+E = Petals, B+C+E= stamen and C+E = carpels (from Ma, 2005).*

1.3.2. Genetic regulation of pollen and tapetum development

An extensive body of research characterising the roles of genetic signalling components in anther development now exists in model species *Arabidopsis* and rice (Fig. 1.4.) which shows although there are some differences the fundamental principles are conserved (Wilson and Zhang, 2009; Gómez *et al.*, 2015). After the initiation of stamen primordia anther lobes consisting of four non-reproductive cell layers surrounding the microsporocytes are formed. In *Arabidopsis*, the genes *SPOROCTELESS (SPL)/NOZZLE (NZZ)* are required in early anther development and are crucial for differentiation and the correct formation of sporogenous cells and the tapetum (Yang *et al.*, 1999). Furthermore, it appears that expression of *SPL/NZZ* is under the regulation of *AG* (Ito *et al.*, 2004).

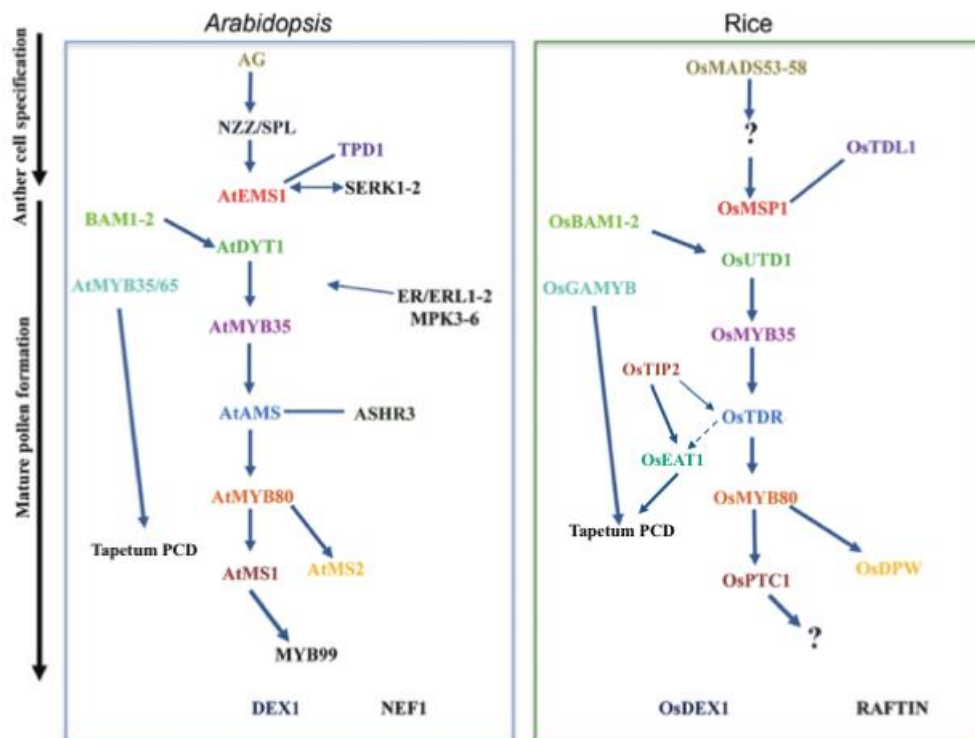


Figure 1.4. Anther development genetic regulatory network in *Arabidopsis* and rice. Colour of gene names relate to equivalent orthologues. Solid arrows indicate characterised relationships, dashed arrows are unconfirmed. Adapted from Gómez *et al.*, (2015)

The expression of two *Arabidopsis* meiocyte and tapetum precursor cell specific genes, *EXCESS MALE SPOROCTYES1* (*EMS1*) and *TAPETUM DETERMINANT1* (*TDR1*), produce a receptor-ligand cell signalling pathway that ensures the correct differentiation of meiocytes and tapetal cells (Canales *et al.*, 2002; Ma, 2005). Both genes are required for tapetum identity with mutant phenotypes displaying excess male sporocytes, the lack of a tapetum and male sterility.

The basic helix-loop-helix (bHLH) transcription factor *DYSFUNCTIONAL TAPETUM1* (*DYT1*) acts downstream of *EMS1/EXS* and *TAPETAL DETERMINANT1* (*TPD1*) and is required for tapetum development (Zhang *et al.*, 2006). During meiosis and young microspore stages in *dyt1* loss-of-function mutants the tapetum becomes vacuolated, with deposition of thin callose walls and a reduction in the expression of other tapetum-preferential genes, including two other transcription factors required for tapetum and

pollen development, *MALE STERILE1 (MS1)* and *ABORTED MICROSPORES (AMS)* (Zhang *et al.*, 2006). *MS1* is a PHD-finger class transcription factor which is expressed in the tapetum during callose breakdown and appears to regulate the expression of at least 260 genes primarily involved in pollen wall and coat formation but also other transcription factors and Cysteine proteases (Yang *et al.*, 2007). The other potential target of *DYT1*, *AMS*, is also a bHLH transcription factor and is also necessary for the expression of tapetal function and postmeiotic pollen wall formation genes (Xu *et al.*, 2010).

A number of genes with important roles in the formation of the pollen coat have been identified but their relationship to the anther regulatory signalling cascade is not yet clear. *DEFECTIVE EXINE 1 (DEX1)* and *NO EXINE FORMATION 1 (NEF1)* are plasma membrane proteins required for pollen exine formation and sporopollenin transport, without which pollen abortion occurs after microspore release from tetrads (Ariizumi *et al.*, 2004; Ma *et al.*, 2013). Similarly, *RAFTIN (OsRAFTIN)* is a cereal specific BURP-domain protein expressed in the tapetum and microspores which is critical for the formation of Ubisch bodies, thought to be instrumental in transporting and depositing sporopollenin from the tapetum on the pollen exine (Wang *et al.*, 2003).

Rice TFs *OsTDR*, *OsUDT1* and *OsGAMYB* mutants all have defective tapetum development phenotypes which suggests that either the tapetum pathway involved in multiple pathways or all of these TFs are upstream of a single PCD “master switch” (Kaneko *et al.*, 2004; Jung *et al.*, 2005; Li *et al.*, 2006a; Parish and Li, 2010). Whilst some information about the likely positions of these TFs in the anther regulatory network can be inferred from their mutant phenotypes and transcription of downstream response genes, expression patterns and protein-protein interaction studies, the precise mechanism through which they bring about tapetum PCD remains unknown.

OsGAMYB is an anther expressed TF which is also involved in mobilisation in the seed aleurone layer suggesting that it may perform a similar function in the tapetum (Millar and Gubler, 2005; Wilson and Zhang, 2009) (see section

1.4.4.). Indeed conversion and transport of carbohydrates is a significant part of the role of the tapetum and is measurably perturbed by abiotic stress (Oliver *et al.*, 2005; Ji *et al.*, 2011). So far however, *OsGAMYB* has been associated only with tapetum PCD regulation and pollen exine formation (Kaneko *et al.*, 2004; Aya *et al.*, 2009).

The absence of PCD in rice *Osgamyb* mutants may be explained by its positive regulation of a group of protease genes which are involved in apoptosis (Aya *et al.*, 2009, Alonso-Pearl *et al.*, 2010). *OsGAMYB* converges with *OsUDT1*, a GA-independent regulator of early tapetum development, to regulate *TAPETUM DEGENERATION* (*OsTDR*) which encodes a basic helix-loop-helix (bHLH) transcription factor which is upstream of essential tapetum and pollen development genes (Li *et al.*, 2010). *OsTDR* is a member of a sequential *bHLH* signalling cascade which operates from early anther cell specification to the execution of tapetum PCD. *TDR INTERACTING PROTEIN2* (*OsTIP2*) promotes the specification of anther cell wall identities and interacts directly with TDR and promotes its expression alongside *ETERNAL TAPETUM 1* (*OsEAT1*; *bHLH141*) (Fu *et al.*, 2014). *OsTIP2* promotes the expression of *OsEAT1* by forming a heterodimer with *OsTDR* and binding to the *OsEAT1* promoter (Ko *et al.*, 2014). *OsEAT1* is a bHLH transcription factor which binds with TDR and the promoter region of at least two aspartic protease genes, *OsAP25* and *OsAP37*, to promote tapetum PCD (Nui *et al.*, 2013). In *Arabidopsis* further interactions between these bHLH TFs in anther development have been described. *DYT1* promotes the expression of *AtbHLH10/AtbHLH89/AtbHLH91*, putative orthologues of *OsEAT1*, which interact with *DYT1* and promote its specific nuclear localisation which is thought to alter its transcriptional activity (Cui *et al.*, 2016)

A possible pathway through which *GAMYB* promotes tapetum PCD by enhancing the *TDR-EAT1* upregulation of aspartic proteases can be envisaged (Fig. 1.5). However, as both *OsGAMYB* and *OsUDT* are upstream of *OsTDR* and the *bHLH* signalling cascade, it remains unclear as to precisely which aspects of tapetum development and PCD GA and non-GA-mediated signalling

pathways control. *OsUDT1* is an early anther development gene whose interaction with *OsTIP2* appears to be crucial for early tapetum differentiation processes (Liu *et al.*, 2010) and is down-regulated by *OsTIP2* in a feedback loop (Fu *et al.*, 2014), whereas *Ostip2*, *Osgamyb*, and *Ostdr* mutants share a similar tapetum-hypertrophy phenotype (Li *et al.*, 2006, Aya *et al.*, 2009, Fu *et al.*, 2014), suggesting their roles are in controlling tapetum size and the initiation of PCD (Fu *et al.*, 2014). Furthermore, whilst the *Oseat1* mutant also displays non-initiation of PCD, it is not accompanied by the increase in tapetum cell enlargement seen in *Osgamyb*, *Ostip2* and *Ostdr* (Nui *et al.*, 2013, Fu *et al.*, 2014). This confirms the post-initiation, PCD execution role of *OsEAT1* and suggests that the temporal expression and accumulation patterns of these transcription factors depends upon the initial “commitment” to tapetum PCD which may be GA-mediated via *OsGAMYB* up-regulation of the *bHLH* signalling cascade.

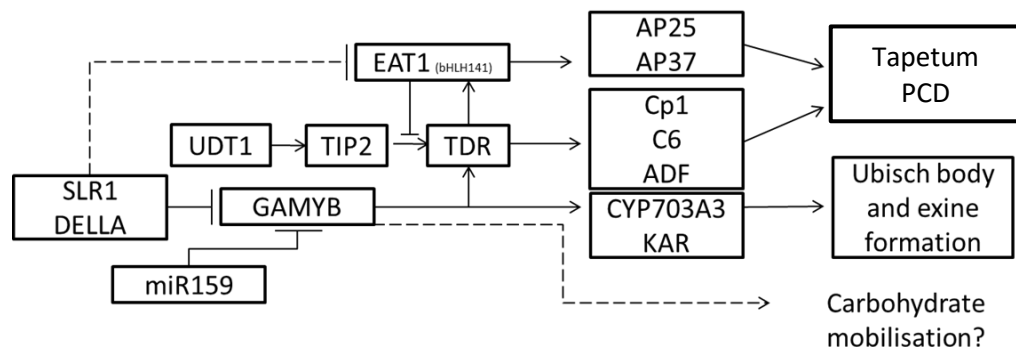


Figure 1.5 Proposed GA-signalling pathway regulating tapetum PCD in rice. Arrows indicate positive regulation; flat bars indicate negative regulation. Dashed lines represent hypothetical pathway. Signalling pathway is based on interactions described in literature.

1.4. Gibberellin signalling in anther development

Gibberellins (GAs) are a group of tetracyclic diterpenoid carboxylic acids produced by plants, some of which have biological activity promoting growth and development (Hedden, 2012). GAs are essential for seed germination,

stem elongation, trichome formation, floral transition and male reproductive development (Sun, 2010; Plackett *et al.*, 2012; Daviere and Achard, 2013).

Plants tightly regulate cellular levels of precursor and active forms of gibberellins in response to developmental and environmental cues (Hedden, 2012). Active gibberellin (GA₁ and GA₄) is a biochemical signal which needs to be perceived and relayed to induce transcriptional changes in response to the stimulus. Although not strictly the correct nomenclature, here the shorthand GA refers to gibberellin generally unless otherwise specified. Through study of GA-deficient and insensitive mutants in model species, a “relief of repression” model of GA-signalling has emerged in which active GA promotes growth and development by promoting the degradation of growth-inhibiting DELLA proteins (Peng *et al.*, 1997; Silverstone *et al.*, 2001).

GA-biosynthesis is a multi-step process requiring the expression of widely conserved gene families, some of which contain multiple, functionally diverse paralogues (Plackett *et al.*, 2012). The primary biologically active GAs in higher plants are GA₁ and GA₄ and their relative abundance varies between species and tissue, with the highest concentrations being found in anthers and developing seeds (Hedden, 2012). GA-biosynthesis occurs in three stages. Firstly, *trans*-geranylgeranyl diphosphate (GGPP) is converted by *ent*-copalyl diphosphate synthase (CPS) and *ent*-kaurene synthase (KS) into *ent*-kaurene in plastids (Hedden, 2016). Two endoplasmic reticulum associated P450s, *ent*-kaurene oxidase (KO) and *ent*-kaurenoic acid oxidase convert *ent*-kaurene into GA₁₂. At this point the GA-biosynthesis bifurcates into two parallel pathways; the 13-hydroxylation pathway, resulting in GA₁ and the non-13-hydroxylation pathway resulting in GA₄, depending on whether or not GA₁₂ is 13-hydroxylated by GA13OX to form GA₅₃ (Hedden, 2012, 2016).

Formation of the bioactive GA₁ and GA₄ requires the oxidation of intermediates by soluble 2-oxoglutarate dependent dioxygenases GA 20-oxidases (GA20OX) and GA 3-oxidases (GA3OX) whilst deactivation of GAs is carried out primarily by GA 2-oxidases (GA2OX) (Hedden, 2012, 2016).

Figure 1.6. shows a simplified GA-biosynthesis pathway in which modifications by GA-oxygenase family enzymes creates precursor compounds which can be readily converted into active and inactive forms. There are multiple *GA20OX* and *GA3OX* genes with varying, but often overlapping, expression profiles in specific tissues depending on developmental stage (Rieu *et al.*, 2007; Plackett *et al.*, 2012; Hedden, 2012). A number of genes encoding GA-biosynthesis enzymes have been identified in wheat (Huang *et al.*, 2012) and their tissue specific expression patterns investigated (Pearce *et al.*, 2015) but little is known about their expression during wheat reproductive development.

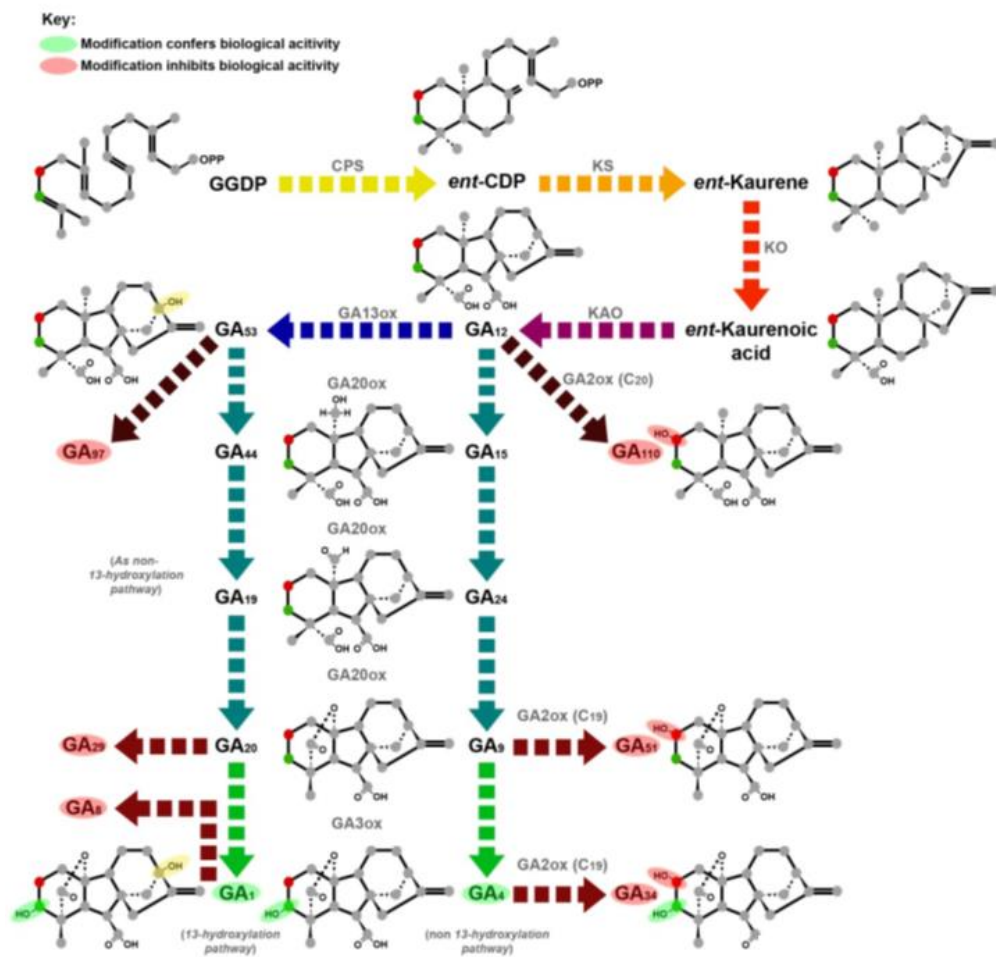


Figure 1.6. The Gibberellin biosynthesis pathway. Coloured arrows represent enzyme or enzyme families which convert precursor compounds into GAs named in black. Green and red highlighting of GA compound and position on chemical structure indicates modification confers or inhibits biological activity respectively (from Plackett *et al.*, 2011).

GA metabolism is an important mechanism of regulating GA-responsive growth. The concentration of bioactive and precursor forms of GA is controlled via the developmental, homeostatic and environmental regulation of GA-biosynthesis and deactivation genes (Hedden, 2012; Colebrook *et al.*, 2014). Over-accumulation of bioactive GAs is prevented by the upregulation of *GA2OX* genes whilst *GA20OX* and *GA3OX* genes are promoted by the repression of GA-signalling and other growth promoting signals such as the hormone auxin (Hedden, 2012). Likewise, environmental stresses which result in the restriction of growth and reduction in GA levels is brought about by the upregulation of *GA2OX* genes and stabilisation of GA-signalling repressors (Achard *et al.*, 2008; Colebrook *et al.*, 2014).

Plants which lack the ability to produce bioactive forms of GA are severely dwarfed but can be rescued by exogenous GA application (Koornneef and van der Veen, 1980; Dawson *et al.*, 1993; Cheng *et al.*, 2004). The identification of a GA-insensitive mutant, *gai-1*, which had a similar appearance to GA-deficient mutants but did not respond to either GA or a GA-inhibitor, paclobutrazol (PAC), led to the discovery of DELLA proteins, the negative regulators which GA opposes (Peng *et al.*, 1997; Silverstone *et al.*, 1997; Dill and Sun, 2001; Silverstone *et al.*, 2001). Since then, a comprehensive understanding of the mechanisms through which GA stimulates growth and development by relieving the repression imposed by DELLAs has emerged primarily through the study of GA-signalling mutants in model species *Arabidopsis* and rice (Fig. 1.7.).

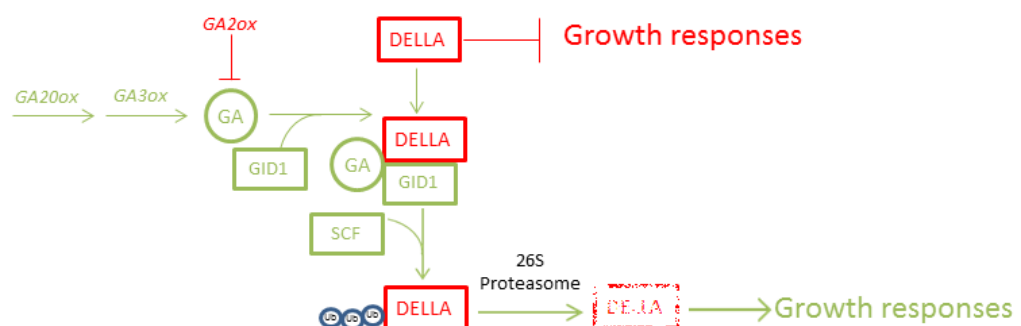


Figure 1.7. The Gibberellin signalling pathway. *Arrows indicate positive regulation whilst closed arrows denote negative regulation, likewise growth promoting and repressive components are green and red respectively. Ub – Ubiquitin, SCF – Skp, Cullin, F-box tripartite complex. (Adapted from Colebrook et al., 2014)*

In the absence of GA DELLA proteins constitutively repress GA responses. The presence of bioactive GA is perceived by the soluble receptor protein GIBBERELLIN INSENSITIVE DWARF (GID1) which has a binding affinity for GA (Ueguchi-Tanaka *et al.*, 2005). The binding of GA by GID1 causes a conformational change which allows GID1 to bind directly with DELLA (Ueguchi-Tanaka *et al.*, 2005; Griffiths *et al.*, 2006). The rice GID1 receptor contains a binding pocket with a strong affinity for GA₄. Binding with GA₄ causes the N-terminal lid to fold over the pocket, creating a hydrophobic surface which is involved in the interaction with SLR1 (Shimada *et al.*, 2008). The formation of a GID1-DELLA complex promotes the interaction between DELLA and the SLEEPY1 (SLY1) F-box component of the SCF^{SLY1} complex (Griffiths *et al.*, 2006). The SCF E3 ubiquitin ligase complex rapidly tags DELLA with ubiquitin resulting in its proteolysis via the ubiquitin/26S pathway (McGinnis, 2003; Sasaki *et al.*, 2003). The degradation of DELLA via this pathway results in rapid, GA-responsive transcriptional changes (Zentella *et al.*, 2007; Locascio *et al.*, 2013).

However, the absence of a DNA-binding domain make it unclear through which mechanisms DELLAs enact transcriptional regulation (Chandler *et al.*, 2002; Zentella *et al.*, 2007; Locascio *et al.*, 2013). The C-terminal GRAS domain region of DELLAs contain two Leucine heptad repeats which are thought to be involved in protein and nucleic acid binding (Dill *et al.*, 2004; Sun *et al.*, 2012; Hirano *et al.*, 2012). Direct interaction with transcription factors by DELLAs is one mode through which they regulate the expression of target genes. The first such interaction was demonstrated with the DNA binding domains of *Arabidopsis* transcription factor PHYTOCHROME INTERACTING FACTOR 4 and 3 (de Lucas *et al.*, 2008; Davière *et al.*, 2008). PIFs are bHLH family TFs which

promote hypocotyl elongation in the absence of light-activated Phytochrome B (de Lucas *et al.*, 2008). The sequestration of PIFs by DELLA into deactivated complexes prevents them from binding to cognate promoter regions of cell elongation genes until their release by GA-induced DELLA degradation (Fig. 1.8. a).

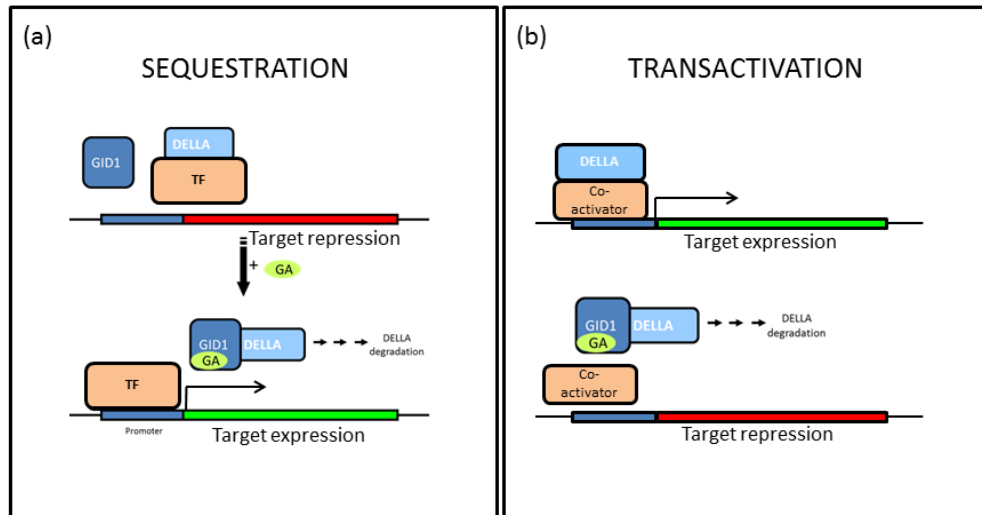


Figure 1.8. Transcriptional regulation by DELLAs. *a) Under low GA-levels DELLAs bind directly to TFs (demonstrated with bHLHs) and prevent association with target gene promoter. GA-mediated DELLA degradation releases repression of TF and transcription is promoted. b) DELLAs promote expression of growth restricting genes by enhancing the association of a co-activating TF with downstream promoter regions. In this case increasing GA concentration downregulates transcription.*

DELLAs also possess transactivational ability, regulating target gene expression through interaction with its promoter region facilitated by an intermediary co-factor (Fig. 1.8. b). IDD2/GAF1 interacts with GAI to upregulate GA-biosynthetic and perception genes, *GA20ox2*, *GA3ox1* and *GID1b* (Fukazawa *et al.*, 2015). The ability of DELLAs to not only repress GA signalling but also regulate the expression of GA-biosynthesis genes enables a homeostatic feedback mechanism (Zentella *et al.*, 2007).

The molecular mechanisms through which GA regulates transcription via DELLAs remain unclear, with only a number of downstream targets identified

so far. To date, only one GA-responsive TF, GAMYB, downstream of DELLA with a role in anther development has been characterised (Aya *et al.*, 2009).

1.4.1. GAMYB is a GA-responsive transcription factor crucial for anther development

The R2R3-MYB family transcription factor GAMYB was first identified as a GA-signalling component in cereal seed aleurone where it mediates GA-induction of α -amylase expression during germination (Gubler *et al.*, 1995). GAMYB activates α -amylase by binding directly to *cis*-acting 21 bp gibberellin responsive element (GARE) (Skriver *et al.*, 1991; Gubler *et al.*, 1999; Woodger *et al.*, 2003). α -amylase is secreted by the aleurone to hydrolyse starch endosperm to provide carbohydrates during germination (Gubler *et al.*, 2002; Aoki *et al.*, 2014). During this process, the aleurone layer undergoes PCD in which GA-signalling has been implicated (Ishibashi *et al.*, 2012; Aoki *et al.*, 2014). Clearly, the aleurone and the tapetum share some similarities; they both have secretory functions, undergo PCD and require GAMYB.

PCD of the anther tapetum layer also requires *GAMYB*. Overexpression of *HvGAMYB* results in smaller and paler anthers than wild type which, despite apparently otherwise normal development, fail to dehisce (Murray *et al.*, 2003). By contrast, sterility in rice *Osgamyb* mutants (Kaneko *et al.*, 2004; Aya *et al.*, 2011; Liu *et al.*, 2010) is due to failure of the tapetum layer to vacuolate and initiate PCD after PMC meiosis. Instead, the tapetum layer becomes hypertrophic, swelling to fill the anther locule and crushes the developing microspores (Fig 1.9.).

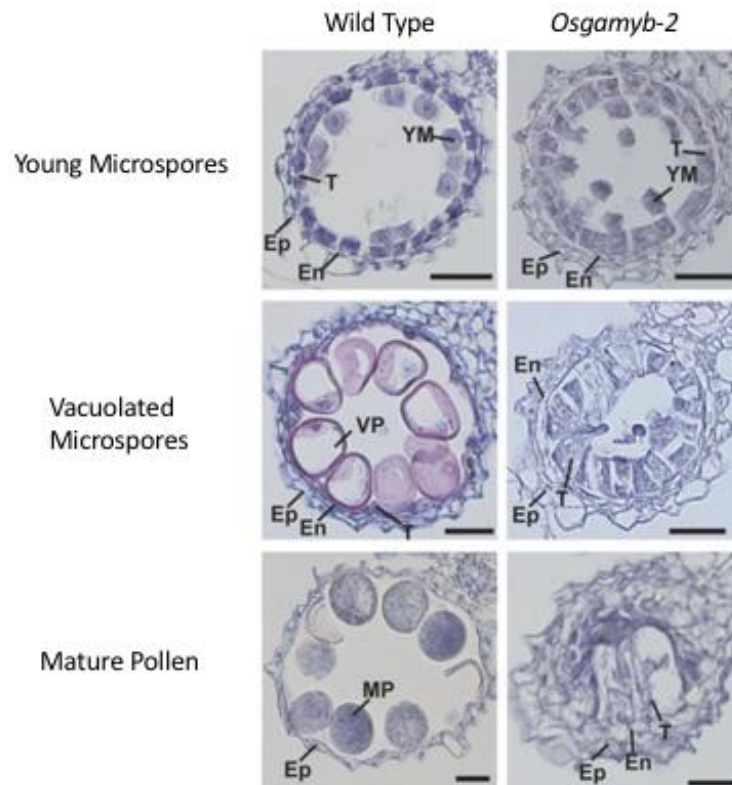


Figure 1.9. Cross sections of rice *gamyb-2* mutant and wild type anthers during young microspore, vacuolated microspore and mature pollen development stages. *Failure to initiate tapetum PCD prevents microspore development beyond young microspores.* En – Endothecium, Ep – Epithecium, MP – Mature pollen, T – Tapetum, YM – Young microspore, VP – Vacuolated microspore. Scale bars = 25 μ m. (Taken from Aya *et al.*, 2009).

The timing of *GAMYB* expression appears to be critical for anther development and induction of tapetum PCD. A number of downstream targets have been identified which give some explanation as to the mechanisms through which *GAMYB* co-ordinates pollen and tapetum developmental processes (Tsuji *et al.*, 2006; Aya *et al.*, 2009). However, further work is needed to extend this understanding to anther development in wheat.

1.4.2. GA-dependent regulation of *GAMYB*

Expression of *GAMYB* in the aleurone is promoted by GA (Gubler *et al.*, 1999; Woodger *et al.*, 2003). Embryoless half seedlings secrete α -amylase when treated with GA₃. In rice *gamyb* mutants, exogenous GA application does not induce α -amylase expression (Kaneko *et al.*, 2004), whilst α -amylase is induced constitutively in the absence of GA₃ in *Slr-1* mutants (Ikeda *et al.*, 2001) demonstrating that *GAMYB* expression is regulated by the GA-DELLA pathway. Indeed, microarray analysis confirms that almost all GA-mediated gene expression in the aleurone is mediated via DELLA and *GAMYB* (Tsuji *et al.*, 2006).

GAMYB expression in the anther appears also to be negatively regulated by DELLAs and induced by GA (Murray *et al.*, 2003). *Osgamyb* and upstream GA-signalling and biosynthesis mutants, *Osgid-1* and *Oscps1-1* share common defective anther phenotypes, confirming the GA signal promoting PCD is transduced via DELLA regulation of *GAMYB* (Aya *et al.*, 2009). However, unlike in the aleurone, post-transcriptional regulation of *GAMYB* by a microRNA (miR159) also occurs in anther tissue (Alonso-Peral *et al.*, 2010). In all other tissue, *GAMYB* is expressed but post-transcriptionally cleaved via repression by microRNA (miR159) (Wang *et al.*, 2012). This is also true in the anthers until a repression of miR159 expression stabilises *GAMYB* transcript levels, demonstrated by the negative correlation in abundance of both transcripts (Tsuji *et al.*, 2006). When miR159 is over expressed plants show delayed flowering and severe anther defects to the point of sterility, similar to that of *gamyb* knockout mutants (Kaneko *et al.*, 2004; Tsuji *et al.*, 2006; Aya *et al.*, 2009; Wang *et al.*, 2012). As expression of miR159 is not regulated by GA (Tsuji *et al.*, 2006), the question remains as to what exactly is the 'master switch' which permits the upregulation of *GAMYB*, and therefore enables GA mediated anther development.

1.4.3. GAMYB regulates secretory functions and PCD

Despite the many functional similarities between tapetum and aleurone tissue, GAMYB appears to have diverse mechanisms of transcriptional regulation. Microarray studies of rice *gamyb* plants show that there is very little overlap between GAMYB-activated genes in aleurone and post-meiotic anthers (Tsuji *et al.*, 2006). Whilst many of these target genes contain the cis-acting GARE elements which allow GAMYB to directly interact with target gene promoters, some do not. This further suggest that, like DELLAs, GAMYB may require interaction with additional co-factors to affect transcriptional regulation (Washio, 2003; Tsuji *et al.*, 2006).

GAMYB has been shown to form heterodimers with other MYB TFs during the regulation of carbohydrate metabolism in germinating seeds (Hong *et al.*, 2012). In response to sugar starvation conditions, GA-signalling promotes the formation of GAMYB-MYBS1 complex which facilitates their redistribution from the cytoplasm to the nucleus where simultaneous binding to both GARE and TA-box elements enhances α -*amylase* expression (Hong *et al.*, 2012). A major function of the tapetum is the delivery of soluble carbohydrates to developing pollen cells which at this point have become a major resource sink (Oliver *et al.*, 2005) and indeed, initiation of *AtMYB33/65* expression coincides with mobilisation of tapetum soluble carbohydrates to pollen cells (Millar and Gubler, 2005; Parish and Li, 2010). However, no direct link between *GAMYB* gene expression in anthers and expression of carbohydrate metabolism genes has yet been established.

GAMYB also directly interacts with the promoter regions of two lipid metabolism genes *cytochrome P450 hydroxylase (CYP703A3)* and β -*ketoacyl-reductase (KAR)*, to promote their expression between meiosis and pollen maturation (Aya *et al.*, 2009). Both genes are thought to be involved in lipid metabolism and given the role of the tapetum in biosynthesis and transport of sporopollenin precursors and pollen coat formation (Scott *et al.*, 2004; Huang *et al.*, 2009), supporting the role of *GAMYB* in tapetum secretory function.

Indeed, GA-biosynthesis mutant *Ososcps1-1*, signalling mutants *Osgid-2* and *Osgamyb-2*, and *Oscyp703a* are all lacking or deficient in Ubisch body formation, the tapetum vesicles which supply sporopollenin, proteins, phenolic and fatty acid compounds to microspores (Aya *et al.*, 2009).

GA-mediated PCD occurs in both tapetum and aleurone cell layers (Guo and Ho, 2008; Aya *et al.*, 2011). PCD of tapetum cells is an apoptotic process which requires GAMYB (Parish and Li, 2010), whilst PCD of barley aleurone protoplasts is enhanced by, but does not require *HvGAMYB* (Guo and Ho, 2008) suggesting aleurone cell PCD may occur via a different pathway. The repression in *Osgamyb* of protease genes encoding enzymes known to be involved in the execution of apoptotic PCD (Tsuji *et al.*, 2006; Aya *et al.*, 2009) suggest that *GAMYB* is upstream of a signalling cascade which commits the tapetum to PCD (see section 1.3.2). One such TF, *OsC6* is a Cysteine protease known to be involved in PCD and contains a *GAMYB*-binding element in its promoter region (Li *et al.*, 2006a; Aya *et al.*, 2009; Plackett and Wilson, 2016).

Tsuji *et al.*, (2006) hypothesised that *GAMYB* aleurone/tapetum specific function is achieved via interaction between *GAMYB* and other differentially expressed transcription factors to activate distinct downstream targets. MYB proteins have been shown to form a transcriptional complex with bHLH and WD-repeat transcription factors which are directly regulated by GA and JA signalling components during trichome formation (Qi *et al.*, 2011; Tian *et al.*, 2016). The ability of MYB proteins to form hormonally regulated complex with bHLH transcription factors may be relevant to the role of *GAMYB* in tapetum PCD as a number of bHLHs have been implicated in the initiation of PCD via direct interactions with aspartic protease gene promoters (Niu *et al.*, 2013)

The accumulation of cell damaging reactive oxygen species (ROS) in both the tapetum and aleurone is also thought to contribute to the initiation of PCD (Ishibashi *et al.*, 2012; Zhang and Yang, 2014; Yi *et al.*, 2016) A burst of ROS is observed in tapetal cells at the initiation of PCD and loss of *DEFECTIVE TAPETUM CELL DEATH 1 (DTC1)*, a TF downstream of the *TDR/UDT/EAT1* bHLH

cascade (see section 1.3.2.) which regulated ROS-scavenging activity, resulting in failure to initiate tapetum PCD and microspore abortion (Hu *et al.*, 2011; Yi *et al.*, 2016) as seen in *gamyb* mutants. DELLAs and ABA promote the expression of ROS-scavenging enzymes and GA induces their production in aleurone cells (Achard *et al.*, 2008; Ishibashi *et al.*, 2012; Kocheva *et al.*, 2014; Aoki *et al.*, 2014), suggesting that GAMYB could bring about PCD through the upregulation of ROS producing enzymes. However, ROS instead appear to be a GA-inducible signalling molecule which promote GAMYB expression in aleurone cells prior to PCD rather than the executors of it themselves (Ishibashi *et al.*, 2012). It therefore remains unclear what link, if any, there is between GAMYB and ROS in the induction of PCD.

1.4.4. GA controls multiple aspects of male reproductive development

The genetic signalling network governing anther development (see section 1.3.2.) is subject to regulation by hormone signalling (Chandler, 2010). Gibberellin signalling in particular is critical to anther and pollen development and exerts control over tapetum PCD via the TF GAMYB (see section 1.4.3.). Furthermore, GA has been shown to regulate the expression of hundreds of anther specific genes in developing anthers via DELLA (Hou *et al.*, 2008). Numerous GA-biosynthesis and signalling mutants have further revealed some information about the developmental processes regulated by GA, however, the precise mechanisms through which GA regulation controls anther development are not well understood.

The *Arabidopsis* and rice GA-deficient mutants (*ga1-3* and *Oscps1-1* respectively) fail to complete pollen development beyond the uninuclear microspore stage apparently due to disruption of the tapetum (Cheng *et al.*, 2004; Aya *et al.*, 2009). A complex picture of the GA-biosynthesis regulation in anthers is emerging; single enzyme, early biosynthesis pathway mutants are severely dwarfed and infertile whereas the partial functional redundancy and specificity within multigene families encoding downstream steps results in variable, semi-fertile phenotypes (Rieu *et al.*, 2007; Plackett *et al.*, 2012).

GA20OX and *GA3OX* family member expression has been reported in the tapetum prior to its degradation and PMCs during meiosis, supporting the observed points of developmental arrest seen in mutant phenotypes (Hu *et al.*, 2008; Chandler, 2010; Plackett *et al.*, 2012). Like *ga1-3*, *Atga20ox* triple mutants are also male sterile but pollen cells appear to progress beyond the uninuclear stage and sterility is instead attributed to failure of the tapetum to undergo PCD (Plackett *et al.*, 2012). Clearly there is functional significance to the location and timing of GA-biosynthesis in the developing anther, especially in relation to tapetum PCD and PMC meiosis which is currently not well understood.

Signalling mutants demonstrate a range of phenotypes; *gid1* mutants fail to undergo differentiation between stamen and filament tissue resulting in a mechanical barrier to fertilisation (Griffiths *et al.*, 2006), whilst *DELLA* loss-of-function mutants in GA-deficient background show varying degrees of reduced filament extension and post-meiotic microspore abortion (Wen and Chang, 2002; Cheng *et al.*, 2004; Plackett *et al.*, 2014). However, in most early studies spontaneous recovery and maintenance of basal levels of fertility was observed in *DELLA* mutants in the *Ler Arabidopsis* background. Plackett *et al.*, (2014) demonstrated that *DELLA* mediated GA-signalling is required to maintain male fertility in the *Col-0* background; in *rga-28.gai-td1* mutants male fertility was completely abolished due to post-meiotic developmental defects. Reintroduction of a functional *DELLA* could restore pollen development to these mutants and the observation that its expression in either the microspores or tapetum cell layer could reinstate fertility supports the hypothesis that the role of *DELLA*s in anther development may be to ensure synchrony between microspore and tapetum development (Plackett *et al.*, 2014).

DELLA mutants demonstrate that GA-signalling is dependent upon functional domains within the protein. Semi-dwarf wheat varieties associated with the green revolution (see section 1.1.) carry an in-frame premature stop codon mutation in the N-terminal domains of *Rht-B1* or *Rht-D1* which abolished

binding with GID1, resulting in GA-insensitivity (Peng *et al.*, 1999; Pearce *et al.*, 2011). It is hypothesised that transcriptional re-initiation after the N-terminal stop codons creates a truncated RHT-1 protein which lacks the domains required for GA-mediated degradation but retains C-terminal domains which repress the expression of growth promoting genes (Pearce *et al.*, 2011). In comparison, mutations in the C-terminal coding region of DELLA genes result in a “slender” phenotype which are hypersensitive to GA and lack the ability to repress growth promoting gene expression (Ikeda *et al.*, 2001; Chandler *et al.*, 2002; Chandler and Harding, 2013). However, there are no further reports upon the specific effect of *Rht-1* mutations on male fertility.

1.5. Anther hormonal signalling responses to HT-stress

HT-stress responses during anther and pollen development have been shown to involve several hormone signalling pathways. Indeed, a complex network of crosstalk between hormone and secondary metabolic signals elicits the physiological and genetic responses seen in HT-injured anthers (Parish *et al.*, 2013; Müller and Rieu, 2016) (Fig. 1.10.), however the significance of many individual components remains unclear.

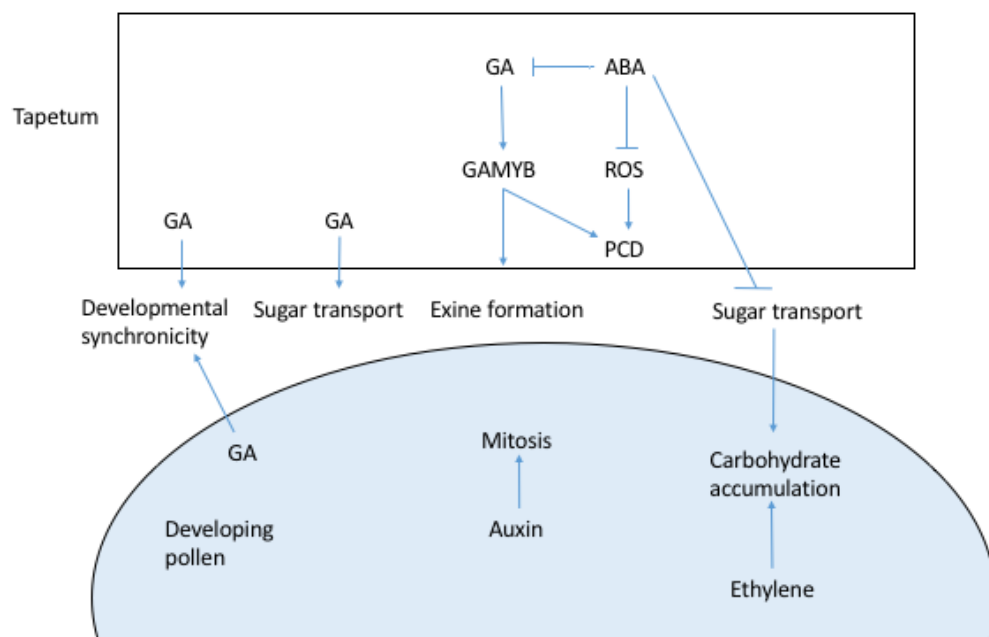


Figure 1.10. Hormonal regulation of anther HT-defects. *Common anther and pollen HT-induced defects are under the regulation of hormone signalling*

pathways. GA-signalling is required for correct tapetum PCD, pollen exine formation and developmental synchronicity between tapetum and pollen cells, all of which are perturbed by HT-stress. ROS may contribute to PCD either by causing oxidative damage or as secondary signalling molecules. GA and ABA have characterised roles in ROS-homeostatic regulation. Carbohydrate transport and uptake via invertase proteins is antagonistically regulated by GA and ABA and modulated by ethylene under HT. Auxin is required for pollen cell mitosis which is also negatively affected by HT. (Adapted from Müller and Rieu, 2016).

The overall effect of HT-stress during male reproductive development of self-fertilising plants is to reduce yield by inhibiting the formation of viable pollen (see section 1.1.1.). Numerous physiological symptoms of HT-stress in the anther have been observed under varying experimental conditions but which of these are the primary causes of infertility is yet to be established (Müller and Rieu, 2016). However, the most common anther developmental defects (premature tapetum PCD, aberrant microspore nuclear division and disrupted sugar metabolism) to some extent all involve hormone signalling pathways.

1.5.1. GA-signalling in anther HT-responses

The role of GA in ensuring the correct timing of tapetum PCD (see section 1.4.3.) and the hastening of PCD by HT suggest that the tapetum GA-signalling pathway may be involved in HT responses. Indeed, downregulation of tapetum-specific GAMYB-responsive genes during HT-stress has been reported in rice (Endo *et al.*, 2009) whilst the *Osgamyb-1* mutant phenotype is enhanced at higher temperature (Kaneko *et al.*, 2004). Anther GA concentration declines under HT conditions (Tang *et al.*, 2007), perhaps explaining the increased frequency of *Osgamyb-1* phenotypes and downregulation of GAMYB targets. Without further information about *GAMYB* expression under HT or the downstream mechanisms through which *GAMYB* elicits PCD, it's unclear whether HT-induced premature PCD is a direct consequence of HT-effects in *GAMYB* function.

HT-stress occurring post-meiosis adversely affects the transport of carbohydrates to young microspores (Firon *et al.*, 2006, De Strome and Geelen, 2013) instead resulting in an accumulation of soluble sugars in the locular fluid (Pressman *et al.*, 2002). In drought stressed plants, tapetum and microspore invertases, which cleave hexose units from sucrose, are specifically down-regulated by ABA (Oliver *et al.*, 2005; Ji *et al.*, 2011). GA promotes the expression of tomato invertase *Lin7* in both the tapetum and microspores (Proels *et al.*, 2006). In the aleurone, a similar secretory tissue type, GAMYB is required for the mobilisation of carbohydrates (see section 1.4.1.). During germination and seedling growth GA promotes the co-nuclear import of a GAMYB/sugar-responsive MYBS1 complex and enhances their binding to α -*amylase* promoter GAREs (Hong *et al.*, 2012), whilst under conditions of abiotic stress, ABA, the GA-antagonist, promote the sequestration of MYBS1 in the cytoplasm (Lin *et al.*, 2014). Whether changes to anther carbohydrate metabolism are mediated via *GAMYB* has not been resolved, although the downregulation of one hexokinase, a sugar metabolic regulator, has been reported in *gamyb* anthers (Tsuji *et al.*, 2006).

After exposure to 39/30 °C day/night at the microspores stage, rice pollen grains appear normal but fail to adhere to and germinate on receptive styles (Endo *et al.*, 2009), showing that HT at this stage prevents pollen exine from developing correctly. *GAMYB* is known to contribute to the development of Ubisch bodies which are required for the correct deposition of sporopollenin on the exine through upregulation of tapetum lipid metabolism genes *CYP703A3* and *KAR* (Aya *et al.*, 2009) (see section 1.4.3.). It is not yet known if the malformation of the pollen coat is due to disruption of tapetal or microspore function or premature collapse of tapetum cells before sporopollenin deposition is complete.

Many modern wheat varieties have GA sensitivity reduced by the presence of *Rht-1* alleles (see section 1.1.), which might be expected to affect response to anther HT. Given the effect of *gamyb* and *gid-1* signalling mutations on tapetum function and PCD, the constitutive repression of *GAMYB* in GA-

insensitive *Rht-1* plants may affect their response to HT-stress. Indeed, Law and Worland, (1984) demonstrated an increase in susceptibility to HT during reproductive development associated with GA-insensitivity in *Rht-1* allele carrying lines. However, this effect has found to also depend heavily on water status and genetic background, making a strong link between GA-sensitivity and male reproductive vulnerability to HT difficult to establish (Alghabari *et al.*, 2014).

On the other hand, DELLAs have been shown to promote stress tolerance by restraining the accumulation of ROS (Achard *et al.*, 2008; Colebrook *et al.*, 2014). Wheat DELLA mutants carrying the *Rht-B1b* and *Rht-B1c* mutations are more able to suppress osmotic stress-induced ROS damage, presumably through constitutive expression of ROS-scavenging genes (Achard *et al.*, 2008; Kocheva *et al.*, 2014). A short-lived burst of ROS occurs in tapetum cells prior to PCD which is brought about through genetic regulation (Hu *et al.*, 2011; Xie *et al.*, 2014; Yi *et al.*, 2016). Damage caused to tapetum mitochondrial membranes by ROS may contribute to the initiation and execution of PCD (Parish and Li, 2010). Alternatively they may act as secondary signals which enhances the execution of PCD via other pathways; ROS production in the barley aleurone is promoted by GA but does not contribute to PCD, instead appearing to act as a GAMYB upregulating signal (Ishibashi *et al.*, 2012; Aoki *et al.*, 2014).

1.5.2. Other hormone signalling pathways in anther HT-responses

Anther ABA levels increase and IAA levels decrease in rice in response to HT (Tang *et al.*, 2014,). HT represses the expression of auxin biosynthesis *YUCCA* genes in barley and *Arabidopsis* and is associated with a further down-regulation of auxin-promoted DNA replication genes (Oshino *et al.*, 2011, Higashitani *et al.*, 2013). Application of exogenous auxin to barley ears prior to HT was sufficient to reverse male sterility (Sakata *et al.*, 2010), suggesting that auxin depletion is an HT-effect rather than an acclimation response (Müller and Rieu, 2016). Auxin accumulates in anthers after PMC meiosis and is required for microspores to undergo mitosis (Feng *et al.*, 2006). Failure to progress beyond

mitosis I is a common observation in HT-treated anthers along with downregulation of auxin-responsive nuclear and organellar DNA-proliferation (Oshino *et al.*, 2011).

Carbohydrate metabolism also links ethylene signalling to anther HT-responses. HT-induces the expression of an ethylene biosynthesis and signalling transcripts in tomato pollen and ethylene-insensitivity increases HT-sensitivity and reduced pollen sucrose accumulation (Firon *et al.*, 2012). A cotton casein kinase (*GhCK1*) which inhibits starch synthase activity is induced in anthers by HT (Min *et al.*, 2013). Overexpression of *GhCK1* down-regulates starch synthase activity. The resultant increase in glucose in early-stage anthers promotes the accumulation of ABA which disrupts ROS homeostasis causing premature tapetum PCD (Min *et al.*, 2013). Conversely, in a HT-sensitive cotton line, HT results in a decline in anther glucose levels and increased auxin accumulation in later stage anthers (Min *et al.*, 2014). The authors hypothesise that in the HT-sensitive lines, auxin biosynthesis is regulated by soluble sugars via PIFs, which have previously been shown to upregulate auxin biosynthesis under HT (Franklin *et al.*, 2011) and interact with DELLAs (de Lucas *et al.*, 2008) (see section 1.4.), demonstrating a potential hormonal crosstalk mechanism in HT-response regulation involving GA, auxin and ABA.

It is likely that the overlapping roles and crosstalk between hormones during anther development and in response to HT will require any approach to improving fertility under HT to consider the “fine balance” of all components rather than individual hormones in isolation.

1.6. Aims and objectives

The sensitivity of wheat anther development to HT is an issue with potential ramifications for global food security in the near future (See section 1.1.1.). Much work has been done in model species to understand the hormonal and genetic signalling networks which control reproductive development the effects of HT upon them (see section 1.5.). With the publication of a high-coverage reference genome (IWGSC., 2014), the powerful tools of modern

functional genomics can now be applied to wheat. This project aims to begin the process of translating the understanding of reproductive development in rice and barley into wheat with a view to identifying potential targets for improving anther and pollen HT-tolerance.

As described above, it is clear that GA-signalling is crucial to male reproductive development and many of the processes it regulates, particularly tapetum PCD and pollen exine formation, are common HT-induced defects. This project will therefore seek to identify important genetic components involved in wheat anther and pollen development downstream of *Rht-1* and investigate the response of anther hormone and genetic signalling to HT-stress. To achieve this there are three main aims of this project:

1. Develop procedures for non-destructive staging of wheat anther development.
2. Identify and characterise wheat orthologues of *OsGAMYB* and *OsEAT*, potential GA-signalling components in tapetum function and PCD
3. Use whole transcriptomic and global hormone profiling approaches to characterise the response of wheat anthers to HT-stress.

CHAPTER 2: GENERAL MATERIALS AND METHODS

2.1. Plant Material and Growing Conditions

Triticum aestivum cv. Cadenza, a spring variety, was used for all molecular, physiological, TILLING and transformation experiments unless otherwise stated. Plants were grown in 13 cm diameter plastic pots also containing Rothamsted prescription mix compost (75% peat, 12% sterilised loam, 3% vermiculite, 10% grit). Controlled environment (CE) growth conditions in rooms and cabinets were 20 °C/15 °C day/night temperatures under 16 hour photoperiods provided by tungsten fluorescent lamps providing 500 $\mu\text{molm}^{-2}\text{s}^{-1}$ PAR unless otherwise specified. Irrigation and relative humidity was maintained at 65 %/75 % day/night in all experiments. Standard glasshouse conditions used the same pots and compost mixture. Temperature was maintained at 18-20 °C day and 14-15 °C night under a 16 h photoperiod using natural light supplemented with 400-1000 500 $\mu\text{molm}^{-2}\text{s}^{-1}$ PAR from SON-T sodium lamps.

2.2. Molecular biology

2.2.1 DNA Extraction

Approximately 1 g of young leaf tissue (GS13) was freeze dried and ground into a fine powder using a GenoGrinder (SPEX SamplePrep, Metuchen, New Jersey, U.S.A.). The homogenate was incubated in 1 ml PVP-extraction buffer (pH 9.5) at 65 °C for 1 hour. Extraction buffer contained 1.2% w/v Trizma base, 7.5% w/v potassium chloride, 2% v/v 0.5M EDTA, 0.75% w/v polyvinylpyrrolidone and 0.36% w/v sodium bisulphate. All reagents manufactured by Sigma-Aldridge, St. Louis, Missouri, U.S.A. 333 μl 5 M Potassium acetate (pH 5.8) was added to each sample before spinning in a bench microfuge for 2 minutes to pellet tissue debris at the bottom of the tubes. 1 ml of cleared supernatant was transferred to fresh tubes and 500 μl pre-chilled isopropanol was added, mixed and allowed to incubate at room temperature for 10 minutes. Samples were spun at 13,000 rpm for 10 minutes

after which supernatant was discarded. Pelleted gDNA was washed in 500 μ l 70% ethanol, spun briefly and allowed to dry at room temperature. gDNA was resuspended in 200 μ l TER buffer (containing Pancreatic RNase), incubated at 50 °C for 1 hour and stored overnight at 4 °C. gDNA was quantified using a Nanodrop™ ND-1000 spectrophotometer (LabTech International Ltd, U.K.).

2.2.2 Polymerase Chain Reaction

PCR conditions vary depending upon primer, target, template properties and downstream purpose of product. For general genotyping GoTaq® Flexi DNA polymerase (Promega, Madison, Wisconsin, U.S.A.) was used to amplify target sequences in 20 μ l reactions consisting of:

| | |
|--|---------------|
| 5X reaction buffer (7.5 mM MgCl ₂) | 6 μ l |
| dNTP mix (10 mM) | 0.5 μ l |
| Forward primer mix (10 μ M) | 0.5 μ l |
| Reverse primer mix (10 μ M) | 0.5 μ l |
| Distilled, purified H ₂ O | 11.35 μ l |
| DNA polymerase | 0.15 μ l |
| Template DNA | 1 μ l |

Reactions were carried out in a DNA Engine Tetrad 2 thermal cycler (Bio-Rad Laboratories, Hercules, California, U.S.A.) using the following standard conditions:

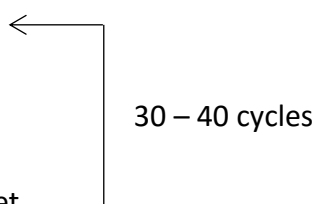
98 °C 5 minutes

97 °C 30 seconds

55-70 °C 30 seconds

72 °C 1 minute/kb target

72 °C 6 minutes



4 °C Hold

Where synthesised product was intended for cloning, a high-fidelity proofreading Phusion[®] High-Fidelity DNA Polymerase (New England Biolabs UK Ltd, Hitchin, U.K.) was used. Reactions were 20 µl in volume and proceeded as follows:

| | |
|--------------------------------------|---------|
| 5X Phusion GC Buffer | 4 µl |
| dNTP mix (10 mM) | 0.4 µl |
| Forward primer mix (10 µM) | 1 µl |
| Reverse primer mix (10 µM) | 1 µl |
| Distilled, purified H ₂ O | 14.4 µl |
| Phusion DNA polymerase | 0.2 µl |
| Template DNA | 1 µl |

PCR cycling conditions:

98 °C 1 minute

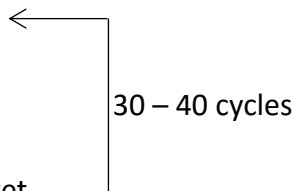
98 °C 10 seconds

55-70 °C 30 seconds

72 °C 1 minute/kb target

72 °C 6 minutes

4 °C Hold



2.2.3 Agarose Gel Electrophoresis

Completed PCR reactions were mixed with 1X Loading Dye containing bromophenol blue and xylene cyanol FF, (Thermo Scientific, Hemel Hempstead, U.K.) (Phusion reactions only) and run on TBE-buffered (45 mM Tris-borate, 1 mM EDTA, pH 8.3) 1-2 % (w/v) agarose gel (Fisher Scientific,

Loughborough, U.K.) containing 0.5 µg/µl Ethidium bromide. 1 kb GeneRuler™ DNA ladder or 100 bp DNA ladder (Thermo Scientific, Hemel Hempstead, U.K.) was run alongside products to assist band size estimation. Electrophoresis was usually carried out at 100 mV for 35 minutes. PCR products were visualised by ethidium bromide fluorescence under UV excitation using SynGene GelDoc imaging equipment (Synoptics Ltd, Cambridge, U.K.).

2.2.4 Extraction and Purification of PCR Products from Agarose Gel

Gel fragments containing amplified DNA products were excised from agarose gel under UV light and purified using the QIAquick® Gel Extraction kit (QIAGEN, Hilden, Germany) according to the manufacturer's instructions.

2.2.5 Primer Design

PCR primers were designed using Primer3Plus online interface (Untergasser *et al.*, 2007) and its respective plugin interface in Geneious (v. 8.1.3, Biomatters Ltd, Auckland, New Zealand). Optimal primer conditions were set to T_m 58 - 62 °C, GC content 50 - 60 % and 18 - 24 bp in size. Primer target specificity was analysed using the Basic Local Alignment Tool (BLAST) against the IWGSC1+popseq wheat genome assembly (IWGSC, 2014; Chapman *et al.*, 2015) on the EnsemblPlants online genome browser (EMBL-EBI, Hinxton, U.K.).

The following primers were used in this project:

| Primer name | Sequence | Tm °C | Purpose |
|-----------------|-----------------------------------|-------|------------------------|
| qGAMYB_RNAi_F1 | GGAGCTCCCTCACTCCAAG | 61.4 | qRT-PCR |
| qGAMYB_RNAi_R1 | TTCCAAGAGACCGCTGTTC | 59.4 | qRT-PCR |
| qTabHLH_RNAi_F1 | ATGTTGCAAGGTTCTTGATG | 57.3 | qRT-PCR |
| qTabHLH_RNAi_R1 | GGTTGGAAGTGTCCGGAGGAG | 61.4 | qRT-PCR |
| TaActin_F | CCTCTCTGCGCCSSTCGT | 58.2 | qRT-PCR |
| TaActin_R | TCAGCCGAGCGGAAATTGT | 59.4 | qRT-PCR |
| bHLH_BamHI_R | TTGGATCCTTTCATCCTCAACTG | 65.1 | RNAi cloning |
| bHLH_BglII_F | AAAGATCTACAGGAGTGGCAGCA | 66 | RNAi cloning |
| GAMYB_BamHI_R | TTHHATCCTAGTCCCTGAGCTT | 65 | RNAi cloning |
| GAMYB_BglII_F | AAAAGATCTATAGCTGGCTAAG | 59.6 | RNAi cloning |
| AdH_F1 | CCTTCTGGCGGCTTATCTG | 62.1 | Sequencing |
| Nos_R1 | AAGACCGGCAACAGGATTCA | 62.9 | Sequencing |
| Nos_R2 | CGGCCGCGATCTAGTAACAT | 59.4 | Sequencing |
| OsAct_F1 | GTGACAAATGCAGCCTCGTG | 59.4 | Sequencing |
| MzeADHlnF3 | TCTAATCAGCCATCCATTTGTG | 58.9 | TaqMan Zygosity |
| MzeADHlnR3 | GGAGTCTGCCCCTAAGACAGATAA | 62.7 | TaqMan Zygosity |
| MzeADHlnP | Fam-AACAACCTCGCGTTGACTTGCGC-Tamra | 67.5 | TaqMan Zygosity |
| HvCon2F1 | TGCTAACCGTGTGGCATCAC | 59.4 | TaqMan Zygosity |
| HvCon2R1 | GGTACATAGTGTGCTGCATCTG | 62.4 | TaqMan Zygosity |
| HvCon2P | VIC-CATGAGCGTGTGCGTGTCTGCG-TAMRA | 71.1 | TaqMan Zygosity |
| 106_GAMYB_B_F | TCAGTAAATCGGAGTGTGC | 57.3 | TILLinG |
| 106_GAMYB_B_R | CAGGAGAAAAGTTTGAGAGCTG | 60.3 | TILLinG |
| 317_GAMYB_D_F | ATTTCTCAAAAAGACTGTACTACA | 57.4 | TILLinG |
| 317_GAMYB_D_R | AGGAAGAAATCATGCAAGGCT | 55.9 | TILLinG |
| 664_GAMYB_A_F | CCGACCCATTGAAAAATAG | 55.3 | TILLinG |
| 664_GAMYB_A_R | CTCGCCGAGTTGAAATCG | 58.8 | TILLinG |
| Rht-D1_GRAS_F1 | ATGGATCCCCGCGTGCCTGCTG | 84.3 | Yeast 2-Hybrid cloning |
| Rht-D1_GRAS_R1 | ATGATATCACGGCCCCGCGAGGCG | 81.2 | Yeast 2-Hybrid cloning |
| TaHLH141_F1 | ATCCATGGTCATGATTGTTGGAGGTGACTAT | 73.2 | Yeast 2-Hybrid cloning |
| TaHLH141_F2 | GGATGAGCAAGACAATCAGCT | 63.3 | Yeast 2-Hybrid cloning |
| TaHLH141_R1 | ATCTCGAGCTAGTTGAATATGCAAGTGCC | 70.2 | Yeast 2-Hybrid cloning |

Table 2.1. PCR primers, oligonucleotide sequences, predicted melting temperatures and experimental purpose.

2.2.6 PCR Product Sequencing

Purified DNA was sent pre-mixed with appropriate sequencing primers to Eurofins Genomics (Wolverhampton, U.K.). Reading and alignment of DNA and amino acid sequences were carried out using Geneious (v 8.1.3, Biomatters Ltd, Auckland, New Zealand).

2.2.7 DNA Cloning and Modification

Purified DNA fragments, amplified using proof-reading Phusion[®] (New England Biolabs UK Ltd, Hitchin, U.K.) polymerase, were cloned into vectors in 10 µl ligation reactions in which insert and vector were present at a molar ratio of 3:1 respectively. The ligation reaction was mixed with 1 µl T4 DNA Ligase (5u/µl) and 1X T4 DNA ligase buffer (Promega, Madison, Wisconsin, U.S.A.) and incubated at room temperature for one hour. Self-ligation of cut

vector was reduced by treatment with calf intestinal alkaline phosphatase (CIAP) (Invitrogen) which removes 5' phosphate groups. 1 µl CIAP (10 u/µl) was used in 10 µl reactions with 1X CIAP buffer (Invitrogen, Carlsbad, California, U.S.A.) which were incubated at 37 °C for one hour. Inactivation of CIAP required 15-minute incubation at 65 °C.

Blunt-ended PCR fragments - amplified using proof-reading polymerase - were ligated into the blunt cloning vector pSC-B (Stratagene, San Diego, California, U.S.A.). Plasmids were transformed into SoloPack competent cells (Stratagene, San Diego, California, U.S.A.) by heat shock and plated onto 2YT plates supplemented with 0.01 mg/ml X-Gal and 0.1 mg/ml carbenicillin. Positive transformants were selected using blue-white screening.

The following plasmids and their selection methods were used in this project:

| Plamid | Selection | Purpose |
|-------------------------|--------------------------------|---------------------------------------|
| pSC-b | Carbenicillin, <i>LacZ</i> | Blunt-end PCR product cloning |
| pRRes::HMW::AdH::Nos | Carbenicillin, | RNAi expression sub-cloning |
| pENTR-11 Dual Selection | Chloramphenicol, Kanamycin | Yeast 2-Hybrid sub-cloning |
| pDEST-22 | Carbenicillin, Chloramphenicol | Yeast 2-Hybrid Prey expression vector |
| pDEST-32 | Chloramphenicol, Gentamicin | Yeast 2-Hybrid Bait expression vector |

Table 2.2. Plasmids and their respective selection methods used for cloning and transformation in this project.

2.2.8. Bacterial strains used

Routine cloning and amplification of plasmid was carried out using chemically competent cells of the Escherichia coli bacterial strain DH5α (ϕ 80dlacZΔM15, recA1, endA1, gyrAB, thi-1, hsdR17(rK-, mK+).

Competent bacterial cells were produced according to Inoue et al., (1990). Cells were cultured on Luria-Bertani (LB) plates containing 1.5% (w/v) agar and incubating overnight at 37°C. Twelve colonies were added to 250 ml of sterile SOB media (0.5% (w/v) yeast extract, 2% (w/v) tryptone, 10mM NaCl, 2.5mM KCl, 10mM MgCl₂, 10mM MgSO₄ (pH 7.0)) in a 1 litre flask and cultured at 19°C to an OD₆₀₀ of 0.5 – 0.6. The flask was then chilled on ice for 10 minutes and cells pelleted by centrifuging at 2500 g for 10 minutes at 4°C.

The cell pellet was re-suspended in 80 ml ice-cold TB solution (10mM PIPES, 15mM CaCl₂, 250mM KCl, 55mM MnCl₂, pH 6.7 and 1.4 ml dimethyl sulphoxide (DMSO) and stored on ice for a further 10 minutes. Cells were pelleted once more by centrifuging at 2500 g for 10 minutes at 4°C and re-suspended in 20 ml TB solution. Cells were dispensed into 50 µl aliquots and immediately frozen in liquid nitrogen before storing at -80°C.

StrataClone SoloPack (Stratagene, San Diego, California, U.S.A.) competent cells (Tet^r. Δ(mcrA)183 Δ(mcrCB-hsdSMR-mrr)173, *endA1*, *supE44*, *thi-1*, *recA1*, *gyrA96*, *relA1*, *lac*, Hte [F'*proAB*, *lacI^qΔM15*, Tn10, (Tet^r), Amy, Cam^r]) were used for blunt-end cloning with pSC-b

2.2.9. E-coli transformation

Plasmids were transformed into competent DH5α *E. coli* cells by incubation on ice for 45 - 60 minutes followed by a 42 °C heat shock for 45 seconds and 2-minute incubation on ice. 500 µl SOC media (20 g/l Bacto-tryptone, 5 g/l Bacto-yeast extract, 0.5 g/l NaCl, 20 mM glucose, 2.5 mM KCl, 10 mM MgCl₂ pH 7.0) was added and then incubated at 37 °C rotating at 180 rpm for 1 hour. Reaction mixture was plated on 2YT agar plates (16 g/l Bacto-tryptone, 10 g/l Bacto-yeast extract, 5 g/l NaCl, 1.5% (w/v) agar pH 7.0) supplemented with 0.1 mg/ml carbenicillin and 0.01 mg/ml X-Gal to allow positive selection and identification of transformants by blue/white screening. Plates were incubated overnight at 37 °C.

Single, positive transformant colonies were picked and cultured overnight at 37 °C in 5 ml SOC media supplemented with 0.1 mg/ml carbenicillin. Purified plasmid DNA was obtained from the culture using the QIAprep Plasmid Mini Kit (QIAGEN, Hilden, Germany) as per the manufacturer's instructions. Confirmation of fragment insertion was then obtained by appropriate restriction enzyme digestion and subsequent sequencing using the M13 or custom sequencing primers (Eurofins Genomic, Wolverhampton, UK).

Alternatively, colony-PCR was used to select positive transformants. Single colony plaques were nicked with a sterile toothpick and used as the template in standard GoTaq PCR for genotyping.

2.2.10. Yeast strains used

Colonies of yeast strain MaV203 were streaked from glycerol stock onto YPED agar plates (20 g/L Peptone, 10 g/L yeast extract, 5 g/L ammonium sulphate, 1.8 % [w/v] agar) and grown at 30 °C for three days. Single colonies were selected and cultured overnight in YPED broth at 30 °C at 160 rpm rotation until the culture reached OD₆₀₀ 1 - 1.5. Cells were harvested by centrifugation at 8,000 rpm for 10 seconds and washed twice with TE buffer and resuspended in 0.1 M LiAC followed by incubation at 30 °C for 1 hour rotating at 160 rpm. 50 µl aliquots were stored at -80 °C.

2.2.11. Gateway cloning for yeast expression

Yeast expression plasmids were cloned using the Gateway® LR reaction as described by the manufacturer (Invitrogen, Carlsbad, California, U.S.A.) as follows:

In a 1.5 µl microfuge tubes mix:

| | |
|-----------------------------|------|
| pENTR-11::GOI (50 - 150 ng) | 1 µl |
| Destination vector (150 ng) | 1 µl |
| TE Buffer (pH 8) | 6 µl |
| LR Clonase II | 2 µl |

The reaction was mixed by vortexing and incubated at room temperature for at least 1 hour. The reaction was terminated by the addition of 1 µl Proteinase K solution and incubation at 37 °C for 10 minutes. The expression clones were then transformed, cultured and purified from *E. coli* as described above

For Yeast 2-Hybrid interaction assays, bait and prey plasmids were cloned, amplified and tested using the ProQuest™ Two-Hybrid System (Invitrogen, Carlsbad, California, U.S.A.) as per the manufacturer's instructions. Co-transformation of yeast cells with bait and prey expression vectors proceeded by mixing 1 µg of each plasmid with 150 µl of competent yeast cells, 350 µl 50 % PEG3350 and 1 µl salmon sperm. The reaction mixture was mixed by inversion and incubated at 30 °C for 1 hour. Cells were then heat shocked at 42 °C for 30 minutes. 200 µl of this reaction mix was plated on SD Agar plates supplemented with -Leu -Trp/-His mixture for positive selection of *His3* reporter gene expression. To confirm interactions, replica plating of master plates on to SC-Leu-Trp-His plates containing 5 mM, 10 mM, 20 mM, 30 mM, 40 mM and 50 mM 3--Amino-1,2,4-Triazole to test *HIS3* induction

2.2.12. Restriction enzyme digests

Restriction enzyme digests were carried out in 20 µl volumes consisting of 1 µl total restriction enzyme(s) (10-12 units), 2 µl of the appropriate buffer, 0.2 µl Bovine Serum Albumen, the required volume for 1 µg of plasmid DNA and the remaining volume made up with sterile, distilled water. Enzymes and associated reagents were manufactured by Promega, Madison, Wisconsin, U.S.A. Incubation was carried out as specified by the enzyme manufacturer. Where double digestion was not possible a sequential digest was performed. Cut plasmid was purified after digestion with the first enzyme using the QIAgen PCR Purification Kit (QIAgen, Hilden, Germany) as described by the manufacturer. Eluted plasmid was then subjected to digestion by the second enzyme and fragments separated and purified from agarose gel electrophoresis as described above.

2.3. Quantitative reverse-transcription PCR

2.3.1 Extraction of RNA

Tissue samples were harvested and flash-frozen using liquid nitrogen prior to storage at -80 °C. Samples were ground to a fine powder using pre-cooled

stainless steel ball bearings in a TissueLyser (QIAgen, Hilden, Germany). RNA was extracted from ground tissue samples (in most cases >100 mg) using the RNeasy Extraction Kit (QIAgen, Hilden, Germany) in accordance with the manufacturer's instructions. This included the incorporation of the on-column DNase I protocol to remove DNA contamination. A modified DNase incubation step was used in which 80 µl of the DNase/RDD buffer solution was added to the column and allowed to incubate for 1 hour at 37 °C after which a further 80 µl was added and allowed to incubate at 37 °C for an additional hour. Alternatively, 10 µg of eluted RNA (as determined by NanoDrop (LabTech International Ltd, U.K.) quantification) was treated with Turbo DNase (Invitrogen, Carlsbad, California, U.S.A.) as per the manufacturer's instructions. RNA quality and accurate quantification was carried out on an Agilent Bioanalyser 2100 using Agilent RNA 6000 Nano Reagent Kit (Agilent, Santa Clara, California, U.S.A.) according to the manufacturer's instructions. DNase treated RNA samples were stored at -80 °C.

2.3.2. cDNA Synthesis

cDNA was synthesised from 1 µg total RNA (samples were normalised to 100 ng/µl) using the SuperScript III First Strand Synthesis System for Reverse-Transcriptase PCR with an Oligo dT₍₂₀₎ primer (Invitrogen, Carlsbad, California, U.S.A.). The modified protocol for First Strand Synthesis of Transcripts with High GC content included in manufacturer's online instructions was used. cDNA samples were stored at -20 °C.

2.3.3. Quantitative Reverse-Transcription PCR

qRT-PCR was carried out using the ABI 7500 Real Time PCR System (Applied Biosystems, Foster City, California, U.S.A.) using the cDNA equivalent of 1 µg diluted by a factor of 1.5. 20µl reactions were prepared as follows:

SYBR Green Master Mix (0.2 % ROX) 10 µl

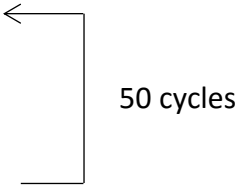
Primer mix (250 nM / primer) 5 µl

cDNA 5 µl

PCR conditions were:

95 °C 10 minute

95 °C 1 minute
59-61 °C 30 seconds
72 °C 1 minute



50 cycles

Dissociation curve

Non-RT control samples (cDNA synthesis mixture minus Reverse Transcriptase) corresponding to cDNA samples were also tested to assess the level of genomic DNA contamination of cDNA samples. Amplification of target genes was assessed by measurement of reaction well fluorescence during the 72 °C elongation step of each cycle. Genomic DNA contamination, non-specific amplification and primer-dimer formation was assessed by visual inspection of reaction well dissociation curves.

2.3.4. Data Analysis

Ct and Rn (cycle fluorescence) values for each reaction were obtained using ABI 7500 software (v2.0.5). Primer efficiencies for each reaction were calculated using LinRegPCR software (v12.3 (Ruijter *et al.*, 2010)). All qRT-PCR reactions were carried out in duplicate for three replicates of each biological sample. Ct values were normalised using the following equation:

$$NE = \text{Primer Efficiency}^{-Ct}$$

Normalised relative expression (NRQ) of target genes were then determined:

$$\text{Target NRQ} = \text{Target NE} \div \text{Reference NE}$$

The mean NRQ value across the biological replicates and its respective standard error was then calculated.

2.4. Generation of transgenic plants

2.4.1. Cloning of wheat RNAi vectors

RNAi trigger constructs were cloned using the HWM::AdH::Nos modular sub-cloning system developed by Drs Hutley and Vaughan at Rothamsted Research, U.K. which takes advantage of cross-compatibility between *BglIII* and *BamHI* restriction sites.

Short fragments of target sequences were amplified by PCR using Phusion *Taq* and another cDNA template. Forward and reverse primers with 5' *BglIII* and *BamHI* extensions respectively were used. The amplified products were gel extracted and purified before being blunt sub-cloned into the pSC-b amp/kan holding vector and transformed into DH5 α *E. coli* competent cells.

The transformation mixture was plated on selective agar plates containing 1 mg/ml carbenicillin (ampicillin analogue). Transformant colonies were selected and cultured overnight in SOC broth also containing 1 mg/ml carbenicillin. Bulk plasmid was obtained by column miniprep (QIAGEN, Hilden, Germany).

RNAi trigger sequences with 5' *BglIII* and 3' *BamHI* overhangs were obtained by digesting the holding vectors with *BglIII/BamHI* and gel extracting the product. Simultaneously, *HMW::AdH::Nos* was digested with *BglIII*, creating a compatible site with which the target fragment and also gel purified. The target fragment was ligated in a sense orientation between *HMW* and the *AdH* intron. This vector was then transformed into *E. coli* and bulked up as above. The sense fragment-containing vector was digested with *BamHI*, creating a ligation site between the *AdH* intron and *Nos* terminator with which the target fragment overhangs are only compatible in an antisense orientation. The fragment and vector were ligated as such and bulked as described.

A *HindIII/Sall* digest of this construct was then conducted to remove the *HMW* promoter. The *OsAct* promoter, previously shown to drive expression of transgenes in wheat anther and pollen tissue (S. Vaughan, pers. comm.) pGEM-t::*OsAct* (obtained from Dr. David Lloyd) was also digested with *HindIII/Sall* and the *OsAct* with 5' *HindII* and 3' *Sall* overhangs was gel purified. The promoter was then ligated into the RNAi expression vector which was transformed and bulked as described. Sequencing confirmed the insertion and orientation of the RNAi trigger and *OsAct* promoter sequences.

2.4.2. Transformation of wheat by biolistics

Purified plasmid was delivered to the Rothamsted Transformation Unit at a concentration of 1 µg/µl for transformation into wheat (var. Cadenza) via biolistics (see Sparks and Jones, 2009). Transformant plants were selected in tissue culture for herbicide resistance due to *Barnase* gene included in transformation vector. Selected plants were grown under standard glasshouse conditions. Further validation of transformation was obtained by PCR genotyping. Positive lines were allowed to self-seed and taken through to T1 generation. Null lines and suspected somatic clones were discarded.

2.4.3. TaqMan Zygosity Assay

The TaqMan zygosity assay indicates dosage of a target gene relative to an endogenous control gene of known copy number. In this work the assay was used to determine the zygosity of RNAi constructs in the progeny of transformed wheat lines based on amplification of the *MaizeADH* intron region of the construct. The assay had previously been developed by Dr. Archana Patil at Rothamsted Research.

Genomic DNA from wheat leaf tissue was extracted as described in 2.2.1 and normalised to 10 µg/µl. Primer and probe mixes made from 100 nM stocks were prepared as follows:

| | |
|--------------------------|--------------|
| ADH F3 | 1.2 μ l |
| ADH R3 | 1.2 μ l |
| ADH Probe 2 | 1.2 μ l |
| <i>HvCon2</i> F | 2.4 μ l |
| <i>HvCon2</i> R | 2.4 μ l |
| <i>HvCon</i> Probe | 2.4 μ l |
| Sterile, distilled water | 49.2 μ l |

The following reaction mix was then prepared in 96-well PCR plates:

| | |
|------------------------------|------------|
| Primer/Probe mix | 2 μ l |
| 2X Absolute* qPCR Master mix | 10 μ l |
| Sterile, distilled water | 3 μ l |
| gDNA | 5 μ l |

*(Thermo Fisher Scientific, Hemel Hempsted, U.K.)

qPCR was then carried out on the samples with conditions as in 2.3.3. with the modification of 40 cycles, annealing temperature 60 °C, the removal of the elongation step and the detection of specific fluorophores to either TaqMAN probe (ADH Probe 2 - FAM, *HvCon* Probe - VIC)

Fluorescence was measured during the annealing step of each cycle. Primer Ct and amplification efficiency for each sample was calculated as described in 2.3.4. The dCt value for each sample was calculated as the difference between the AdH Ct and *HvCon* Ct. More negative dCt values indicate high transgene copy number and/or homozygosity. dCt values were also plotted on XY scatter plots to identify distinctive clustering of values which may further suggest homozygosity within the population.

2.5. Breeding of TILLInG mutants

2.5.1. Plant Breeding

Selected female parents were emasculated by excision of pale green/yellow immature anthers 1-2 days prior to anthesis. The first 3 and last 2 spikelets and innermost two florets of all remaining spikelets were removed and the tips of lammela cut off. Emasculated spikes were enclosed in transparent plastic crossing bags. When selected male parents entered anthesis, single pollen shedding spikes were excised and placed upside-down inside the crossing bag with the emasculated spike. After agitation to spread pollen around all available floret positions, pollen donor spikes were held in place upside-down against the female parent using paperclips. Pollen donor spikes were replaced as required.

2.5.2. Embryo Rescue

Spikes containing immature grain no older than 25 days post-fertilisation were excised and seeds removed. Seeds were surface-sterilised by washing first in 70% Ethanol for 5 minutes followed by 15 minutes in 0.5% Sodium Hypochlorite and 1 drop of Tween20 (Sigma-Aldridge, St. Louis, Missouri, U.S.A.) solution before 3 rinses in sterile, distilled water.

Embryos were extracted from grain under a Leica MZ6 dissecting microscope (Leica, Wetzlar, Germany) and mounted upon autoclave-sterilized growth medium contained in plastic blood cell counter vials. Growth medium consisted of the following:

0.5% w/v Type A agar (Sigma-Aldridge, St. Louis, Missouri, U.S.A.)

1X Standard Murashige and Skoog powder (Duchefa Biochemie, Haarlem, Netherlands)

0.05% w/v MES buffer (Melford Laboratories Ltd, Ipswich, U.K.)

1X Sucrose (Sigma-Aldridge, St. Louis, Missouri, U.S.A.)

Potassium hydroxide (Sigma-Aldridge, St. Louis, Missouri, U.S.A.) as required to achieve pH 5.8

Vials containing mounted embryos were stored in controlled environment conditions as described above. Embryos which successfully germinated were transplanted to Rothamsted prescription mixture compost in P24 plastic trays and allowed to continue growing under glasshouse conditions.

2.6. Histology

2.6.1 Fixation of Tissue

Samples were excised and placed immediately in cold vials of 4% Paraformaldehyde + 0.05% Gluteraldehyde solution. Vials were allowed to rotate for 4 hours at room temperature before storage overnight at 4 °C. Samples were then loaded into a Leica EM TP automatic sample preparation machine (Leica, Wetzlar, Germany) and subjected to a fixation and agitation with continuous agitation. Samples were submerged for 1 hour in 0.05M Phosphate buffer (pH 7.2), followed by an ethanol dehydration series, beginning with 10% and increasing by 10% increments, 1 hour at each concentration. At the 70% ethanol step samples were submerged for 12 hours and the temperature was dropped from ambient to 4 °C. The dehydration series up to 100% ethanol was then completed at ambient temperature. Infiltration of samples with LR Resin (Agar Scientific, Standted, U.K.) was also carried out in a sequential concentration series; ethanol 100% : LR resin 1:4, 3:2, 2:3 and 4:1 (v/v) for 1 hour followed by 100% LR white for 6 hours at 4 °C. Infiltrated tissue was then placed in a 0.5 ml thin-walled PCR reaction tube, orientated as desired and filled with fresh LR resin. Samples were embedded in the resin by baking for at least 24 hours in a 60 °C oven purged of oxygen.

2.6.2 Sectioning, Staining and Visualisation of Samples

Thin sections (1-2 µm) of samples were taken using a glass knife in a Reichert-Jung Ultracut microtome (Leica, Wetzlar, Germany). Samples were mounted

on glass slide cover slips and allowed to dry at room temperature overnight. A drop of Toluidine blue (0.05%) was placed on each section for 0.5 - 1 minute and then gently rinsed off using sterile, distilled water. Sections were placed on a warm plate and allowed to dry. Sections were then mounted on a glass microscope slide using DPX (Sigma-Aldridge, St. Louis, Missouri, U.S.A.).

Initial inspection of sections was carried out using Olympus BH-2 light microscope (Olympus, Shinjuku, Japan). For digital image capture slides were visualised using a Zeiss Axiophot light microscope (Zeiss, Jena, Germany) equipped with a Retiga digital camera (Q-Imaging, Surrey, Canada). Images were processed and captured using MetaMorph[®] (Molecular Devices (UK) Ltd, Wokingham, U.K.) imaging software.

2.6.3 Alexander Pollen Viability Staining

Anthers on the cusp of dehiscence were excised and placed in 2 ml microfuge tubes containing Carnoy's fixative (Ethanol: Chloroform: Acetic Acid 6:3:1 [v/v]) and stored at room temperature. After at least 24 hours anthers were removed from the fixative, placed under a dissecting microscope and sliced longitudinally using a razor blade. Anthers were then placed in microfuge tubes containing 100 µl Alexander stain which was prepared as follows:

For 100 ml add (in order):

10 ml 90% ethanol (Sigma-Aldridge, St. Louis, Missouri, U.S.A.)

1 ml Malachite green (1% solution in 95% ethanol) (Hopkins and Williams Ltd, Chadwell Heath, U.K.)

50 ml distilled water

25 ml glycerol (Sigma-Aldridge, St. Louis, Missouri, U.S.A.)

5 ml Acid fuchsin (1% (w/v) solution in water) (Hopkins and Williams Ltd, Chadwell Heath, U.K.)

0.5 ml Orange G (1% (w/v) solution in water) (Hopkins and Williams Ltd, Chadwell Heath, U.K.)

4 ml Glacial acetic acid (Sigma-Aldridge, St. Louis, Missouri, U.S.A.)

Add 8.5 ml distilled water to bring up to 100 ml

Samples were incubated at 30 °C for 30 minutes and mixed by vortexing regularly. A known volume of the Alexander stain solution was placed on a glass slide and covered with a coverslip. Total viable and nonviable cells visible in the aliquot were counted using a light microscope and multiplied by dilution factor to obtain a total anther value.

CHAPTER 3: NON-DESTRUCTIVE STAGING OF MALE REPRODUCTIVE DEVELOPMENT IN WHEAT

3.1. Introduction

Much of the regulatory networks which control anther cell identity specification, anther cell division and differentiation, gametophyte meiosis, pollen development and anthesis have been described in model species *Arabidopsis* and rice (Ma, 2005; Wilson and Zhang, 2009; Ge *et al.*, 2010; Plackett *et al.*, 2011; Zhang *et al.*, 2011) (see section 1.3.). Indeed there appears to be a great deal of conservation of signalling pathways between *Arabidopsis*, a brassicaceous eudicot, and monocot species (Wilson and Zhang, 2009), allowing the identification of many genes of interest in crop species based on sequence homology with already annotated genes in related species. An improved understanding of these genetic regulatory pathways in major cereals such as wheat, barley, rice and maize is imperative for development of hybrid and double haploid varieties, genetic containment and breeding for abiotic stress tolerance in preparation for future climate change scenarios (see section 1.1.). So far there has been very little study of genetic regulation of anther and pollen development in wheat, but with recent developments in genome sequence availability (Chapman *et al.*, 2015; Pingault *et al.*, 2015) and reverse genetics tools (Chen *et al.*, 2014) further accelerated progress is anticipated.

Wheat progresses through a series of phenological changes which can be easily recognised by external morphological features, allowing the definition of distinct developmental stages (Zadoks *et al.*, 1974). These developmental scales have proven useful, becoming embedded within national agronomic advice and the global agricultural vocabulary. Modern molecular genetics techniques provide experimenters with the tools to describe the function of specific genes within a given tissue, cell, developmental period, *etc.*, provided that the material used is accurately staged. However, for many of studies of reproductive development, plant material is collected by age (Gómez and

Wilson, 2012) or according to external development scales, neither of which provide accurate enough prediction of internal development for experimental purposes.

In order to characterise the molecular regulation of anther and pollen development it is necessary to identify and define important anther cytological and morphological stages in the studied species. Although the physiological processes involved in anther development appears to be broadly conserved amongst angiosperms (see section 1.2.), there are nonetheless differences which mean that staging developed for species other than that under investigation cannot be relied upon to translate directly. Therefore, when characterising the function of a gene based on orthology, identical interspecies expression profiles and function cannot be presumed. For example, the expression of *Arabidopsis* transcription factor *DYSFUNCTIONAL TAPETUM1 (DYT1)* is preferentially expressed in tapetum cells prior to PMC meiosis (Zhang *et al.*, 2006) whereas its putative rice orthologue *UNDEVELOPED TAPETUM1 (UDT1)* is expressed for a period spanning pollen cell meiosis to mitosis (Jung *et al.*, 2005). The development of systems relating the stage of anther development, which in cereal plants occurs enclosed within the culm, to external morphological markers is therefore necessary to ensure selected material is suitably representative of the development stage under investigation.

In order to establish a means of identifying and collecting suitable wheat anther material for molecular and physiological studies, the internal and visible external growth and development of wheat was characterised. Specifically, the series of developmental processes that occur during wheat anther and pollen development were characterised and divided into defined stages. Concomitant changes to external morphology were also studied with the aim of relating external characteristics to internal development in the form of a non-destructive staging model.

3.1.1. External development

Wheat is a member of the *Poaceae* family of grass species which, like other cereal crops within the family, has undergone substantial domestication and selective breeding pressure which has modified its phenology and morphology to suit prevailing cultivation practices (Salamini *et al.*, 2002; Simons *et al.*, 2006). Modern wheat varieties vary in height, vernalisation requirement, grain hardness and many other features such as the presence of awns. However, sufficient similarity in growth and development between wheat varieties allows for description of important stages in broadly applicable terms. The UK national agricultural Levy Board (ADHB) provides a standardised guide to wheat growth which uses a numerical scale based on the work of Zadocks *et al.*, (1974) and Trottmann (1987) to assist growers in applying agronomic interventions to at appropriate growth stages (Fig. 3.1.) (ADHB, 2015). Above ground development is broadly categorised in to seven groups (seedling growth, tillering, stem elongation, booting, ear emergence, flowering and grain development (Fig. 3.1.)) which encompass the most clearly defined phases of vegetative and reproductive growth and development

Seedling growth (GS10-19) begins with the emergence of the first leaf from the coleoptile (GS11), with each subsequent growth stage describing the incremental increase in number of leaves (GS13 – three leaves; GS15 – five leaves: *etc.*).

Growth stages

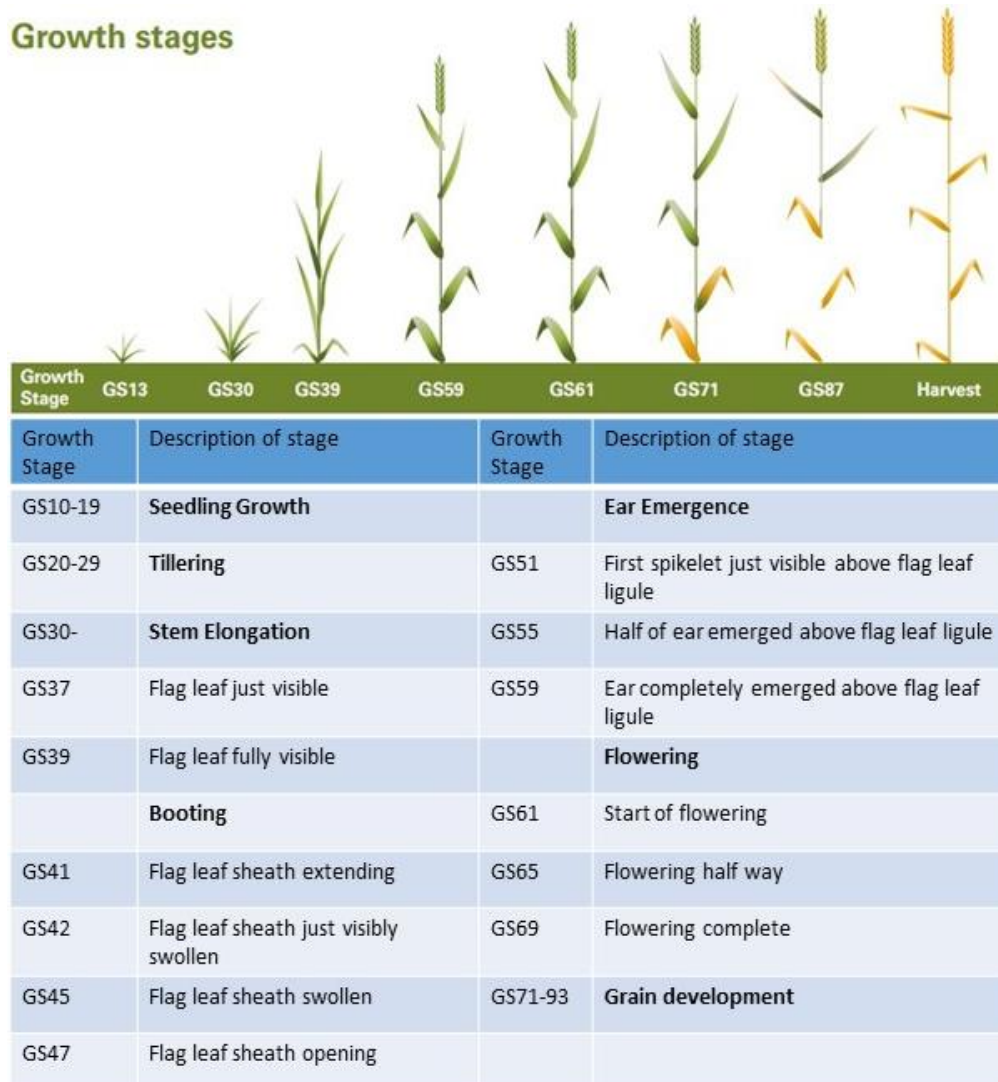


Figure 3.1. Growth stages of wheat based on external morphological development. *Distinct developmental phases of broad relevance to reproductive development shown in bold. Specific growth stages during which male reproductive development and processes relevant to this project are given with a brief description of distinguishing morphological features. GS – Growth stage. Adapted from ADHB (2015)).*

The number of tillers produced by a plant is an important determinant of yield and is carefully regulated according to environmental conditions (Power and Alessi, 1978; Sparkes *et al.*, 2006). During tillering (GS20-29), the number of tillers, each capable of producing a grain-containing spike, increases rapidly until the initiation of the stem elongation phase (GS30-39) and reproductive development in the main tiller. At this point competition for resources

between the developing spikes instigates abortion of laggard tillers. The duration of tiller production and number of tertiary tillers aborted is determined by the plant sensing of nitrogen and light availability (Sparkes *et al.*, 2006). Stem elongation is characterised by the appearance of nodes as the pseudostem extends, driven by internode elongation. At GS37 the tip of the rolled flag leaf emerges from the ligule of the last leaf (Fig. 3.2. a.), continuing to GS39 when the entire flag leaf blade has emerged (Fig. 3.2. b).

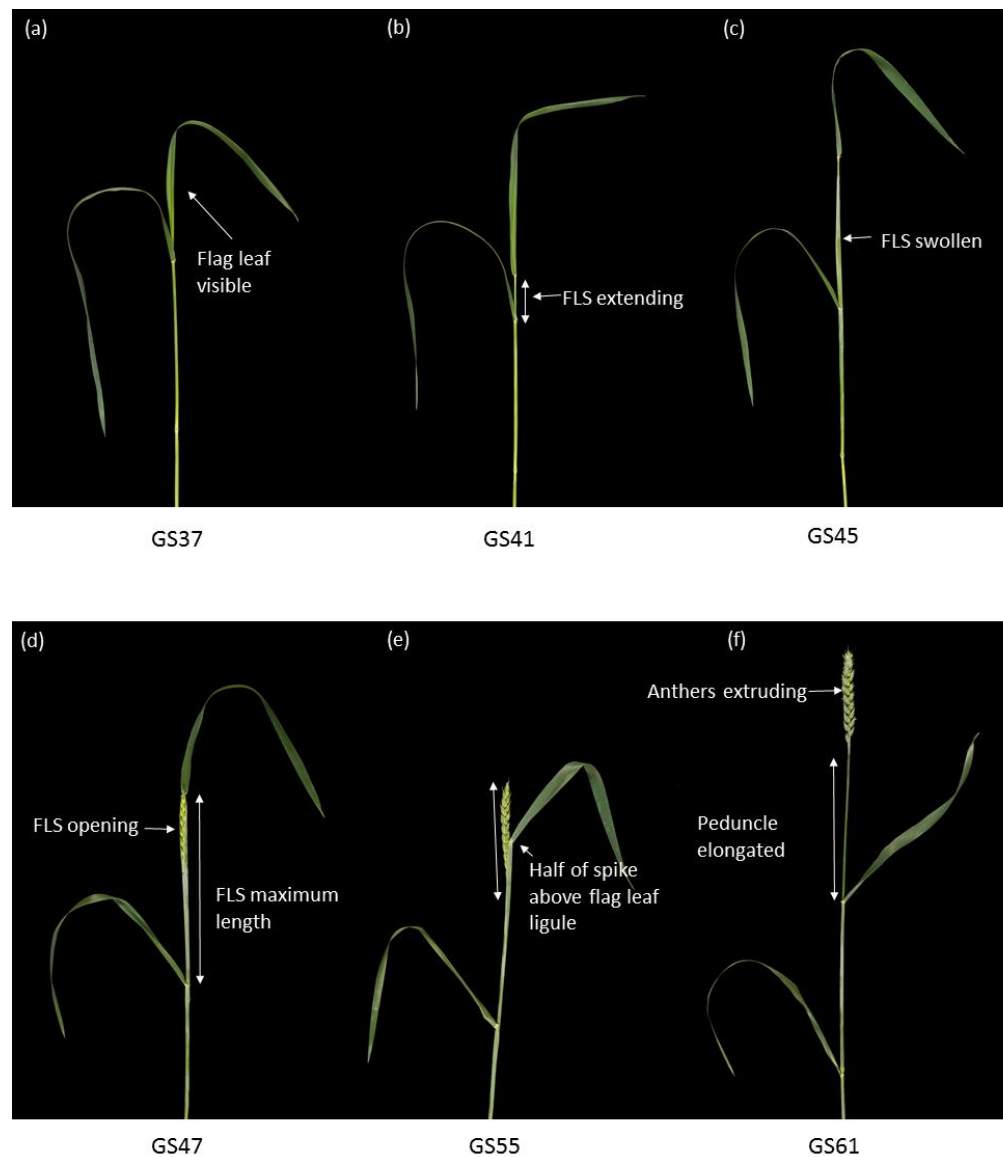


Figure 3.2. Defining morphological features of wheat (var. Cadenza) according to Zadocks scale. *Wheat plants at 6 distinct stages of development according to the Zadocks scale. Growth stage numerical code is stated below each tiller.*

Stage defining features according to Figure 3.1 are annotated in white. (a) GS37, (b) GS41, (c) GS45, (d) GS47, (e), GS55, (f) GS61.

Booting (GS41-47) describes the transitional period in which the external morphology of plants shifts from vegetative to reproductive characteristics. The extension of the true stem driven by internode elongation exposes the flag leaf sheath (FLS) which continues to elongate during GS41 (Fig. 3.2. b). Internal growth and development of the spike and further internode elongation forces the spike into the FLS causing it to become visibly swollen (GS43-45) (Fig. 3.2. c) At this point awns may become visible protruding from the flag leaf ligule in awned varieties. The spike itself starts becoming visible at GS47 as it enlarges to the point of forcing the flag leaf sheath open (Fig. 3.2. d).

Ear emergence (GS51-59) is caused by the extension of the peduncle, the true stem connecting the spike to the previous node, propelling first the first spikelet above the ligule of the flag leaf (GS51), followed by half the spike (GS55) (Fig. 3.2. e) and finally the entire spike (GS59).

Flowering begins at GS61 at anthesis when the first anthers become visible protruding from the floret (Fig. 3.2. f). The first floret positions to enter anthesis and directional progression of anthesis along the spike varies between genotypes. Similarly, the open or closed habit of florets during flowering varies between cultivars. Upon completion of flowering (GS69) the remaining growth stages (GS71-93) describe the appearance and characteristics of the maturing grain up to the point at which they are ready to be harvested.

3.1.2. Development of the wheat anther and pollen

Reproductive development begins in wheat after the transition of the apical meristem to reproductive growth and continues through a series of definable processes until anthesis, many of which occur whilst the immature spike is enclosed within the culm (Vahamidis *et al.*, 2014). A number of staging scales

for wheat reproductive development have been suggested, many with the aim for assisting the timing of agronomic interventions such as fertiliser and growth regulator applications (Waddington *et al.*, 1983; Vahamidis *et al.*, 2014). Much of this male reproductive development takes place before GS51, when the spike first becomes externally visible. Therefore, in order to investigate the effect of any treatment upon these processes or collect material at specific developmental stages, a means of accurately linking distinct external morphological features to anther development stages whilst it is enclosed within the culm is required.

Male reproductive development begins in wheat with the specification of stamen primordia on the apical meristem and reaches completion upon dehiscence when the pollen is released from the anther, some remaining inside the floret and falling upon its own stigma (De Vries, 1971). The nuclear division of wheat pollen cells proceeds through meiosis of a sporophytic pollen mother cell, the release of unicellular microspores from tetrads and their subsequent mitosis to form mature pollen cells (Goss, 1968) as occurs in other species. El-Ghazaly and Jansen (1986) and Mizelle *et al.*, (1989) used transmission electron microscopy (TEM) to investigate the changes that occur within wheat anthers during pollen development in order to characterise the effect of a chemical hybridising agent. They divided wheat anther development into 7 distinct stages: 1) precallose, 2) central callose – prophase I meiosis, 3) dyad and tetrad, 4) young, free microspores, 5) vacuolated microspore, 6) vacuolated pollen grain, 7) near-mature, tri-nuclear pollen grain. Saini *et al.*, (1984) also described 7 stages of wheat anther development (Fig. 3.2.) but described the mitosis of vegetative and generative nuclei as two distinct events prior to pollen maturation.

| Stage of microspore development | Feature of anther anatomy |
|---------------------------------|---|
| Pre-meiosis | Anther wall consists of epidermis, endothecium, middle layer and a tapetum surrounding PMC |
| Meiosis | Each PMC enclosed within a callose wall |
| Young microspores | Callose walls are broken down. Microspores aporate, thin-walled with large nuclei align along the periphery of the anther lumen. Degeneration of tapetum commences |
| Vacuolated microspores | Microspores irregularly shaped and in contact with the tapetum. Wall and pore formation continues. Pro-Ubisch bodies form on inner walls of degenerating tapetum cells. Anther diameter increases |
| Mitosis I | Microspore nucleus divides to form vegetative and generative nuclei. Pollen begins to accumulate starch |
| Mitosis II | Generative nucleus divides to form two ovoid sperm nuclei. Tapetal cells degenerated. Pollen becomes spherical |
| Mature Pollen | Only two outer layers of anther wall remain. Pollen consists of an outer 3-layered exine, middle Z-layer and inner 2-layered intine |

Table 3.1. Description of wheat anther and pollen development. *Wheat anther and pollen development stages, beginning at the formation of sporogenic Pollen Mother Cells (PMCs), gametogenesis via meiosis and mitosis and concomitant development of anther and tapetum cell layers. Pollen development is complete with the formation of trinuclear cells with fully formed outer layer and accumulated starch reserves.* Adapted from Saini *et al.*, (1984).

During the pre-meiosis stage, large sporogenous cells are present surrounded by four cell layers, the innermost being comprised of rectangular, single nuclear tapetum cells with heavily staining cytoplasm. Mizelle *et al.*, (1989) define the beginning of the meiosis stage by the expansion of the microsporangium, creating a locule into which the secretion of callose causes a distinctive star shape to be formed. As meiosis progresses and dyads followed by tetrads are formed inside callose envelopes, tapetum cells become binuclear, their plastids become dense and the primary wall expands as pro-Ubisch bodies become evident within the cytosol and on the plasma membrane surface (El-Ghazaly and Jensen, 1986; Mizelle *et al.*, 1989).

Upon release of young microspores, the tapetum primary wall completely degrades and a pore forms within the microspore orientated towards the tapetum, and Ubisch bodies assume their distinctive spiked shape as sporopollenin is deposited upon them. The nucleus of the young microspore migrates from the centre of the cell to the periphery and the cell becomes vacuolated (Mizelle *et al.*, 1989). The rapid expansion of the microspores during vacuolation appears to compress the tapetum layer and Mizelle *et al.*, (1989) define this as the beginning of tapetum degeneration. Mitosis I occurs after the vacuolated pollen grain stage (Table 3.1.), resulting in a vegetative and generative cell. Tapetum degeneration continues throughout this stage with tapetal cytosol precipitating into the locule and large lipid deposits becoming evident. Throughout this period sporopollenin deposition on the microspore continues leading to a visible increase in exine thickness (El-Ghazaly and Jensen, 1986; Mizelle *et al.*, 1989).

Unlike Saini *et al.*, (1984), Mizelle *et al.*, (1989) group Mitosis II and mature pollen stages together. At the near-mature tri-nuclear pollen grain stage the generative cell divides to form two sperm cells whilst the vegetative cell migrates to the pore (Goss, 1968). The cytoplasm now proliferates into the central vacuole and becomes rich in starch-storing plastids which stain heavily. At this stage the tapetum layer is in an advanced stage of degeneration, however, although some debris such as plastids and endoplasmic reticulum fragments can still be recognised (Mizelle *et al.*, 1989), it is not clear whether these components retain any function at this point in pollen development.

Interestingly, this description of anther development in wheat indicates that the tapetum layer is degenerating but still present during pollen mitosis II. In rice the tapetum layer is generally described as disintegrating immediately prior to pollen mitosis (Li *et al.*, 2006a; Huang *et al.*, 2009) and in *Arabidopsis* degeneration starts much earlier, during meiosis, and is complete before the end of mitosis (Parish and Li, 2010). This suggests that despite common processes occurring during anther development, there are important

differences between species. The secretory function of the tapetum and correct timing of its PCD is vital for wheat fertility and is vulnerable to abiotic stress (see section 1.5.) and it is therefore necessary to ensure that any anther development scale incorporates accurate descriptions of the changes that occur in tapetum cells.

3.1.3. Existing non-destructive reproductive development staging methods

In order to investigate the effects of experimental treatment(s) upon male reproductive development in cereals, non-destructive means of estimating internal developmental stage based on measurement of external characteristics have been established. Like wheat, early stages of reproductive development in barley occur whilst the spike is enclosed within the pseudostem. In order to complete molecular studies on developing barley anthers, a non-destructive staging method was established to avoid first having to dissect and damage the spike (Gómez and Wilson, 2012). The authors determined that the Zadocks scale was inadequate for predicting the size of the developing spike between GS31 and GS49 and therefore introduced substages to better resolve more easily detectable morphological markers where Zadocks scale descriptors were overlapping or ambiguous. Between GS31-37 the Zadock's scale could predict the length of the developing spike, which itself was correlated to anther development stage. Upon the emergence of the flag leaf at GS37 the proceeding Zadocks scale stages were replaced with four last flag elongation (LFE) stages which further refine the Zadocks scale definitions with the addition of the FLS elongation measurements (Table 3.2.). This combined scale was shown to be an accurate predictor of anther development stage between anther cell differentiation and pollen maturation. Cytological analysis of anthers and expression analysis of putative orthologues of anther genes with known temporal profiles confirmed the accuracy of the technique.

The negative impact of environmental stresses on reproductive development in rice has prompted the detailed investigation of anther and pollen development, necessitating an appropriate non-destructive staging method. Like barley and wheat, large periods of reproductive development take place whilst the spike is enclosed within the pseudostem. An auricle distance (AD) measurement, the distance between the auricles of the flag leaf and the previous leaf, for staging anther development has been used to determine the most vulnerable stages of pollen development to cold stress (Satake and Hayase, 1970) and for the application of drought stress treatments for molecular studies of anther hormonal signalling (Oliver *et al.*, 2005; Ji *et al.*, 2011). AD could be considered to be analogous to LFE as they both essentially characterise FLS length, however the rice inflorescence (panicle) differs from wheat and barley in that it consists of a branched rachis off which numerous secondary or lateral, spikelet-bearing rachises emanate which bear spikelets (Itoh *et al.*, 2005). The age of spikelets can vary by as much as 7 days and therefore care must be taken with the AD method to target only main stems and to restrict sampling to synchronously developing tillers and to restrict sampling to a defined region of the branch (Satake and Hayase, 1970).

| Stage | Characterisitcs | Spike length (cm) | Anther and pollen development stage |
|-------|--|-------------------|--|
| 31 | One node. | 1.17±0.54 | Primary sporogenous cells. |
| 32 | Two nodes | 2.46±0.97 | Secondary sporogenous cells to pollen mother cells. Four layers. |
| 33 | Three nodes | 3.14±0.72 | Pollen mother cells undergo meiosis. Tapetum layer is prominent. |
| 34 | Four nodes | 3.9±1.15 | Microspores released from the tetrad. Tapetum vacuolated. |
| 35 | Fifth node detectable / last flag emerged completely before the fifth node was detectable. | 4.77±0.89 | Free microspores. Middle layer undergoes crushing. The prominent tapetum layer starts to degenerate. |
| 37 | Last flag completely emerged, still rolled. | 6.11±1.12 | Microspores become vacuolated. Tapetum degenerating. |
| LFE1 | Flag leaf emerged completely and unrolling, ligule may be visible; last flag sheath extended 0.5–5 cm. | 7.14±1.29 | Mitosis I. Tapetum degenerating, but still present. |
| LFE2 | Last flag sheath extended 5–10 cm. Boot swelling obvious. Awns may be visible. Spike still inside the sheath, rachis has not started elongating. | 9.38±1.27 | |
| LFE3 | Flag leaf opening and awns clearly visible. Last flag sheath extended over 10 cm. Rachis starts elongation, moving the spike upwards towards the last flag sheath. | 9.19±0.77 | Binuclear pollen. Mitosis II occurs. |
| LFE4 | Spike has completed its upward movement and was entirely localized within the last flag sheath. Heading is imminent. | - | Trinuclear pollen. Septum breakage |

Table 3.2. Non-destructive anther staging method in barley. *Anther development stage in two double-rowed barley variety Optic grown at 15/12 °C day/night 16/8h light/dark is related to spike size which can be predicted by external growth stage. From Gómez and Wilson (2012).*

The aim of the following experiments was to determine if the LFE/AD staging method could be extended to wheat in order to conduct heat stress experiments and characterisation of anther and pollen regulatory genes. Specifically, the spring wheat variety Cadenza is the standard variety used for wheat molecular biology research at Rothamsted Research, including TILLING and transgenesis, due to its receptiveness to transformation and tissue culture and shortened life cycle due to its spring habit. As Cadenza was used for other anther molecular genetic investigations, described in the following

chapters, a non-destructive staging method was required to ensure correct material collection and treatment targeting.

3.2. Materials and Methods

3.2.1. Growing conditions

Spring wheat plants (var. Cadenza) were grown in controlled environment conditions (see section 2.) until the beginning of the booting period. Material was collected from secondary tillers between GS39 (flag leaf fully visible) and GS51 (ear emergence) (see section 3.1.1.).

3.2.2. Material collection and measurement

Based on previous work (see section 3.1.3.) material collection was carried out during the booting stages of wheat development to suit the further aims of this project to characterise aspects of anther development likely to take place during this period. The beginning of booting was defined as GS39 in the AHDB Wheat Growth Guide (AHDB, 2015) (Fig. 3.1.). At this point the flag leaf has fully emerged from the pseudostem and as the flag leaf sheath elongates during GS41 the distance between the ligule of the flag and previous leaf become measurable. To reduce the introduction of intra-ear variability into the data, collection and staging of anthers was restricted to the outer florets of mid-spike spikelets.

3.2.3. Histological analysis of anther development

Whole wheat florets or individual anthers were fixed in resin in order to characterise developmental stage by light microscopy. At earlier stages, when florets were too small for individual dissection the whole spike was fixed. Harvested material was immediately subject to chemical fixation as described in section 2.6.

Prepared resin blocks were mounted in a microtome and cross sections were taken using a glass knife. Section thickness varied from 0.5 to 4 μm depending

upon hardness of the resin. Sections were floated and allowed to expand on fresh water and then recovered with a glass coverslip and placed on a drying plate. Once dried, sections were stained by covering in 0.05% Toluidine blue for 30 seconds and rinsed with water and returned to the drying plate overnight and chemically mounted as described in section 2.6. Samples were observed under a light microscope (Zeiss Axiophot, Carl Zeiss AG, Oberkochen, Germany).

3.3. Results

3.3.1. Identification of wheat anther development stages

In order to determine if FLS length is a viable proxy measurement for staging anther development in spring wheat (var. Cadenza), it was necessary to first establish a standardised anther development scale against which to assign stages. To do this, light microscopy was used to observe the internal morphology of thin cross sections of anthers and determine if discrete developmental stages could be interpreted based on common features.

Anther material was collected from Cadenza plants ranging from GS39 to GS47 and prepared for light microscopy as described above. This external stage range was chosen to attempt to encompass the anther development stages which are of specific interest to other experimental aims (see sections 4 and 5). Progression of wheat anther development has been observed as previously described and assigned to discrete stages (see section 3.1.2) (Table 3.1.).

Anthers observed in the youngest material collected around GS39 were undergoing division of archesporial cells and differentiation of other anther cell layers. The four-lobed condition was also becoming evident at this stage (Fig. 3.3. a). It was possible to identify 3 distinct stages prior to meiosis as described in other species; the presence of archesporial cells surrounded by an epidermal and primary parietal cell layers (Stage 1, Fig. 3.3. a), then three differentiated cell layers of the endodermis, endothecium and secondary

parietal cells (Stage 2, Fig. 3.3. b). Lateral division of the secondary parietal layer gives rise to the differentiated middle and tapetum layer and archesporial cells divide to form sporogenous PMCs (Fig. 3.3. c). The beginning of the PMC meiosis is marked by the heavy staining of the sporogenous cell nuclei followed by swelling and increased vacuolisation of the tapetum layer (Stage 4, Fig. 3.3. d). The distinctive callose star formation appears in the locule during this period.

Although more detailed characterisation of the distinct stages of PMC meiosis in wheat has occurred elsewhere, this level of detail was not necessary for the purposes of this project as the focus of later physiological and genetic studies is on events in the tapetum after meiosis. Therefore, meiosis was considered as a single event spanning the initiation of nuclear division to the release of haploid microspores from tetrads. Furthermore, whilst the formation of the anther locule during this stage caused by the separation and contraction of microspore cluster-containing callose envelopes, differentiation between dyads and tetrads required the use of fluorescent dyes such as DAPI which was not used during this project.

Upon completion of meiosis, haploid microspores are released from the microspore cluster. At this stage, microspores are encased in a callose envelope which is degraded by the action of enzymes secreted by the tapetum, allowing free microspores to align to the tapetum during which time their vacuoles enlarge (Stage 5, Fig. 3.3. e). The swelling of the tapetum cell layer at this stage becomes such that the middle layer becomes compressed and degrades (Stage 6, Fig. 3.3. f). The migration of microspore nuclei from central to peripheral locations as described in section 3.1.2 can be observed at this point.

A significant change in developing anther and pollen cell morphology occurs as the microspores begin to take an irregular form and the tapetum layer becomes dense and compressed as it degrades (Stage 7, Fig. 3.3. g). From this point pollen cell Mitosis I (Stage 8, Fig. 3.3. h) and II (Stage 9, Fig. 3.3. i) give

rise to the generative and vegetative pollen cell nuclei. The migration of the generative nucleus to the locule-facing pole of the cell is evident at stage 9 but the orientation of the vegetative nucleus towards the tapetum is not visible in Figure 3.3. i. As the tapetum cells continue to degrade, the pollen coat stains more heavily as increasing quantities of sporopollenin accumulate and the cells become increasingly spherical in shape. During this period, the vacuole is reduced as the cytoplasm proliferates. Plastids begin to accumulate starch which stain densely and become immediately recognisable as nearly mature pollen grains (Stage 10, Fig. 3.3. j). Upon completion of starch accumulation, the tapetum layer has completely degraded but cellular debris can still be seen lining the locule. Further degradation of the endothecium is accompanied by septum breakage, joining two anther locules before dehiscence, when breaking of the endodermis releases mature pollen from the anther (Stage 11, not shown).

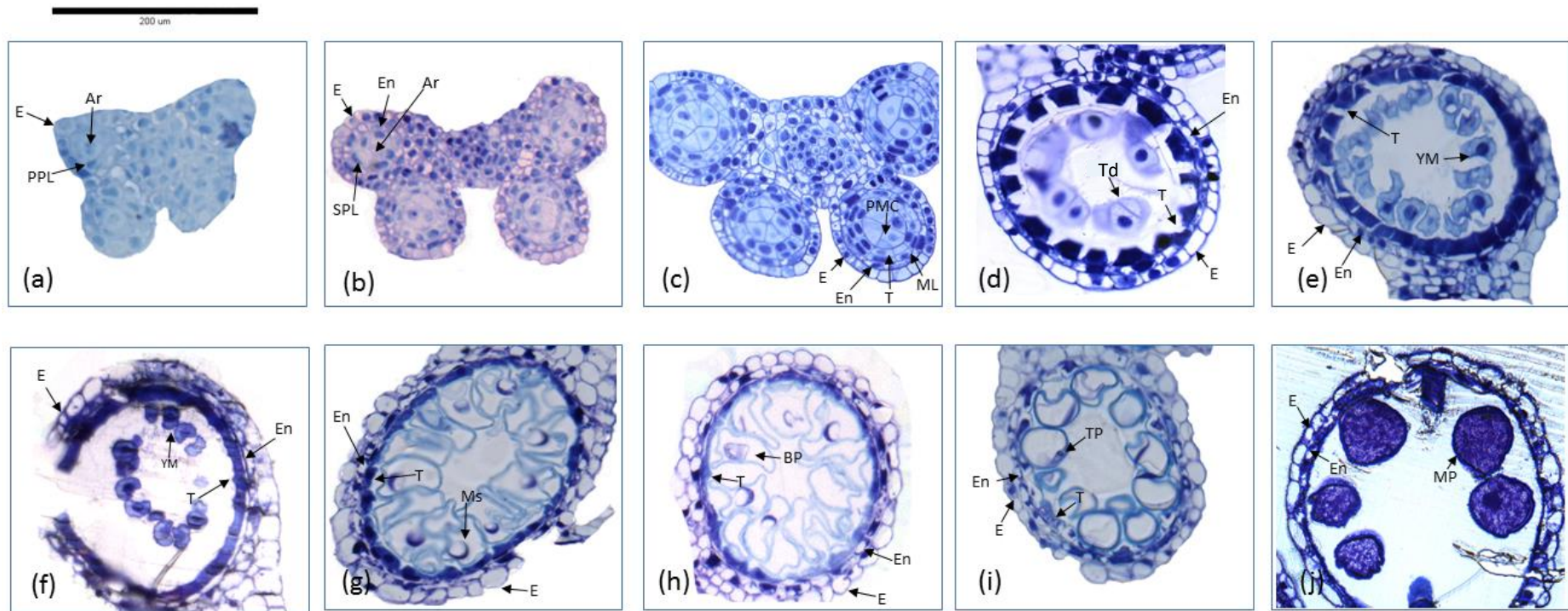


Figure 3.3. Staging of wheat anther development in wheat. *10 distinguishable stages were identified between the initiation of the four lobed condition (a) and completion of pollen development prior to dehiscence (j). Stages 1-2 (a and b) are defined by the presence of archesporial (Ar) and primary (PPL) and secondary parietal cells (SPL) surrounded by an endothecium (En) and epidermis (E). At stage 3 (c) the parietal cells have*

differentiated creating a middle layer (ML) and Tapetum (T). Meiosis of PMCs begins at stage 4, some tetrads (Td) visible (d) and is characterised by the crushing of the middle layer and prominence of the tapetum. Young microspores (YM) are released from the callose envelope at stage 5 (e) and tapetum degeneration is evident at stage 6 (f). The vacuolation of pollen cells at stage 7 (h) marks the beginning of progress through mitosis I (Stage 8, (h)) creating bicellular pollen (BP), followed by mitosis II (stage 9) creating tricellular pollen (TP). At Stage 10 (j), mature pollen (MP) is filled with starch, the tapetum layer has completely degraded prior to dehiscence (Stage 11).

| Stage | Anther and Pollen development |
|--------------|--|
| 1 | Archisporial cells present |
| 2 | Primary archisporial cells surrounded by three cell layers |
| 3 | Pollen Mother Cells surrounded by differentiated endodermis, endothecium, middle layer and tapetum |
| 4 | PMCs undergo meiosis, tapetum layer is prominent, Middle layer crushed |
| 5 | Young microspores released from tetrad |
| 6 | Young microspores align to tapetum. Tapetum degeneration evident |
| 7 | Vacuolation of microspores. |
| 8 | Mitosis I. Binuclear pollen beginning to develop coat layer |
| 9 | Mitosis II. Trinuclear pollen beginning to accumulate starch |
| 10 | Pollen cells completely filled with starch |
| 11 | Dehiscence |

Table 3.3. Description of wheat anther development stages as shown in Figure 3.3. For each stage, defining morphological characteristics which can be easily recognised using light microscopy are listed. Adapted from barley anther development stages in Gómez and Wilson (2012).

3.3.2 Flag leaf sheath length can be used to stage wheat anther development

Having established a developmental scale for anther development in wheat (var. Cadenza) a study of internal and external development was carried out to determine if anther development stage can be accurately predicted by non-

destructive measurement of external morphology. In order to develop a method for easily identifying and collecting material at specific anther development stages, the suitability of the LFE method described in barley by Wilson and Gómez (2012) was investigated.

Gómez and Wilson, (2012) found that the Zadocks scale for barley became non-sequential and inadequate for describing external development of tillers during the booting stages. Therefore, additional stages describing changes in morphology during this period were introduced. Upon emergence of the flag leaf and creation of an externally measurable distance between auricles 4 additional LFE scale stages could be used to define development between flag leaf emergence and emergence of the ear. The authors found a correlation between a combination of Zadocks scale and LFE growth stages with anther and pollen development, sufficient for non-destructive staging of reproductive development. The growth and development of wheat (var. Cadenza) was observed to determine if similar adaptations of the growth scale were required. The flag leaf blade becomes completely visible and unrolled at GS39 (Fig. 3.4. a) defining the beginning of booting stages. The next developmental stage (GS41) is simply defined as “Flag leaf sheath extending”, but encompasses around 10 cm of FLS growth (Fig. 3.4. b and c) and the extension of the developing spike and its peduncle to fill the FLS cavity (Fig. 3.4. d.).

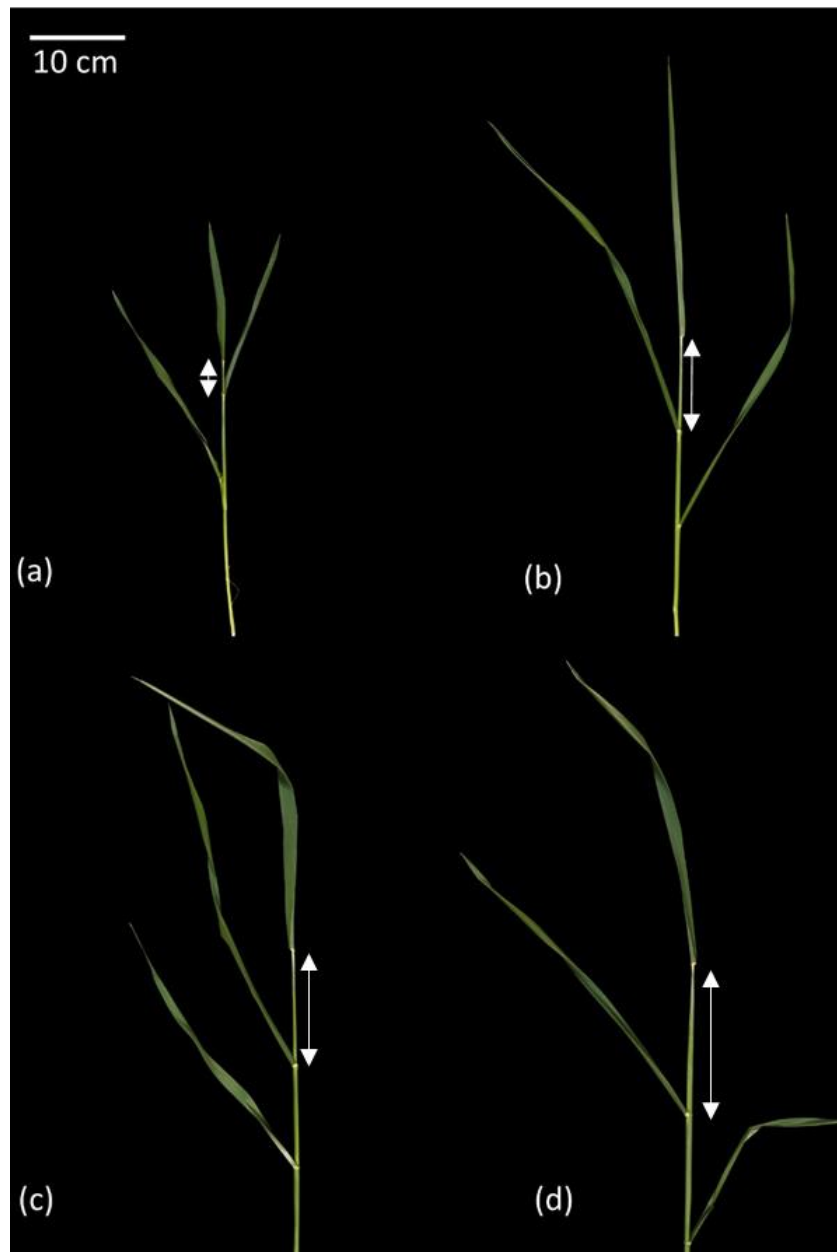


Figure 3.4. Extension of the flag leaf sheath during booting stages. (a) *Wheat tiller at GS39 with the entire flag leaf visible marking the end of the stem elongation phase and the beginning of booting phase during which anther development was staged.* (b) *FLS and flag leaf continued extension becomes obvious as the plant enters GS41* (c) *FLS extension exceeds 10 cm and the spike begins to enter the FLS cavity.* (d) *The flag leaf sheath begins to swell as the developing spike fills the cavity at GS43.* White arrows indicate the FLS.

The internal development of the spike was also assessed (Fig. 3.5.). At GS39 the immature spike remains inside the pseudostem below the level of the leaf

previous to the flag leaf. The spike was around 1 cm in length at this stage (Fig. 3.5. a). Extension of the spike in the proceeding stages is driven by elongation and enlargement of the rachis and spikelets (Fig. 3.5 a). An important transition in spike development is the initiation of peduncle elongation which by GS43 has extended the spike to completely fill the flag leaf sheath cavity. At this stage individual green anthers measuring around 1 mm and with a pronounced, visible four-lobed morphology can be readily harvested from spikes (not shown).

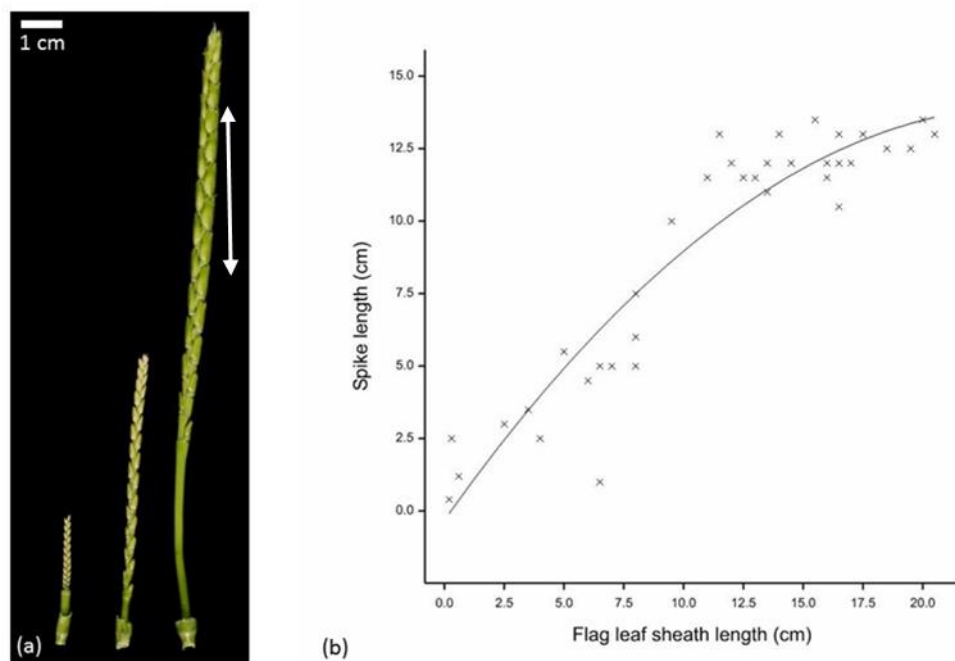


Figure 3.5. Development of the immature wheat ear.

(a) *The immature wheat ear at GS39, 41 and 43 (left to right). White double-headed arrow indicates mid-spike positions to which anther harvesting was restricted to maintain developmental consistency.* (b) *The relationship between flag leaf sheath length and spike length can be described by a*

*polynomial regression with the parameters $Y = (1.166*x^2) + (-0.024*x) + -0.313$ with an r^2 of 0.87.*

The length of 36 FLS and corresponding spikes were measured and compared to establish if a predictive relationship existed (Fig. 3.5.b). A positive relationship between FLS length and spike length was identified by regression

analysis of FLS and spike lengths ($r^2 = 0.87$). After 10 cm FLS length the rate of spike elongation appears to decrease. This is possibly explained by the initiation of elongation of the peduncle which causes the spike to fill the FLS cavity. The relationship between FLS and spike elongation demonstrates that external vegetative development can be predictive of internal reproductive development

Having established a link between internal and external development, it was necessary to determine if the relationship extends specifically also to anther development. To test if the barley LFE anther staging method could be applied to wheat, the length of the FLS of 20 secondary tillers in a population of Cadenza plants was recorded prior to extraction of anthers from mid-spike (Fig. 3.5. a), outer floret positions and their chemical fixation and staging by light microscopy as described (see section 3.2.). The anther development stage of each sample was plotted against the corresponding FLS length (Fig. 3.6.).

A logistic correlation describes the relationship between anther development stage and length of the FLS ($p \leq 0.001$, $r^2 0.89$). The model shows that pre-meiotic development progresses independently of FLS extension. Anther development between meiosis (stage 4) and mitosis I (stage 9) correlates positively with FLS extension between 15 and 17.5 cm. It may therefore be possible to target material collection and experimental treatments to these anther development stages based on flag leaf sheath FLS lengths. The anther development stages appear to be grouped; pre-meiosis (stage 1-3) at FLS length ≤ 7.5 cm, meiosis to vacuolated microspores (stage 4-7) at FLS length 8 – 13.5 cm, mitosis I to pollen maturation (stage 7-10) at FLS length ≥ 14 cm.

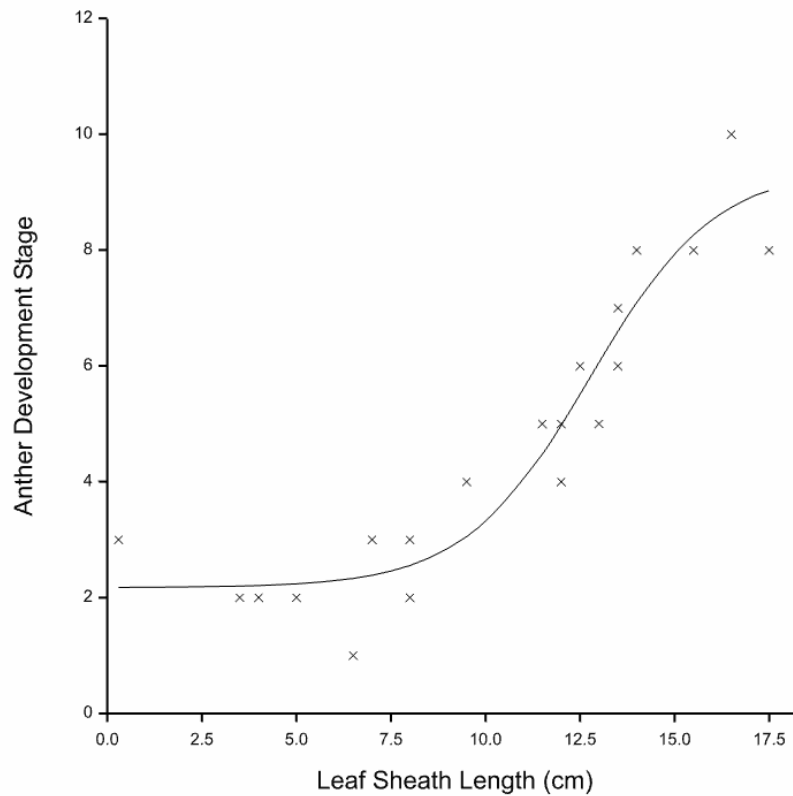


Figure 3.6. Logistic model of relationship between wheat anther developmental stage and flag leaf sheath length in the spring variety Cadenza. *The four parameter model ($Y = A + C / (1 + \exp(-B \cdot (x - M)))$) of 20 observations fits the data with an r^2 of 0.89 and an estimated standard error of observation of 0.83.*

To confirm this, anthers were taken from secondary cadenza tillers measuring 5, 10 and 15 cm and GS43 when the flag leaf sheath FLS has reached its maximum length and the ear is swelling. Using the model parameters, the expected anther development stages of these samples would therefore be 2, 3, 8 and stage 9 onwards respectively (Table 3.4.).

| Flag leaf sheath length (cm) | Predicted anther stage | Standard Error |
|---------------------------------|---------------------------|----------------|
| 5 | 2.236 | 0.32 |
| 10 | 3.314 | 0.437 |
| 15 | 7.937 | 0.395 |
| 20 (GS43) | 9.324 | 0.906 |

Table 3.4. Predicted anther development stages based on logistic staging model for user defined flag leaf sheath lengths. *Predicted anther stage, S, was calculated using the equation $S = A+C/(1+exp(B*(L-M)))$ where L is the flag leaf sheath length value.*

Samples were fixed, sectioned and visualised as described above. Three biological replicates were assessed for each flag leaf sheath FLS length and cross sections of all samples, except for FLS 10 cm, are shown in Figure 3.7. For example, stages 1-3 are represented in the 5 cm FLS group and can be considered collectively as a pre-meiosis stage (Fig. 3.7. a, b, c). The logistic regression model predicted anther development stage 2 at 5 cm FLS which was observed in Figure 3.7. b. The loss of two replicates at FLS 10 cm prevents a comparative analysis of the accuracy of the model at this FLS length. However, despite the longitudinal orientation of the cross section, the presence of PMCs within callose envelopes and vacuolation of tapetum cells indicate that meiosis has been initiated (Fig 3.7. d). Stages 5, 6 and 7 (Fig. 3.7. e, f and g respectively) were observed at FLS 15 cm which encompass the release of microspores from the meiotic complex to the initiation of microspore mitosis. However, the logistic model predicts anther development stage 8 at FLS 15 cm. At GS43 the predicted anther development stage is 9 and indeed this is observed in Figure 3.7. j. These stages can be recognised by the shift from irregular to ovoid shape of microspores, the division of nuclei which align to the non-tapetum facing end, the degeneration of tapetum cells and the increasing thickness of the microspore cell wall as exine is laid down. A high degree of variability between replicates was observed. However, based

on the stages described in Table 3.2., it is clear that broadly similar processes are occurring within each of the four FLS categories.

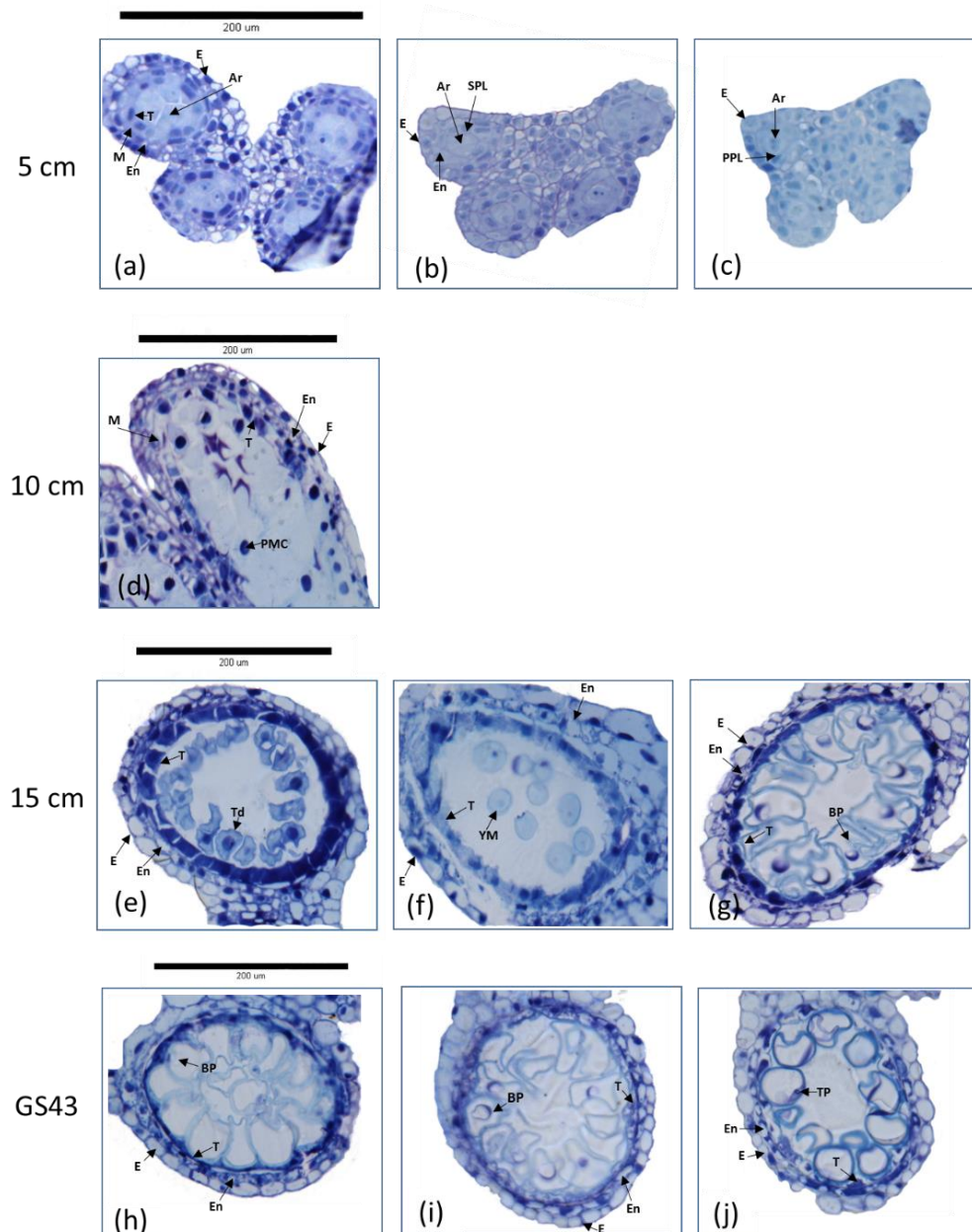


Figure 3.7. Microscopic analysis of wheat pollen development during FLS extension. *The anther development stages of samples taken from 5 cm FLS were (a) – Stage 3, (b) – Stage 2 and (c) – Stage 1. At 10 cm (d) PMCs undergoing meiosis are visible – Stage 4. At 15 cm FLS anther development stages were (e) – Stage 5, (f) – Stage 6 and (g) – Stage 7. At GS43 anther developmental stages were (h) – Stage 8, (i) – Stage 8 and (j) – Stage 9.*

Clearly, there is a disparity between anther development stages predicted by the logistic regression model (Table 3.3) and those observed *in planta* (Fig. 3.7.). Therefore, by grouping anther stages which constitute more general developmental processes, the FLS length can be used to identify material which fall in to the pre-meiotic (stage 1-3), meiotic (stage 4), pre-mitotic (stage 5-7) and mitotic (stage 8-9) categories of pollen and anther developmental stage.

3.4. Discussion

The characterisation of regulatory gene networks controlling wheat anther and pollen development and the impact of HT upon these networks is crucial for attempts to maintaining wheat fertility as extreme temperature events become more frequent during the growing season. Such investigations have been restricted by the difficulty in collecting developmentally uniform material as wheat reproductive development mostly takes place whilst the inflorescence is contained within the pseudostem. Accurately staged material is a prerequisite of molecular studies, especially those investigating the temporal and/or tissue specific gene expression. Similarly, physiological studies investigating the impact of HT and other abiotic stresses on anther and pollen development require the experimenter to determine the developmental stage(s) exposed to stress in order to characterise the response. Anther developmental stage can be determined by light microscopy; however, this is time consuming and requires the destructive sampling of often limited experimental material. Therefore, an investigation was undertaken to determine if a non-destructive anther development staging method previously described in barley (Gómez and Wilson, 2012) could be modified for use in wheat.

Light microscopy was used to identify distinguishable stages of wheat anther and pollen development (Fig. 3.3.). Previous classifications of wheat anther development defined 7 stages at which specific cytological processes or features can be recognised (Table 3.1.) (Saini *et al.*, 1984; Mizelle *et al.*, 1989).

Here, analysis of the youngest material incorporated anthers at two earlier stages of development, prior to differentiation of the primary (Stage 1, Fig. 3.3. a) and secondary parietal layers (Fig. 3.3. b) into tapetum and middle cell layers surrounding archesporial cells. These stages were also described by Gómez and Wilson (2012) and included in their non-destructive anther development staging model. Therefore, the previous seven stages of wheat anther development were extended to include the two earlier stages of parietal cell differentiation observed in this investigation (Table 3.1.). Also, other anther development scales divide the process of meiosis, in particular the formation of dyads and tetrads into discrete stages. Whilst the contraction of the callose envelopes surrounding the meiotic PMCs expanding the locule was evident at this stage (Fig. 3.3. c, d), distinguishing between bi- and tetra-cellular microspore clusters was difficult and therefore a single stage defining meiosis as beginning at the prominence of the PMC and ending with the release of haploid microspores was used.

In order to characterise genetic regulators of anther development and the impact of high temperature stress, the LFE/AD staging method was extended to the experimental material and conditions used in this project. The LFE method utilises the relationship between FLS length and anther developmental stage (Gómez and Wilson, 2012). Initial extraction of material for the characterisation of anther development in wheat revealed that at GS39 the developing spike is around 1 cm long (Fig. 3.5. a) and contained anthers at stages 1-2 (Fig. 3.3. a-b). As this project is primarily concerned with the role of GA-signalling and impact of HT-stress on the development of the tapetum, which is not yet formed at these stages, it was not necessary to characterise anther development in relation to spike length prior to booting. Instead, investigation focused on establishing a relationship between FLS length after GS39 and anther development stages incorporating specific developmental processes of interest, namely meiosis, tapetum PCD and pollen cell mitosis and maturation. A logistic regression model was found to best fit the data (Fig. 3.6.); however, individual observations at a given FLS length

were often found to span up to three anther developmental stages. Indeed, a test of the predictive accuracy of the logistic regression model (Table 3.4. and Fig. 3.7) showed that the model underestimates anther development stage in the middle of the FLS length range. This is potentially problematic as characterisation of anther regulatory gene expression requires the collection of developmentally uniform material, especially where expression is highly developmentally regulated. Anther development rate in wheat has been shown to differ between floret positions within a spikelet (Miralles *et al.*, 1998) and between spikes (Lukac *et al.*, 2012) and this is most likely the source of variation in observed anther development stage between tillers of the same FLS length (Fig.3.7). Therefore, without further refinement it is highly likely that use of this method to collect material for molecular analysis will result in the inclusion of multiple developmental stages and reduce the developmental stage-specificity of HT treatments.

Increasing the number of observations in the staging model may further improve the predictive accuracy of the FLS method. Similarly, further restriction of the spikelets and floret positions staged may reduce the level of variation caused by intra-spike differences in developmental rate, however, this would also reduce the amount of material which could be collected via this method. Nonetheless, the non-destructive staging model presented here has been shown to be able to distinguish between material at pre-meiotic, meiosis, young and vacuolated microspores and mitosis (Fig. 3.7.). Whilst this approach may preclude the targeting of specific certain anther development stages, the ability to non-destructively stage meiosis, stages incorporating tapetum PCD, pollen mitosis and maturation will permit a comprehensive characterisation of wheat anther GA and HT signalling networks.

CHAPTER 4: INVESTIGATING THE ROLES OF TaGAMYB AND TabHLH141 IN GA-MEDIATED WHEAT ANTHER DEVELOPMENT

4.1. INTRODUCTION

GA-signalling is crucial for anther development, particularly regulation of tapetum function and timing of PCD (see section 1.4.). These anther development processes are disrupted by HT-stress leading to reduced male fertility and loss of yield suggesting that the GA-signalling response to HT may be a source of HT-associated anther defects (see section 1.5.1.). Therefore, having described the morphological development of wheat anthers and pollen (see section 3), the characterisation of two putative wheat orthologues of rice anther GA-signalling TF *OsGAMYB* and tapetum PCD regulator *OsEAT1* (see section 1.3.2.) was carried out to establish the identity and function of wheat anther regulatory genes and determine their level of regulation by GA-signalling.

4.1.1. GAMYB

GAMYB is a transcription factor expressed in rice and barley anthers which is crucial for tapetum and pollen development (see section 1.4.1.). Furthermore, it is the central TF in the anther GA-signalling pathway, downstream of DELLA, which controls tapetum PCD and pollen development (Aya *et al.*, 2009). Loss-of-function *Osgamyb* mutants fail to correctly initiate tapetum PCD (Kaneko *et al.*, 2004; Aya *et al.*, 2009) leading to male infertility, whilst overexpression of *HvGAMYB* results in the formation of non-viable pollen. Transcriptional analysis shows that *GAMYB* directly regulates a number of genes involved in PCD and formation of the pollen exine which is critical for viability (see section 1.4.3.) (Tsuji *et al.*, 2006; Aya *et al.*, 2009). Premature degradation and damage of the tapetum resulting in microspore abortion and non-viability are frequently observed HT-stress defects (see section 1.1.1.), suggesting that *GAMYB* could be involved in regulating anther HT-responses.

Furthermore, loss-of-function *gamyb* mutants exhibit a more severe sterility phenotype under elevated temperatures (Millar and Gubler, 2005; Kaneko *et al.*, 2004). The observation that a number of *GAMYB* anther target transcripts are also downregulated under HT (Endo *et al.*, 2009) suggests that *GAMYB* function may be sensitive to temperature. Some characterisation of *TaGAMYB* and its role in wheat aleurone function has been carried out (see section 1.4.1.), however, there is currently little information about its function in wheat anther development. Given its central role in GA-signalling during anther development and potential involvement in HT-stress responses, a reverse genetics approach was taken to characterising the *TaGAMYB* and its function in wheat anther development.

4.1.2. *bHLH141*

The rice gene *ETERNAL TAPETUM 1 (EAT1)* is a basic helix-loop-helix (bHLH) family TF which is expressed in tapetum cells during anther development and has a role in the instigation and execution of PCD (Niu *et al.*, 2013) (see section 1.3.2.). Like *Osgamyb*, *Oseat1* exhibits delayed tapetum PCD and exine malformation and aborted microspores but without tapetal cell hypertrophy. *OseAT1* is expressed in tapetum cells between late meiosis and the completion of tapetum degradation, acting to upregulate the expression of two PCD executing aspartic proteases.

OseAT1 is under the regulation of *OstDR1* and is slightly downregulated in *Osgamyb* and *Osudt1*, suggesting that GA-signalling may converge with another regulatory pathway to execute PCD via *OseAT1*. Furthermore, an *EAT1 Arabidopsis* orthologue *AtbHLH089* was identified as a putative interactor with RGA in a yeast 2-hybrid anther cDNA library screen (S. Thomas, pers. comm.). DELLA-bHLH interactions have previously been described in the hormonal regulation of other developmental signalling networks (see section 1.4.). Given the evidence suggesting partial transcriptional regulation by *GAMYB* and direct regulation by DELLA, a characterisation of the *OseAT1* wheat orthologue, *TabHLH141*, was carried out to determine its function in

tapetum function and PCD and determine its involvement in the wheat anther GA-signalling pathway

4.1.3. Reverse genetic approaches to characterising wheat anther gene function

The size, complexity and hexaploidy of the bread wheat genome has restricted the expansion of molecular genetic research which has been experienced in less genetically complex crop species such as rice, barley and maize (Berkman *et al.*, 2012). As well as its polyploidy, the wheat genome is 17-Gb and is 80% comprised of highly repetitive transposable elements which has made the assembly of a complete reference genome challenging (Berkman *et al.*, 2012; Pingault *et al.*, 2015). Nonetheless, recent advances in high-throughput sequencing and genetic computational technology have permitted the publication of a draft reference sequence for hexaploid bread wheat (International Wheat Genome Sequencing Consortium (IWGSC) *et al.*, 2014; Chapman *et al.*, 2015). As the availability of wheat reference genomic sequence and accompanying positional and gene structural information continues to catch up with that of model species such as rice, it becomes increasingly feasible to translate understanding of well-studied genes and regulatory networks into wheat.

As a member of the *Poaceae* family, wheat shares a common ancestor with related grass species such as rice and barley and the model species *Brachypodium distachyon*. Therefore, a degree of synteny between wheat and other grass species allows the identification of orthologous genes based on sequence conservation (Bolot *et al.*, 2009; Kumar *et al.*, 2009). This approach of using known gene sequences in related species to identify orthologous genes in the wheat reference genome has been used here to assist with the molecular characterisation of their function in the wheat anther regulatory network. RNA interference (RNAi) is an established approach for investigation of gene function in plants (Fu *et al.*, 2007) based on a double-stranded RNA mediated post-transcriptional pathogen defence and gene expression

regulatory mechanism (Baulcombe, 2004). RNAi induces post-transcriptional gene silencing through recognition by eukaryotic cells of cognate double stranded RNA usually expressed as a transgene or delivered by viral vector. This endogenous mechanism can therefore be manipulated to induce the down-regulation of a native gene via the expression of an inverted repeat of a short fragment with homology to the target gene. The ability of RNAi to simultaneously target multiple homoeologous copies of a gene makes it ideally suited to investigations in polyploid species such wheat in which the A, B and D homoeologous genomes share 95% sequence similarity (Fu *et al.*, 2007).

RNAi is also well known to result in varying levels of gene silencing resulting in a range of phenotype severity (Small, 2007). Therefore, confirmation of similar silencing phenotypes in independent transgenic events and evidence of reduced target gene mRNA abundance is required in order to validate results. For these reasons, Small, (2007) suggests that RNAi is ideal for an initial screen for interesting phenotypes which must then be validated by more robust means.

An alternative approach is Targeted Induced Legions in Genomes (TILLInG) an extension of established plant breeding chemical mutagenesis techniques for fundamental functional genomic research (Mac Key, 1968; Slade *et al.*, 2005; Chen *et al.*, 2014). TILLInG is a PCR based approach for high-throughput screening of DNA libraries from thousands of individuals treated with ethyl methanesulfonate (EMS), an alkylating, radiomimetic chemical mutagen for single nucleotide polymorphisms (SNPs) (Slade *et al.*, 2005). Whilst far less precise than transgenesis, TILLInG does not involve the introduction of foreign DNA and is therefore subject to far fewer regulatory restrictions and barriers to commercial registration of resulting varieties. Furthermore, TILLInG can generate complete knockout in a given target gene with more consistency than RNAi gene silencing and, unlike transgenic gene silencing and transposon-DNA insertion, can generate allelic series which are more useful for dissection of gene function (Dong *et al.*, 2009; Chen *et al.*, 2014).

A population of EMS treated population of spring wheat var. Cadenza for TILLInG was established at Rothamsted Research U.K., in 2004-5 and characterised in the field for agronomic traits in the M₃-M₆ generations (Rakszegi *et al.*, 2010). A batch of around 2000 M₄ seed of the Cadenza TILLInG population was established of which around 1200 underwent exon-capture sequencing; the coding sequence of 1,831 known cDNAs and 15 hand-annotated GA-biosynthesis and signalling coding sequences formed an exon-capture array used to enrich gDNA extracted from each line which was then sequenced using Illumina GAII 110 bp paired end reads and mapped to the IWGSC CSS reference genome (King *et al.*, 2015). The reads were mapped to the IWGSC CSS reference and where coverage was lacking for genes of interest reads were also mapped to the W7984 whole-genome shotgun assembly (Chapman *et al.*, 2015). Data from SNP calling and annotation analysis was compiled into a searchable data base cross referenced to M₄ seed library serial numbers (A. Phillips, pers. comm.) permitting easy identification of EMS-induced mutations in target genes.

This chapter presents evidence obtained using reverse and molecular genetic experimental approaches which shows that the wheat orthologues of *OsGAMYB* and *OsEAT1* play a crucial role in ensuring male fertility. Both genes were identified in the wheat reference genome based on sequence homology with characterised orthologues in rice and barley. Loss-of-function mutants were obtained using transgenic gene silencing and mutagenesis which confirm that both genes are required for pollen development in wheat. Based on previously observed interaction between *Arabidopsis* DELLAs and *OsEAT* paralogues AtbHLH89/91 (S.Thomas pers. comm.) the full length cDNA sequences of *TabHLH141* were co-expressed with a truncated *Rht-D1* sequence to test for interactions. The apparent interaction between RHT-D1 and TabHLH141 provides evidence that TabHLH141 is involved in GA-mediated tapetum PCD.

4.2. MATERIALS AND METHODS

All molecular and cytological techniques used in this chapter are described in section 2.

4.3. RESULTS

4.3.1. Identification of *TaGAMYB* and *TabHLH141* orthologues

In order to carry out functional characterisation of *TaGAMYB* and *TabHLH141* confirmation of full length genomic sequences were required to facilitate amplification, cloning, RNAi target design and TILLING. In the case of *GAMYB*, previous work had cloned and confirmed the sequence of the three *TaGAMYB* homoeologues (Haseneyer *et al.*, 2008), however, since the more recent publication of the wheat reference genome it was decided to validate *TaGAMYB* sequences using the updated resources.

The *OsGAMYB* (Os01g0812000) and *OsEAT1/bHLH141* (Os04g0599300) annotated genomic sequences were extracted from The Rice Annotation Project Database (rapdb.dna.affrc.go.jp). Although *AtbHLH089* has been shown to interact with DELLA, *OsEAT1* was used as the query sequence as rice is more closely related to wheat and phylogenetic analysis has shown that most *bHLH* genes are conserved amongst angiosperms (Li *et al.*, 2006b). The translated proteins of both genes were then used as the query input for a protein Basic Local Alignment Search Tool (BLASTP) search for orthologues and paralogues in *Brachypodium*, *S. bicolor*, and *Z.mays* in Phytozome (phytozome.jgi.doe.gov). Exported protein hits were assembled in a phylogenetic tree in Geneious (Biomatters, Auckland, New Zealand) to identify the most closely related *Brachypodium* sequences. For *OsGAMYB* this was Bradi2g53010 and for *OsEAT1/bHLH141* Bradi5g20397. The coding DNA sequences (cds) of *BdGAMYB* and *BdEAT1/bHLH141* were then used as the query input for a TERA-BLASTN search in the Decypher package (TimeLogic, Carlsbad, CA, U.S.A.) against the IWGSC chromosome sequence survey (CSS)

assembly curated by the Applied Bioinformatics group at Rothamsted Research, U.K.

Decypher returned scaffold contigs which contained hits with identity to the *Brachypodium* cds sequences. The highest ranking hits were extracted and aligned individually with annotated rice and barley sequences to confirm intron-exon boundaries. To confirm correct annotation of coding sequence, predicted proteins from each putative homoeologue sequence were extracted and aligned with the known protein sequences of *OsGAMYB* and/or *HvGAMYB* (Fig. 4.1.).

Cereal GAMYB proteins shared 91.8% pairwise identity (Fig. 4.1. a). Moreover, the three wheat homoeologues and *HvGAMYB* are identical in the functional tandem R2 and R3 MYB-domains which has previously been described (Haseneyer *et al.*, 2008). Furthermore, the three wheat homoeologues contained three highly conserved functional domains (Box 1, 2 and 3; see Gocal *et al.*, (2001)) which have been implicated in functional specificity in the aleurone which are only partially shared in rice *GAMYB-like* genes (Tsuji *et al.*, 2006). The presence of an R2R3 MYB domain and other conserved domains indicates that the identified sequences are *GAMYB* orthologues.

Full length coding sequences could be assembled from CSS contigs for all three *TabHLH141* homoeologues (Fig. 4.1. b). Pairwise alignment with *OsEAT1/bHLH141* and *BdEAT1/bHLH141* reveal significant conservation of sequence homology (86.5% pairwise identity) with the putative wheat homoeologues. All three *TabHLH141* homoeologues share a high degree of similarity in the rice and *Brachypodium* HLH domain (amino acids 256 – 364) and the C-terminal Domain of Unknown function (DUF). Previous work determined that *OsEAT1* shares around 40% homology in both domains with rice homoeologue *OsBHLH142 (OsTIP2)* and three *Arabidopsis* homoeologues *AtbHLH89*, *AtbHLH91*, *AtbHLH10* (Niu *et al.*, 2013). Therefore, the observation of 86.5% amino acid identity between *OsEAT1*, *BdEAT1* and the three wheat homoeologues identified here indicates that they are orthologous.

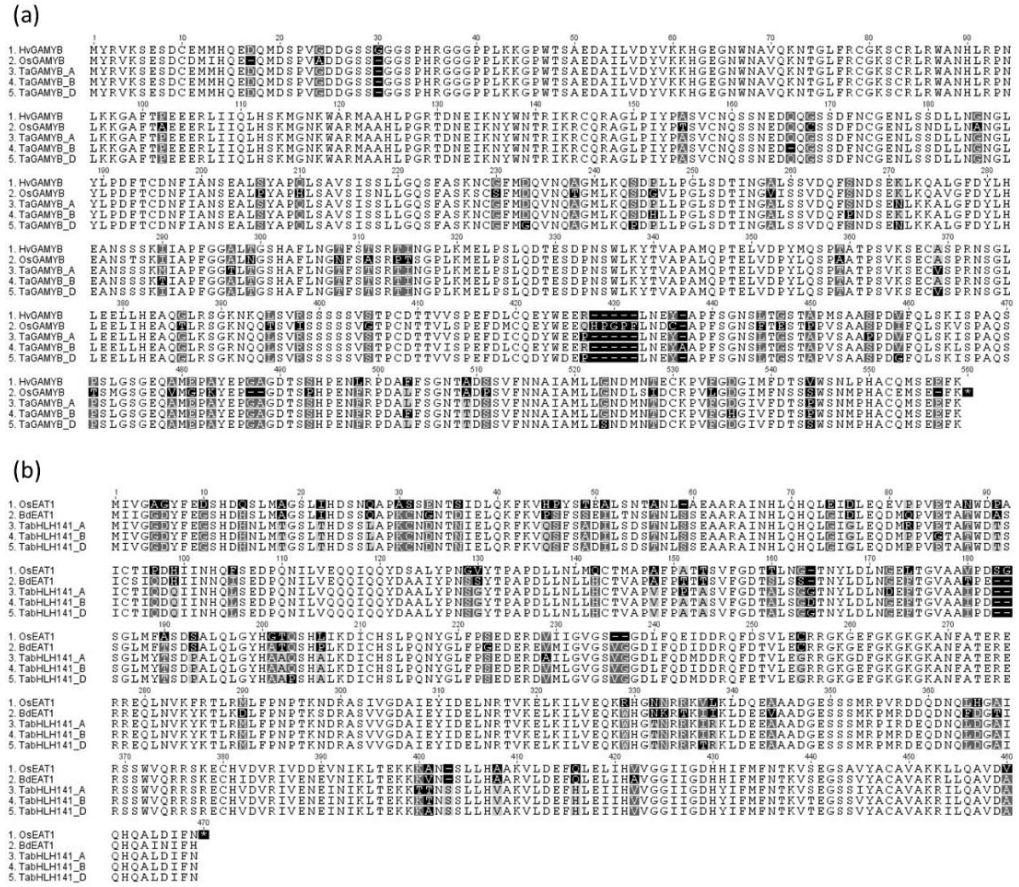


Figure 4.1. Protein alignments of putative a) *TaGAMYB* and b) *TabHLH141* sequences predicted from sequence isolated from IWGSC CSS. *The most closely related Brachypodium orthologues to OsGAMYB and OsEAT1/bHLH141 were used to identify wheat genome sequences containing shared sequence identity. Predicted cds translation proteins were aligned with rice and barley sequences to confirm orthology. Alignments were carried out in Geneious using the MUSCLE tool. Alignments contained 91.8% and 86.5% pairwise identity respectively, indicating the wheat sequences identified are target gene orthologues.*

Both *TaGAMYB* and *TabHLH141* belong to large gene families which are conserved amongst angiosperms and have undergone extensive evolutionary divergence. It is therefore important to compare putative orthologues to known orthologues in other species to establish the phylogenetic relatedness of the candidate sequences to known orthologues and distinguish between potential paralogues. A previous search for *TaGAMYB* sequences in an EST

library found two sequences containing the reverse complement of the miR159 binding site (see section 1.4.2.) and therefore identified a second *GAMYB-like* transcript (Wang *et al.*, 2012). This nucleotide sequence was identified in the IWGSC reference genome named *TaMYB15*. The three homoeologues cds sequences of *TaMYB15* were extracted and placed in a phylogenetic tree with the putative *TaGAMYB* orthologues identified above and other related *GAMYB* and *GAMYB-like* sequences to establish their evolutionary relationship and further confirm their identity. The wheat *TaGAMYB* sequences were most similar to barley, rice and *Brachypodium* orthologues as previously shown by sequence alignments (Fig. 4.2. a). *TaMYB15* (*GAMYB-like*) and *OsGAMYB-like* sequences formed separate clades confirming their evolutionary separation from *TaGAMYB*. The presence of closely related paralogues resulting from gene duplication is evident in dicot species which obviously segregated from the monocot cereal species. *TabHLH141* is most closely related to rice and *Brachypodium* orthologues (Fig. 4.2. b). Interestingly, other members of the rice *bHLH* family which include TFs with characterised functions in anther development form a separate clade. *OsTDR*, *OsEAT1* and *OsTIP2* form a consecutive signalling cascade and it has previously been suggested that they might have arisen from gene duplications during evolution (Fu *et al.*, 2014) (see section 1.3.2.).

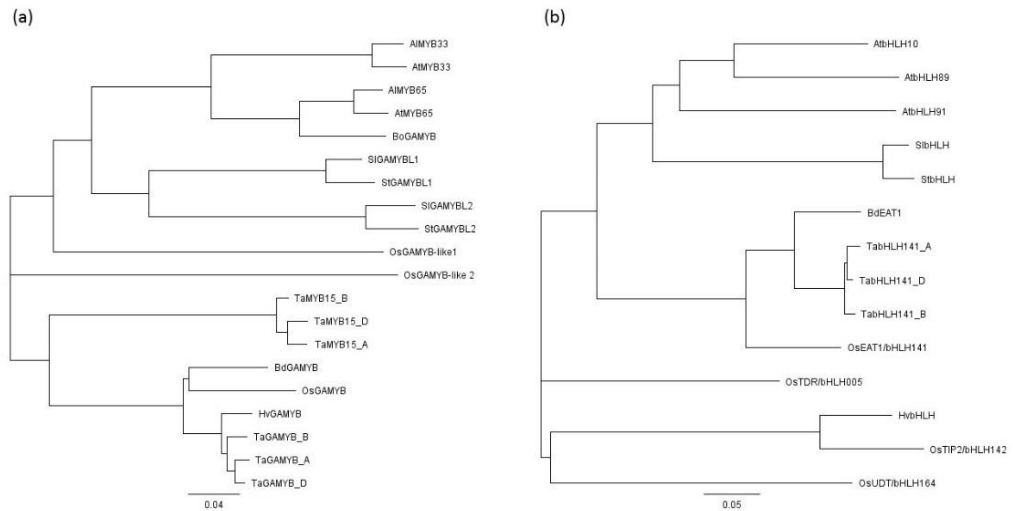


Figure 4.2. Phylogenetic trees for *TaGAMYB* and *TabHLH141*. Putative orthologue sequences from *Arabidopsis thaliana* (*At*), *Arabidopsis lyrata* (*Al*), tomato (*Sl*), potato (*Sl*) rice (*Os*), wheat (*Ta*), *Brachypodium distachyon* (*Bd*) and barley (*Hv*) were compared to similar sequences in other species using the Geneious tree builder tool using the Neighbor-joining method. a) *TaGAMYB* homoeologues are most closely related to orthologous cereal species and *OsGAMYB*-like and *TaMYB15* (*GAMYB*-like) form separate clades. b) *TabHLH141* is most closely related to rice and *Brachypodium EAT1* orthologues. Other rice *bHLH* family members show significant divergence from *EAT1*. In both cases the evolutionary separation of dicot and monocotyledonous species is evident.

During the course of this project further improvements were made to the availability and quality of wheat gene sequences. Firstly, an improved IWGSC with some gene annotation became available in which both *TabHLH141* and *TaGAMYB* coding sequences were uniquely labelled with a *TRAES_* identifier. More recently the TGACv1 assembly has significantly expanded the coverage of the wheat reference genome. Both genes have been identified in the updated reference genomes (Table 4.1.). All genes in successive reference genomes were extracted and nucleotide fidelity was confirmed by cds alignment (not shown).

| Homoeologu e | IWGSC identifier | TGAC v1 identifier |
|-----------------|--|--|
| | | TRIAE_CS42_3AL_TGACv1_195431_AA064950 |
| TaGAMYB_A | TRAES_3AL_F09C7CA19 TRAES_3BF027700010CFD_t | 0 |
| TaGAMYB_B | 1 | TRIAE_CS42_3B_TGACv1_223446_AA0782290 |
| TaGAMYB_D | TRAES_3DL_D9A29948B | TRIAE_CS42_3DL_TGACv1_253186_AA0893720 |
| TabHLH141_ A | TRAES_2AL_6FC5FIFDO | TRIAE_CS42_2AL_TGACv1_094707_AA0301850 |
| TabHLH141_ B | TRAES_2BL_1DDA22EA3 | TRIAE_CS42_2BL_TGACv1_129925_AA0399500 |
| TabHLH141_ D | TRAES_2DL_9DD224B48 | TRIAE_CS42_2DL_TGACv1_158620_AA0523420 |

Table 4.1. Gene identification labels in reference genome assemblies. *Both TaGAMYB and TabHLH141 are found in the wheat genome reference assemblies and gene structures have been annotated according to the respective gene models used.*

To further confirm the identity and confirm the expression during anther development of identified *TaGAMYB* and *TabHLH141* orthologues, qRT-PCR was carried out on wheat (var. Cadenza) anthers cDNA collected from plants grown in standard controlled environment conditions at 5 cm, 10 cm, 15 cm and GS43 FLS (see section 3 for further information on developmental staging) (see section 2 for primers and qRT-PCR materials and methods). *TaActin* was selected based on the previous use of *OsActin* as an anther reference gene (Aya *et al.*, 2009) and previous characterisation of its consistent, stable

expression in wheat anthers during development (J. González, pers. comm.)

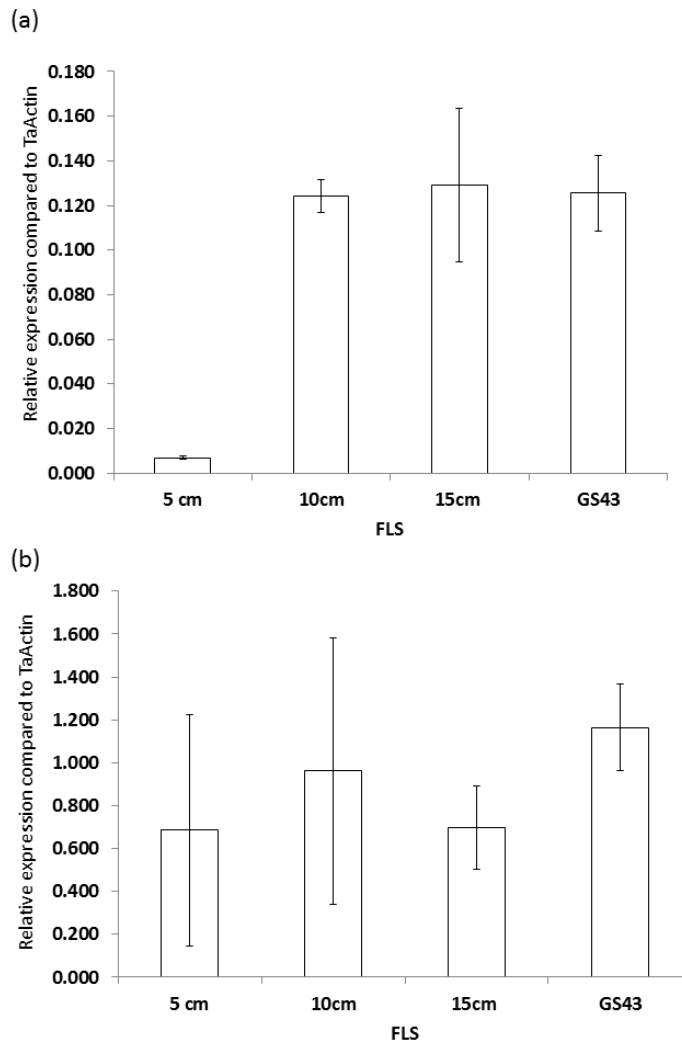


Figure 4.3. Quantification of (a) *TaGAMYB* and (b) *TabHLH141* expression during wheat anther development. Anther samples were taken from plants at four FLS lengths. Normalised relative expression was quantified using the reference gene *TaActin*. Mean normalised expression of three biological replicates are shown. Error bars represent one standard error of the mean.

The expression of *TaGAMYB* is highly up regulated between FLS 5 cm and 10 cm after which it is consistently expressed to mature pollen (Fig. 4.3. a). This is consistent with previous observations of *OsgAMYB* and *HvGAMYB* (Murray *et al.*, 2003; Aya *et al.*, 2009), suggesting that the putative *TaGAMYB*_orthologues identified above share a conserved expression profile in cereal species and provides further evidence that they are true orthologues of characterised

GAMYB sequences in other species. The expression profile observed for *TabHLH141* is less comparable to that recorded for its rice orthologue. *OsEAT1* expression is highly expressed between pollen cell meiosis and mitosis (Niu *et al.*, 2013) whereas *TabHLH141* expression was also observed in pre-meiosis (FLS 5 cm) and pollen maturation (GS43) (Fig. 4.3. b). Whilst these data confirm that *TabHLH141* is expressed in wheat anthers, further work is needed to clarify its specific expression profile.

4.3.2. *Tagamyb-RNAi* and *Tabhlh141-RNAi* plants are male sterile

RNAi constructs targeting *TaGAMYB* and *TabHLH141* were generated and transformed into wheat to characterise their function through the knocked-down phenotype. RNAi triggering expression cassettes were designed, cloned and transformed in to wheat via biolistics (see section 2.4.2.). Stable transformant T₀ plants from independent transgenic events were identified by genotype and grown to seed to form segregating lines (see section 2.4.2.). Positive T₂ and T₃ lines showed dramatic reductions in fertility compared to the null segregants. The loss of fertility was attributed to a failure to complete anther and pollen development, confirming the role of both genes in male reproductive development in wheat.

4.3.2.1. RNAi target design

With careful design, it is possible to silence all three homoeologous copies of a wheat gene with a single construct. At the same time, it is also important to ensure target specificity of all potential RNAi triggers generated by a construct.

Firstly, to ensure the silencing of all homeoalleles, the protein coding nucleotide sequences obtained above were aligned in Geneious and inspected for regions of continuous homoeologous identity (Fig. 4.4.).

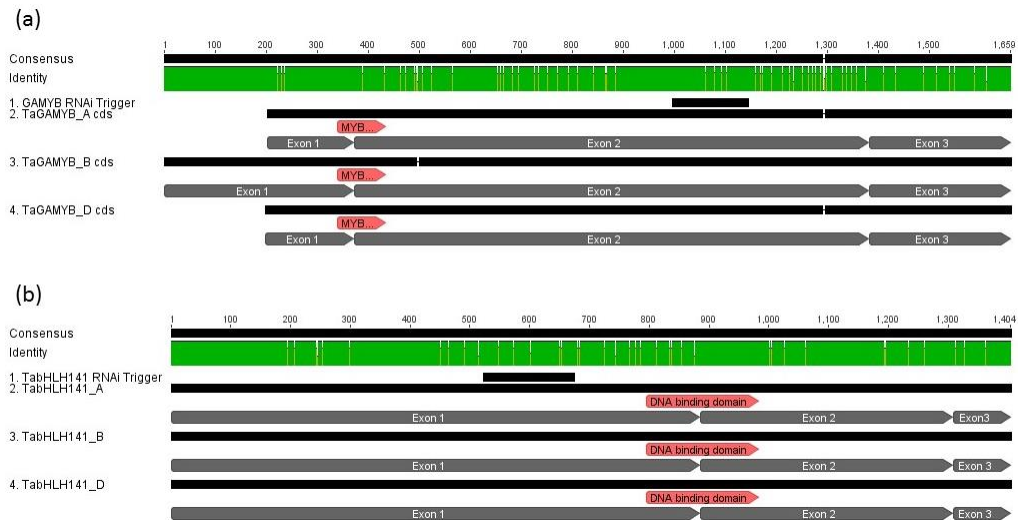


Figure 4.4. Schematic showing selection of RNAi trigger sequences for *TaGAMYB* and *TabHLH141*. Regions of 100% sequence homology between homoeologues are indicated by the green identity bar. Highly conserved functional domains have been annotated in red. a) a *TaGAMYB* RNAi trigger was identified in exon 2 and b) in exon 1 for *TabHLH141* (black bar).

100 – 250 bp sections of consensus sequence with 100% identity were compared to the IWGSC CSS reference genome using BLAST. Sections containing hits longer than 21 bp matching genes other than the target gene were rejected as they might trigger off-target silencing. No suitable continuously identical regions of sequence were suitable for target-specific silencing. The cellular RNAi machinery digests double stranded RNA triggers into 21-26mer guide siRNAs, meaning that a small number of single nucleotide polymorphisms between homoeologues can be tolerated in the trigger sequence provided it contains at least 1 21mer which is 100% identical to all three homoeologues. A 147 bp region in exon 2 of *TaGAMYB* (Fig. 4.4. a) and 151 bp region in exon 1 of *TabHLH141* (Fig. 4.4. b) were selected and confirmed as target-specific RNAi trigger sequences by BLAST search against the IWGSC CSS reference genome.

RNAi plasmids *pOsAct::GAMYB::RNAi* and *pOsAct::bHLH141::RNAi* were then cloned and transformed into wheat (var. Cadenza) as described in section 2.

4.3.2.2. Selection of transgenic lines

A total of 38 *pOsAct::TaGAMYB::RNAi* and 39 *pOsAct::TabHLH141::RNAi* T₀ plants were recovered from independent transgenic events from 2 separate bombardments with each construct.

Four positive lines from each bombardment were randomly selected and 1 T₁ seed sown, established and genotyped by PCR using AdH intron and Nos terminator specific primers (see Table 2.1.) Once plants reached the grain filling stage it became obvious that certain individual transformant plants had significantly reduced fertility, although other plants in which the transgene was present showed normal grain filling. In all instances there was obvious variation in grain number, with some plants having many unfilled grain positions.

Based on the phenotypic and genotypic characterisation of *pGAMYB::RNAi* and *pbHLH141::RNAi* lines, good candidates with reduced fertility and a high likelihood of being homozygous for the transgene were identified. The following plants were selected for continuation and renamed as follows:

pGAMYB::RNAi R3P20e 6 – *gamyb-RNAi* 1

pGAMYB::RNAi R8P4b 5 – *gamyb-RNAi* 2

pGAMYB::RNAi R7P1 Null – *gamyb-RNAi* Null

pbHLH141::RNAi R9P8 6 – *bhlh141-RNAi* 1

pbHLH141::RNAi R6P3 2 – *bhlh141-RNAi* 2

pbHLH141::RNAi R6P7b Null – *bhlh141-RNAi* Null

4.3.2.3. Characterisation of positive lines

T₂ seed from the selected null lines were potted and established in standard glasshouse conditions (see section 2.1.). TaqMan zygosity testing was carried out on gDNA extracted from all plants as described above in order to ensure phenotypic characterisation of homozygous individuals (Fig 4.5.).

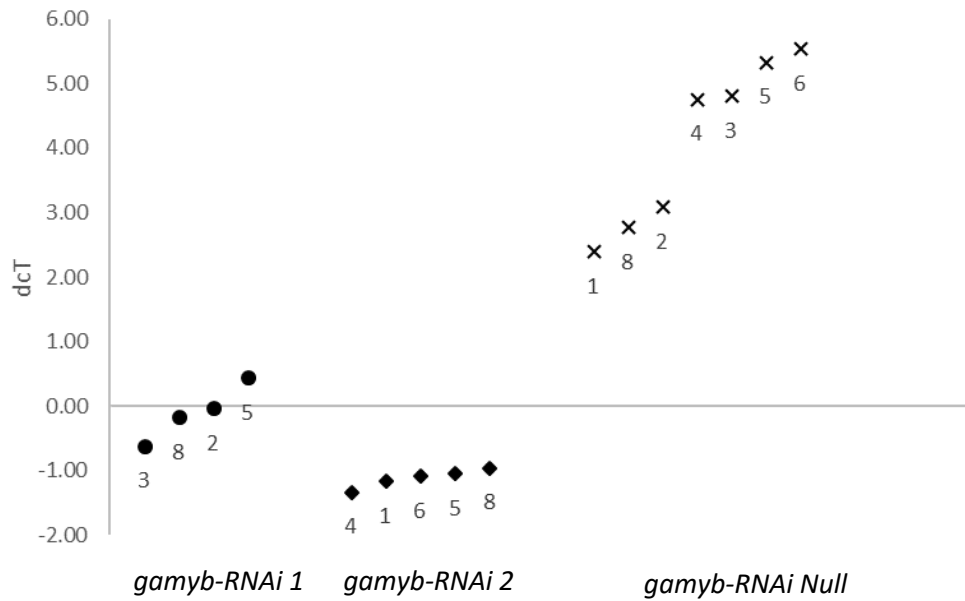


Figure 4.5. Zygoty of T₂ *gamyb-RNAi* plants. *dcT* is a relative value indicating the difference in amplification of a known, single copy, reference gene and an RNAi construct-specific fragment i.e. plants with the most negative scores are likely to be homozygous. Four *pGAMYB::RNAi* lines contain individuals with - *dcT* values double that of the highest scoring plant suggesting that they are homozygous for the transgene.

Figure 4.8 shows that most of the zygoty and copy number of *pOsAct::GAMYB::RNAi* based on relative amplification of the transgene to a known, single copy reference gene *HvCon* (see section 2.4.3.) Individuals with a negative *dcT* value can be inferred to have a higher dose of the transgene than the reference gene. Relative amplification of the transgene target in homozygous plants should be double that of a heterozygous plant whilst null plants should have *dcT* values approaching 0 but are more likely to have positive values as technical inefficiencies. Furthermore, multiple insertions would further distort amplification ratios. It would therefore be expected that in *dcT* values clustering into positive and 0 null values, and negative heterozygous and homozygous groups. Although this did not occur in these lines, organising *dcT* in ascending order assists in identifying individuals with negative *dcT* scores double that of the highest scoring heterozygous individual which are therefore most likely to be homozygous. In some cases, the inferred

genotype from the Taqman assay conflicts with that obtained by PCR. These individuals were discarded. Zygosity could not be resolved in *bHLH141-RNAi* plants and therefore plants were selected on PCR genotype (not shown), however, this could only be achieved in *bHLH141-RNAi 2* plants.

Three individual biological replicate plants were grown for each line for comparative analysis. Based on the observed reduction in fertility of the parents in the previous generation a more comprehensive analysis of reproductive development was carried out to better understand the roles of *TaGAMYB* and *TabHLH141* in wheat anthers.

Reduced fertility in *gamyb-RNAi 1* and -2 compared to the null line was evident in the T₂ generation (Fig. 4.6.). All floret positions formed anthers with normal appearance in both *gamyb-RNAi* lines. Just prior to GS61 (anthesis), anthers were harvested from all lines and prepared for pollen viability staining (see section 2.6.). In *gamyb-RNAi 1* and -2 pollen grains were irregular in shape, lacking in sufficient cytoplasm to cause the vacuole to fill the cell and in some cases completely lacking in cytoplasm (Fig. 4.6. a.) whilst the null line pollen appeared normal (Fig. 4.6. b.).

Some evidence of tapetal hypertrophy and locular disorganisation at stage 7-8 was evident in *gamyb-RNAi* plants (Fig. 4.6. c.) whilst null plants appeared normal (Fig. 4.6. d.). Upon completion of flowering, developing grain become easily distinguishable as they accumulate assimilate and swell sufficiently to force florets open (Fig. 4.6. e). Figure 4.9. e. shows a clear difference in the number of floret positions filled with developing grain between transgenic and null segregant spikes. At this stage the total number of grain and floret positions on three secondary spikes was counted on all lines. Presence of the transgene had a significant effect on average grain number per spike ($P < 0.001$); *gamyb-RNAi 1* and -2 had significantly fewer grains per spike compared to the null line (L.S.D. 1% and 5% respectively). Average floret positions were counted and found not to differ between lines (not shown)

confirming that reduced grain number was due to a loss of fertility rather than smaller spikes *per se*.

Kaneko *et al.*, (2004) reported a shortening of the final internode length (the distance between the junction of the stem with the culm/spike and the previous stem node) of rice *Osgamyb* T-DNA insertion lines. Final internode length was also found to be significantly reduced in *gamyb-RNAi 1* compared to the null line ($p < 0.001$; L.S.D. 5%) (Fig. 4.6. e) but not in *gamyb-RNAi 2* (Fig. 4.6. f). Based on the grain number and internode length measurements, this suggests that the phenotype of *gamyb-RNAi 2* may be due to a reduced level of silencing of GAMYB than in *gamyb-RNAi 1*.

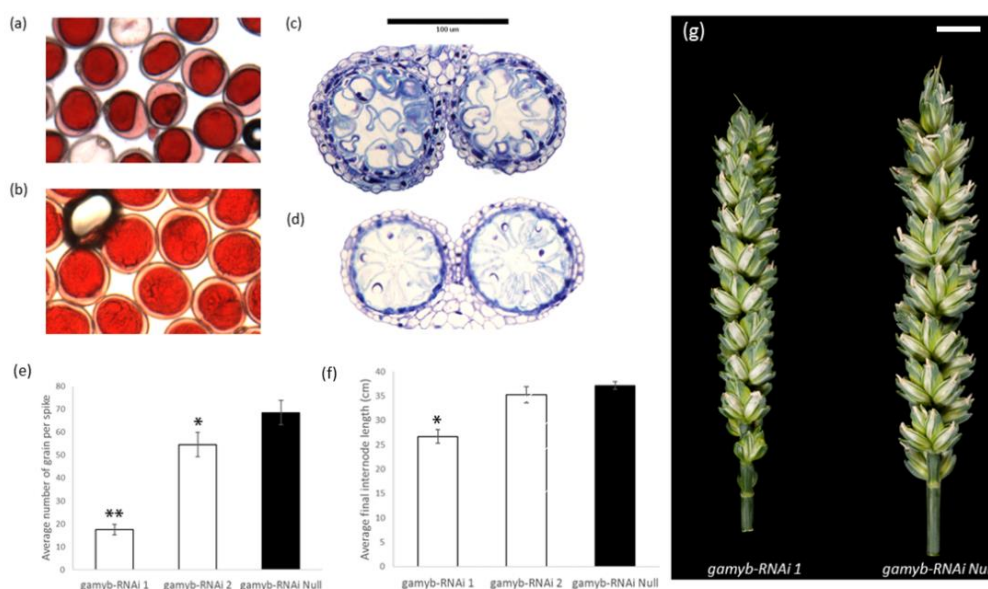


Figure 4.6. Phenotypic characterisation of *gamyb-RNAi 1*, -2 and Null lines. Pollen viability was assessed by Alexander stain in a representative RNAi line (a) and the Null line (b). Internal anther morphology was examined using light microscopy (c and d). Mean grain numbers (e) and mean final internode distance (f) on three main tillers were for three biological replicates were calculated for *gamyb-RNAi* lines (open bars) and the null line (black bar). Error bars are one standard deviation of the mean. * is statistically different to the Null mean by 1 least significant difference $P \leq 0.05$, ** $P \leq 0.001$. Representative spikes were photographed (g), Scale bar = 1 cm.

To further resolve the cause of observed male fertility defects in *gamyb-RNAi 1* and *2*, thin sections of anther tissue at stage 7-8 was examined by light microscopy at an increased magnification (Fig. 4.7.). *gamyb-RNAi* tapetum cells have evident vacuolation of tapetum cells and the middle layer is still present. At the same stage null tapetum cells have become condensed, a sign of degradation and the middle layer has degenerated.

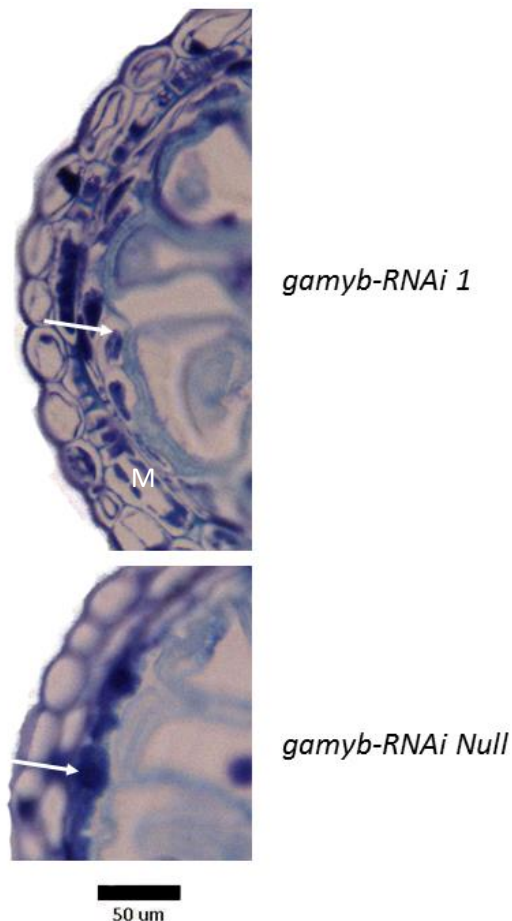


Figure 4.7. Increase magnification of *gamyb-RNAi 1* and *Null* tapetum. Anthers at vacuolated pollen stage are shown. White arrows indicate tapetum cells, M – Middle layer.

Although two independent *bHLH141-RNAi* lines were selected, consistent genotypic and phenotypic characterisation of *bHLH141-RNAi 1* could not be obtained and it was therefore excluded from the analysis. Unlike the *gamyb-RNAi* line, pollen in the transgenic lines (Fig. 4.8. a) appears similar to the null wild type (Fig. 4.8. b) with a regular shape and packed cytosol.

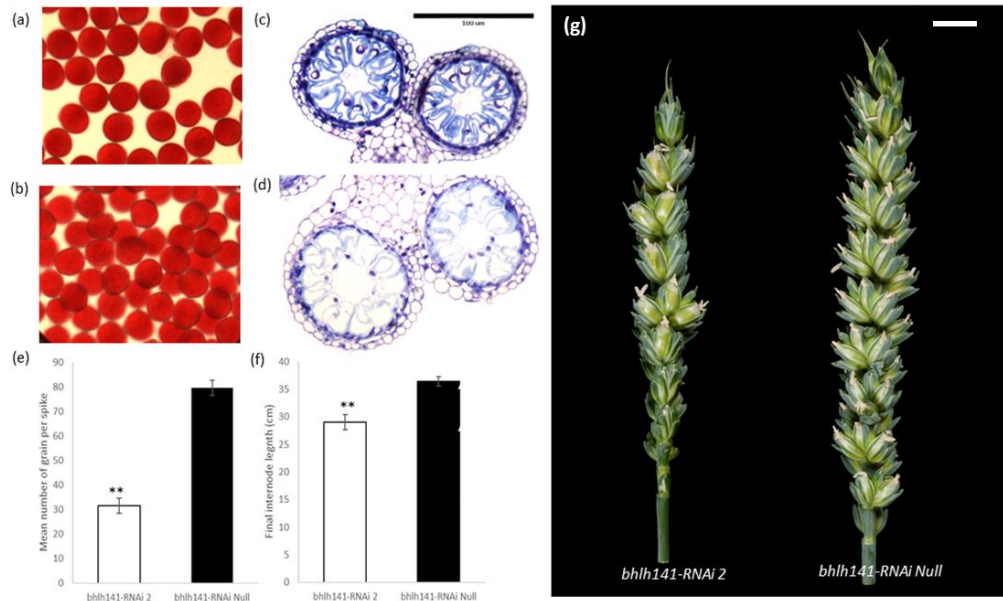


Figure 4.8. Phenotypic characterisation of *bhlh141-RNAi 2* and Null lines.

*Pollen viability was assessed by Alexander stain in a representative RNAi line (a) and the Null line (b). Internal anther morphology of a representative bhlh141-RNAi 2 (c) and Null (d) plant was examined using light microscopy. Mean grain numbers (e) and mean final internode distance (f) on three main tillers were for three biological replicates were calculated for bhlh141-RNAi lines (open bars) and the null line (black bar). Error bars are one standard deviation of the mean. ** is statistically different to the Null mean by 1 least significant difference $P \leq 0.001$. Representative spikes were photographed (g).*

Likewise, despite a pronounced loss of fertility, no obvious differences in internal anther morphology could be detected between selected *bhlh141-RNAi 2* (Fig. 4.8. c) and null (Fig. 4.8. d) anthers. Average grain number (Fig. 4.11. e) was significantly reduced in *bHLH141-RNAi 2* compared to the wild type ($P \leq 0.001$; L.S.D. 1%) which again was not due to reduced spike size *per se* as there was no significant difference in average number of florets (not shown). Final internode length was also found to be significantly reduced in the transgenic line ($P \leq 0.001$; L.S.D. 1%) (Fig. 4.8. f). Figure 4.8. g shows the same sporadic floret grain setting phenotype compared to the null in *bHLH141-RNAi 2* plants as observed in the *gamyb-RNAi* lines.

To confirm silencing of *TabHLH141* qRT-PCR was carried out on anther samples taken from *bhlh141-RNA 2* and null line plant. Anthers were harvested at GS43, when both *TaGAMYB* and *TabHLH141* are expected to be expressed based on previous analysis (Fig. 4.3.).

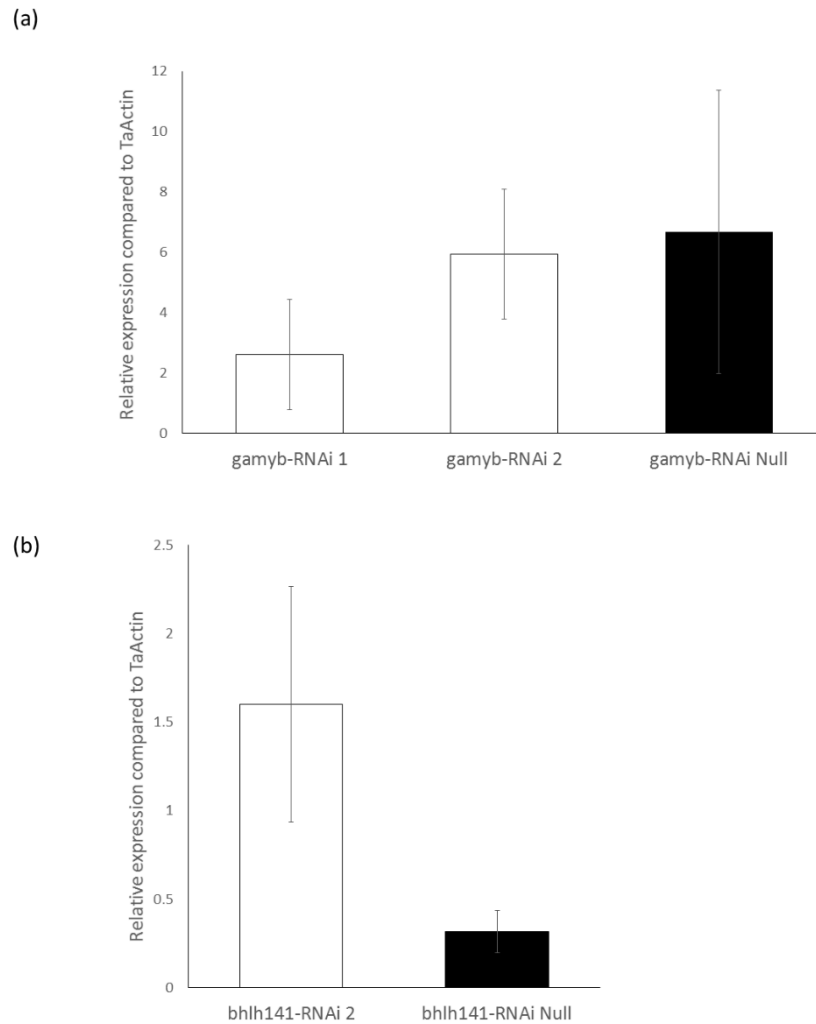


Figure 4.9. Quantification of target transcript relative abundance in RNAi and Null lines. (a) *gamyb-RNA 1* and *-2* (open bars) and Null line (black bar). (b) *bhlh141-RNAi 2* (open bar) and Null line (black bar). Values are mean normalised expression values (NRQ) of the target gene compared to the *TaActin* reference gene. Averages were taken of NRQs 3 biological replicates (with the exception of *gamyb-RNAi 2* which is 2 replicates). Error bars represent one standard error of the mean.

Expression of *TaGAMYB* in the T₂ plants appears to be more reduced in *gamyb-RNAi 1* than -2, which are both lower than the null line (Fig. 4.9. a). This agrees with the severity of the male sterile phenotype observed in these plants (Fig. 4.6. e and g). This suggests that more complete RNAi gene silencing of *TaGAMYB* in *gamyb-RNAi 1* is responsible for the more severe loss of fertility and reduction in internode length compared to *gamyb-RNAi 2*. However, in *bHLH141-RNAi 2* expression of the target gene was higher than in the null line despite also showing a strong male sterility phenotype (Fig. 4.8.b). No statistically significant differences when compared by general ANOVA were observed between any lines. Clearly, very little can be inferred from these data and further investigation will be required to confidently attribute the observed phenotypes to silencing of the targeted genes.

4.3.3. *Tagamyb* lines generated by TILLInG are male sterile

The use of RNAi to silence *TabHLH141* and *TaGAMYB* expression in wheat has provided some evidence that both genes are required for anther and pollen development. However, in both instances silencing was not complete resulting in variable phenotypes which are difficult to interpret. TILLInG was therefore used in an attempt to generate complete loss-of-function mutants for validation of phenotypic abnormalities observed in gene silenced lines. A search of the Cadenza M₄ TILLInG SNP database identified lines carrying predicted premature stop codons in the coding sequence of the three *TaGAMYB* homoeologues (see annex I). Only one premature stop codon in *TabHLH141_A* coding sequence was identified whilst all other mutations in *TabHLH141_B* and *_D* resulted in either missense or synonymous changes. In the absence of evidence that missense mutations would result in loss-of-function, TILLInG in *TabHLH141* was not pursued any further. In order to produce complete knock-out *Tagamyb* lines the SNPs were validated and stacked by crossing.

4.3.3.1. Validation of *TaGAMYB* SNPs

Identified SNPs were mapped to coding regions of *TaGAMYB* and confirmed to result in in-frame introduction of premature stop codons (Fig. 4.10.).

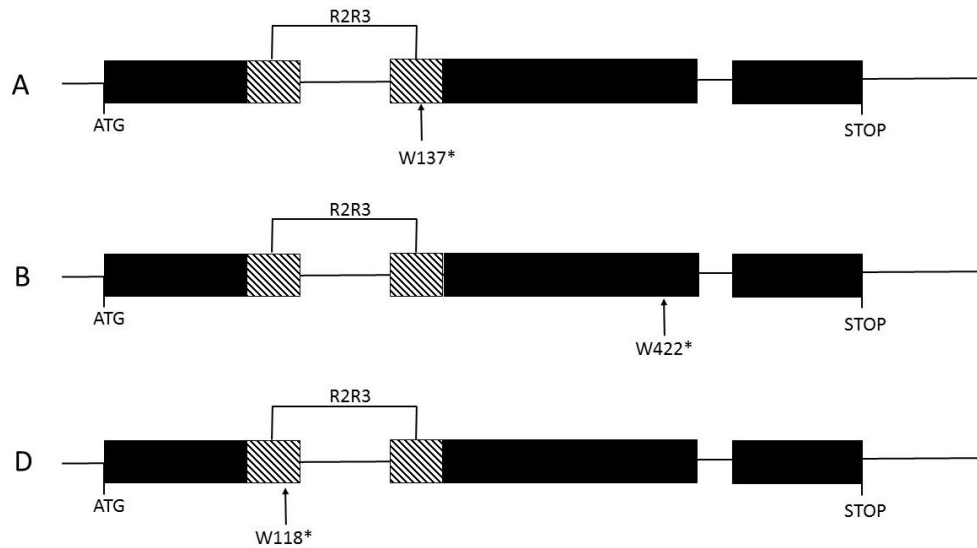


Figure 4.10. Schematic representation of SNP positions in *TaGAMYB* homoeologues. Exons are black boxes. Arrows represent approximate position of nucleotide change. Hashed regions represent conserved R2R3 Myb domain. Letter indicates wildtype residue, numbers nucleotide position, * stop codon.

To confirm the position and zygosity of the SNPs, BAM files containing the Illumina reads mapped to the reference sequence genome for M₄ lines (obtained from Dr. Phillips) were visually inspected in Integrative Genomics Viewer v2.3 software (Broad Institute, Cambridge, M.A., U.S.A.). Figure 4.11. shows the alignment of sequencing reads of three M₄ lines each containing SNPs in *TaGAMYB_A*, *_B* and *_D* respectively. In each case the region containing the SNP is well covered by individual mapped reads to support the call. The number of SNP called reads (shown in green) compared to wild type (grey) in the *TaGAMYB_A* and *B* lines confirms roughly to the mendelian 3:1 ratio which supports the heterozygous call. Likewise, all the reads in the *TaGAMYB_D* line are SNP called confirming that the mutation is homozygous in this line. In all cases the sequencing confirms that the SNPs result in a TGG

codon encoding Trp in coding exons being changed to a TGA stop codon (not shown).

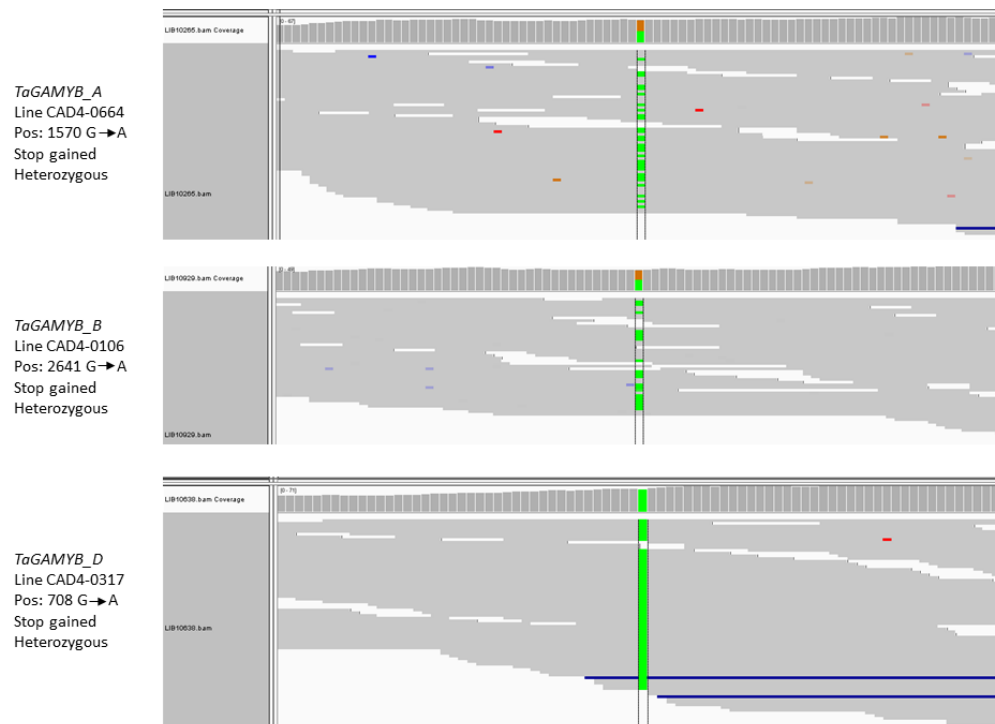


Figure 4.11. Visualisation of exon-capture reads to *TaGAMYB* reference sequence. Grey horizontal bars represent sequencing reads mapped to the reference. Coloured segments indicate mismatched bases to the position, mismatched bases represented in sufficient quantity and consistency to be considered SNPs are coloured green.

Six M₄ seed of each line (obtained from Dr. Phillips) were established under standard glasshouse conditions. Genomic DNA was extracted from seedling leaf material of each plant (see section 2.1.1.). Using homoeologue specific primers (see section 2.5.) genomic fragments incorporating the target SNP were amplified by PCR and gel extracted and purified as described in section 2.2. The amplified fragments of homoeologue specific DNA were then sequenced using the amplification primers (see Table 2.1.) and aligned to the reference sequence in Geneious (BioMatters Ltd, Auckland, New Zealand) (Fig. 4.12).

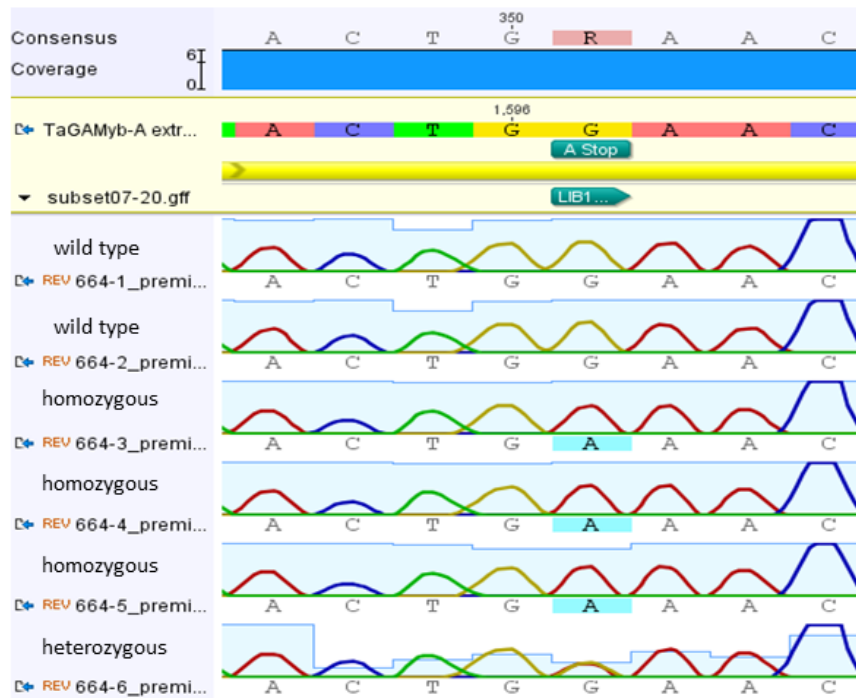


Figure 4.12. Sequencing alignment of TILLInG mutants. 6 M_4 individuals were sequenced with *TaGAMYB* homoeologue-specific primers and aligned to the respective reference sequence. *TaGAMYB_A* sequencing shown to demonstrate genotype calls. SNPs are highlighted in blue. The zygosity of SNP was determined manually and is annotated next to the line name.

Figure 4.12. shows the alignment of sequencing reads to the reference of 6 M_4 individuals of *TaGAMYB_A* homoeologue TILLInG line. SNP zygosity of each line was called manually according to relative amplitude of the base signal. Solid single base peaks were called as either wild type or homozygous depending on the base, heterozygous positions were determined by overlapping peaks of wild type and SNP base signals at around half the amplitude of a homozygous position. Plants in which there were any ambiguity in base call at the SNP position were discarded. In total 3 homozygous and 1 *TaGAMYB_A*, 2 heterozygous *TaGAMYB_B* and 5 homozygous and 1 heterozygous *TaGAMYB_D* TILLInG mutant plants were identified.

These plants and their progeny were crossed as described in section 2.5. Firstly *_A* and *_B* mutants were crossed into homozygous *_D* background.

Combinations of double mutant F1 individuals were then crossed and heterozygous triple mutants were selected in the F2 generation. F2 triple mutants were allowed to self-fertilise and to produce segregating triple and double homozygous and null lines. All selections were made according to genotype data obtained by sequencing as described above.

4.3.3.2. Homozygous *Tagamyb* plants are male sterile

In total 5 plants containing all three homoeologous mutations (*Tagamyb*) in a homozygous state were obtained. Like *gamyb-RNAi 1* and *-2*, *Tagamyb* plants showed reduced fertility, however *Tagamyb* plants were almost completely sterile, producing only a few grain per ear. As plants were not bagged at anthesis it is possible that grains were produced as a result of low frequency outcrossing with neighbouring fertile plants.

Comparative assessment of anther development in *Tagamyb* plants and a segregating wild type plant was carried out to determine if the observed loss of fertility was caused by male sterility (Fig. 4.13.). When wild type plants reached anthesis anthers could be seen extruding from florets. During the same period of development anthers did not extrude in *Tagamyb* plants. Comparable florets were dissected *in situ* and photographed (Fig. 4.13. a). *Tagamyb* anthers are noticeably shorter and darker yellow than the wild type. No filament extension appears to have occurred in *Tagamyb* nor the shedding of any pollen which can also be observed in the wild type. This appears to be the cause of the failure of *Tagamyb* to consistently set grain compared to the wild type (Fig. 4.13. b). To confirm that the observed male developmental defects are the cause of the sterility as opposed to female development, a *Tagamyb* spike was cross-pollinated with a pollen shedding wild type spike. Figure 4.13. c shows that many more grain are produced by *Tagamyb* spikes when fertilised with viable, wild type pollen confirming that *Tagamyb* is male, but not female sterile.

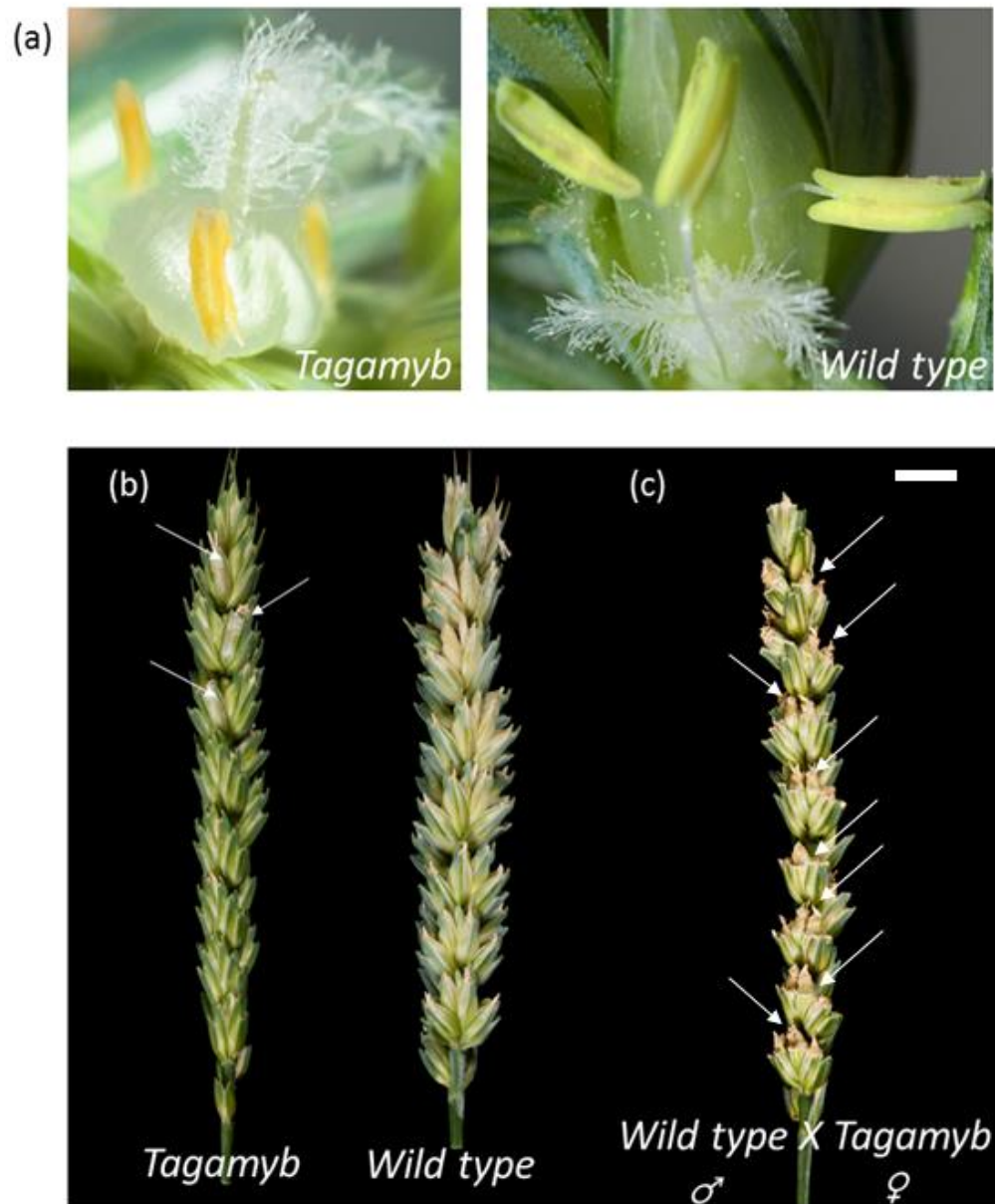


Figure 4.13. Abnormal anther development in *Tagamyb* plants. a) Anthers in *Tagamyb* plants taken at reproductive maturity. b) Whole spikes taken during grain filling.. c) A *Tagamyb* spike during grain filling after cross-pollination with wild type pollen. White arrows indicate positions with a developing grain, wild type 100% fertile. Scale bar = 1 cm.

Given the characterised role of *GAMYB* in anther development, specifically tapetum PCD (see section 1.4.3.) and observed tapetum defects in *gamyb-RNAi* plants (see section 4.3.2.3.), anthers were harvested from *Tagamyb*

plants at early developmental stages (FLS 5 – 10 cm) and later developmental stages (GS43) and prepared for light microscopy as described in section 2.6. Severe defects in internal anther development were observed and lead to a failure to produce viable pollen (Fig. 4.14.).

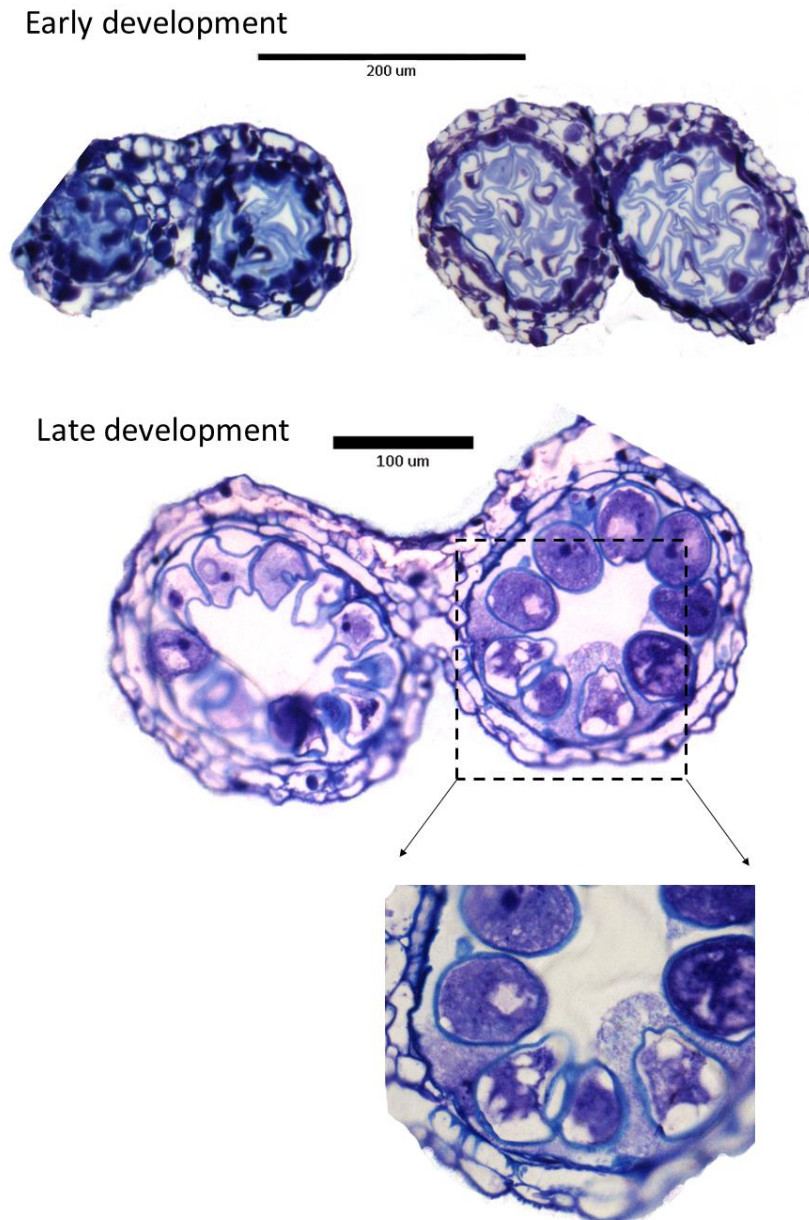


Figure 4.14. Thin section of *Tagamyb* anthers at different stages of development.

Internal morphology of *Tagamyb* at early stages (see section 3.3.) indicates that pollen development has progressed beyond meiosis with what appears to be crescent shaped nuclei distinctive of the vacuolated pollen stage (stage 7 –

see section 3). However, wild type anthers locules at this stage are more uniformly organised with easily definable microspores aligned to the tapetum surrounded by a distinguishable elliptical cell wall (Fig. 3.3. g). Here, microspores are irregularly shaped and individuals cannot be easily defined. This suggests that *TaGAMYB* may have a role in determining post-meiotic anther organisation, however, the effect may also be caused by constriction due to the reduced size of *Tagamyb* anthers. At the later stage of development, when mitosis and pollen maturation is occurring in wild type anthers (see section 3.3.1.), *Tagamyb* anthers have an accumulation of staining material within the locule which has not previously been observed in wild type anthers. Furthermore, some *Tagamyb* pollen cells have not taken a regular, spherical shape nor appear to have accumulated as much carbohydrates as others. This is consistent with observed phenotypes in other GA-signalling and biosynthesis mutants (see section 1.4.). However, further work is required to establish if the observed defects are the cause of male sterility in these plants and to what extent *Tagamyb* affects anther and pollen developmental processes.

4.3.4. TabHLH141 interacts with RHT-1

The Arabidopsis homoeologue of TabHLH141, AtbHLH089 was previously shown to bind with the DELLA protein RGA, in a yeast 2-hybrid screen of anther-expressed cDNA (S. Thomas, pers. comm.). Having demonstrated that *TabHLH141* is required for male fertility (see section 4.3.2), the role of GA-signalling in regulation of TabHLH141 was investigated by yeast 2-hybrid assay. Yeast 2-hybrid assays are an established method for studying specific protein-protein interactions by co-expression of one gene as a GAL4 trans-activation domain (AD) fusion (bait) and the other as the DNA-binding domain (DBD) (prey). Interaction between the two encoded proteins brings the GAL4 AD and DBD into close proximity, driving the expression of the *HIS3* reporter gene. Interaction can be quantitatively assessed by growing co-transformed strains on His⁻ media containing HIS3 competitive inhibitor 3-AT; strains

expressing strongly interacting proteins are able to tolerate higher concentrations of 3-AT.

TFs often have native trans-activational ability and as such DELLA::AD fusion proteins have previously been shown to self-activate in the absence of an interacting prey::DBD protein (S. Thomas, pers. comm.). Therefore, a truncated version of RHT-D1 containing only the C-terminal GRAS domain thought to suppress plant growth by interacting with target promoter regions (Hirano *et al.*, 2012) was used in this study in order to minimise background trans-activation of *HIS3*. All fusion protein vector cloning, transformation was carried out as described in as described in section 2. Positive control known interactors AtGAI - AtARF-19 were supplied by Dr. S. Thomas.

The RHT-D1GRAS domain was found to interact with the full length TabHLH_141_B protein (Fig. 4.15). Growth of strain 4 (Rht-D1GRAS – bHLH141) is maintained at 50 mM whereas growth of strain 2 (Rht-D1GRAS – empty prey) is abolished at 40 – 5030 mM 3-AT indicating that interaction between RHT-D1GRAS and bHLH141 is driving stronger expression of *HIS3* above the background level of RHT-D1GRAS self-activation. Likewise, growth of strain 3 (empty bait – bHLH141) is inhibited at 30 mM 3-AT, showing that *HIS3* expression requires the interaction between RHT-D1GRAS and bHLH141. Growth of the strain 4 (Rht-D1GRAS – bHLH141) is not as strong at 50 mM 3-AT as strain 5 (AtGAI – AtARF-19), demonstrating suggesting that the assayed interaction is weaker than the positive control. Growth of strain 6 (bHLH141 – empty prey) at 50 mM 3-AT shows that bHLH141 can transactivate *HIS3*, as is common in TFs used as bait.

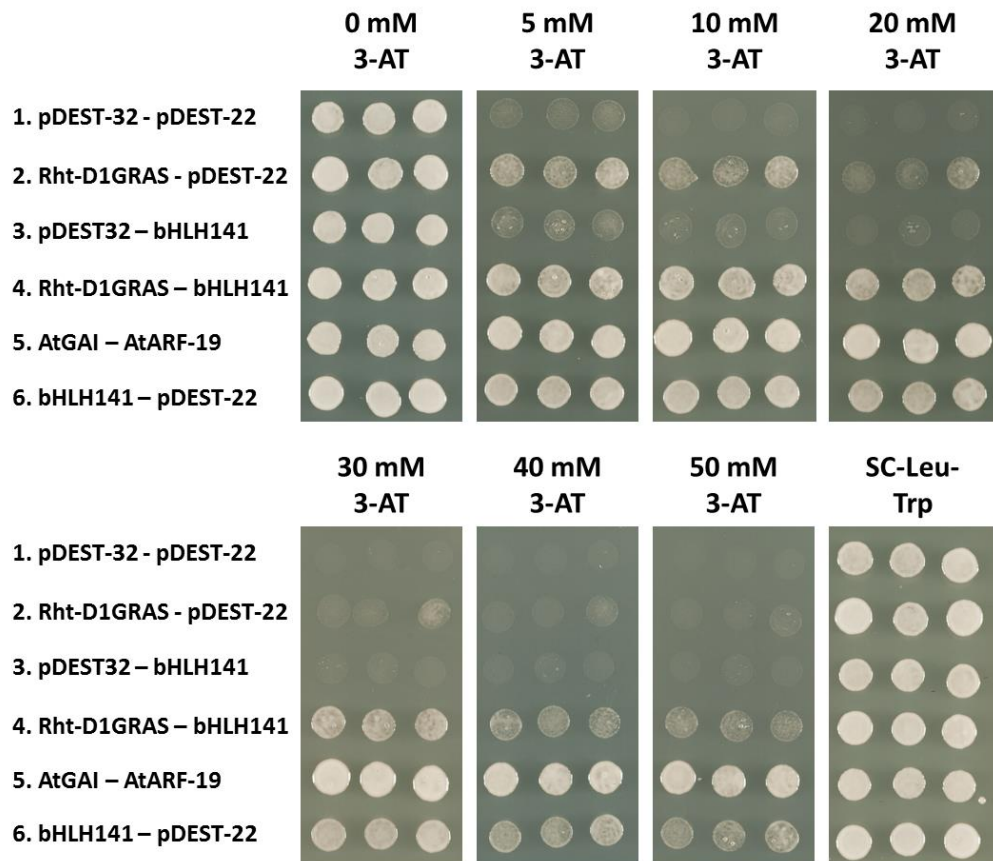


Figure 4.15. Interaction between RHT-D1-GRAS and TabHLH141. Co-transformed yeast strains were grown on SC-Leu-Trp/His⁻ plates containing 0, 5, 10, 20, 30, 40 and 50 mM 3-AT and a SC-Leu-Trp plate containing His⁻ (negative control). 1 – empty vector control, 2 – bait only self-activation control, 3 – prey only control, 4 – interaction assay, 5 – known interaction positive control, 6 – prey as bait self-activation control.

The observed interaction between RHT-D1GRAS and bHLH141 observed here indicates a potential role for GA-signalling in the regulation of tapetum PCD via the post-transcriptional regulation of bHLH141. However, further work will be required to confirm if this interaction occurs *in planta* and if so, how binding by DELLAs affects function and transcriptional regulation by bHLH141.

4.4. DISCUSSION

Wheat orthologues of two genes of interest, *TaGAMYB* and *TabHLH141*, have been identified and their functions in male reproductive development

investigated through the generation and characterisation of reduced or loss-of-function mutants. Clearly, both transcription factors have important roles in ensuring pollen development, however, from the phenotypes observed in the above experiments significant questions remain as to the mechanisms in which they are involved.

Taking advantage of the high levels of synteny between related cereal species genomic DNA sequences for *TaGAMYB* and *TabHLH141* were identified in the wheat reference genome (section 4.3.1.). *GAMYB* has been the focus of previous research for its role in cereal germination and seedling establishment (see section 1.4.1.) and therefore full length genomic sequence data in wheat was available at the beginning of the project whilst *bHLH141* was only characterised in rice as *OsEAT1* (Niu *et al.*, 2013). Nonetheless, both genes were identified in the IWGSC CSS reference with a high degree of confidence based on encoded protein identity with inter-species orthologues (Fig 4.1.) and phylogenetic relationships therein (Fig. 4.2.). BLAST searches of the CSS reference suggested that both genes are present in single copies like in rice and barley and have not undergone any further duplication. This conclusion was further supported by the more complete TGAC v1 reference in which paralogues of either gene are not present.

Expression analysis carried out by qRT-PCR demonstrated that both genes are expressed in developing wheat anthers (Fig.4.3. a). The expression profile of *TaGAMYB* was consistent with the stable expression of *HvGAMYB* and *OsGAMYB* in anthers after the formation of PMCs through to pollen maturity (Murray *et al.*, 2003; Tsuji *et al.*, 2006). Further work is required to quantify *TaGAMYB* expression at specific developmental stages and tissue localisation. The latter could be addressed using *in situ* hybridisation or laser-microdissection of specific anther tissues as described by Suwabe *et al.*, (2008). The expression of *TabHLH141* could not be as clearly resolved (Fig 4.3. b). *OsEAT1* expression overlaps with *GAMYB* but is most strongly expressed between late meiosis and young microspores, consistent with its role in executing tapetum PCD (Niu *et al.*, 2013). Therefore, staging of anther

material to specific stages may be required to in order to reduce the amount of variation associated with observed mean *TabHLH141* expression profile.

4.4.1. The role of *TaGAMYB* in wheat male fertility

Having obtained genomic sequences for all three homoeologues of *TaGAMYB* an investigation into their functions during male reproductive development was carried out using RNAi-mediated gene silencing and TILLING. As shown by previous studies in rice (Kaneko *et al.*, 2004; Aya *et al.*, 2009; Liu *et al.*, 2010), *TaGAMYB* plays an important role in tapetum and pollen development (Fig. 4.6.). Some evidence of tapetal hypertrophy was observed in *gamyb-RNAi 1* plants (Fig. 4.7.) although not with the same severity as seen in the rice mutants. Indeed, the pollenless and hypertrophic tapetum phenotype of the rice mutants is not replicated in these plants, suggesting that sterility is due to disruption of tapetum processes support of pollen development rather than PCD.

Tagamyb plants showed a more severe and consistent male sterility phenotype (see section 4. 3.3.). In plants with homozygous copies of all three homoeologous premature stop codon mutations anthers are severely stunted (Fig. 4.13. a) with highly disorganised internal morphology (Fig. 4.14.), although no tapetal hypertrophy was observed. Where pollen development progressed, pollen cells lacking in cytoplasm and locules full of material were observed (Fig. 4.14.) as they were in the RNAi mutants. Furthermore, the fertilisation of *Tagamyb* florets with wild type pollen shows that female fertility is not effected by the loss of *TaGAMYB* function (Fig 4.13. c.). No obvious loss of fertility was incurred by plants carrying single or double homozygous SNPs nor in the triple heterozygous lines (not shown). Although no statistical comparisons of grain numbers were carried out, the observation nonetheless indicates that even a basal level of *TaGAMYB* expression is sufficient to ensure fertility and a high level of homoeologous functional redundancy is likely.

Together, these mutants demonstrate that *TaGAMYB* is critical for the completion of anther and viable pollen development in wheat. GA-signalling co-ordinates anther and pollen development through *GAMYB* (Aya *et al.*, 2009). Generally, GA-signalling mutants display some degree of male sterility attributable to aberrant microspore meiosis, pollen wall formation and desynchronisation of tapetum development (see section 1.4.1.) although phenotypes are often incomplete and variable even at the ecotype level (Plackett *et al.*, 2014). Therefore, whilst it's clear that GA-signalling plays some role in ensuring synchronicity between tapetum and pollen, it's not yet clear how downstream components such as *GAMYB* are involved in such coordination. For example, *OsGAMYB* expression is tapetum-specific, but Kaneko *et al.*, (2004) observed disrupted pollen mother cell meiosis in *Osgamyb* mutants, suggesting a role in cell-cell communication. Here, mature pollen cells lacking cytoplasm and the accumulation of material in post-meiotic anthers of *gamyb-RNAi* and *Tagamyb* plants (Fig. 4.7., Fig. 4.14) was also observed, further supporting the implication of *GAMYB* in microspore as well as tapetum development.

The presence of material inside the locule which has not been taken up by pollen cells in *gamyb-RNAi* and *Tagamyb* plants may be indicative of a loss of ability to correctly package and transport metabolites by the tapetum. A similar phenotype was observed in *rga.gai* mutants (Plackett *et al.*, 2014), indicating that the DELLA-*GAMYB* anther signalling module is involved in the regulation of metabolite transport and uptake. So far two of the most comprehensively characterised functions of *GAMYB* are in the GA-mediated upregulation of carbohydrate mobilisation in developing grain (see section 1.4.3) and promoting the expression of two sporopollenin biosynthesis genes *KAR* and *CYP703A3* in the tapetum (Aya *et al.*, 2009). In the absence of the aberrant PCD phenotype, the male sterility of the wheat *gamyb* mutants appears to be caused by non-viable pollen. Therefore, further biochemical analysis of mutant locular fluid and pollen cell wall and cytoplasmic constituents using scanning electron microscopy (SEM) might give further

indication of the precise role of *GAMYB* in the preparation of pollen components. Furthermore, identification of *KAR* and *CYP703A3* orthologues wheat and investigation of the effect of loss of *TaGAMYB* on their transcription would help to further confirm the role of *TaGAMYB* in wheat pollen development.

Alternatively, it may be that an alternative pathway in wheat ensures that PCD occurs and the loss of *GAMYB* is only a minor perturbation of the initiation process. Liu *et al.*, (2010) showed that *OsgAMYB* and *OsuDT1* independently regulate the expression of *OstDR*, an important component of tapetum PCD regulatory signalling (Li *et al.*, 2006a) and PCD fails to initiate in mutants of all three genes (Jung *et al.*, 2005; Li *et al.*, 2006a; Liu *et al.*, 2010). Quantification of *TDR* expression in *gamyb-RNAi 1* and *-2* would help to determine these pathways are also connected in wheat; their existence would seem likely given their conservation between dicot *Arabidopsis* and closely related cereal and monocot rice (Liu *et al.*, 2010). The DNA staining assay TUNEL is regularly used to detect DNA fragmentation associated with apoptotic PCD (see section 1.3.2.) and could be deployed in a developmental series of *gamyb-RNAi* anthers to determine if and when the developmental programme of the tapetum is disturbed by silencing of *TaGAMYB*. Similarly, further confirmation of gene silencing, such as quantification of *TaGAMYB* in anther tissue by western blot, is required to verify that the observed phenotype is associated with *TaGAMYB* silencing.

Interestingly, Lui *et al.*, (2014) recognised that the position of T-DNA and stop-codon mutations in rice *gamyb* mutants has an effect on the resulting phenotype. For example, in the *Osgamyb-2* mutant, which carries an insertion in the third exon, pollen development is arrested after meiosis whilst in *Osgamyb-1* and *-3*, in which the insertion is in the second exon, abnormal meiosis is observed (Kaneko *et al.*, 2004). Downstream targets of *GAMYB* have so far been identified based on the presence of *GAMYB* binding motifs in upstream promoter regions (Aya *et al.*, 2009). It is therefore conceivable that *GAMYB* proteins truncated, or reinitiated prior to certain domains are able to

retain some functions, indeed GAMYB contains three interspecies conserved motifs additional to the MYB domain which are thought to function in transcriptional regulation (Gocal *et al.*, 2001). *Tagamyb* contains premature stop codons in the A and D MYB domain regions and upstream of Box 2 in the B homoeologue (Fig. 4.10.). It is possible that some transcriptional function is retained by the B homoeologue if a truncated protein carrying a functional MYB domain and conserved Box 1 and 2. It is therefore important that alternative alleles are identified and tested to further confirm the role of GAMYB. A number of other premature stop codon and missense SNPs in *TaGAMYB* coding sequence were identified in the exon capture array (not shown), investigation of SNPs in other domains may reveal more information about how the structure of GAMYB affects its function.

Likewise, the RNAi target region was located in the 3' region of exon 2 and therefore incomplete cleavage of transcripts could lead to the translation of a truncated protein which may explain the variability and incompleteness of the phenotype. The observation of significantly different levels of sterility in two positive *gamyb-RNAi* lines (Fig. 4.6. f.) highlights the inherent limitations of RNAi as a reverse genetics technique. Whilst incomplete silencing of a target gene may be of benefit in terms of propagation of male sterile lines, it is difficult to determine if the observed phenotype is the complete loss-of-function. This could be alleviated by robust molecular, quantitative assaying of target transcript and protein levels however, Figure 4.9. demonstrates that determining RNAi gene silencing by qRT-PCR in wheat is also problematic. Firstly, as discussed in Chapter 3, staging of anther development in wheat can be achieved by measurement of the FLS, however, final internode length was significantly reduced in *gamyb-RNAi 1* plants (Fig. 4.6. g.) and therefore without specific characterisation of *gamyb-RNAi 1* internal and external development it is likely that highly developmentally variable anther material was tested. This perhaps explains why the mean expression levels of both target genes are associated with large standard errors and do not differ significantly from the null. Secondly, qRT-PCR primers for wheat genes must

be designed in a similar manner to that of the RNAi target, ensuring target specificity and identity with all three homoeologues. Whilst extensive validation of the primers used here was carried out (not shown), attempts to quantify *TaGAMYB* and *TabHLH141* in wild type anther tissue had also yielded similarly variable results (Fig. 4.3.) suggesting that further technical refinement could assist in linking observed phenotype to loss of gene function.

The *Tagamyb* mutants presented in this work represent the segregating homozygotes from a population of the progeny of selfed heterozygotes. Therefore, there were insufficient numbers of segregating triple mutants and null types to complete a statistical comparison of fertility traits such as grain numbers. Furthermore, several rounds of marker-assisted backcrossing will be required to ensure that no other mutations are influencing the phenotype. Similarly, the limitations of RNAi restrict the amount which can be inferred from the mutant phenotypes. Other transgenic approaches, such as transcriptional repressor fusion domains or overexpression of the native *TaGAMYB* negative regulator *mR159* (see section 1.4.2.), could be useful alternatives but still depend on transgenesis and therefore many of the same limitations apply.

The shortening of the final internode of both *gamyb-RNAi* lines (Fig. 4.6. g) is a curious observation. Kaneko *et al.*, (2004) also reported reduced final internode lengths in *Osgamyb* insertion mutants, raising the possibility that *GAMYB* is somehow involved in the regulation of peduncle growth. Reduced stem elongation is a common phenotype in GA-signalling mutants (see section 1.4.), however at present there is no evidence for the involvement of *GAMYB*. Exposure of *Arabidopsis* shoot apex to GA₄ or inductive conditions causes an increase in the expression of *GAMYB-like* genes and the floral regulator *LEAFY* (Gocal *et al.*, 2001) whilst loss of a rice floral repressor *EARLY FLOWERING 1*, a DELLA phosphorylating kinase which regulates GA responses during floral transition, results in male sterility by essentially overexpressing *OsGAMYB* (Kwon *et al.*, 2015). Clearly, the spatio-temporal activation of GA-signalling

during early floral development also has ramifications for later anther development and the restriction the peduncle elongation may represent an early perturbation of a GA-signalling feedback system. However, the shortened final internode phenotype was also present in the *bhlh141-RNA 2* plants (Fig. 4.8. f.). The expression or potential functions of *bHLH141* in stem elongation, if any, is unknown. Therefore, caution should be taken when interpreting the role of GAMYB in peduncle elongation when the same phenotype is seen in an independent TF mutant. Without further information about the location of the transgene insertions, the possibility that a functional locus has been disrupted cannot be discounted.

4.4.2. The role of *TabHLH141* in wheat male fertility

A significant loss of fertility was observed in *bhlh141-RNAi 2* plants (Fig. 4.8. e). However, internal anther morphology (Fig. 4.8. c) and pollen viability (Fig. 4.8. a) appeared normal in the anthers selected for analysis. Rice orthologue EAT1 directly regulates the expression of two aspartic proteases (Niu *et al.*, 2013) and two cysteine proteases (Ji *et al.*, 2013) in the rice tapetum which trigger PCD. *eat1-1* mutants have delayed tapetum PCD, but not the hypertrophy associated with *GAMYB* and *TDR* mutants (Niu *et al.*, 2013). Therefore, without specific analysis of the timing of PCD initiation through TUNEL in *bhlh141-RNAi* mutants, it is not possible to determine if PCD is delayed in these plants.

The dramatic reduction in grain numbers in *bhlh141-RNAi 2* provides strong evidence that *TabHLH141* is required for fertility. However, the phenotype was incomplete with some positions setting grain. As plants were not bagged at anthesis it is not clear whether this is the result of a leaky RNAi phenotype or outcrossing with fertile siblings. However, as discussed in the context of *gamyb-RNAi*, RNAi is often leaky and the formation of grains in certain positions may be due to some anthers “escaping” the targeting of *TabHLH141*. In this case, the apparently random distribution of fertile and infertile floret positions (Fig. 4.8. f) makes it difficult to select the ideal material for

cytological and molecular analysis, perhaps accounting for the unexpectedly high expression levels of *TabHLH141* in *bhlh141-RNAi* 2 plants (Fig. 4.9. b).

4.4.3. Regulation of TabHLH141 by RHT-1

The observation that TabHLH141 interacts with the GRAS domain of RHT-D1 in the yeast 2-hybrid system (Fig. 4.15.) provides further evidence for a role for GA-signalling in the regulation of the tapetum in wheat anthers. DELLAs have previously been demonstrated to interact directly with PIF bHLH TFs during light-responsive hypocotyl growth (de Lucas *et al.*, 2008) (see section 1.4.). The consequence of this physical interaction is that, DELLAs restrict growth by binding with the PIF bHLH DNA-binding domain, preventing PIFs from associating with target gene promoters until relieved by GA-induced DELLA degradation. Therefore, it may be that GA promotion of RHT-1 degradation in the tapetum releases TabHLH141 from sequestration, allowing it to activate the expression of PCD-inducing genes.

Whilst yeast 2-hybrid is an established method of investigating protein-protein, further work is needed to confirm that the observed RHT-1 – TabHLH141 interaction occurs *in planta*. Whilst yeast 2-hybrids give an indication of the strength of an interaction between two proteins, they are both very highly expressed in yeast cells and in the absence of other competing and regulating factors which may occur in plant cells. Interaction between two proteins *in planta* can be determined by co-immunoprecipitation (Co-IP) in which precipitation from a tissue lysate of both proteins by an antibody specific to only one of the proteins of interest. However, previous attempts to raise specific antibodies against RHT-1 have so far been unsuccessful (Pearce *et al.*, 2011). An alternative approach is biomolecular fluorescence complementation (BiFC) in which both proteins are expressed in fusion with corresponding fragments of the yellow fluorescent protein (YFP). Interaction between the fusion proteins brings the two fragments into proximity, forming a functional YFP, creating an interaction signal which can be visualised by confocal microscopy. However, this

approach depends on the successful generation of stable transgenic wheat plants, the limitations of which are discussed above.

The rice orthologue, OsEAT, is downstream of OsTDR with which it forms a heterodimer which enhances the expression of lipid transfer and PCD – executing genes (Ji, Niu). *OsGAMYB*, *OsSLR1* and *OsTDR* are expressed in the tapetum between meiosis and young microspores during the initiation of PCD (Li *et al.*, 2006; Plackett *et al.*, 2011). *OsEAT1* is strongly upregulated at these stages but continues to be expressed during tapetum degeneration (Niu *et al.*, 2013). Therefore, it may be the case that *OsGAMYB* and *OsTDR* co-promote the expression of *OsEAT1* during tapetum PCD-initiation but its transcriptional activity is tightly regulated by competitive binding by SLR1 and TDR. *GA3OX*, which catalyses the final step in the biosynthesis of bioactive GA, is upregulated in degenerating tapetum cells and bicellular pollen (Plackett *et al.*, 2011), which based on the observed interaction between TabHLH141 and RHT-D1GRAS (Fig. 4.15.), would be expected to release DELLA repression of TabHLH141 and enhancing tapetum cellular degeneration. Therefore, based on the observed interaction between RHT-D1GRAS and TabHLH141 and previously described mutant phenotypes in both wheat and rice, a putative GA-signalling pathway in wheat anthers during tapetum PCD is proposed (Fig. 4.16.)

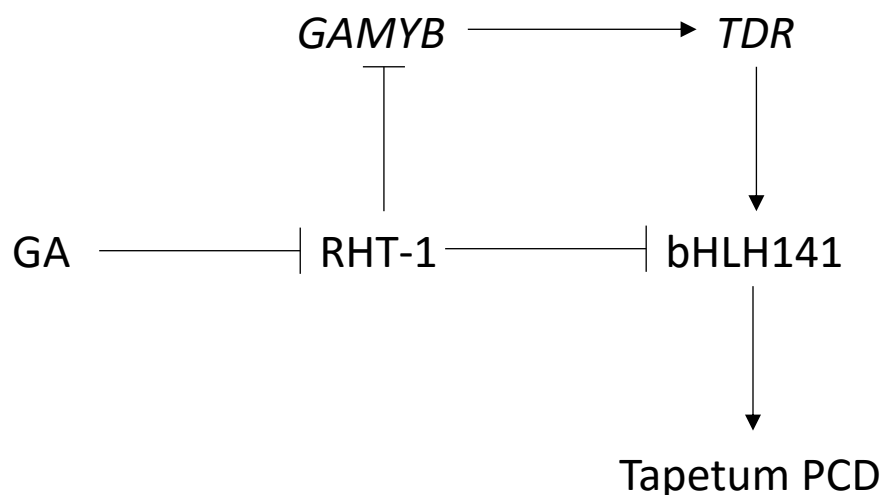


Figure. 4.16. Putative tapetum PCD GA-signalling pathway. Bioactive GA production during tapetum degeneration releases the repression of TabHLH141 by RHT-1. GA may further promote the expression of *TabHLH141* by promoting the expression of *TDR* via *GAMYB* (based on rice mutants).

However, further work will be required to confirm this signalling pathway in wheat anthers. The development of *Tabh141* and *Tagamyb* mutant (see section 4.3.1.) presents an opportunity to identify downstream targets of both TFs. Furthermore, to our knowledge this is the first example to show a direct interaction between RHT-1 and another protein other than GID1. Therefore, further dissection of this interaction could provide further explanation of the role of functional domains within RHT-1. The GRAS domain first leucine-heptad repeat is thought to be required for interaction with bHLH TFs (de Lucas *et al.*, 2008) which could explain why different *Rht-1* alleles have varying effects on male reproductive development.

MYB proteins have also been demonstrated to interact with bHLH and other TFs to form transcriptionally active complexes (see section 1.3.2.). *GAMYB* is thought to be upstream of bHLH141, possibly regulating its expression via upregulation of *TDR* (Li *et al.*, *TDR*, Niu *et al.*, 2013). A similar yeast 2-hybrid study to determine whether *GAMYB* can also interact with TabHLH141 should also be carried out to determine if *GAMYB* enhances tapetum PCD through interaction with bHLH141. MYB and bHLH proteins have also been demonstrated to form tripartite regulatory complexes with WD-repeat proteins (Qi *et al.*, 2011; Tian *et al.*, 2016) which therefore should also be investigated. Likewise, characterisation of the wheat orthologue of *OsTDR* and generation of knock-out mutants will be vital in establishing the relative contributions of *Rht-1*, *GAMYB* and the non-GA regulated *UDT-TDR* pathway to wheat tapetum PCD execution by *TabHLH141*.

CHAPTER 5: THE TRANSCRIPTIONAL AND HORMONAL RESPONSE TO HT IN WHEAT ANTHERS

5.1. Introduction

HT stress during wheat reproductive development is predicted to become one of the most yield-limiting consequences of climate change in Northern Europe (Semenov and Shewry, 2011). Exposure to prolonged periods of HT causes irreversible damage to the developing anthers and microspores contained within, resulting in sterility (see section 1.1.1.). Whilst the full detail of the underlying causes of HT-induced sterility remain unclear, much progress has been made in establishing the associated changes in anther metabolism, gene expression and hormonal signalling that occur in response to HT stress.

Microarray and qPCR studies have been particularly useful in identifying HT-responsive genes in the anthers. Such genes in barley anthers identified by microarray could be categorised into stress-related, hormone signalling-related groups as well as specific genes involved in lipid metabolism, DNA replication and PCD (Abiko *et al.*, 2005; Oshino *et al.*, 2007; Sakata and Higashitani, 2008), conforming with the cytological defects observed in HT-stressed anthers (see section 1.5.). Indeed, the observed premature progression of anther development led to the hypothesis that HT-injury is associated with an acceleration of the expression of anther development genes (Oshino *et al.*, 2007).

Furthermore, numerous gene expression studies on HT-treated anthers have implicated changes in hormone signalling and biosynthesis gene expression in HT-stressed anthers (Oliver *et al.*, 2005; Sakata *et al.*, 2010; Ji *et al.*, 2011; Oshino *et al.*, 2011). ABA, GA and auxin are all required for development of the tapetum and pollen cells (Parish *et al.*, 2013) and the effect of HT-stress on their biosynthesis and signalling contributes to the disruption of anther and pollen development (Müller and Rieu, 2016). Auxin biosynthesis is reduced in barley anthers exposed to HT and has been linked to defective cell

proliferation and DNA replication (Oshino *et al.*, 2011) which can be restored by exogenous application of auxin (Sakata *et al.*, 2010). ABA is a stress hormone which can cause male sterility similar to that caused by HT (Saini *et al.*, 1984). Rice lines with reduced ABA biosynthesis in stressed anthers are better able to maintain carbohydrate supply to pollen cells via the tapetum (Ji *et al.*, 2011). ABA is an antagonist of GA which has a critical role in anther and tapetum development (see section 1.4.). A number of GA-signalling, tapetum-specific genes are down regulated in rice lines exposed to HT (Endo *et al.*, 2009) and wheat GA-signalling mutants have defects in tapetum PCD and microspore development (see section 4) similar to those seen under HT. Indeed, HT-tolerant rice lines are better able to maintain anther GA and IAA biosynthesis and repress ABA biosynthesis under HT (Tang *et al.*, 2007).

Clearly, anther hormonal and transcriptional responses to HT are interdependent but how they interact to elicit anther HT-responses is not very well understood. Here, analysis of whole transcriptome and global hormone changes in wheat anthers under control (20 °C) and HT (34 °C) was undertaken to better understand the relationship between developmental and stress-induced differential gene expression in the context of the anther hormonal status. Therefore, as well as identifying candidate genes for improving wheat HT-tolerance, improved understanding of hormonal regulation of anther HT responses may assist in the formulation and targeting of chemical interventions to maintain normal anther development under stress conditions.

RNA-Seq is a high throughput approach to transcriptome profiling that uses deep sequencing of total or fractionated RNA-derived cDNA fragments (Wang *et al.*, 2009). Mapping of these short reads to a reference genome, transcriptome or *de novo* assembly enables the simultaneous discovery of transcripts and quantification of their abundance (Wang *et al.*, 2009; Trapnell *et al.*, 2010). A major advantage of this approach over chip based hybridisation microarrays and qPCR is the potential of RNA-seq to quantify the

abundance of all transcripts and their isoforms within a sample (Garber *et al.*, 2011).

With the regular improvement of the wheat reference genome (IWGSC *et al.*, 2014; Chapman *et al.*, 2015) an increasing number of genes and their transcript variants are being identified and functionally annotated. It is now feasible in terms of sequencing cost, computational requirements and available genomic reference data to utilise RNA-Seq in wheat for whole transcriptome analysis.

This approach was used to investigate the transcriptional response in anthers to HT throughout a time course. The objectives of this experiment were to 1) identify genes which are differentially expressed in response to HT as candidates for further investigation, 2) determine the effect of HT on the temporal regulation of the anther transcriptional programme and 3) use gene ontology (GO) enrichment to investigate the impact of HT on biological processes occurring within the anther. In addition, the analyses will also provide a comprehensive list of the wheat genes which are expressed in the anthers.

Using RNA-Seq to carry out comparative global transcriptome profiling, a number of promising candidate genes which are differentially expressed under HT conditions were identified. In particular, the significant upregulation of transcripts potentially associated with tapetum metabolism, PCD and Ubisch body formation suggests that HT causes a detrimental acceleration of development resulting in loss of male fertility. Furthermore, combining hormone quantification with expression analysis of known GA-biosynthesis and signalling genes has revealed the fascinating possibility that HT causes alterations to the biochemical pathway through which GA is synthesised in the anther.

5.2. Materials and methods

5.2.1 RNA-Seq plant material

A total of 48 individual wheat plants (var. Cadenza) were established in a large growth room under standard conditions as described in section 2. When plants entered the stem elongation phase (GS30) they were divided equally into two groups of 24 and transferred to two Sanyo growth cabinets to acclimate for a period of 4-6 weeks. Standard controlled environment conditions (see section 2.1.) were used as the experimental control conditions in this experiment. When plants entered the booting stage, they were randomly divided into groups of 4, representing 1 experimental unit, which were randomly allocated control or HT treatment. There were three replicate experimental units for each treatment.

Using the non-destructive staging method described in section 3, it was established that at 5 cm FLS length anthers would be in the pre-meiotic stages of development. This stage was selected to ensure HT treatment coincided with meiosis and a period of high tapetum metabolic activity. When plants entered the booting stage, 10 tillers within each experimental unit measuring $4 \text{ cm} \pm 0.5 \text{ cm}$ were tagged and randomly allocated to a time point for sampling. After 24 hours the experimental procedure began and anthers from tillers allocated to T_0 were harvested. Experimental units allocated to HT treatment were transferred to a Sanyo cabinet with the following conditions 34/20 °C day/night, 16/8 h light day/night, 65/75% relative humidity and irrigation maintained. Anthers were harvested from the tagged tillers after 6 h (T_1), 12 h (T_2), 24 h (T_3) and 48 h (T_4), with T_0 occurring at the beginning of the 16 h photoperiod (Fig. 5.1.). Harvested anthers were immediately frozen in liquid nitrogen and stored at -80 °C.

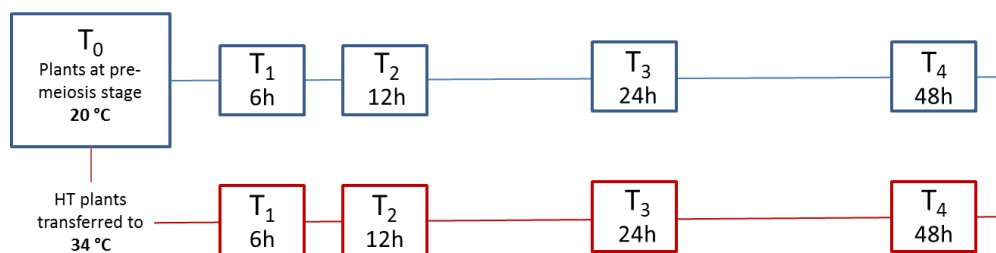


Figure 5.1. Experimental time course structure of RNA-Seq experiment. *Three biological replicates were collected at each time point.*

Total RNA was extracted, quantified and checked for integrity as described in section 2.3.

To investigate the effect of the HT-stress conditions on anther development, anthers harvested at T₃ (+24h) and +72h were fixed in resin and prepared for examination by light microscopy as described in section 2.6.

5.2.2. Sequencing of total mRNA

27 samples (3 x Control T₀, 3 x Control T₁₋₄, 3 x HT T₁₋₄) of total RNA was delivered to The Oxford Genomics Centre, Wellcome Trust Centre for Human Genetics, Oxford, U.K. for sequencing. Short read sequencing was completed using an Illumina HiSeq 4000 (Illumina, San Diego, CA, U.S.A.). cDNA libraries were prepared using PolyA selection to deplete ribosomal RNA contamination. Forward strand-specific sequencing of cDNA was carried out using 150 bp paired-end reads. Four technical replicates of each paired-end sequencing reaction were carried out on independent sequencing lanes.

5.2.3. Quality control and pre-processing of short reads

A total of 216 (27 samples x 4 technical replicates x 2 direction of read) fastq files were returned containing 150 bp read nucleotide sequence and accompanying quality metadata. All bioinformatics analysis was carried out within Rothamsted's Galaxy user interface instance (Sloggett *et al.*, 2013) unless otherwise stated. In order to visualise the sequencing quality information, each fastq file was entered into the FastQC tool (Babraham Bioinformatics, U.K.) which summarises various categories of sequence

quality. In general, all reads were of high quality. In all cases, base content and Kmer analysis returned warnings of overrepresented sequence. This was expected as contamination from short sequencing adapter oligonucleotides is common.

To remove the sequencing adapters, filter out short reads and trim low quality sequencing from the ends of reads, fastq files were processed using the Trimmomatic tool (Bolger *et al.*, 2014). First, each of the 4 pairs of fastq files for each sample were assembled into paired dataset collections which allows Trimmomatic to process them simultaneously. Each data list was then processed by Trimmomatic using default conditions other than the specification of TruSeq III adapter sequence removal, removal of reads shorter than 100 bp (MINLEN) and removal of read-end bases with quality scores lower than 15 (TRAILING).

After pre-processing approximately 50% of the sequenced reads had been discarded. This resulted in an effective sequencing depth of approximately 21x of the 361.58 Mbp TGACv1 transcriptome reference.

5.2.4. Mapping to a whole genome reference and counting

Initially, sequenced reads were aligned to a whole genome reference sequence to allow transcript identification and counts. The IWGSC whole genome reference is curated within the Rothamsted galaxy instance, the version used was the publically available IWGSC reference scaffold, T.Aestivum_Dec. 2015 (IWGSC1.0+popseq/ENSEMBLEv29 (genome) available from Ensembl and was selected as the reference genome in the TopHat alignment tool (Kim *et al.*, 2013). TopHat aligned sequencing reads to the reference genome using default parameters with the exception of the following: library type: FR First Strand, supply own junction data: use gene annotation model. The gene annotation model used was `Triticum_aestivum.IWGSC1.0_popseq.29.gtf`.

TopHat is a multifunctional spliced aligner which allows mapping of sequenced reads which span introns, permitting the use of a whole genome reference sequence (Kim *et al.*, 2013). TopHat produces a BAM file (a binary Sequence Alignment/Map file) which contains a list of read alignments. The 4 BAM files produced by each technical replicate were combined using the MergeSamFiles tool to produce 1 BAM file for each of the 27 samples and sorted by mapped chromosomal coordinates.

The Cufflinks tool (Trapnell *et al.*, 2010, 2012) uses an algorithm which assembles aligned reads into likely transcripts and calculates their abundance. A significant advantage of this tool is its ability to detect transcripts which are not contained within the reference gtf file. Across all samples, total of 170,351 genes with 366,729 transcripts were detected. Using the Cuffmerge tool (Trapnell *et al.*, 2010), the newly identified transcripts were merged with the IWGSC1.0_popseq.29 reference annotation to create an another custom reference annotation against which read count for each gene could be counted.

To determine relative expression levels of transcripts in an RNA-Seq experiment it is necessary to count the number of short sequencing reads which have been mapped to a given transcript. However, when using a whole genome reference sequence which includes intronic and non-coding regions any read counting tool needs to be able to distinguish between mismapped reads and those which span exon junctions or splice variations. The htseq-count tool creates a digital expression matrix using read counts and has three built in modes for assigning reads which overlap with more than one gene feature (Anders *et al.*, 2015). Htseq-count was used to determine the number of reads mapping to transcripts mapping to genes annotated within the custom reference described above. Default parameters were used with the exception of specification of the union mode for handling reads overlapping features and the specification that the data is forward strand specific. The union mode classes any read spanning or overlapping an annotated intron/exon junction as a count for the given gene, any reads which map to

two different genes are listed as ambiguous. A tabular count file was generated.

5.2.5. Mapping to a transcriptome reference and counting

During the course of analyses using the IWGSC whole genome reference, a significantly improved reference genome (TGACv1) became available. Having already invested significant time and resources in mapping and aligning to the IWGSC whole genome, and given limitations on the time remaining to complete the project, it was decided not to repeat whole genome mapping with the updated reference. Instead, the predicted cDNA transcriptome model containing 273,739 predicted transcripts was used as the reference sequence. This approach significantly reduced the time and computational resources required to complete alignment of sequencing reads to the reference. However, unlike when mapping to a whole genome reference, the use of a transcriptome reference restricts analysis to transcripts included in the annotation, so that the discovery of new transcripts is not possible.

Rapid alignment of sequencing reads to the transcriptome reference was carried out using the Bowtie 2 tool (Langmead *et al.*, 2009; Langmead and Salzberg, 2012). As a transcriptome reference was used in this case there was no need for a splice aligner such as TopHat and therefore the simpler mapping tool Bowtie 2 could be used. Default parameters were used with the exception of the -a setting for reporting options which permits Bowtie 2 to search for an unlimited number of alignments for each read.

The resulting BAM files were sorted by read name and merged for each biological replicate. Transcript abundance was quantified for every transcript in the reference transcriptome using the eXpress software package (Roberts and Pachter, 2012) for each sample and merged into a tabular matrix file.

5.2.6. Identifying differentially expressed transcripts

Differential gene expression analysis was completed by A. Gonzalez (Applied Bioinformatic, Rothamsted Research, U.K.) using the edgeR software package

(Robinson *et al.*, 2010) in the RStudio software environment (v. 0.99.484) (R Core Team, 2016). Analysis of the similarity between samples was carried out. Initially, General Linear Modelling (GLM) within edgeR was used to attempt to identify clusters of genes that have changes in expression which are explained by the interaction between time and temperature treatments (Fig. 5.2.). This approach was intended to allow differentiation between gene expression which changes only in response to temperature (Fig. 5.2. a) from developmental gene expression profiles which do not respond to HT (Fig. 5.2. b) and genes which respond to the interaction between time and temperature (Fig. 5.2. c). Given previously observed acceleration of anther development in response to HT, it was hypothesised that many genes would also show a premature peak in expression under HT relative to the control developmental expression profile.

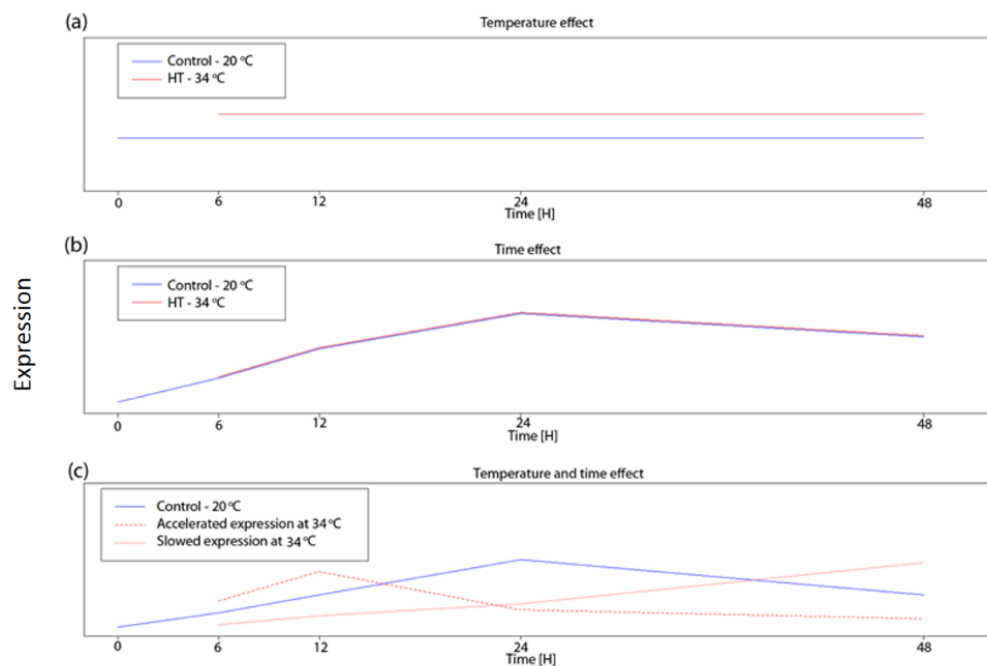


Figure 5.2. Treatment and interaction effects on an example transcript. (a) Transcript is differentially expressed in response to HT. (b) Transcript is differentially expressed in response to time (developmentally). (c) Transcript expression responds to temperature and time.

5.2.7. Assigning gene annotations and GO terms

Gene ontology enrichment was carried out on lists of differentially expressed transcripts in order to investigate the effect of treatment on another biological processes. Lists of differentially expressed transcripts were imported into Blast2Go (v.3.3.) (BioBab, Valencia, Spain) and using the built in BLASTx tool (minimum 10 matched, threshold E-value 1×10^{-5}) searched against a custom wheat annotation reference for homologues; GO-terms are then extracted by mapping accepted hits to online databases of gene annotation data (Conesa *et al.*, 2005). Statistical analysis of over- or under-represented GO-terms for a given transcript list was carried out using the built-in Fisher's exact test function which ranks GO-terms based on their P value after correction for false discovery rate (0.01 threshold FDR = 5%).

5.2.8. Global hormone quantification plant material

An initial study was undertaken to determine the minimum volume of tissue required for accurate hormone quantification. Material was collected from wheat plants (var. Cadenza) grown under standard glasshouse conditions (see section 2). Global hormone analysis (carried out at Olomouc, Czech Republic) and GA-specific quantification (carried out at Rothamsted Research, U.K.) confirmed that all major hormones could be detected in as little as 20 mg dry weight of anthers collected from tillers ranging from 13 cm to 18.5 cm FLS length (covering predicted stages 6 – 9, young microspores – mitosis II). Based on these findings a completely randomised experiment to investigate hormone levels in anther tissue at two stages of development at 20 °C and 34 °C was planned.

24 wheat plants were established in controlled environment conditions as previously described (see section 5.2.1). Plants were grown in a completely randomised design. When plants entered the booting stage (GS40) they were designated to either control or HT at either 10 cm or 15cm FLS length treatment (estimated anther development stages, meiotic and pre-mitotic development respectively). Having initially been unable to identify any GAs by

LC-MS, it was decided that GA-specific quantification by GC-MS would be carried out at Rothamsted Research. Therefore, half of the plants were designated for global analysis and the other half GA analysis. There were therefore three biological replicates for each treatment. It had been intended to use a similar experimental design to that used in section 5.2.1 in which staggering of plant transfer to HT-treatment conditions allows for the optimum material to be selected. However, due to malfunctioning of the secondary cabinet intended for use as the HT treatment, the following amendments were made:

As only one experimental growth cabinet was available, staggering of treatments to match individual plant development was not possible. Therefore, anthers from mid-spike positions from two tillers measuring 10 ± 0.5 cm or 15 ± 0.5 cm per control group plant were harvested and two other tillers with the same measurements were tagged. The controlled environment settings were then changed from 20 °C control conditions to the HT 34 °C conditions (see section 5.2.1.). After 24 h the tagged anthers were also harvested.

Due to these restricted experimental conditions some plants had to be sampled under both treatments to ensure sufficient material for analysis. Repeat sampling of experimental units results in overpowering of statistical comparisons, increasing the likelihood of finding statistically significant results (S. Powers, pers. comm.). Therefore, caution must be taken when interpreting these data. General Analysis of Variance (ANOVA) was carried out in GenStat (v17, VSNI, Hemel Hempstead, U.K.).

All samples were immediately frozen in liquid nitrogen and stored at -80 °C. Prior to extraction samples were freeze dried and weighed in the collection tube. The dry weight of the sample was determined as the difference to the empty collection tube weight.

5.2.9. Extraction and quantification of GAs

GA analysis was carried out as described in Griffiths *et al.*, (2006). Anthers were extracted in 80% methanol primed with known quantities ^3H - and $^2\text{H}_2$ -labeled GA internal standards at 4 °C overnight. The GA containing acidic fraction was then separated by chromatography using QAE-Sephadex (Sigma-Aldrich, St. Louis, Missouri, U.S.A.) anion-exchange and Sep-Pak C₁₈ (Waters Ltd, Milford, Massachusetts, U.S.A.) columns. Samples were then methylated in ethereal diazomethane and the GA-containing organic phase isolated by partitioning in water and ethyl acetate. Further purification by removal of remaining unmethylated acid components was achieved by passing the organic phase through NH₂ anion-exchange columns (Agilent, Santa Clara, California, U.S.A.) and retaining the eluate. No High Performance Liquid Chromatography (HPLC) separation of fractions was carried out as previous studies had shown this to be unnecessary in this case (P. Hedden pers. comm.). Quantification of GA family members was carried out by Prof. Peter Hedden using Gas Chromatography – Mass Spectrometry (GC-MS) with selected ion monitoring based on established calibration curves for the labelled internal standards.

5.2.10. Extraction and quantification of all other hormones

Global hormone analysis was carried out by Jan Simura using Liquid Chromatography – Mass Spectrometry (LC-MS) at the Laboratory of Growth Regulators & Department of Chemical Biology and Genetics, Palacky University and Institute for Experimental Botany, Olomouc, Czech Republic.

5.3. Results

5.3.1 The impact of HT on wheat anther development

A number of different HT-stress phenotypes, ranging in severity, have been reported in cereal anthers (see section 1.5.). Therefore, before undertaking transcriptional analysis of anthers it was necessary to establish the effects of

the experimental HT-stress condition on anther development in wheat. This would then allow any observed changes in transcription to be understood in the context of the resulting developmental defects. Anthers from plants exposed to the experimental control and HT conditions were investigated by light microscopy to determine the effect of HT-stress on internal morphology and development. Cytological analysis of anthers exposed to HT for 24 and 72 h confirmed that 34 °C caused developmental defects consistent with disruption of the post-meiotic function of the tapetum and pollen cell maturation (Fig. 5.3.).

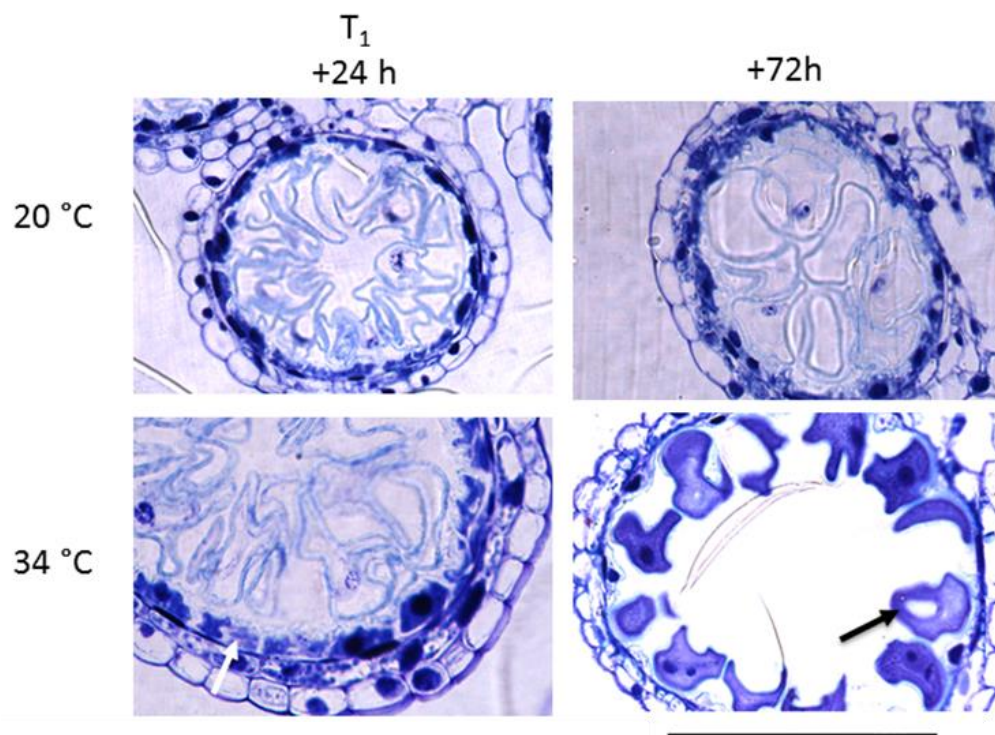


Figure 5.3. The effect of HT on anther development and morphology. *Anthers were harvested from control and HT-treated plants and examined by light microscopy. Anthers exposed to HT show granulation of the tapetum cells (white arrow) and accelerated progression of pollen development which have become irregular in shape (black arrow). Scale bar 200 μ m.*

Consistent with previous observations, premature acceleration of the anther development programme is induced by exposure to HT. Tapetum decay appears to have begun by T₁ at 20 °C and 34 °C with loss of the tapetum

primary wall and internal degradation becoming evident (Fig. 5.3. white arrow). However, 24 hours after the completion of the experimental time course (+72h) the tapetum layer is completely degraded at 34 °C but still present as microspores undergo vacuolation and mitosis at 20 °C. This acceleration of development results in the formation of misshapen pollen cells which have not completely filled with carbohydrates (Fig. 5.3. black arrow). Whilst pollen viability or grain set of these plants was not tested, the anther phenotypes observed above confirm that 34 °C is an adequate experimental treatment for the induction of HT stress.

5.3.2 Hierarchical clustering of total expressed transcripts

Hierarchical clustering analysis of differentially expressed genes was carried out in edgeR using the hclust function with the intention of grouping genes according to the three expression responses described above (Fig. 5.2.) However, it became clear that such a complex analysis would not be possible within the timeframe of the project; a high degree of variability and large number of differentially expressed transcript resulted in undefinable clusters (Fig. 5.4.).

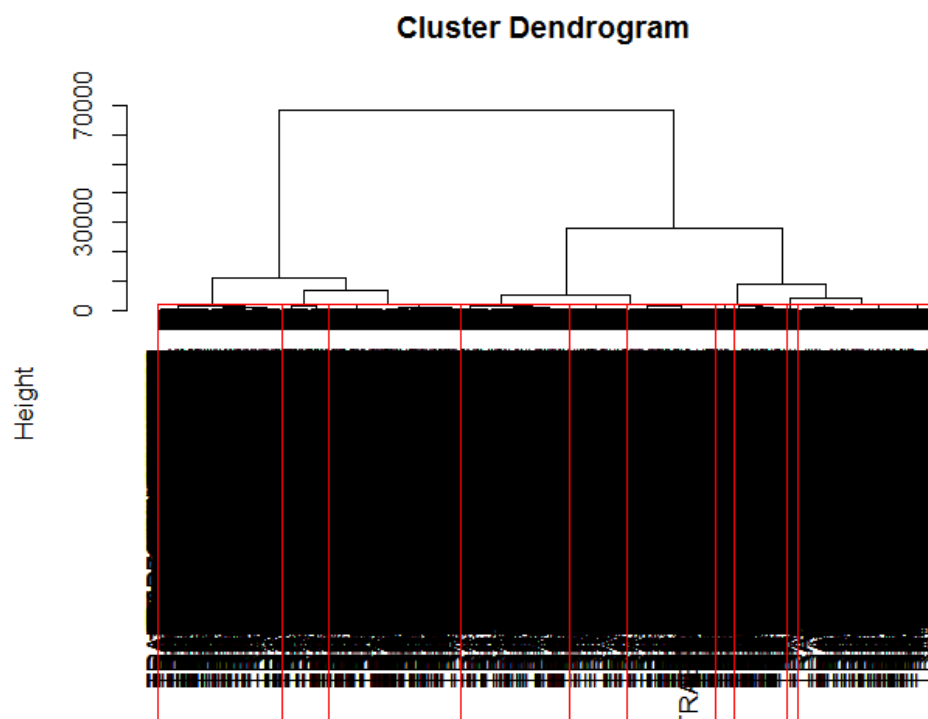


Figure 5.4. Cluster dendrogram for all differentially expressed genes. *Clustering analysis carried out in edgeR reveals poor definition between differentially expressed gene groups. Red boxes indicate software-suggested clusters.*

The failure of the clustering analysis to distinguish between differential expression profiles indicates that there is insufficient difference between comparative samples. In order to establish the biological variability captured by the experimental sampling regime, a multidimensional scaling (MDS) plot visualising the relative similarity of each sample based on counts per million kilobases was created in edgeR using the plotMDS function (Fig. 5.5.). The scattering of points around the plot demonstrates the variability captured within the samples and offered some explanation as to why clustering failed.

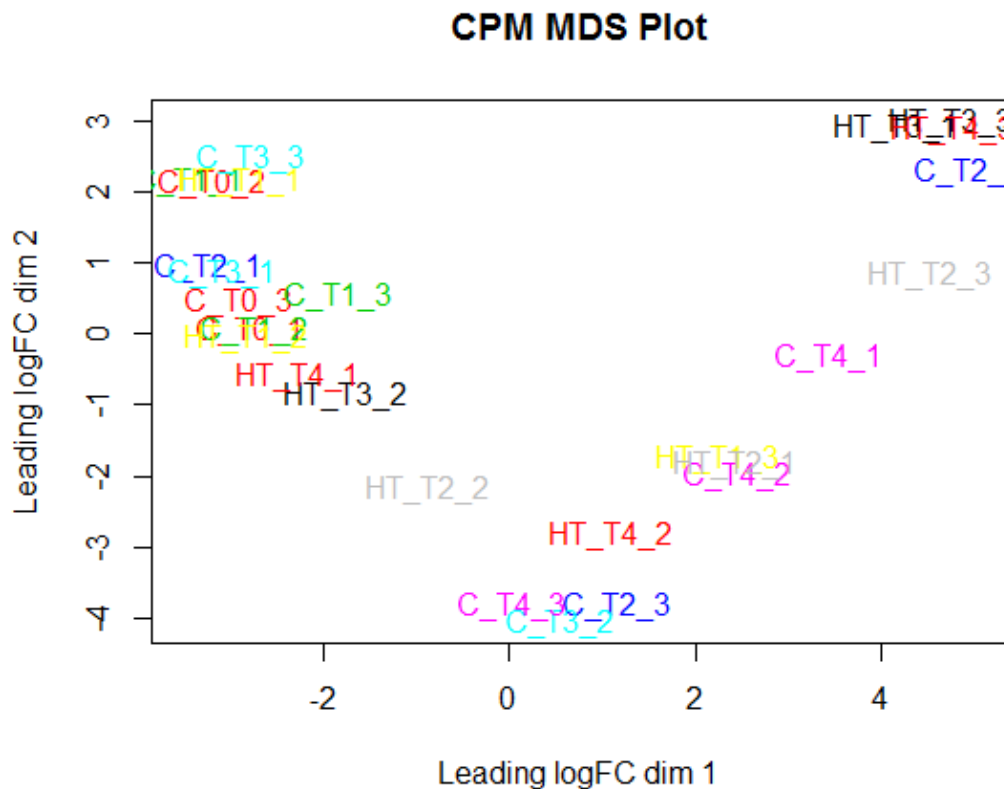


Figure 5.5. MDS plot of RNA-seq samples mapped to IWGSC whole genome reference. *Biological replicates are the same colour. Samples are named by their treatment group (C – control, HT), time point and biological replicate number.*

Ideally, biological replicate samples should group together whilst a clear separation between treatment samples should be evident. In this case, biological replicates are spread across both axes whilst time point and temperature time points can be seen to overlap each other. This indicates that samples which should be biologically distinct in fact account for large portions of the same variation. Therefore, a comparative analysis of all time-points and treatments would be unlikely to provide useful results.

5.3.3. Transcriptional regulation of anther development

In light of the obvious difficulty in assessing such variable results when considering the HT experiment as a whole, it was decided to investigate if any pairwise comparisons could be made between comparable samples with less variable replicates. By systematically comparing time point samples variation on MDS plots it was established that biological replicates 1 and 3 could be used for a comparison of gene expression between samples collected at T_3 (+24 h) for a comparison of control and HT treatments (Fig. 5.6.). Despite a large degree of variation in the second component between the two control samples, a good separation of HT and control samples in the first dimension permits valid comparisons between the two experimental treatments.

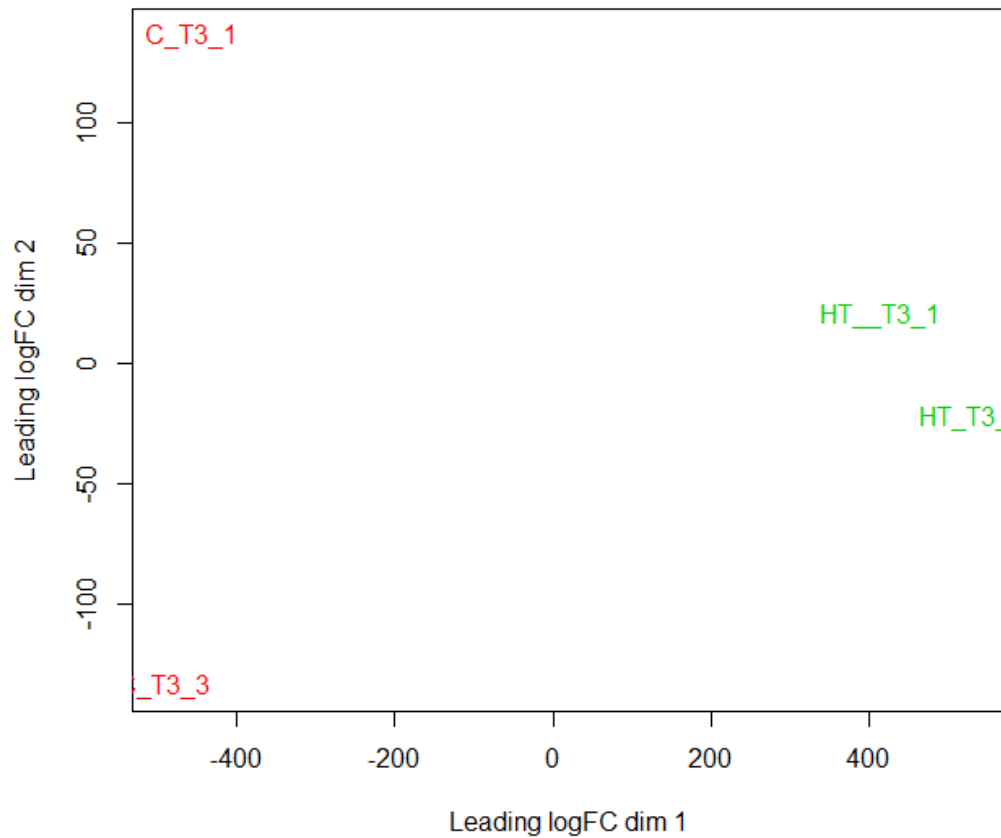


Figure 5.6. MDS plot of whole genome aligned expressed genes in two biological replicates of T₃ control and HT samples.

Read counts for the two selected replicates of both samples were extracted and differential gene analysis comparing the HT samples to C was carried out using edgeR. A total of 9943 differentially expressed transcripts were detected. The top 20 most significantly differentially expressed genes and their gene function annotations are presented in Table 5.1.

| Transcript ID | Annotation | Fold change | FDR |
|---------------------|---|-------------|----------|
| XLOC_026217 | #N/A | 10.84 | 4.66E-84 |
| Traes_2BL_255108047 | #N/A | 10.96 | 2.90E-82 |
| Traes_2BL_87AA8B551 | meiotic serine proteinase-like protein | 10.22 | 4.60E-71 |
| XLOC_030553 | #N/A | 10.51 | 1.25E-68 |
| Traes_4BS_9A1950277 | #N/A | 9.76 | 2.23E-65 |
| Traes_2AS_15562C23D | protein pfc0760c-like | 10.92 | 6.38E-65 |
| Traes_2AL_A634C94CA | meiotic serine partial | 8.95 | 1.61E-63 |
| Traes_4AS_BE9625780 | fatty acyl- reductase 2-like | 9.66 | 3.74E-62 |
| Traes_4AL_BD68A9279 | #N/A | 10.17 | 3.57E-61 |
| Traes_4DL_021634BC0 | fatty acyl- reductase 2-like | 9.54 | 7.44E-60 |
| Traes_2AL_187E80B24 | cytochrome p450 87a3-like | 10.44 | 2.52E-58 |
| Traes_1BS_6A84E22E2 | hvk7_orysj ame: full=hexokinase-7 ame: full=hexokinase-6 | 9.09 | 3.76E-57 |
| Traes_6DS_2EDFCBCA4 | #N/A | 6.94 | 5.12E-56 |
| Traes_2BS_81588BD1F | protein pfc0760c-like | 10.44 | 8.64E-55 |
| Traes_7DL_439CC6EA0 | abc transporter g family member 26 | 9.89 | 8.96E-55 |
| Traes_7AS_91F6E710D | #N/A | 7.60 | 1.69E-53 |
| Traes_7AL_3B2536995 | hypothetical protein TRIUR3_24487 | 7.08 | 8.02E-53 |
| Traes_2BS_E4D5800DD | #N/A | 8.10 | 6.89E-52 |
| Traes_4DS_D1C345CDE | #N/A | 9.98 | 3.84E-51 |
| XLOC_139738 | #N/A | 7.83 | 9.55E-51 |

Table 5.1. Top 20 DEGs in anther tissue after 24 h exposure to HT. *DEGs were ranked by most significant FDR value of significance of fold change in counts between HT and control samples.*

Half of the top 20 DEGs have no associated gene function annotation. The annotated functions of the remaining transcripts provide evidence that HT has a dramatic effect on the function of the tapetum. Two meiotic serine proteinase transcripts are significantly upregulated under HT at 24 h (Table 5.1.). Serine proteinases are hypothesised to have a role in the release of microspores from meiotic callase envelopes and the execution of PCD (Taylor *et al.*, 1997). Similarly, the tapetum plays a major role in the biosynthesis and transport of exine and the upregulation of two fatty acid reductase, one cytochrome P450 and one ABC transporter transcript suggest these functions may also be affected. Also, tapetum development TF *TaDYT_A* (see section 1.3.2.) and Traes_7DS_CB7D748CC, which is annotated as tapetum differentiation TF TIP2-like, appear in the DEG list (-5.9 fold and -4.6 fold change at HT +24 h, respectively). Additional searches revealed no significant differential expression of known GA-biosynthesis, signalling or other known

anther development transcripts. All differential gene expression data will be made available in an online repository.

In order to further investigate the effect of HT on transcriptional regulation of anther development processes, GO-terms were assigned to the 9943 DEGs using Blast2Go (see section 5.2.7.). The top 50 most frequently assigned GO-terms are presented in Figure 5.7. The most frequently assigned GO-terms are representative of biological processes common to anther development (Fig 5.7.). Terms relating to meiosis, mitosis and pollen development specifically are highly represented. Similarly, metabolic processes such as carbohydrate metabolism, protein turn over and transmembrane transport appear in top 50 most represented terms.

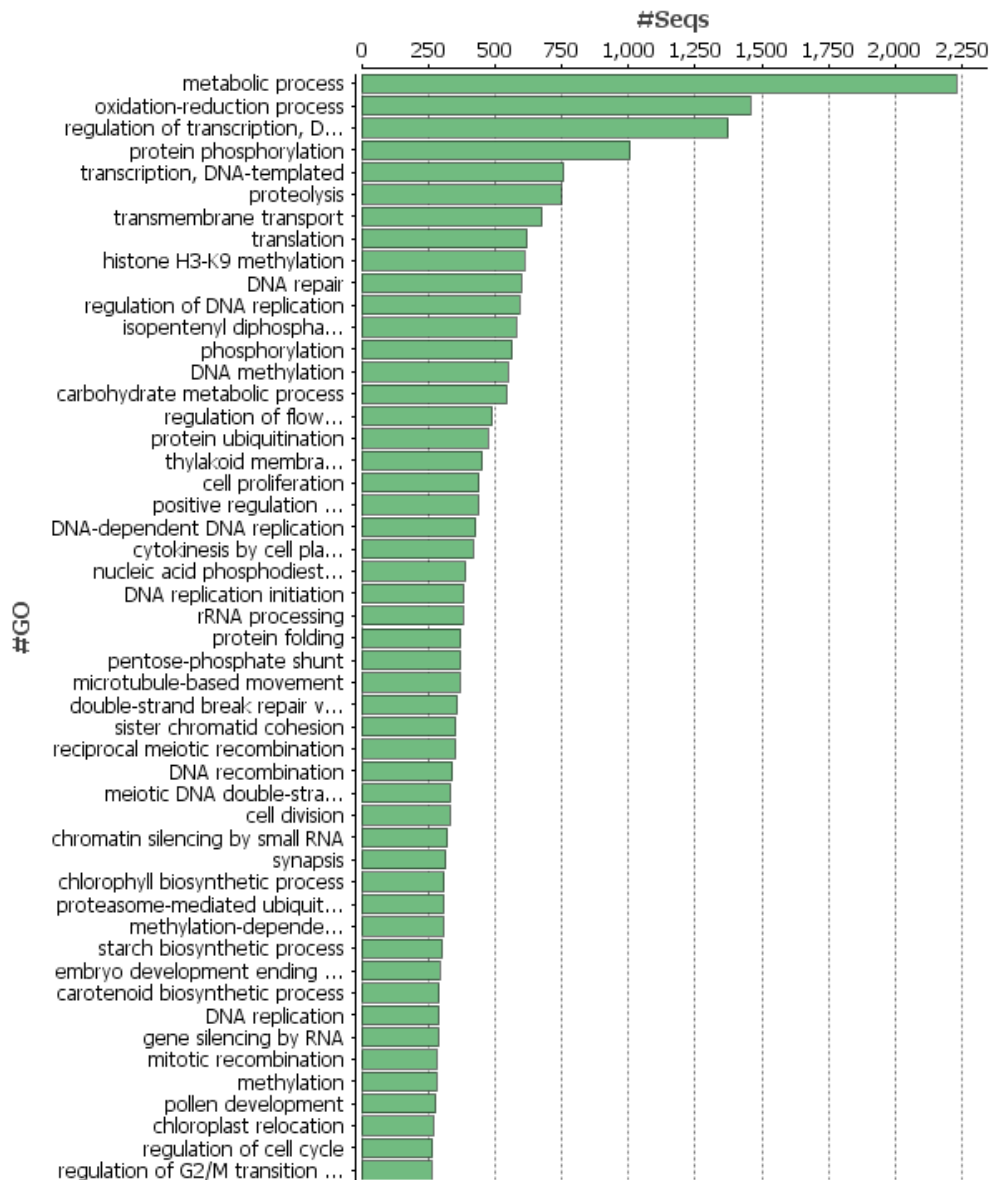


Figure 5.7. Top 50 most abundant GO-terms amongst DEGs at 24 h HT treatment. *Transcripts were assigned GO-terms using the annotation function in Blast2Go.*

It is notable that many of the most abundant GO-terms are associated with processes previously shown to be negatively affected by HT-stress. The presence of a number of terms relating to meiosis, mitosis, DNA replication and cell proliferation indicate that microsporogenesis has been affected by HT. Interestingly, pollen development terms also appear in the top 50 most abundant. Given that transcript analyses were exclusively for developing anthers; it is perhaps surprising that the term pollen development did not

account for more of the expressed transcripts. However, this is most likely caused by the limitation of the gene annotations used.

Fisher's Exact test was carried out comparing this list of annotated DEGs to the whole genome annotation in order to investigate the impact of HT on transcriptional regulation of biological processes in the anther. A total of 467 GO-terms were found to be significantly under- or over-represented in the DEGs list. Keyword searches were used to extract terms related to hormone signalling and biosynthesis and the genetic regulation of anther and pollen development (Table 5.2.).

| GO-ID | Term | FDR | P-Value | Over/Under |
|--|-----------------------------------|----------|----------|------------|
| Hormone biosynthesis and signalling | | | | |
| GO:0009739 | response to gibberellin | 6.96E-04 | 1.15E-04 | UNDER |
| GO:0009734 | auxin-activated signaling pathway | 4.44E-07 | 4.54E-08 | UNDER |
| GO:0060918 | auxin transport | 6.48E-04 | 1.05E-04 | UNDER |
| GO:0009737 | response to abscisic acid | 5.84E-05 | 7.82E-06 | UNDER |
| GO:0016102 | diterpenoid biosynthetic process | 1.83E-05 | 2.24E-06 | UNDER |
| Anther and pollen development | | | | |
| GO:0048443 | stamen development | 1.28E-04 | 1.81E-05 | UNDER |

Table 5.2. Selected GO-terms extracted from Fisher's Exact Test output.

Keyword searches were used to identify terms associated with hormonal and genetic regulation of anther and pollen development in list of significantly under- or over-represented terms in 24 h HT DEGs list.

GO-terms associated with gibberellin, auxin and ABA biosynthesis and signalling were all significantly under-represented in DEGs indicating that HT has caused a modulation of hormonal responses. However, the observation that transcription relating to ABA response is suppressed after 24 hours but is over-represented in the overall analysis indicates that ABA signalling may be prominent at earlier time points. Likewise, no further meiosis, mitosis or pollen development specific terms were identified at 24 h except for stamen development which was under-represented. Again this suggests that HT causes dramatic changes to the anther transcriptome within the first 24 h. No terms relating to jasmonate, brassinosteroid or ethylene biosynthesis or signalling were identified.

5.3.4. Transcriptome profiling using a cDNA reference

During the analysis of sequencing data using the IWGSC whole genome reference, a significantly improved reference genome, TGACv1 which covers more than 13.5 Gbp of the highly repetitive 17 Gbp wheat genome (compared to 6.5 Gbp covered by the IWGSC whole genome reference) also became available. Given the limited time remaining to complete analysis, a re-mapping of processed sequencing reads (see section 5.2.3.) to the TGACv1 predicted cDNA transcriptome as opposed to the entire genome assembly was undertaken as this required much less computational processing and could be completed rapidly.

The cDNA reference FASTA file and GFF annotation file for the TGACv1 assembly were imported into Galaxy and Trimmomatic processed FASTQ were mapped to the reference using Bowtie 2 and counted by eXpress (see section 5.2.5.). Read counts for a total of 273,739 transcripts were calculated. An effective counts matrix was generated and a comparison of differential gene expression of two T₃ (+24 h) time-point replicates under control or HT conditions, was carried out in edgeR as described above. A total of 6083 DEGs were identified, of which 2726 were downregulated and 3357 were upregulated. The functional annotations of these genes were assigned using Blast2Go as described (see section 5.2.7.). The top 20 most significant DEGs, their annotation, log fold change value and FDR are presented in Table 5.3.

The finding that the two most significantly upregulated transcripts in response to HT contain BURP-domain containing proteins is potentially of great importance. *TaRAFTIN* is an anther specific BURP-domain protein which has a crucial role in the delivery and assembly of tapetum-manufactured sporopollenin on the pollen exine (Wang *et al.*, 2003) (see section 1.3.2.). The Log₂FC 10-fold upregulation of transcripts with annotated similarity to a gene critical to Ubisch body function in response to HT suggests this might be one mechanism through which HT induces male sterility. However, further

investigation of these transcripts is required to determine their function in wheat anther development.

| Transcript ID | Annotation | Log Fold Change | FDR |
|--|---|-----------------|----------|
| TRIAE_CS42_2DL_TGACv1_15893 4_AA0529130.1 | BURP domain-containing 4-like | 10.93 | 5.83E-58 |
| TRIAE_CS42_2BL_TGACv1_13066 8_AA0415660.1 | BURP4_ORYSJ ame: Full=BURP domain- containing 4 Short= 04 Flags: Precursor | 10.72 | 4.63E-57 |
| TRIAE_CS42_2DL_TGACv1_16121 0_AA0557440.1 | meiotic serine ase | 9.41 | 1.37E-52 |
| TRIAE_CS42_2AS_TGACv1_11259 9_AA0341990.1 | pectinesterase 66 | 10.59 | 2.19E-51 |
| TRIAE_CS42_2DS_TGACv1_17928 1_AA0605850.2 | pectinesterase 66 | 10.26 | 1.27E-50 |
| TRIAE_CS42_2AL_TGACv1_09296 3_AA0268200.1 | cytochrome P450 87A3-like | 9.96 | 1.27E-50 |
| TRIAE_CS42_4BS_TGACv1_32796 8_AA1080080.1 | classical arabinogalactan 9-like | 9.37 | 8.58E-49 |
| TRIAE_CS42_4BL_TGACv1_32098 8_AA1053040.2 | fatty acyl- reductase 2-like | 9.75 | 2.85E-47 |
| TRIAE_CS42_4AS_TGACv1_30839 9_AA1027760.1 | Cytochrome P450 704C1 | 10.26 | 1.62E-46 |
| TRIAE_CS42_4AS_TGACv1_30702 2_AA1016260.1 | fatty acyl- reductase 2-like | 10.17 | 1.62E-46 |
| TRIAE_CS42_4DS_TGACv1_36120 0_AA1163460.1 | classical arabinogalactan 9-like | 10.08 | 1.85E-45 |
| TRIAE_CS42_1BS_TGACv1_05001 3_AA0165940.1 | HXX7_ORYSJ ame: Full=Hexokinase-7 ame: Full=Hexokinase-6 | 8.59 | 5.43E-45 |
| TRIAE_CS42_1DS_TGACv1_08222 4_AA0264200.1 | HXX7_ORYSJ ame: Full=Hexokinase-7 ame: Full=Hexokinase-6 | 8.73 | 6.02E-45 |
| TRIAE_CS42_2BL_TGACv1_12934 1_AA0379410.1 | meiotic serine ase | 10.04 | 1.04E-44 |
| TRIAE_CS42_4DL_TGACv1_34281 8_AA1122940.1 | fatty acyl- reductase 2-like | 10.37 | 1.25E-44 |
| TRIAE_CS42_7DL_TGACv1_60481 7_AA2002000.1 | ABC transporter | 9.58 | 1.54E-43 |
| TRIAE_CS42_7BS_TGACv1_59181 2_AA1922120.6 | Sucrose synthase 1 | 7.99 | 9.95E-40 |
| TRIAE_CS42_1AS_TGACv1_02029 2_AA0076360.1 | hypothetical protein TRIUR3_07253 | -7.95 | 1.37E-39 |
| TRIAE_CS42_1AS_TGACv1_02039 9_AA0077180.1 | hexokinase partial | 8.03 | 1.99E-39 |
| TRIAE_CS42_3B_TGACv1_221086 _AA0729940.1 | aquaporin NIP4-1-like | 10.76 | 2.62E-38 |

Table 5.3. Top 20 most significant DEGs at 24 h HT. *DEGs were ranked by most significant FDR value of significance of fold change in counts between HT and control samples.*

As was seen in the DEG list using the IWGSC whole genome reference (Tab. 5.3.), two meiotic serinease transcripts are significantly upregulated (9.41, and 10.04 log fold increase respectively) along with two pectinesterase transcripts (10.59 and 10.26 log fold increase respectively). Serinase has previously been

reported to be secreted during microsporogenesis and is thought to be involved in the degeneration of the callose envelope surrounding tetrads and the tapetum PCD (Taylor *et al.*, 1997). Similarly, pectinesterases are highly expressed in developing anthers and have been implicated in regulation of plant cell wall degradation and have been shown to be highly upregulated by HT (Wu *et al.*, 2015). Together, the upregulation of these transcripts suggests that tapetum cell degradation, which requires the decomposition of the tapetum primary cell wall, may have been accelerated by HT. During the post-meiotic, pre-mature pollen development stage, a major function of the decaying tapetum is to support the synthesis and construction of the pollen coat which has been shown to require the expression of a number of lipid and carbohydrate metabolism and transport genes (see section 1.2.2.). Therefore, an acceleration of the tapetum life cycle is further supported by the upregulation of genes potentially involved in lipid biosynthesis (fatty acid reductases and cytochrome P450s), carbohydrate metabolism (sucrose synthase and hexokinases) and transmembrane transport (ABC transporter and aquaporin NIP4-1-like).

In order to further investigate the biological processes affected by HT using the TGAC v1 transcriptome, GO-enrichment on the DEGs list was carried out using the annotation function in Blast2Go (see section 5.2.7.). The top 50 most commonly assigned terms (based on number of matching sequences) is shown in figure 5.8. As previously observed, a number of general terms which describe well characterised biological processes occurring in developing anthers and pollen. Indeed, the metabolism and transport of carbohydrates, lipids and other metabolites indicates that the anther is highly active at this stage. The presence of stress associated terms such as oxidation-reduction process, DNA repair, defence responses to fungus and cellular oxidant detoxification also suggest that cells are transcriptionally responding to HT treatment.

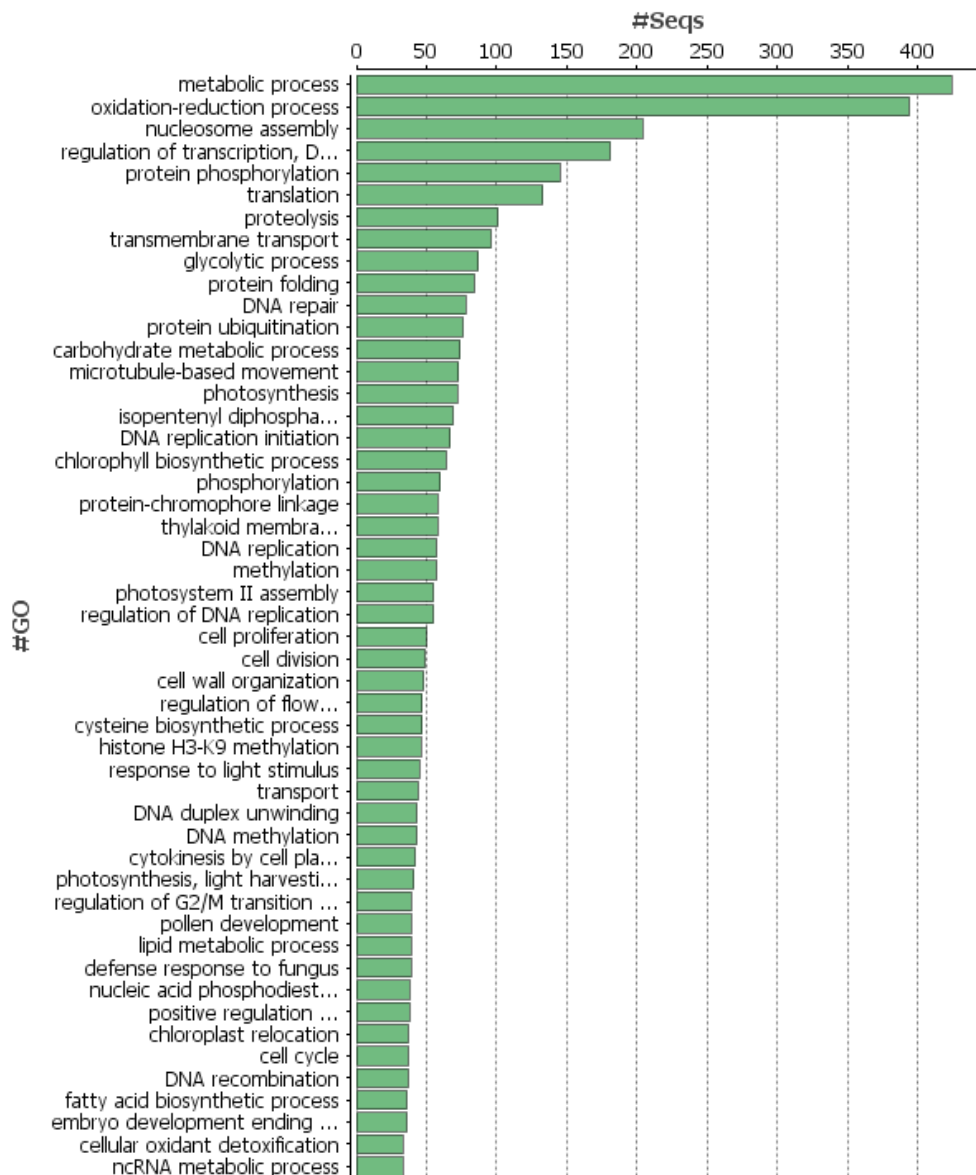


Figure 5.8. Top 50 most frequently represented GO-terms in 24 h DEGs list using TGACv1 transcriptome reference.

5.3.5. The impact of HT on expression of GA-signalling and biosynthesis genes.

Global transcriptome analysis of anthers established that exposure to HT-stress causes dramatic changes to gene expression associated with developmental processes taking place in the tapetum and microspores. GA-signalling is involved in the regulation of these processes, particularly tapetum PCD and the biosynthesis and laying down of the sporopollenin component of the pollen coat, suggesting that a negative effect of HT-stress on GA-signalling

may contribute to some of the HT-defects previously described. Therefore, in order to investigate if HT-stress has any effect on the GA-signalling pathway in wheat anthers, the expression profiles under control and HT conditions of a number of known GA-signalling and biosynthesis components were compiled based on read counts mapped to TGACv1 reference transcripts.

A list of gene identifiers for known GA-signalling and biosynthesis transcripts (Annex II) was obtained and used to extract the effective count data from the eXpress output of the transcriptome reference analysis pipeline. The transcriptome reference was used in this study as a greater number of transcripts of interest are included than in the IWGSC whole genome reference. Transcripts with counts not exceeding effective counts of 50 at any time point were excluded. Mean counts for each homoeologue were calculated; the overall expression was calculated as the homoeologue average. Mean effective counts (reads per transcript corrected for fragment length bias) were plotted for 7 GA biosynthesis, 2 confirmed and 1 putative GA-signalling component under control and HT conditions (Fig. 5.9.). It is important to repeat that given the high variability that exists between replicate samples caution should be taken when interpreting comparative results.

lines indicate the mean effective counts of the given homoeologues of the respective gene. Effective counts were calculated for 5 time points beginning at T_0 for control conditions (top graph) and HT conditions (bottom graph). Two early GA-biosynthesis genes were identified, *TaCPS* (a) and *TaKAO* (b), two *TaGA13OX* paralogues, 1 (c) and 2 (d), two *TaGA20ox* paralogues, 1 (e) and 2 (f) and *TaGA20X_3* (g). The receptor *TaGID1* was also identified (h) as well as the signalling component *TaGAMYB* (i). Only the *_B* homoeologue of *TabHLH141* was identified and therefore the mean effective counts at control (solid line) and HT (dashed line) are presented on one graph.

The transcription of early GA-biosynthesis genes *TaCPS* (Fig.5.9. a) and *TaKAO* (Fig. 5.9. b) remains relatively stable during control time points and a slight elevation in transcript level can be seen before and after $T_1 +6h$ respectively. Interestingly, expression of *TaGA13OX_1* is noticeably increased after 12 hours of HT (Fig. 5.9. c). This suggests that one of the effects of HT may be to drive GA-biosynthesis down the 13-hydroxylation pathway (Fig. 5.11.). The expression of *TaGA20OX_1* (Fig. 5.9. d) and *TaGA20OX_2* (Fig. 5.9. e) also appears to respond to HT. A peak of effective counts of *TaGA20OX_1* at T_1 is amplified at HT whilst a peak of expression at T_3 of *TaGA20OX_2* under control conditions is suppressed by HT. Also of note is the rapid increase in the expression of the GA-inactivating *TaGA20X_3* under HT which is otherwise expressed at only a basal level (Fig. 5.9. f). Similarly, the GA-receptor *TaGID1* has a stable expression profile under control conditions but its expression begins increasing after T_2 under HT treatment (Fig. 5.9. g.).

The expression of *TaGAMYB* has been shown to be vital for wheat male fertility (see section 4). Here, the expression profiles suggest that *TaGAMYB* expression remains relatively stable during anther development and is not dramatically effected by HT treatment, although a relative increase in mean effective counts at HT_4 can be observed (Fig. 5.9. h.). *TabHLH141* is also required for male reproductive development in wheat and is a putative GA-responsive PCD elicitor (see section 4). Only the B homoeologue could be identified in the expression data, although expression of all three

homoeologues in whole wheat spikes at GS39 has previously been reported (Choulet *et al.*, 2014), which suggests that exclusive expression of *TabHLH141_B* is unlikely. Expression of the *B* homoeologue transcript appears to be activated at T₁, peak at T₂ and then decline and stabilise under control conditions (Fig. 5.9. i). HT appears to accelerate the expression of *TabHLH141_B* until T₂ when it also begins to decline as seen under control conditions.

5.3.6. Quantification of anther endogenous hormone levels in response to HT

The role of hormones in anther development and responses to HT have been well studied (see section 1.5.). Transcriptional data collected above suggest that HT causes changes to the genetic regulation of GA-biosynthesis and signalling in the anther which may be of significance to the developmental response. However, hormone biosynthesis pathways are complex, multistep processes (see section 1.4.) and the expression of a given catabolism paralogue does not necessarily relate to changes in cellular hormone content. Analysis of hormone concentrations in mature rice anthers has shown that accumulation of GA₄ and auxin in tricellular pollen may be achieved through the earlier expression of biosynthetic genes in microspore and tapetum cells and the storage of precursor forms (Hirano *et al.*, 2008). Transcriptional analysis of wheat anthers has demonstrated altered expression of GA-biosynthesis genes when exposed to HT, which could potentially affect the production of bioactive GA at later stages. Furthermore, whilst low, stable levels of ABA, JA and BR were detected in mature rice anthers, transcriptional analysis nonetheless demonstrates that their biosynthesis and signalling pathways are highly regulated during pollen development (Hirano *et al.*, 2008). Given that other studies have demonstrated the importance of maintaining GA and auxin whilst suppressing ABA levels in response to HT for rice male fertility (Tang *et al.*, 2007), there is clearly a need to better understand the impact of HT-stress on hormone biosynthesis in wheat anthers.

Therefore, an analysis of anther global hormone content under control and HT conditions was carried out. The objective was to determine if changes in anther hormone concentrations could be detected which would provide further explanation for observed transcriptional responses to HT. Specific analysis of active and precursor forms of GA was carried out in order to establish how HT-responsive biosynthesis gene expression affects hormone concentrations. Quantification of many major plant hormones and their precursor forms in developing wheat anthers and in response to HT would represent a novel and potentially very useful resource for further investigation of developmental and stress response regulation, especially when combined with transcriptomic data described in section 5.3.5.

Prior to undertaking global hormone analysis, a pilot study to determine the minimum tissue requirements for detection of GAs by GC-MS was undertaken (see section 5.2.9.). In 0.8 mg dry weight of anthers extracted around the mature pollen stage a total of 450 ng/g of GA₄ and 4910 ng/g of GA₉ were detected. This is consistent with previous observations which describe an accumulation of large amounts of non-13-hydroxylated GA₄ in mature rice anthers (Hirano *et al.*, 2008).

Global hormone analysis carried out using LC-MS shows dynamic regulation of hormone concentrations within the anther during development and in response to HT stress (Fig. 5.10.). Major active and inactive members of the abscisic and salicylic acid, auxin, brassinosteroid, cytokinin, gibberellin and jasmonate families were measured. Quantification of all family member compounds can be found in annex III. Only the bioactive forms of each family are presented (Fig 5.10.), except for the gibberellins where all detected family members are reported (Fig. 5.12).

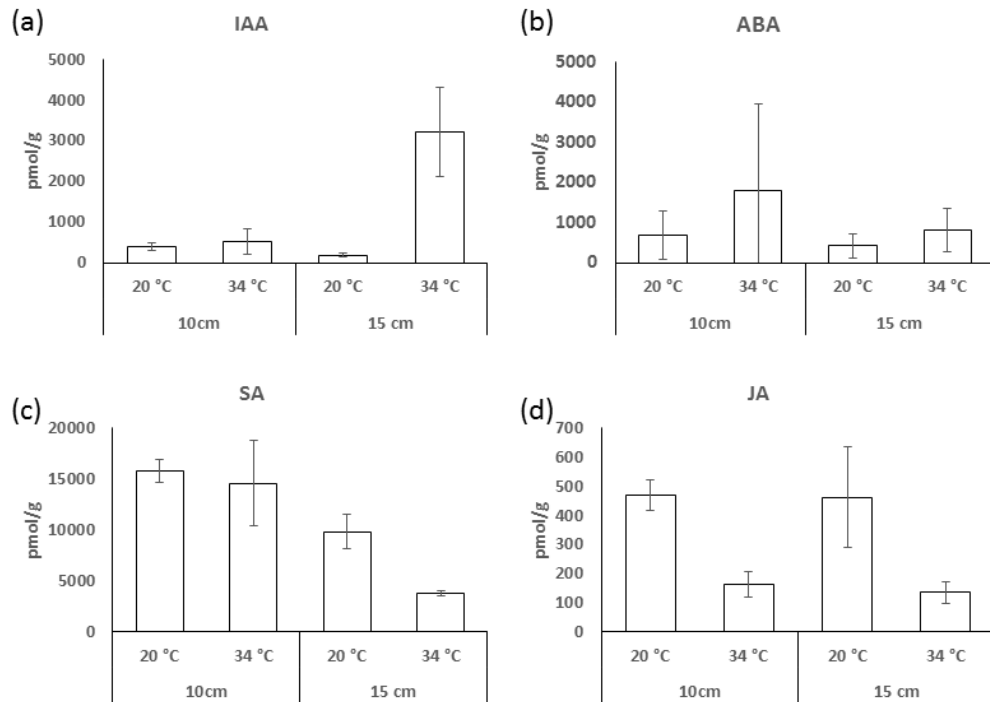


Figure 5.10. Hormone concentrations (pmol/g) in anthers at two development stages (10 cm or 15 cm FLS length) under control and HT conditions. (a) IAA – *Indole-3-acetic acid*, (b) ABA - *Abscisic acid*, (c) SA – *Salicylic Acid*, (d) JA - *Jasmonic acid*. Values shown are means of three biological replicates, error bars are one standard deviation of the mean. Individual pairwise comparisons were made using 5% L.S.Ds (not shown).

Endogenous IAA has been demonstrated to have a role in tapetum PCD and anther sugar-signalling responses under HT (Oshino *et al.*, 2011; Min *et al.*, 2013) and exogenous application of IAA can protect male reproductive development from HT (Sakata *et al.*, 2010) (see section 1.5.2.). Here, anther auxin concentration was found to respond significantly to developmental stage ($p < 0.05$), temperature ($p < 0.01$) and the interaction term ($p < 0.01$) (Fig. 5.10. a). Clearly, HT causes a dramatic increase in IAA biosynthesis, from 118.97 pmol/g to 3207.02 pmol/g, at the later stage of development.

ABA is a well characterised stress hormone and an increase in biosynthesis would be expected in response to HT treatment. Indeed, at both developmental stages, endogenous ABA concentration is elevated in response

to HT (Fig. 5.10. b.), however due to large amounts of variation within replicated samples no statistically significant differences were detected. Salicylic acid (SA) concentrations decline significantly as anthers age ($P < 0.01$) (Fig. 5.10. c.). Furthermore, SA concentrations are significantly reduced by HT at the later developmental stage ($p < 0.05$) but does not respond at the early stage. Information relating to the role of SA in anther and pollen development is scarce. However, it has been shown that exogenous application of SA can protect rice pollen development from HT possibly through the upregulation of ROS-scavenging enzyme levels (Mohammed and Tarpley, 2009).

Jasmonic acid (JA) is an important regulator of anther developmental pathways, particularly filament elongation, anther dehiscence and the final stages of pollen maturation (Qi *et al.*, 2015). JA concentrations are significantly reduced ($P < 0.01$) by HT at both anther developmental stages. No differences in concentration was detected between control samples of the two developmental stages suggesting that JA levels remain relatively stable during this period in the materials collected.

A number of GA-family members were detected by LC-MS (Fig. 5.11.), however GA₁₅, GA₂₄, GA₅₁, GA₂₉, GA₆, GA₅ and the bioactive form GA₄ were not detected in any experimental samples. Earlier precursors prior to GA₁₂ were not examined.

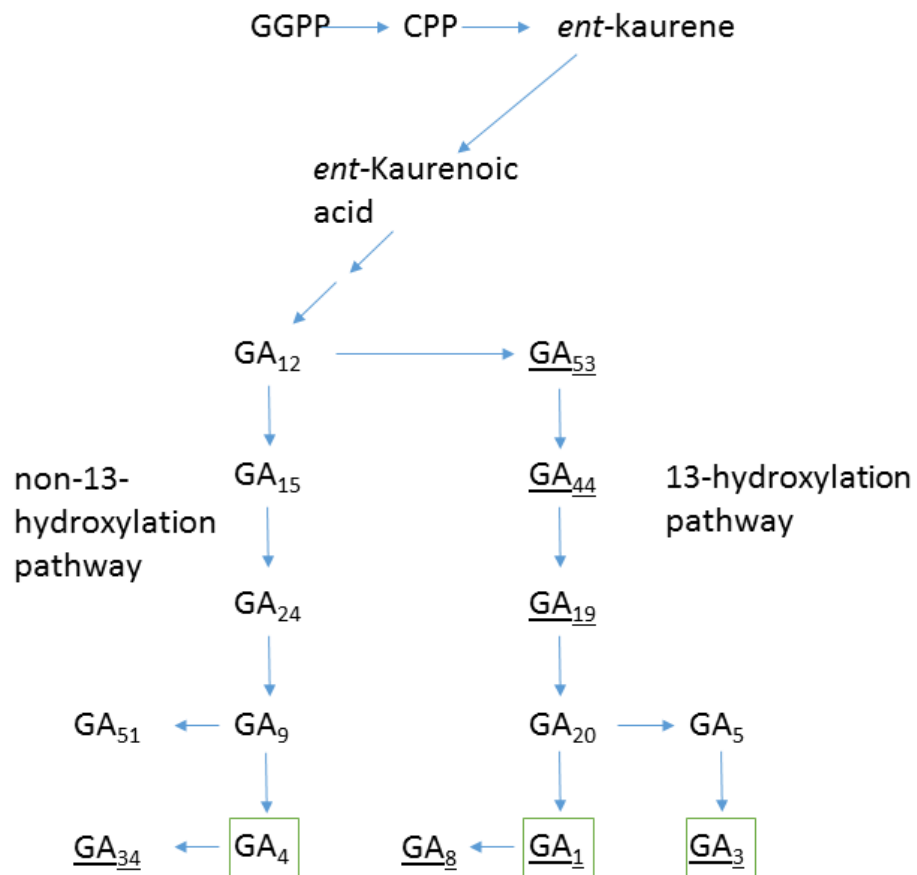


Figure 5.11. The 13-hydroxylated and non-13-hydroxylated GA-biosynthesis pathway. The 13 and non-13-hydroxylation pathways and their intermediary forms are shown. GAs in green squares are have biological activity, underlining indicates detection in this assay. Double arrows indicates intermediaries not show. GGPP – *trans*-geranylgeranyl diphosphate, CPP – *ent*-copalyl diphosphate.

The majority of detected GA family members belong to the early-13-hydroxylation pathway (Fig. 5.12), which is surprising given previous reports showing GA₄ is the dominant form of bioactive GA in closely related rice anther (Hirano *et al.*, 2008) and the observation of large quantities of GA₄ and GA₉ in wheat anthers analysed by GC-MS.

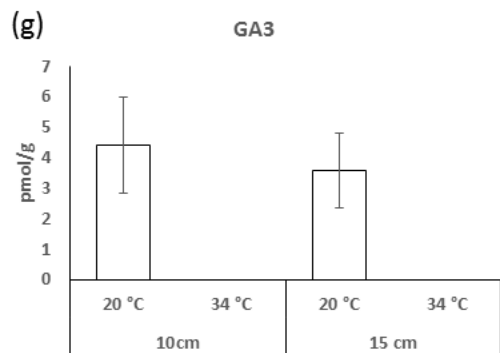
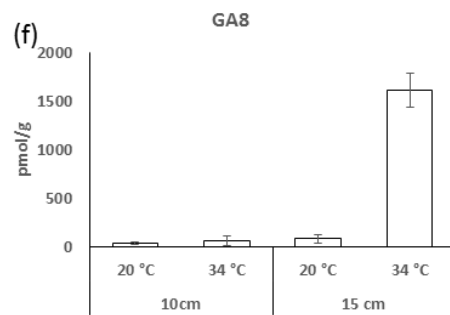
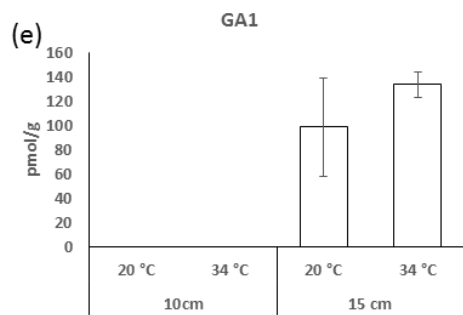
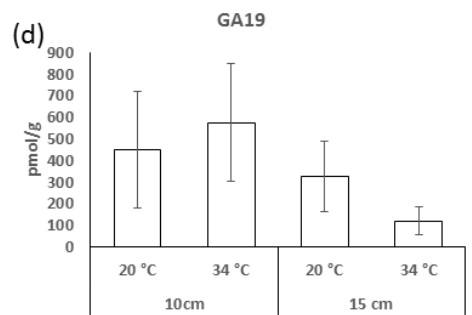
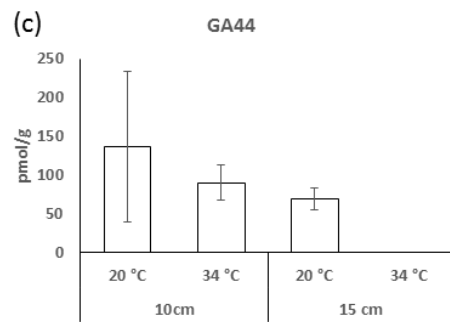
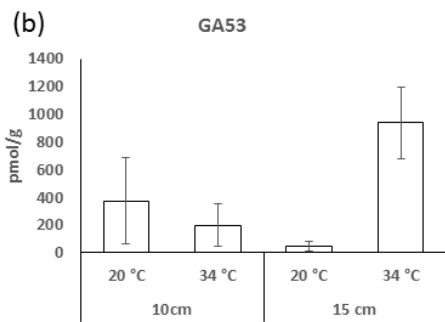
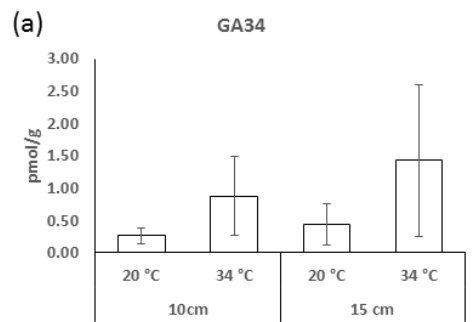


Figure 5.12. Quantification of gibberellins in anthers at two development stages (10 cm or 15 cm FLS length) under control and HT conditions.

Biologically inactive precursor forms were detected: GA₅₃ (b), GA₄₄ (c), and GA₁₉ (d); and the inactive catabolites GA₃₄ (a) and GA₈ (f). Two biologically active forms were also detected; GA₁ (e) and GA₃ (g). Values shown are means of three biological replicates, error bars are one standard deviation of the mean. Individual pairwise comparisons were made using 5% L.S.Ds (not shown).

GA₃₄, the 2 β -hydroxylated deactivated form of the non-13-hydroxylated bioactive GA₄, was found at extremely low concentrations, elevating slightly in response to HT at both stages but not interacting significantly with either treatment (Fig. 5.12. a). GA₅₃ is the first product of the early-13-hydroxy-pathway after the bifurcation at GA₁₂. Concentration of GA₅₃ responds significantly to the interaction between stage and HT ($p < 0.01$) and is significantly elevated in response to HT at the later developmental stage ($p < 0.05$) (Fig. 5.12. b). The next, two precursor forms produced by GA20ox-family enzymes, GA₄₄ (Fig. 5.12. c) and GA₁₉ (Fig. 5.12. d) do not differ significantly between treatments, although GA₄₄ could not be detected under HT at the later development stage. However, the final intermediate produced by the GA20ox family in this pathway, GA₂₀ (Fig. 5.11.), was not detected.

The bioactive GA product of the 13-hydroxylation pathway, GA₁, was not detected in either of the early stage samples but was significantly elevated at the later developmental stage ($p < 0.01$) (Fig. 5.12. e). Cellular concentration of its 2 β -hydroxylated inactive form GA₈ was significantly increased by HT in the later stage of development ($p < 0.05$) (Fig. 5.12. f), suggesting HT affects the rate of turnover of bioactive GA. Likewise, another biologically active form, GA₃, was detected under control conditions at both developmental stages but is absent under HT (Fig. 5.12. g). However, given the low concentrations of GA₃ detected (max. 6 pmol/g), this observation may be of little biological relevance.

GA₁ and GA₃₄ were also detected in samples analysed using GA-specific GC-MS, supporting the findings of the global LC-MS analysis. However, due to interfering peaks, it was not possible to quantify them by GC-MS without further separation of samples by High Performance Liquid Chromatography (HPLC).

5.4. Discussion

In this chapter a combined transcriptomic and global hormone analysis approach has revealed previously unknown information about the genetic and hormonal regulation of wheat anther responses to HT stress. Gene expression and ontology analysis using two separate bioinformatics pipelines independently show that HT stress causes significant upregulation of genes associated with hormone-mediated processes in tapetum and developing pollen cells. Furthermore, global hormone quantification demonstrated HT stress alters the hormonal profile of anthers, potentially explaining some of the observed changes in gene expression.

The ambitious aim of these experiments was to create comparable gene expression and hormone quantification datasets which would allow the dissection of hormonal regulation of gene expression during normal development and under HT-stress conditions. Both analyses were carried out using a HT-stress treatment of 34 °C for 24 h, comparable to previous experiments which have demonstrated a negative effect of HT on anther development, specifically perturbing hormonal biosynthesis and signalling pathways (Saini *et al.*, 1984; Sakata and Higashitani, 2008; Oshino *et al.*, 2007, 2011). RNAseq analysis was targeted to the PMC anther development stage, whereas hormonal analysis was carried out on two later anther development stages (meiotic and pre-mitotic development). Similar experimental approaches in rice have suggested that synthesis of GA-precursors and metabolic enzymes may occur in the tapetum, followed by the completion of bioactive GA formation using these components in mature pollen cells (Hirano *et al.*, 2008; Plackett *et al.*, 2012). Therefore, whilst the transcriptional and

hormone concentration datasets do not overlap temporally, understanding the effects of HT on the expression of biosynthesis and signalling components during early development may help to explain later irregularities in anther hormone profiles.

Both studies have been negatively affected by the developmental variation of the experimental samples. Principle component analysis of sample variance (Fig. 5.5.) shows the impact of sample biological variability on the output from RNA-Seq differential gene expression analysis. The result of this was an inability to distinguish manageable clusters of genes with shared developmental and HT transcriptional responses (Fig. 5.4.). It was therefore decided to perform a differential gene expression analysis on a single time point with samples more suitably divided by treatment and grouped by cluster (Fig. 5.7.). However, only two biological replicates for either treatment samples were considered in the analysis which is not statistically ideal and dramatically reduces the confidence with which observations can be considered. Likewise, large amounts of variation in hormone levels detected were present amongst biological replicates of individual samples.

The source of this variation is most likely to be differences in developmental stage of anthers within replicates. The FLS length method described in chapter 3 was used in both experiments. Asynchronous anther development between floret positions is likely to have been a source of some of this variability. Furthermore, at 10 cm FLS the spikes are very small and dissecting out specific-anthers in sufficient quantity is technically challenging. It is therefore possible that some damage may have occurred to the experimental material. Clearly, the limitations of this approach have been reached by these experiments which require relatively large quantities of very accurately staged material. Further refinement of the staging method is obviously a pre-requisite to any future attempts to repeat these experiments.

A further limitation of any RNA-Seq experiment is the quality of the reference genome and annotation used for mapping (see section 5.2.5). During the

course of this analysis the quality, coverage and annotation of the wheat reference genome improved significantly. The TGACv1 reference includes 273,739 gene transcripts as opposed to 112,496 gene transcripts in the IWGSC gene version. Using a whole genome reference allows the use of Cufflinks which is able to identify additional genes which do not appear in the reference sequence. In comparison, using a transcriptome reference restricts analyses to genes already identified and listed in the TGACv1 gene annotation.

Nonetheless, the significantly increased number of annotated genes within the TGACv1 cDNA reference (273,739 compared to 112,469 in the IWGSC reference) and its suitability for use in a less complex and computationally demanding bioinformatics pipeline allowed for a useful analysis to be carried out in a very short period of time. Furthermore, the overall similarity in DEGs and GO-terms identified in both analyses suggest using a well annotated transcriptome reference is preferable to more demanding pipelines using a lower quality genomic reference.

5.4.1. Acceleration of the tapetum development programme

The role of the tapetum is to provide crucial nutrients, cellular components and developmental signals to developing pollen cells and undergo PCD, all of which is disrupted by HT stress (Parish *et al.*, 2013). After 24 h exposure to HT around meiosis, the most significantly differentially expressed genes in wheat anthers are associated with the processes known to be occurring in tapetum cells at that stage. These analyses provide a comprehensive list of candidate HT-responsive wheat anther genes for further investigation as well as providing important information about the expression profiles of anther development genes, such as *TaGAMYB* and *TabHLH141*, which have previously been difficult to obtain by qRT-PCR.

Using the TGACv1 cDNA reference, the two previously unannotated most significantly upregulated transcripts encode BURP domain containing proteins (Table 5.3.). Whilst BURP domain proteins have been found to be expressed in diverse developmental contexts in a number of plant species, to date

TaRAFTIN is the only reported wheat BURP domain gene in the literature. Expression of *OsRaftin* has been reported in tapetum and to a lesser extent in microspores (Wang *et al.*, 2003; Suwabe *et al.*, 2008). RAFTIN is found in the peritapetal wall, Ubisch bodies and exine, which suggest that it plays a role in the accumulation of sporopollenin on Ubisch bodies and its correct assembly on the pollen exine (Wang *et al.*, 2003) (see section 1.). However, BLAST search of the TGACv1 assembly using a rice transcript annotated as *OsRaftin* (LOC_Os08g0496800) found that a different transcript (TRIAE_CS42_7BS_TGACv1_591818_AA1922490) was a more likely candidate for *TaRaftin* ($E = 1.73 \times 10^{-54}$, 91.3% identity), whereas the first and second DEGs shared 52.3% and 52.6% pairwise identity respectively with *OsRaftin* when aligned using the Geneious (BioMatters, Auckland, New Zealand) aligner with default parameters. Therefore, further work is required to establish the function of the BURP-domain annotated DEGs.

Similarly, significant upregulation of genes annotated as meiotic serinases, which may be involved in callase production and PCD (Taylor *et al.*, 1997), along with arabinogalactans and pectinesterases which regulate the formation and degradation of cell walls (Table. 5.3.) (Wu *et al.*, 2015) could be responsible for aberrant tapetum function and/or pollen wall formation. Indeed, Wu *et al.*, (2015) found 5 pectinase genes to also be highly upregulated in rice floral organs under HT. It's possible that the upregulation of these genes is indicative of an acceleration of the tapetum PCD programme. However, further information about the location of their expression and their functions is required to confirm this.

Production and transport lipid biosynthesis precursors is performed by the tapetum and is a crucial component of the sporopollenin synthesis pathway (Huang *et al.*, 2009). Therefore, the significant upregulation of fatty acid reductase and cytochrome P450 annotated transcripts in response to HT agrees with the emerging trend of modulation of tapetal metabolism under HT. Likewise, the upregulation of hexokinase transcripts indicates a similar change in anther carbohydrate metabolism occurs under HT. Hexokinase

catalyses the ATP-dependent conversion of hexose to hexose 6-phosphates; one hexokinase gene *OshxK10* is specifically expressed in the anther and is required for rice pollen germination (Cho *et al.*, 2006; Xu *et al.*, 2008) Some authors have pointed to sugar-starvation as the HT-induced cause of sterility (Parish *et al.*, 2013); however, it is equally possible that altered carbohydrate metabolism is part of a metabolic adjustment to HT rather than a symptom of HT-injury (Müller and Rieu, 2016)

GO-term enrichment of DEGs further supports the observation that tapetal metabolic processes are affected by HT. Specific terms associated with lipid and carbohydrate metabolism were all highly represented in DEG sequences along with meiosis, pollen development and cell death terms (Fig 5.7.). Oshino *et al.*, (2007) proposed that HT stress causes the premature progression of the anther developmental programme which is the underlying cause of HT-injury. Analysis of whole transcriptome changes undertaken here seem to support this hypothesis. Indeed, cytological analysis of wheat anthers under control and HT treatment display a marked divergence in developmental rate (Fig. 5.3). However, Endo *et al.*, (2009) found no difference in the expression of *OsRaftin*, *OsC6* or *OsTDR* in response to heat stress and instead conclude that specific tapetal mechanisms must be disrupted as opposed to tapetum development *per se*. Indeed, pollen from HT-injured anthers appeared normal, taking up Alexander stain, but failed to adhere to and germinate on receptive stigma (Endo *et al.*, 2009). Further biochemical analysis of pollen and anther ultra-structures is required to determine the biological outcomes of HT-responsive transcription.

Many of the DEGs and HT-enriched GO-terms relate to anther and pollen developmental processes which are known to involve hormone signalling. Tapetum PCD and Ubisch body formation is regulated by GA via *GAMYB* (see section 1.4.2.). No significant changes in the expression of *TaGAMYB* or other GA-biosynthesis or signalling genes were detected, consistent with other studies. Endo *et al.*, (2009) noted that a cluster of significantly HT-down-regulated genes contained a large number of transcripts also down-regulated

in the *gamyb* mutant (Kaneko *et al.*, 2004). Microarray studies of *gamyb* and other GA-signalling mutants indicates that almost all GA-regulation of transcription in the anther requires *GAMYB* (Aya *et al.*, 2009). The discovery that RHT-D1 directly binds to the PCD elicitor TabHLH141 (see section 4) demonstrates a potential *GAMYB*-independent regulation of tapetum function. It may be the case that HT causes changes to hormone signalling in anthers which alters the stability or binding ability of negative regulators of PCD and tapetum function, resulting in the apparent acceleration of development. Likewise, *GAMYB* converges with *UDT1* on the bHLH signalling cascade which regulates PCD (see section 1.3.2.). The observed increase in *TabHLH141_B* expression (Fig. 5.9. j) and significant downregulation of *TIP2-like* and *AMS-like* annotated transcripts after 24 h HT suggest a regulatory factor other than *GAMYB* is involved in the HT response.

Fisher's exact test was used to determine which biological function GO-terms were significantly under- or over-represented in DEGs under HT compared to control conditions (Table 5.2.). Specific under-representation of GA and IAA biosynthesis and signalling at 24 h HT agrees with previous observations (Oshino *et al.*, 2011). Both hormones have been shown to have a role in pollen cell meiosis and mitosis (Liu *et al.*, 2010; Cecchetti *et al.*, 2015; Müller and Rieu, 2016) and indeed terms related to cellular division, DNA replication etc. were highly represented GO-term enrichments. The under-representation of ABA-signalling terms was unexpected (Table 5.2.). ABA is a stress hormone which has been shown to accumulate in anthers during abiotic stress, negatively affecting carbohydrate transport to developing microspores (Oliver *et al.*, 2005; Ji *et al.*, 2011). Significant upregulation of carbohydrate metabolism genes could represent attempts to mobilise additional resources required to support a HT-stress induced, heightened metabolic state (Müller and Rieu, 2016). ABA and GA have been shown to differentially regulate the expression of *INVERTASE* genes which regulate the conversion and transport of sucrose assimilate for tapetum and pollen cell metabolism and storage (De Storme and Geelen, 2014).

5.4.2. Modulation of the anther hormone profiles in response to HT

Analysis of anther whole transcriptome responses to HT revealed a number of hormone-mediated processes are affected. In order to better understand these observations in the context of absolute hormone concentrations, comparative global hormone analysis was carried out (Fig. 5.10. and 12.).

Significant changes in hormone concentrations attributable to developmental stage and HT stress were observed. Previous reports have suggested that transcriptional changes in HT-injured barley anthers is accompanied by a decrease in auxin biosynthesis (Oshino *et al.*, 2007; Sakata *et al.*, 2010; Higashitani, 2013). However, in cotton HT-tolerant varieties show an increase in anther auxin concentration in response to HT-stress (Min *et al.*, 2014) . Here, however, auxin levels are dramatically elevated by HT at the later developmental stage (Fig 5.10. a). it should be noted that the barley studies focused on earlier stages of anther development, beginning prior to the establishment of the tapetum layer (Oshino *et al.*, 2011), whereas here anthers were examined between PMC meiosis and mitosis stages. Also, in these studies, auxins were quantified by immune-detection (Sakata *et al.*, 2010) which is of limited sensitivity and has since been superseded by LC/GC-MS (Forcat *et al.*, 2008). Ability to maintain auxin biosynthesis under HT is thought to be a determinant of thermotolerance (Tang *et al.*, 2007) possibly due to its role in cell division (Sakata *et al.*, 2010). However, a more complex picture of auxin signalling in HT responses is emerging. HT in late stage cotton anthers results in sugar-signalling mediated upregulation of *PIFs* which themselves upregulate auxin biosynthesis which appears to be a trait more associated with HT-sensitive genotypes (Min *et al.*, 2014). The precise role of auxin signalling in HT responses, and particularly its involvement in crosstalk with sugar-signalling remains unclear but evidently could be an important point of convergence between metabolic and hormonal stress response signals.

ABA content was not found to differ significantly between developmental or temperature treatments although increases in response to HT were observed (Fig. 5.10. b). There was pronounced variation in ABA content between biological replicates which indicates that specific developmental stage might be particularly important in determining HT-induced biosynthesis levels. In the barley aleurone ABA inhibits PCD by suppressing GA-induced ROS production (Ishibashi *et al.*, 2012). This suggests that, additional to its role in carbohydrate metabolism, increased ABA concentrations in response to HT may be a response mechanism to ROS accumulation due to cellular injury. Furthermore, ABA stabilises DELLAs thus negatively regulating GA-signalling pathways (Sun, 2010). As GA- and ROS-signalling are known to induce tapetum PCD (see section 1.4.3.) it is possible that accumulation of ABA in the 24 hours preceding initiation of HT is targeted at restricting the premature acceleration of tapetum PCD.

SA is a stress responsive hormone which has been shown, along with ABA and ethylene to alleviate oxidative damage to cells caused by HT (Larkindale and Knight, 2002). SA levels were found only to differ significantly between developmental stages and not in response to HT (Fig. 5.10. c). The significance of SA in anther and pollen development is unclear. JA is also a stress responsive hormone which positively regulates the later stages of pollen maturation (Qi *et al.*, 2015). Transcription of JA-biosynthesis and signalling genes has been demonstrated to be active at all stages of rice tapetum development and JA is preferentially synthesised at the tricellular pollen stage (Hirano *et al.*, 2008) Here, JA concentration is significantly reduced by HT (Fig. 5.10. d). Further information about the role of JA in HT responses is scant: however, a bHLH TF appearing to act oppositely to positively regulate ABA-signalling whilst repressing JA-signalling has been identified (Nakata *et al.*, 2013). Furthermore, JA also is involved in antagonistic crosstalk with GA and ethylene (Song *et al.*, 2014) suggesting that JA may be important for attenuating the responses to other signalling pathways. Further work will be needed to identify wheat orthologues of JA-biosynthesis and signalling genes

and to quantify their response to HT using the whole transcriptome analysis (see section 5.3.4.). However, the dramatic reductions in JA levels under HT at both developmental stages suggests that regulation of JA biosynthesis in anthers is negatively affected by HT-stress.

The detection of GAs primarily from the 13-hydroxylation pathway is a curious observation. It had previously been reported that GA₄, produced via the non-13-hydroxylation pathway is favoured in reproductive development (Kobayashi *et al.*, 1989). Indeed, pilot analysis of anthers nearing maturity using GC-MS detected high levels of GA₄ and its precursor GA₉ (see section 5.3.6). Here, only very low levels of GA₃₄, the product of GA₄ catabolism were detected (Fig. 5.12. a), suggesting that the non-13-hydroxylation pathway is functional in the anther tissue analyses but turned over very rapidly. Three precursor forms of the 13-hydroxylation pathway, GA₅₃, GA₄₄, and GA₁₉ were present at both stages of anther development (Fig. 5.12 b, c, d). Expression of *GA13OX* genes required to divert GA₁₂ from the non-13- to the 13-hydroxylation pathway is extremely low during earlier anther development (Fig. 5.10. c, d). This suggests that a preference for either pathway may depend on developmental stage and could be reflective of the changing tissue composition of the anther during development. The detection of products of both pathways in maize pollen anther tissue has prompted the suggestion that sporophytic and pollen tissue have differing GA-biosynthesis profiles (Yamaguchi *et al.*, 1990). Indeed, Hirano *et al.*, (2008) demonstrated that expression of GA-precursor genes was detectable in the tapetum, but production of bioactive GA₄ takes place in maturing pollen where the *GA20* and *GA30OX* genes which catalyse the final activation steps are highly expressed. Much further work is needed to determine if this is indeed the case and what the biological significance of favouring GA₁ or GA₄ is for reproductive development.

The overall effect of HT on GA-biosynthesis is unclear; production of the bioactive GA₃, a by-product of the 13-hydroxylation pathway, is abolished by HT (Fig. 5.12. g) and the production of de-activated GA₁ in the form of GA₈ is

dramatically elevated by HT at the later stage of development (Fig. 5.12. f). Transcriptional data also suggests that HT causes an increase in the expression of *TaGA13OX* and *TaGA20OX* (Fig 5.10. c, d, e, f) which might explain the observed elevation in GA₁ and GA₈. Previous studies have shown a decrease in anther GA levels in response to HT (Tang *et al.*, 2007). The HT-induced upregulation of *TaGID1* may also be an indication of declining levels of bioactive GA as it has been shown to be negatively regulated by exogenous GA₃ (Li *et al.*, 2013). GA₃ is bioactive and decreases significantly to HT (Fig. 5.12. g) However, it is present in very small concentrations under control conditions, most likely as a by-product of GA₁ biosynthesis (P. Hedden, pers. comm.), and therefore its biological significance is unclear. Some minor changes in the expression of *TaGA20OX* paralogues was observed under HT suggesting some transcription upregulation of GA-biosynthesis is taking place (Fig. 5.10. d, e) and this perhaps corresponds to changes in GA₅₃, GA₄₄ and GA₁₉ concentrations (Fig. 5.12. b, c, d). Hirano *et al.*, (2008) hypothesise that the *GA20OX* and *3OX* genes expressed in rice microspores have a higher affinity for non-13-hydroxylated precursors. Therefore, it is possible that HT-induced alteration to the expression of specific *TaGA20* and *3OX* paralogues (Fig. 5.9. e, f, g) are a response to depletion of non-13-hydroxylated precursors. However, further information about the contribution of specific paralogues to GA-biosynthesis in wheat is required in order to make any further inferences about these observations.

The transcriptomic and global hormone analyses presented in this chapter highlight the complexity of the HT response in developing wheat anthers. The most dramatic changes in gene expression primarily relate to tapetum processes involved in formation of the pollen exine and carbohydrate metabolism and PCD. This is consistent with previous observations, suggesting that either through acceleration of the developmental programme *per se* or disruption of specific pathways, HT stress prevents critical processes carried out by the tapetum. However, a number of questions about the events leading to sterility remain; does upregulation of tapetum metabolism genes

contribute to premature PCD by 'overloading' cellular metabolic capacity? Does a sudden surge in Ubisch body and sporopollenin promoting genes somehow disturb pollen exine patterning? Answering these questions will require more in depth knowledge of wheat tapetum function. For example, the exact role of Ubisch bodies and their formation is not well understood (Gómez *et al.*, 2015), highlighting a knowledge gap important to understanding HT-responses. Furthermore, secondary metabolites such as ROS and carbohydrates themselves act as signalling molecules which elicit PCD and crosstalk with hormone signalling (Parish and Li, 2010; Ishibashi *et al.*, 2012; Parish *et al.*, 2013). It therefore needs to be resolved as to whether these molecules are signals or executors of HT-injury. Some progress has been made on addressing a similar question on the role of ROS in aleurone PCD signalling using biochemical ROS quantification in hormone signalling mutants (Ishibashi *et al.*, 2012; Aoki *et al.*, 2014) and similar approaches could be applied to the wheat anther.

The signalling mechanisms which control anther HT-responses are still poorly understood. HT-stress touches on processes in which several hormonal signalling pathways are involved, particularly GA, ABA and IAA. Changes in hormonal concentrations and transcription of biosynthesis and signalling genes have been observed. GA-signalling is required for tapetum PCD and although down-regulation of GA-responsive genes under HT has been observed, no link has yet been established between HT-induced tapetum defects and GA-signalling. A complex picture of GA-biosynthesis appearing to switch between biosynthetic pathways at different stages of development emerged in this study. Further work is required to determine if this is the case, at what point the transition occurs and the functional relevance. One possibility is that either pathway is favoured by pollen and sporophytic cells separately; as anther development progresses, pollen accounts for an increasing amount of the anther mass and therefore the pollen-preferred pathway comes to dominate. With the increasing availability of wheat reverse genetics tools (see section 4), it would now be possible to generate wheat GA-

biosynthesis mutants for the purpose of dissecting the sites and temporal specificity of GA biosynthesis in wheat anthers as has been done in *Arabidopsis* (Rieu *et al.*, 2007; Plackett *et al.*, 2012).

CHAPTER 6: GENERAL DISCUSSION

6.1. Project Summary

HT-stress during male reproductive development is predicted to become a significant cause of wheat yield loss in Northern Europe by the middle of this century (see section 1.1). The underlying physiological cause of this loss of yield is damage caused by HT to the tapetum, a layer of cells lining the inside of the anther which provide vital nutrients and outer coat components to developing pollen cells (see section 1.5). Studies in wheat and closely related cereals rice and barley, have shown that HT-stress causes fertility-reducing defects such as premature tapetum PCD, aborted microspores and failure to properly form the pollen exine and pollen starch reserves (see section 1.5). The development of the tapetum and the critical timing of its PCD has been shown in model species to be under the control of GA-signalling via the TF GAMYB and a second signalling network which converges with the GA-GAMYB pathway on a bHLH TF cascade that targets *OsEAT1* (see section 1.3).

Given that many of the anther development processes have been shown to be controlled by GA-signalling are negatively affected by HT-stress, development of HT-stress mitigation strategies requires a better understanding of anther GA-signalling and HT-responses. Therefore, in this project translational genomics was applied to identify and characterise two putative wheat anther GA-signalling components; *TaGAMYB* and *TabHLH141*. The whole-anther hormonal and transcriptional responses to HT-stress were investigated by identifying HT-DEGs and HT-induced changes in anther hormone profile using a combined approach of LC-MS hormone quantification and RNA-Seq.

6.2. Limitations of studying anther development in wheat

A major limitation throughout this project was the difficulty associated with accurately staging male reproductive development. Having first characterised anther development stages in Cadenza, the variety used in this project, a non-destructive anther staging method based on the association between FLS

length and anther development was established (see section 3). However, it was clearly demonstrated that the logistic regression on which the staging model was based was not able to overcome the inherent developmental variability between plants, spikes and floret positions. Whilst material could be grouped into broad developmental categories, the selection of developmentally variable material for molecular analyses such as qRT-PCR, RNA-Seq and biochemical analysis of hormones has quite clearly reduced the accuracy of these measurements. Overcoming this is crucial to understanding the highly dynamic developmental and stress-responsive changes to hormone signalling pathways in wheat anthers.

The requirement for selection of developmentally uniform anthers when undertaking molecular analysis necessitates that researchers have some means of establishing development stage prior to harvest or treatment and without damaging the tissue. One approach to achieving this may be the utilisation of advanced plant imaging techniques. Real-time 3D visualisation of internal development in germinating wheat seeds has demonstrated that X-ray computer tomography (micro-CT) can be used to assess developmental changes in internal morphology (Suresh and Neethirajan, 2015). If such a system can be scaled up from individual grains to whole tillers, allowing the visualisation of internal spike characteristics such as spike or individual anther length, the accuracy and predictive power of reproductive staging models could be greatly increased. Indeed, anther length in rice, resolved in mm, has been shown to be a good descriptor of anther development stage between formation of archesporial cells through to Mitosis II (Itoh *et al.*, 2005).

6.3. GA-signalling and the wheat tapetum

GAMYB is the central transcription factor in GA-signalling in the rice tapetum (Aya *et al.*, 2009). A major finding of this project is that wheat *Tagamyb* RNAi and TILLING mutants are also male sterile, suggesting that *GAMYB* anther function is conserved in cereals. However, the tapetal hypertrophy phenotype seen in many rice mutants was not as strong in wheat mutants. Whilst some

excessive tapetum vacuolation was observed, the presence of excessive debris within the anther locule suggests that disruption of tapetum function as opposed to complete failure to initiate PCD is the cause of reduced fertility in wheat mutants. Similarly, RNAi-mediated silencing of *TabHLH141* induced sterility but no causal defective anther phenotype was observed.

Ideally, more extensive characterisation of these mutants would be carried out on T₃ homozygous RNAi and backcrossed TILLING mutants to reduce the impact of background effects. However, given the time required to generate wheat mutant plants by transgenesis and TILLING, only a preliminary characterisation of early mutant generations was possible in this project. Furthermore, additional refinement of PCR based approaches to genotyping and transcript quantification are required in order to confirm the correct selection of homozygous lines and silencing of target genes.

Once homozygous RNAi-knockdown mutants and backcrossed TILLING mutants have been obtained, further characterisation assays should be carried out to clarify the roles of *TaGAMYB* and *TabHLH141* in the wheat tapetum and developing microspores. Firstly, a more detailed comparative analysis of anther morphological development in mutants and segregating nulls, incorporating a greater range of developmental stages, is required to establish precisely which processes are perturbed by the loss of either gene function. In both mutants, no obvious delay of tapetum PCD or hypertrophy similar to that of corresponding rice mutants was observed. The TUNEL assay could be used to definitively resolve if delayed tapetum PCD also occurs in the wheat mutants. Furthermore, having observed the production of pollen cells in all of the mutants generated in this project, it is important to determine the source of their non-viability.

A yeast 2-hybrid interaction study demonstrated that the RHT-1GRAS domain interacts with *TabHLH141* (see section 4.3.4.). This suggests that GA-signalling may positively regulate tapetum PCD by releasing *TabHLH141* from DELLA sequestration. Whilst this interaction must be confirmed *in planta*, it

demonstrates that the role of GA-signalling in tapetum PCD may not solely operate through GAMYB as described in rice (Aya *et al.*, 2009). The rice orthologue *OsEAT1* is transcriptionally regulated by *OsTDR* which itself is co-regulated by *OsUDT1* and *OsGAMYB* (see section 1.3.2.). Therefore, it may be the case that *TaGAMYB* is partially responsible for the upregulation of *TabHLH141* but the commitment to PCD is not carried out until the GA signal releases the repression of *TabHLH141* by RHT-1. Determining the expression profiles of *Rht-1*, *TaGAMYB* and *TabHLH141* in both wild type and the signalling mutants generated here will be crucial to determining the signalling relationship between these GA-signalling components in wheat anther development.

DELLA and JA-signalling negative regulator JA-ZIM DOMAIN (JAZ) have been shown to competitively bind to WD-repeat/MYB/bHLH complexes during the mediation of anthocyanin biosynthesis and trichome initiation (Qi *et al.*, 2011; Tian *et al.*, 2016). It is therefore proposed that RHT-1 and GAMYB are able to form similar complexes with bHLH proteins in the anther which regulate their transcriptional activity in a GA-responsive manner (Fig 6.1.). The binding of GAMYB and bHLH TFs into DELLA-interacting complexes could result in alterations to their transcriptional activity dependent upon the protein domains involved in the interaction. This may therefore explain the apparent dual functions of GAMYB and bHLH141 in initiation of tapetum PCD and formation of the pollen exine.

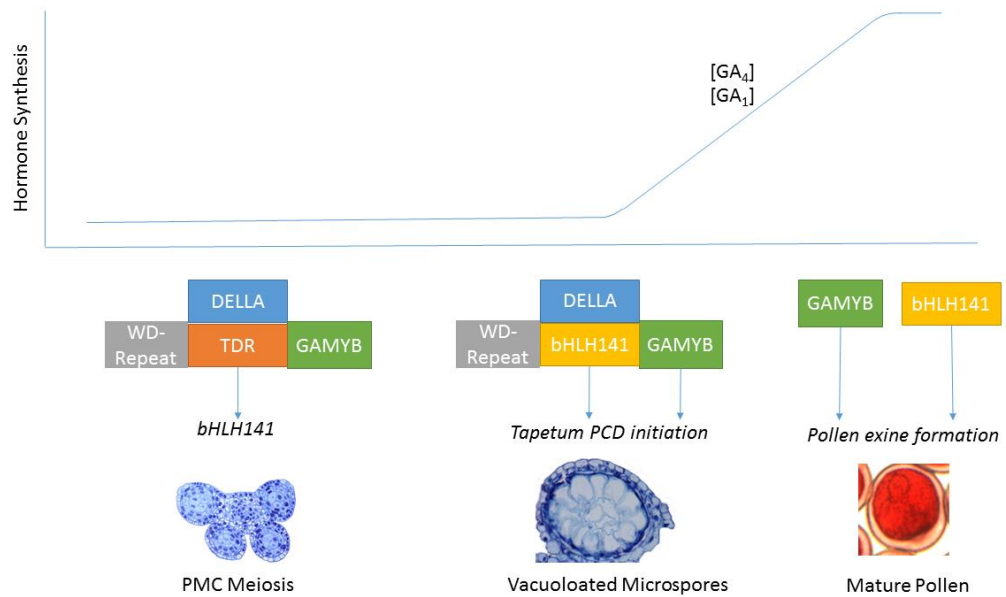


Figure 6.1. Proposed model of anther developmental regulation by GA. *Binding of WD-repeat/bHLH/MYB complexes by DELLA regulates anther development. Perception of a GA signal releases the TFs from complexes, changing their transcriptional functions.*

In the proposed model, the absence of bioactive GA during early anther development promotes the formation of DELLA-interacting WD-repeat/TDR/GAMYB complexes which enhances the expression of *bHLH141*. Tapetum PCD is initiated around the vacuolated microspores stage by *bHLH141* and GAMYB. At this point there is little reported expression of GA-biosynthesis genes in the anther (Hirano *et al.*, 2008) and therefore it would be expected under the proposed model that GAMYB and *bHLH141* would be retained within the DELLA-interacting complex. Anther GA concentration increases rapidly from mitosis to mature pollen cells, resulting in DELLA degradation (Hirano *et al.*, 2008). At this stage, GAMYB and *bHLH141* are released from the regulatory complex, exposing previously bound functional domains which promote the formation of the pollen exine coat. Understanding the environmental regulation of these interactions will be crucial to determining why HT-stress leads to failed pollen and tapetum development. Whilst further work needs to be done to determine the involvement of GAMYB in DELLA-interacting complexes, the RHT-1 – *bHLH141*

interaction provides a model through which the effect of environmental stress on GA-regulation of wheat anther development can be dissected further.

The rapid development of homozygous, triple knock-out *Tagamyb* mutants by exon-capture TILLING represents a step-change in wheat genetic research. Using accelerated-life cycle techniques and high throughput genotyping (see section 4) it was possible to stack three homoeologous SNPs in *TaGAMYB* to obtain homozygous triple mutants in less than 12 months. In comparison, the cloning, transformation and regeneration in tissue culture of T₀ RNAi mutants took nearly twice as long. Whilst RNAi phenotypically demonstrated the importance of *TaGAMYB* and *TabHLH141* to male fertility, robust genotyping and confirmation of silencing in mutants was difficult to achieve and therefore the validity of these results cannot be confirmed. Furthermore, the development of low-cost, high-throughput competitive allele specific PCR (KASP) assays for simultaneous selection and zygosity assignment of TILLING SNPs will further accelerate the process of mutant stacking (Rasheed *et al.*, 2016). With the publication of increasingly high-quality wheat reference sequences, such as TGACv1 and reducing cost of deep sequencing and genotyping assays, TILLING by exon sequence may soon supersede transgenic approaches to wheat gene characterisation.

6.4. HT-stress elicits hormonal and transcriptional responses

RNAseq was used to investigate the effect of HT-stress on the whole transcriptome of the anther (see section 5). HT-DEG transcripts were identified based on analysis using whole genome and predicted transcriptome references which indicate that tapetum processes controlling pollen coat formation, carbohydrate transport and PCD are affected HT-stress. Most of the DEGs were highly upregulated in response to HT which suggests that overstimulation of metabolic activity of the tapetum may become detrimental to its function. GO-enrichment analysis supported this hypothesis, demonstrating that terms associated with tapetum construction of pollen coat

and carbohydrate transport were considerably over-represented in HT-responsive DEGs.

Initially, RNA-seq analysis was carried out using the IWGSC whole genome reference with the intention of distinguishing between gene expression which varied over the course of anther development and those which vary in response to HT. However, due to the developmental variation within the sequenced material, it was not possible to achieve such in-depth resolution of anther developmental and stress transcriptional responses. Instead, a comparison of samples taken at 24 h after meiosis at HT and control conditions was made using two replicates with similarly distributed variation. Analysis of DEGs was carried out having mapped sequence reads to both the IWGSC whole genome reference sequence and the updated TGACv1 transcriptome reference. Both analyses showed that HT causes a significant upregulation of transcripts associated with pollen exine formation, carbohydrate transport and PCD.

The finding that many HT-responsive DEG transcripts are associated with processes in which GA-signalling has been implicated supports previous observations of negative effects on tapetum function, PCD, pollen exine and transport of carbohydrates to developing pollen (see section 1.4).

Furthermore, significant changes in auxin, GA and JA profiles in response to HT (see section 5.3.6.) confirm that hormonal regulation of wheat anther development is affected by HT-stress. Further identification of auxin, GA and JA-responsive transcripts in the DEG data sets will be required to better understand how the observed changes in anther hormone concentrations contribute to HT-induced damage of anther structures. The rapid generation of hormone signalling mutants by TILLING as described in section 4 may also be a complementary approach to the characterisation of IAA and JA-mediated responses to HT.

GA-biosynthesis and signalling was specifically investigated in greater detail due its role in the regulation of the HT-sensitive tapetum. Preliminary GS-MS

analysis demonstrated that non-13-hydroxylated pathway product GA₄, accumulates in high concentrations in mature anthers, consistent with previous reports (see section 5.3.6). However, this conflicted with LC-MS analysis of younger anthers which detected 13-hydroxylated pathway products (Fig. 5.12.) Some HT-responsive upregulation of *TaGA13OX* transcripts was reported (Fig. 5.9. c, d), suggesting that HT-stress may have some role in modulation of the anther GA-biosynthetic pathway. Further investigation of GA-biosynthesis in wheat anthers is required to clarify the biosynthetic profile under optimal and abiotic stress conditions.

An analysis of the biological processes affected by HT-stress was carried out using gene ontology enrichment of DEGs (see section 5.3.). Terms associated with GA-signalling responses were found to be under-represented in HT-responsive DEGs. However, no significant changes to any known GA-signalling component, including the proposed central tapetum regulator *TaGAMYB*, or other known anther development regulators were observed. Therefore, it is not possible from the results of this project to link HT-responsive changes in tapetum metabolism with alterations to GA-signalling and further investigation of the effect of HT-stress on GA-responsive expression in the anther is necessary. The generation of a male sterile *Tagamyb* mutant provides the opportunity to identify GA-GAMYB-regulated genes which are also differentially expressed under HT. Furthermore, some evidence was shown that changes in anther hormone concentrations which would be expected to lead to downstream signalling changes to transcription. However, as this experiment was severely limited by equipment malfunction, the results of global hormone analysis can only be taken as preliminary and will need repeating to further resolve the hormonal response to HT.

Clearly, some further refinement to experimental approaches is required to better understand the wheat anther hormonal response to HT. Both RNAseq and the global hormone analysis were limited by the difficulty in obtaining adequately staged material in sufficient quantity. Laser microdissection is one approach which has been successfully used to separate rice anther tissues in

order to perform tapetum and pollen-specific transcriptomics (Hirano *et al.*, 2008; Suwabe *et al.*, 2008). By specifically selecting the tapetum and pollen tissue it would be possible not only to distinguish between sporophyte and gametophyte responses but also to ensure analysis of a developmentally uniform sample. In conjunction with refined non-destructive staging methods, this kind of approach could be used to extend the work of this project by further investigating the tapetum-specific expression profiles of GA-signalling and biosynthesis components.

REFERENCES

- Abiko, M., Akibayashi, K., Sakata, T., Kimura, M., Kihara, M., Itoh, K., Asamizu, E., Sato, S., Takahashi, H., and Higashitani, A.** (2005). High-temperature induction of male sterility during barley (*Hordeum vulgare* L.) anther development is mediated by transcriptional inhibition. *Sex. Plant Reprod.* **18**: 91–100.
- Achard, P., Renou, J.P., Berthome, R., Harberd, N.P., and Genschik, P.** (2008). Plant DELLAs restrain growth and promote survival of adversity by reducing the levels of reactive oxygen species. *Curr. Biol.* **18**: 656–660.
- Alghabari, F., Lukac, M., Jones, H.E., and Gooding, M.J.** (2014). Effect of Rht Alleles on the Tolerance of Wheat Grain Set to High Temperature and Drought Stress During Booting and Anthesis. *J. Agron. Crop Sci.* **200**: 36–45.
- Alonso-Peral, M.M., Li, J., Li, Y., Allen, R.S., Schnippenkoetter, W., Ohms, S., White, R.G., and Millar, A.A.** (2010). The microRNA159-regulated GAMYB-like genes inhibit growth and promote programmed cell death in Arabidopsis. *Plant Physiol.* **154**: 757–771.
- Anders, S., Pyl, P.T., and Huber, W.** (2015). HTSeq—a Python framework to work with high-throughput sequencing data. *Bioinformatics* **31**: 166–9.
- Aoki, N., Ishibashi, Y., Kai, K., Tomokiyo, R., Yuasa, T., and Iwaya-Inoue, M.** (2014). Programmed cell death in barley aleurone cells is not directly stimulated by reactive oxygen species produced in response to gibberellin. *J. Plant Physiol.* **171**: 615–618.
- Ariizumi, T., Hatakeyama, K., Hinata, K., Inatsugi, R., Nishida, I., Sato, S., Kato, T., Tabata, S., and Toriyama, K.** (2004). Disruption of the novel plant protein NEF1 affects lipid accumulation in the plastids of the tapetum and exine formation of pollen, resulting in male sterility in *Arabidopsis thaliana*. *Plant J.* **39**: 170–181.
- Asseng, S., Ewert, F., Martre, P., Rötter, R. P., Lobell, D. B., Cammarano, D., Kimball, B. A., Ottman, M. J., Wall, G. W..** (2014). Rising temperatures reduce global wheat production. *Nat. Clim. Chang.* **5**: 143–147.
- Aya, K., Ueguchi-Tanaka, M., Kondo, M., Hamada, K., Yano, K., Nishimura, M., and Matsuoka, M.** (2009). Gibberellin modulates anther development in rice via the

transcriptional regulation of GAMYB. *Plant Cell* **21**: 1453–1472.

Barnabas, B., Jager, K., and Feher, A. (2008). The effect of drought and heat stress on reproductive processes in cereals. *Plant Cell Env.* **31**: 11–38.

Baulcombe, D. (2004). RNA silencing in plants. *Nature* **431**: 356–363.

Berkman, P.J., Lai, K., Lorenc, M.T., and Edwards, D. (2012). Next-generation sequencing applications for wheat crop improvement. *Am. J. Bot.* **99**: 365–71.

Bolger, A.M., Lohse, M., and Usadel, B. (2014). Trimmomatic: a flexible trimmer for Illumina sequence data. *Bioinformatics* **30**: 2114–20.

Bolot, S., Abrouk, M., Masood-Quraishi, U., Stein, N., Messing, J., Feuillet, C., and Salse, J. (2009). The “inner circle” of the cereal genomes. *Curr. Opin. Plant Biol.* **12**: 119–125.

Cassman, K.G. (1999). Ecological intensification of cereal production systems: yield potential, soil quality, and precision agriculture. *Proc. Natl. Acad. Sci. U. S. A.* **96**: 5952–9.

Cecchetti, V., Brunetti, P., Napoli, N., Fattorini, L., Altamura, M.M., Costantino, P., and Cardarelli, M. (2015). ABCB1 and ABCB19 auxin transporters have synergistic effects on early and late Arabidopsis anther development. *J. Integr. Plant Biol.*

Chandler, P.M., Marion-Poll, A., Ellis, M., and Gubler, F. (2002). Mutants at the Slender1 locus of barley cv Himalaya. Molecular and physiological characterization. *Plant Physiol.* **129**: 181–90.

Chandler, J.W. (2010). The Hormonal Regulation of Flower Development. *J. Plant Growth Regul.* **30**: 242–254.

Chandler, P.M. and Harding, C.A. (2013). “Overgrowth” mutants in barley and wheat: new alleles and phenotypes of the “Green Revolution” DELLA gene. *J. Exp. Bot.* **64**: 1603–1613.

Chapman, J.A., Chapman, J.A., Mascher, M., Buluç, A., Barry, K., Georganas, E., Session, A., Strnadova, V., Jenkins, J., Sehgal, S., Olikier, L., Schmutz, J., Yelick, K.A., Scholz, U., Waugh, R., Poland, J.A., Muehlbauer, G.J., Stein, N., Rokhsar,

D.S., Weber, J.L., Myers, E.W., Green, P., Smith, J.J., Putta, S., Zhu, W., Pao, G.M., Verma, IM., Hunter, T., Brenchley, R., Spannagl, M., Pfeifer, M., Barker, G.L., D'Amore, R., Allen, A.M., Nystedt, B., Street, N.R., Wetterbom, A., Zuccolo, A., Lin, YC., Scofield, D.G., Zhang, G., Fang, X., Guo, X., Li, L., Luo, R., Xu, F., Luo, M-C., Gu, YQ., You, F.M., Deal, K.R., Ma, Y., Hu, Y., Alkan, C., Sajjadian, S., Eichler, E.E., Feuillet, C., Leach, J.E., Rogers, J., Schnable, P.S., Eversole, K., Myers, E.W., Sutton, G.G., Delcher, AL., Dew, I.M., Fasulo, D.P., Flanigan, M.J., Venter, J.C., Adams, M.D., Myers, E.W., Li, P.W., Mural, R.J., Sutton, G.G., Birol, I., Raymond, A., Jackman, S.D., Pleasance, S., Coope, R., Taylor, G.A., Zimin, A., Stevens, K.A., Crepeau, M.W., Holtz-Morris, A., Koriabine, M., Marçais, G., Xu, X., Pan, S., Cheng, S., Zhang, B., Mu, D., Jia, J., Zhao, S., Kong, X., Li, Y., Zhao, G., He, W., Ling, H.Q., Zhao, S., Liu, D., Wang, J., Sun, H., Zhang, C., Wang, X., Wang, H., Wang, J., Sun, R., Wu, J., Liu, S., Schnable, P.S., Ware, D., Fulton, R.S., Stein, J.C., Wei, F., Pasternak, S., Dolezel, J., Kubalaková, M., Paux, E., Bartos, J., Feuillet, C., Choulet, F., Alberti, A., Theil, S., Glover, N., Barbe, V., Daron, J., Mascher, M., Muehlbauer, G.J., Rokhsar, D.S., Chapman, J., Schmutz, J., Barry, K., Noss, C.W., Havlak, P., Yue, JX., Lv, J., Vincent, K.Y., Brockmann, H.J., Hahn, M.W., Zhang, S.V., Moyle, L.C., Sorrells, M.E., Gustafson, J.P., Somers, D., Chao, S., Bensch, D., Guedira-Brown, G., Brown, P.J., Sorrells, ME., Jannink, J-L., Ho, I., Sunkara, S., Luo, S., Schroth, G.P., Rokhsar, D.S., Arumuganathan, K., Earle, E., Hastie, A.R., Dong, L., Smith, A., Finklestein, J., Lam, E.T., Huo, N., Wilhelm, E.P., Mackay, I.J., Saville, R.J., Korolev, A.V., Balfourier, F., Greenland, A.J., Khlestkina, E.K., Kumar, U., Röder, M.S., Bradnam, K.R., Fass, JN., Alexandrov, A., Baranay, P., Bechner, M., Birol, I., Mochida, K., Yoshida, T., Sakurai, T., Ogihara, Y., Shinozaki, K., Saintenac, C., Jiang, D., Akhunov, E.D., Muñoz-Amatriaín, M., Eichten, S.R., Wicker, T., Richmond, T.A., Mascher, M., Steuernagel, B., Truco, M.J., Ashrafi, H., Kozik, A., Leeuwen, H., Bowers, J., Wo, S.R.C., Neves, L.G., Davis, J.M., Barbazuk, W.B., Kirst, M., Wu, Y., Bhat, P.R., Close, T.J., Lonardi, S., Graner, A., Jahoor, A., Schondelmaier, J., Siedler, H., Pillen, K., Fischbeck, G., Ramsay, L., Macaulay, M., Ivanissevich, S Degli., MacLean, K., Cardle, L., Fuller, J., Devos, K., Dubcovsky, J., Dvořák, J., Chinoy, C., Gale, M., Caldwell, .KS., Dvorak, J., Lagudah, E.S., Akhunov, E., Luo, M.C., Wolters, P., Cavanagh, C.R., Chao, S., Wang, S., Huang, B.E., Stephen, S., Kiani, S., Belova, T., Zhan, B., Wright, J., Caccamo, M., Asp, T., Simkova, H., Oeveren, J., Ruiter, M., Jesse, T.,

Poel, H., Tang, J., Yalcin, F., Kovach, A., Wegrzyn, J.L., Parra, G., Holt, C., Bruening, G.E., Loopstra, C.A., Mascher, M., Richmond, T.A., Gerhardt, D.J., Himmelbach, A., Clissold, L., Sampath, D., Mascher, M., Wu, S., Amand, P.S., Stein, N., Poland, J., Mascher, M., Jost, M., Kuon, J.E., Himmelbach, A., Assfalg, A., Beier, S., Poursarebani, N., Nussbaumer, T., Simkova, H., Safar, J., Witsenboer, H., Oeveren, J., Paux, E., Sourdille, P., Salse, J., Saintenac, C., Leroy, P., Flavell, R., Bennett, M., Smith, J., Smith, D., Williams, L.J., Tabbaa, D.G., Li, N., Berlin, A.M., Shea, T.P., MacCallum, I., Langridge, P., Pruitt, K.D., Brown, G.R., Hiatt, S.M., Thibaud-Nissen, F., Astashyn, A., Ermolaeva, O., Altschul, S.F., Madden, T.L., Schäffer, A.A., Zhang, J., Zhang, Z., Miller, W., Jurka, J., Kapitonov, V.V., Pavlicek, A., Klonowski, P., Kohany, O., Walichiewicz, J., Li, H., Durbin, R., Li, H., Zhang, Z., Schwartz, S., Wagner, L., Miller, W., Altschul, S.F., Gish, W., Miller, W., Myers, E.W., Lipman, D.J., Quinlan, A.R., Hall, I.M., Arend, D., Lange, M., Chen, J., Colmsee, C., Flemming, S., Hecht, D. (2015). A whole-genome shotgun approach for assembling and anchoring the hexaploid bread wheat genome. *Genome Biol.* **16**: 26.

Chen, L., Hao, L., Parry, M.A.J., Phillips, A.L., and Hu, Y.-G. (2014). Progress in TILLING as a tool for functional genomics and improvement of crops. *J. Integr. Plant Biol.* **56**: 425–43.

Cheng, H., Qin, L., Lee, S., Fu, X., Richards, D.E., Cao, D., Luo, D., Harberd, N.P., and Peng, J. (2004). Gibberellin regulates Arabidopsis floral development via suppression of DELLA protein function. *Development* **131**: 1055–1064.

Cho, J.-I., Ryoo, N., Ko, S., Lee, S.-K., Lee, J., Jung, K.-H., Lee, Y.-H., Bhoo, S.H., Winderickx, J., An, G., Hahn, T.-R., and Jeon, J.-S. (2006). Structure, expression, and functional analysis of the hexokinase gene family in rice (*Oryza sativa* L.). *Planta* **224**: 598–611.

Choulet, F., Alberti, A., Theil, S., Glover, N., Barbe, V., Daron, J., Pingault, L., Sourdille, P., Couloux, A., Paux, E., Leroy, P., Mangenot, S., Guilhot, N., Le Gouis, J., Balfourier, F., Alaux, M., Jamilloux, V., Poulain, J., Durand, C., Bellec, A., Gaspin, C., Safar, J., Dolezel, J., Rogers, J., Vandepoele, K., Aury, J., Mayer, Klaus., Berges, H., Quesneville, H., Wincker, P., Feuillet, C. (2014). Structural and functional partitioning of bread wheat chromosome 3B. *Science* (80-.). **345**: 1249721.

- Colebrook, E.H., Thomas, S.G., Phillips, A.L., and Hedden, P.** (2014). The role of gibberellin signalling in plant responses to abiotic stress. *J. Exp. Biol.* **217**: 67–75.
- Conesa, A., Götz, S., García-Gómez, J.M., Terol, J., Talón, M., and Robles, M.** (2005). Blast2GO: a universal tool for annotation, visualization and analysis in functional genomics research. *Bioinforma. Appl. NOTE* **21**: 3674–3676.
- Cossani, C.M. and Reynolds, M.P.** (2012). Physiological traits for improving heat tolerance in wheat. *Plant Physiol.* **160**: 1710–1718.
- Cui, J., You, C., Zhu, E., Huang, Q., Ma, H., and Chang, F.** (2016). Feedback Regulation of DYT1 by Interactions with Downstream bHLH Factors Promotes DYT1 Nuclear Localization and Anther Development. *Plant Cell* **28**: 1078–1093.
- Daviere, J.M. and Achard, P.** (2013). Gibberellin signaling in plants. *Development* **140**: 1147–1151.
- Dawson, J., Wilson, Z.A., Aarts, M.G.M., Braithwaite, A.F., Briarty, L.G., and Mulligan, B.J.** (1993). Microspore and pollen development in six male-sterile mutants of *Arabidopsis thaliana*. *Can. J. Bot.* **71**: 629–638.
- Dill, A. and Sun, T.P.** (2001). Synergistic derepression of gibberellin signaling by removing RGA and GAI function in *Arabidopsis thaliana*. *Genetics* **159**: 777–785.
- Dong, C., Dalton-Morgan, J., Vincent, K., and Sharp, P.** (2009). A Modified TILLING Method for Wheat Breeding. *The Plant Genome* **2**: 39–47.
- El-Ghazaly, G. and Jensen, W.A.** (1986). Studies of the Development of Wheat (*Triticum Aestivum*) Pollen. *Grana* **25**: 1–29.
- Endo, M., Tsuchiya, T., Hamada, K., Kawamura, S., Yano, K., Ohshima, M., Higashitani, A., Watanabe, M., and Kawagishi-Kobayashi, M.** (2009). High temperatures cause male sterility in rice plants with transcriptional alterations during pollen development. *Plant Cell Physiol.* **50**: 1911–22.
- Evenson, R.E. and Gollin, D.** (2003). Assessing the impact of the green revolution, 1960 to 2000. *Science* **300**: 758–62.
- Farooq, M., Bramley, H., Palta, J.A., and Siddique, K.H.M.** (2011). Heat Stress in Wheat during Reproductive and Grain-Filling Phases. *CRC. Crit. Rev. Plant Sci.*

30: 491–507.

- Feng, X.L., Ni, W.M., Elge, S., Mueller-Roeber, B., Xu, Z.H., and Xue, H.W.** (2006). Auxin flow in anther filaments is critical for pollen grain development through regulating pollen mitosis. *Plant Mol. Biol.* **61**: 215–226.
- Ferris, R., Ellis, R.H., Wheeler, T.R., and Hadley, P.** (1998). Effect of High Temperature Stress at Anthesis on Grain Yield and Biomass of Field-grown Crops of Wheat. *Ann. Bot.* **82**: 631–639.
- Firon, N., Pressman, E., Meir, S., Khoury, R., and Altahan, L.** (2012). Ethylene is involved in maintaining tomato (*Solanum lycopersicum*) pollen quality under heat-stress conditions. *AoB Plants* **2012**: pls024.
- Flintham, J.E., Borner, A., Worland, A.J., and Gale, M.D.** (1997). Optimizing wheat grain yield : effects of Rht (gibberellin-insensitive) dwarfing genes. *J. Agric. Sci. Cambridge* **128**: 11–25.
- Forcat, S., Bennett, M.H., Mansfield, J.W., and Grant, M.R.** (2008). A rapid and robust method for simultaneously measuring changes in the phytohormones ABA, JA and SA in plants following biotic and abiotic stress. *Plant Methods* **4**: 16.
- Fu, D., Uauy, C., Blechl, A., and Dubcovsky, J.** (2007). RNA interference for wheat functional gene analysis. *Transgenic Res.* **16**: 689–701.
- Fu, Z., Yu, J., Cheng, X., Zong, X., Xu, J., Chen, M., Li, Z., Zhang, D., and Liang, W.** (2014). The Rice Basic Helix-Loop-Helix Transcription Factor TDR INTERACTING PROTEIN2 Is a Central Switch in Early Anther Development. *Plant Cell* **26**: 1512–1524.
- Fukazawa, J., Ito, T., Kamiya, Y., Yamaguchi, S., and Takahashi, Y.** (2015). Binding of GID1 to DELLAs promotes dissociation of GAF1 from DELLA in GA dependent manner. *Plant Signal. Behav.* **10**: e1052923.
- Gamal El-Ghazaly & William A. Jensen** (1986). Studies of the Development of Wheat (*Triticum Aestivum*) Pollen. *Grana* **25**: 1–29.
- Garber, M., Grabherr, M.G., Guttman, M., and Trapnell, C.** (2011). Computational methods for transcriptome annotation and quantification using RNA-seq. *Nat. Methods* **8**: 469–477.

- Ge, X., Chang, F., and Ma, H.** (2010). Signaling and transcriptional control of reproductive development in Arabidopsis. *Curr. Biol.* **20**: R988-97.
- Giorno, F., Wolters-Arts, M., Mariani, C., and Rieu, I.** (2013). Ensuring Reproduction at High Temperatures: The Heat Stress Response during Anther and Pollen Development. *Plants* **2**: 489–506.
- Gocal, G.F.W., Sheldon, C.C., Gubler, F., Moritz, T., Bagnall, D.J., MacMillan, C.P., Li, S.F., Parish, R.W., Dennis, E.S., Weigel, D., and King, R.W.** (2001). GAMYB-like genes, flowering, and gibberellin signaling in Arabidopsis. *Plant Physiol.* **127**: 1682–1693.
- Godfray, H.C.J., Beddington, J.R., Crute, I.R., Haddad, L., Lawrence, D., Muir, J.F., Pretty, J., Robinson, S., Thomas, S.M., and Toulmin, C.** (2010). Food security: the challenge of feeding 9 billion people. *Science* **327**: 812–8.
- Gómez, J.F. and Wilson, Z.A.** (2012). Non-destructive staging of barley reproductive development for molecular analysis based upon external morphology. *J. Exp. Bot.* **63**: 4085–94.
- Gómez, J.F., Talle, B., and Wilson, Z.A.** (2015). Anther and pollen development: A conserved developmental pathway. *J. Integr. Plant Biol.* **57**: 876–891.
- Goss, J.A.** (1968). Development, Physiology, and Biochemistry of Corn and Wheat Pollen i. *Bot. Rev.* **34**: 333–359.
- Gouache, D., Le Bris, X., Bogard, M., Deudon, O., Pagé, C., and Gate, P.** (2012). Evaluating agronomic adaptation options to increasing heat stress under climate change during wheat grain filling in France. *Eur. J. Agron.* **39**: 62–70.
- Gourdji, S.M. et al.** (2013). An assessment of wheat yield sensitivity and breeding gains in hot environments. *Proc. Biol. Sci.* **280**: 20122190.
- Griffiths, J., Murase, K., Rieu, I., Zentella, R., Zhang, Z.L., Powers, S.J., Gong, F., Phillips, A.L., Hedden, P., Sun, T.P., and Thomas, S.G.** (2006). Genetic characterization and functional analysis of the GID1 gibberellin receptors in Arabidopsis. *Plant Cell* **18**: 3399–3414.
- Gubler, F., Kalla, R., Roberts, J.K., and Jacobsen, J.V.** (1995). Gibberellin-Regulated Expression of a myb Gene in Barley Aleurone Cells: Evidence for Myb

Transactivation of a High-pl [alpha]-Amylase Gene Promoter. *Plant Cell Online* **7**: 1879–1891.

Gubler, F., Raventos, D., Keys, M., Watts, R., Mundy, J., and Jacobsen, J. V. (1999).

Target genes and regulatory domains of the GAMYB transcriptional activator in cereal aleurone. *Plant J.* **17**: 1–9.

Gubler, F., Chandler, P.M., White, R.G., Llewellyn, D.J., and Jacobsen, J. V. (2002).

Gibberellin signaling in barley aleurone cells. Control of SLN1 and GAMYB expression. *Plant Physiol.* **129**: 191–200.

Guo, J.X. and Liu, Y.G. (2012). Molecular control of male reproductive development and pollen fertility in rice. *J. Integr. Plant Biol.* **54**: 967–78, i.

Haseneyer, G., Ravel, C., Dardevet, M., Balfourier, F., Sourdille, P., Charmet, G.,

Brunel, D., Sauer, S., Geiger, H.H., Graner, A., and Stracke, S. (2008). High level of conservation between genes coding for the GAMYB transcription factor in barley (*Hordeum vulgare* L.) and bread wheat (*Triticum aestivum* L.) collections. *Theor. Appl. Genet.* **117**: 321–331.

Hays, D., Do, J.H., Mason, R.E., Morgan, G., and Finlayson, S.A. (2007). Heat stress induced ethylene production in developing wheat grains induces kernel abortion and increased maturation in a susceptible cultivar. *Plant Sci.* **172**: 1113–1123.

Hedden, P. (2003). The genes of the Green Revolution. *Trends in Genet.* **19**: 5–9.

Hedden, P. (2012). Gibberellin Biosynthesis. In eLS (John Wiley & Sons, Ltd).

Hedden, P. (2016). Gibberellin biosynthesis in higher plants. In *Annual Plant Reviews*, Volume 49 (John Wiley & Sons, Ltd: Chichester, UK), pp. 37–72.

Higashitani, A. (2013). High temperature injury and auxin biosynthesis in microsporogenesis. *Front. in Plant Sci.* **4**: 47.

Hirano, K., Aya, K., Hobo, T., Sakakibara, H., Kojima, M., Shim, R.A., Hasegawa, Y., Ueguchi-Tanaka, M., and Matsuoka, M. (2008). Comprehensive Transcriptome Analysis of Phytohormone Biosynthesis and Signaling Genes in Microspore/Pollen and Tapetum of Rice. *Plant Cell Physiol.* **49**: 1429–1450.

- Hirano, K., Kouketu, E., Katoh, H., Aya, K., Ueguchi-Tanaka, M., and Matsuoka, M.** (2012). The suppressive function of the rice DELLA protein SLR1 is dependent on its transcriptional activation activity. *Plant J.* **71**: 443–53.
- Hong, Y.-F., Ho, T.-H.D., Wu, C.-F., Ho, S.-L., Yeh, R.-H., Lu, C.-A., Chen, P.-W., Yu, L.-C., Chao, A., and Yu, S.-M.** (2012). Convergent Starvation Signals and Hormone Crosstalk in Regulating Nutrient Mobilization upon Germination in Cereals. *Plant Cell* **24**: 2857–2873.
- Hou, X., Hu, W.-W., Shen, L., Lee, L.Y.C., Tao, Z., Han, J.-H., and Yu, H.** (2008). Global Identification of DELLA Target Genes during Arabidopsis Flower Development. *Plant Physiol.* **147**: 1126–1142.
- Hu, J., Mitchum, M.G., Barnaby, N., Ayele, B.T., Ogawa, M., Nam, E., Lai, W.C., Hanada, A., Alonso, J.M., Ecker, J.R. and Swain, S.M.,** (2008). Potential sites of bioactive gibberellin production during reproductive growth in Arabidopsis. *Plant Cell* **20**: 320–336.
- Hu, L., Liang, W., Yin, C., Cui, X., Zong, J., Wang, X., Hu, J., and Zhang, D.** (2011). Rice MADS3 Regulates ROS Homeostasis during Late Anther Development. *Plant Cell* **23**: 515–533.
- Huang, M.-D., Wei, F.-J., Wu, C.-C., Hsing, Y.-I.C., and Huang, A.H.C.** (2009). Analyses of advanced rice anther transcriptomes reveal global tapetum secretory functions and potential proteins for lipid exine formation. *Plant Physiol.* **149**: 694–707.
- Huang, Y., Yang, W., Pei, Z., Guo, X., Liu, D., Sun, J., and Zhang, A.** (2012). The genes for gibberellin biosynthesis in wheat. *Funct. Integr. Genomics* **12**: 199–206.
- Ikeda, A., Ueguchi-Tanaka, M., Sonoda, Y., Kitano, H., Koshioka, M., Futsuhara, Y., Matsuoka, M., and Yamaguchi, J.** (2001). slender rice, a constitutive gibberellin response mutant, is caused by a null mutation of the SLR1 gene, an orthologue of the height-regulating gene GAI/RGA/RHT/D8. *Plant Cell* **13**: 999–1010.
- Inoue, H., Nojima, H., and Okayama, H.** (1990). High efficiency transformation of *Escherichia coli* with plasmids. *Gene* **96**: 23–28.
- International Wheat Genome Sequencing Consortium (IWGSC),.** (2014). A

chromosome-based draft sequence of the hexaploid bread wheat (*Triticum aestivum*) genome. *Science* **345**: 1251788.

Ishibashi, Y., Tawaratsumida, T., Kondo, K., Kasa, S., Sakamoto, M., Aoki, N., Zheng, S.-H., Yuasa, T., and Iwaya-Inoue, M. (2012). Reactive oxygen species are involved in gibberellin/abscisic acid signaling in barley aleurone cells. *Plant Physiol.* **158**: 1705–14.

Itoh, J.-I., Nonomura, K.-I., Ikeda, K., Yamaki, S., Inukai, Y., Yamagishi, H., Kitano, H., and Nagato, Y. (2005). Rice plant development: from zygote to spikelet. *Plant Cell Physiol.* **46**: 23–47.

Ji, C., Li, H., Chen, L., Xie, M., Wang, F., Chen, Y., and Liu, Y.G. (2013). A novel rice bHLH transcription factor, DTD, acts coordinately with TDR in controlling tapetum function and pollen development. *Mol. Plant* **6**: 1715–1718.

Ji, X., Dong, B., Shiran, B., Talbot, M.J., Edlington, J.E., Hughes, T., White, R.G., Gubler, F., and Dolferus, R. (2011). Control of abscisic acid catabolism and abscisic acid homeostasis is important for reproductive stage stress tolerance in cereals. *Plant Physiol.* **156**: 647–662.

Ji, X., Shiran, B., Wan, J., Lewis, D.C., Jenkins, C.L., Condon, A.G., Richards, R.A., and Dolferus, R. (2010). Importance of pre-anthesis anther sink strength for maintenance of grain number during reproductive stage water stress in wheat. *Plant Cell Env.* **33**: 926–942.

Jung, K.-H., Han, M.-J., Lee, Y.-S., Kim, Y.-K.Y.-W., Hwang, I., Kim, M.-J., Kim, Y.-K.Y.-W., Nahm, B.H., and An, G. (2005). Rice Undeveloped Tapetum1 Is a Major Regulator of Early Tapetum Development. *Plant Cell Online* **17**: 2705–2722.

Kaneko, M., Inukai, Y., Ueguchi-Tanaka, M., Itoh, H., Izawa, T., Kobayashi, Y., Hattori, T., Miyao, A., Hirochika, H., Ashikari, M., and Matsuoka, M. (2004). Loss-of-function mutations of the rice GAMYB gene impair alpha-amylase expression in aleurone and flower development. *Plant Cell* **16**: 33–44.

Mac Key, J. (1968). Mutagenesis in Vulgare Wheat. *Hereditas* **59**: 505–517.

Kim, D., Perteza, G., Trapnell, C., Pimentel, H., Kelley, R., and Salzberg, S.L. (2013). TopHat2: accurate alignment of transcriptomes in the presence of insertions,

deletions and gene fusions. *Genome Biol.* **14**.

King, R., Bird, N., Ramirez-Gonzalez, R., Coghill, J.A., Patil, A., Hassani-Pak, K., Uauy, C. and Phillips, A.L. (2015). Mutation Scanning in Wheat by Exon Capture and Next-Generation Sequencing. *PLoS One* **10**: e0137549.

Kobayashi, M., Sakurai, A., Saka, H., and Takahashi, N. (1989). Quantitative Analysis of Endogenous Gibberellins in Normal and Dwarf Cultivars of Rice. *Plant Cell Physiol.* **30**: 963–969.

Kocheva, K., Nenova, V., Karceva, T., Petrov, P., Georgiev, G.I., Börner, A., and Landjeva, S. (2014). Changes in Water Status, Membrane Stability and Antioxidant Capacity of Wheat Seedlings Carrying Different Rht-B1 Dwarfing Alleles under Drought Stress. *J. Agron. Crop Sci.* **200**: 83–91.

Koornneef, M. and van der Veen, J.H. (1980). Induction and analysis of gibberellin sensitive mutants in *Arabidopsis thaliana* (L.) heynh. *Theor. Appl. Genet.* **58**: 257–63.

Kumar, S., Mohan, A., Balyan, H.S. and Gupta, P.K. (2009). Orthology between genomes of Brachypodium, wheat and rice. *BMC Res. Notes* **2**: 93.

Kwon, C.-T., Kim, S.-H., Kim, D., and Paek, N.-C. (2015). The Rice Floral Repressor Early flowering1 Affects Spikelet Fertility By Modulating Gibberellin Signaling. *Rice (N. Y.)*. **8**: 58.

Langmead, B. and Salzberg, S.L. (2012). Fast gapped-read alignment with Bowtie 2. *Nat. Methods* **9**: 357–359.

Langmead, B., Trapnell, C., Pop, M., and Salzberg, S.L. (2009). Ultrafast and memory-efficient alignment of short DNA sequences to the human genome. *Genome Biol.* **10**.

Larkindale, J. and Knight, M.R. (2002). Protection against Heat Stress-Induced Oxidative Damage in *Arabidopsis* Involves Calcium, Abscisic Acid, Ethylene, and Salicylic Acid. *Plant Physiol.* **128**: 682–695.

Law, C. and Worland, A. (1984). An effect of temperature on the fertility of wheats containing dwarfing alleles Rht-1, Rht-2 and Rht-3. In *Annual Report of the Plant Breeding Institute*, pp. 69–71.

- Li, A., Yang, W., Li, S., Liu, D., Guo, X., Sun, J., and Zhang, A.** (2013). Molecular characterization of three GIBBERELLIN-INSENSITIVE DWARF1 homologous genes in hexaploid wheat. *J. Plant Physiol.* **170**: 432–43.
- Li, N., Zhang, D.S., Liu, H.S., Yin, C.S., Li, X.X., Liang, W.Q., Yuan, Z., Xu, B., Chu, H.W., Wang, J. and Wen, T.Q.** (2006a). The rice tapetum degeneration retardation gene is required for tapetum degradation and anther development. *Plant Cell* **18**: 2999–3014.
- Li, X., Duan, X., Jiang, H., Sun, Y., Tang, Y., Yuan, Z., Guo, J., Liang, W., Chen, L., Yin, J. and Ma, H.** (2006b). Genome-Wide Analysis of Basic/Helix-Loop-Helix Transcription Factor Family in Rice and Arabidopsis. *Plant Physiol.* **141**: 1167–1184.
- Liu, Z., Bao, W., Liang, W., Yin, J., and Zhang, D.** (2010). Identification of gamyb-4 and analysis of the regulatory role of GAMYB in rice anther development. *J Integr. Plant Biol.* **52**: 670–678.
- Locascio, A., Blazquez, M.A., and Alabadi, D.** (2013). Genomic analysis of DELLA protein activity. *Plant Cell Physiol.* **54**: 1229–1237.
- de Lucas, M., Davière, J.-M., Rodríguez-Falcón, M., Pontin, M., Iglesias-Pedraz, J.M., Lorrain, S., Fankhauser, C., Blázquez, M.A., Titarenko, E., and Prat, S.** (2008). A molecular framework for light and gibberellin control of cell elongation. *Nature* **451**: 480–484.
- Lukac, M., Gooding, M.J., Griffiths, S., and Jones, H.E.** (2012). Asynchronous flowering and within-plant flowering diversity in wheat and the implications for crop resilience to heat. *Ann. Bot.* **109**: 843–50.
- Ma, H.** (2005). Molecular genetic analyses of microsporogenesis and microgametogenesis in flowering plants. *Annu. Rev. Plant Biol.* **56**: 393–434.
- Ma, L., Yang, Z., and Zhang, S.** (2013). DEX1, a plasma membrane-localized protein, functions in microspore development by affecting CalS5 expression in *Arabidopsis thaliana*. *Chinese Sci. Bull.* **58**: 2855–2861.
- Matsui, T., Omasa, K., and Horie, T.** (1999). Mechanism of Anther Dehiscence in Rice (*Oryza sativa* L.). *Ann. Bot.* **84**: 501–506.

- McCormick, S.** (1993). Male Gametophyte Development. *Plant Cell Am. Soc. Plant Physiol.* **5**: 1265–1275.
- McFadden, E.S. and Sears, E.R.** (1946). The origin of *Triticum spelta* and its free-threshing hexaploid relatives. *J. Hered.* **37**: 107–116.
- Millar, A.A. and Gubler, F.** (2005). The Arabidopsis GAMYB-like genes, MYB33 and MYB65, are microRNA-regulated genes that redundantly facilitate anther development. *Plant Cell* **17**: 705–721.
- Min, L., Zhu, L., Tu, L., Deng, F., Yuan, D., and Zhang, X.** (2013). Cotton GhCKI disrupts normal male reproduction by delaying tapetum programmed cell death via inactivating starch synthase. *Plant J.* **75**: 823–835.
- Min, L., Li, Y., Hu, Q., Zhu, L., Gao, W., Wu, Y., Ding, Y., Liu, S., Yang, X., and Zhang, X.** (2014). Sugar and Auxin Signaling Pathways Respond to High-Temperature Stress during Anther Development as Revealed by Transcript Profiling Analysis in Cotton. *Plant Physiol.* **164**: 1293–1308.
- Miralles, D.J., Katz, S.D., Colloca, A., and Slafer, G.A.** (1998). Floret development in near isogenic wheat lines differing in plant height. *F. Crop. Res.* **59**: 21–30.
- Mizelle, M.B., Sethi, R., Ashton, M.E., and Jensen, W.A.** (1989). Development of the pollen grain and tapetum of wheat (*Triticum aestivum*) in untreated plants and plants treated with chemical hybridizing agent RH0007. *Sex. Plant Reprod.* **2**: 231–253.
- Mohammed, A.R. and Tarpley, L.** (2009). High nighttime temperatures affect rice productivity through altered pollen germination and spikelet fertility. *Agric. For. Meteorol.* **149**: 999–1008.
- Müller, F. and Rieu, I.** (2016). Acclimation to high temperature during pollen development. *Plant Reprod.* **29**: 107–118.
- Murray, F., Kalla, R., Jacobsen, J., and Gubler, F.** (2003). A role for HvGAMYB in anther development. *Plant J.* **33**: 481–491.
- Nakata, M., Mitsuda, N., Herde, M., Koo, A.J., Moreno, J.E., Suzuki, K., Howe, G.A., and Ohme-Takagi, M.** (2013). A bHLH-type transcription factor, ABA-INDUCIBLE BHLH-TYPE TRANSCRIPTION FACTOR/JA-ASSOCIATED MYC2-LIKE1, acts as a

repressor to negatively regulate jasmonate signaling in arabidopsis. *Plant Cell* **25**: 1641–1656.

Niu, N., Liang, W., Yang, X., Jin, W., Wilson, Z.A., Hu, J., and Zhang, D. (2013). EAT1 promotes tapetal cell death by regulating aspartic proteases during male reproductive development in rice. *Nat. Commun.* **4**: 1445.

Oliver, S.N., Van Dongen, J.T., Alfred, S.C., Mamun, E.A., Zhao, X., Saini, H.S., Fernandes, S.F., Blanchard, C.L., Sutton, B.G., Geigenberger, P., Dennis, E.S., and Dolferus, R. (2005). Cold-induced repression of the rice anther-specific cell wall invertase gene OSINV4 is correlated with sucrose accumulation and pollen sterility. *Plant, Cell Environ.* **28**: 1534–1551.

Ortiz, R., Sayre, K.D., Govaerts, B., Gupta, R., Subbarao, G.V., Ban, T., Hodson, D., Dixon, J.M., Iván Ortiz-Monasterio, J., and Reynolds, M. (2008). Climate change: Can wheat beat the heat? *Agric. Ecosyst. Environ.* **126**: 46–58.

Oshino, T., Abiko, M., Saito, R., Ichiishi, E., Endo, M., Kawagishi-Kobayashi, M., and Higashitani, A. (2007). Premature progression of anther early developmental programs accompanied by comprehensive alterations in transcription during high-temperature injury in barley plants. *Mol. Genet. Genomics* **278**: 31–42.

Oshino, T., Miura, S., Kikuchi, S., Hamada, K., Yano, K., Watanabe, M., and Higashitani, A. (2011). Auxin depletion in barley plants under high-temperature conditions represses DNA proliferation in organelles and nuclei via transcriptional alterations. *Plant Cell Env.* **34**: 284–290.

Parish, R.W. and Li, S.F. (2010). Death of a tapetum: A programme of developmental altruism. *Plant Sci.* **178**: 73–89.

Parish, R.W., Phan, H.A., Iacuone, S., and Li, S.F. (2013). Tapetal development and abiotic stress: a centre of vulnerability. *Funct. Plant Biol.* **39**: 553.

Pearce, S., Saville, R., Vaughan, S.P., Chandler, P.M., Wilhelm, E.P., Sparks, C.A., Al-Kaff, N., Korolev, A., Boulton, M.I., Phillips, A.L. and Hedden, P. (2011). Molecular characterization of Rht-1 dwarfing genes in hexaploid wheat. *Plant Physiol.* **157**: 1820–31.

Pearce, S., Huttly, A.K., Prosser, I.M., Li, Y.-D., Vaughan, S.P., Gallova, B., Patil, A.,

- Coghill, J.A., Dubcovsky, J., Hedden, P., and Phillips, A.L.** (2015). Heterologous expression and transcript analysis of gibberellin biosynthetic genes of grasses reveals novel functionality in the GA3ox family. *BMC Plant Biol.* **15**: 130.
- Peng, J., Carol, P., Richards, D.E., King, K.E., Cowling, R.J., Murphy, G.P., and Harberd, N.P.** (1997). The Arabidopsis GAI gene defines a signaling pathway that negatively regulates gibberellin responses. *Genes Dev.* **11**: 3194–3205.
- Peng, J., Richards, D.E., Hartley, N.M., Murphy, G.P., Devos, K.M., Flintham, J.E., Beales, J., Fish, L.J., Worland, A.J., Pelica, F. and Sudhakar, D.** (1999). “Green revolution” genes encode mutant gibberellin response modulators. *Nature* **400**: 256–61.
- Pingault, L., Choulet, F., Alberti, A., Glover, N., Wincker, P., Feuillet, C. and Paux, E.** (2015). Deep transcriptome sequencing provides new insights into the structural and functional organization of the wheat genome. *Genome Biol.* **16**: 29.
- Plackett, A.R.G., Thomas, S.G., Wilson, Z.A., and Hedden, P.** (2011). Gibberellin control of stamen development: a fertile field. *Trends Plant Sci.* **16**: 568–78.
- Plackett, A.R.G., Powers, S.J., Fernandez-Garcia, N., Urbanova, T., Takebayashi, Y., Seo, M., Jikumaru, Y., Benlloch, R., Nilsson, O., Ruiz-Rivero, O. and Phillips, A.L.** (2012). Analysis of the developmental roles of the Arabidopsis gibberellin 20-oxidases demonstrates that GA20ox1, -2, and -3 are the dominant paralogs. *Plant Cell* **24**: 941–960.
- Plackett, A.R.G., Ferguson, A.C., Powers, S.J., Wanchoo-Kohli, A., Phillips, A.L., Wilson, Z.A., Hedden, P., and Thomas, S.G.** (2014). DELLA activity is required for successful pollen development in the Columbia ecotype of Arabidopsis. *New Phytol.* **201**: 825–836.
- Plackett, A.R.G. and Wilson, Z.A.** (2016). Gibberellins and plant reproduction. In *Annual Plant Reviews*, Volume 49 (John Wiley & Sons, Ltd: Chichester, UK), pp. 323–358.
- Power, J.F. and Alessi, J.** (1978). Tiller development and yield of standard and semidwarf spring wheat varieties as affected by nitrogen fertilizer. *J. agric. Sci., Cambridge* **90**: 97–108.

- Proels, R.K., González, M.-C., and Roitsch, T.** (2006). Gibberellin-dependent induction of tomato extracellular invertase Lin7 is required for pollen development. *Funct. Plant Biol.* **33**: 547.
- Qi, T., Song, S., Ren, Q., Wu, D., Huang, H., Chen, Y., Fan, M., Peng, W., Ren, C., and Xie, D.** (2011). The Jasmonate-ZIM-domain proteins interact with the WD-Repeat/bHLH/MYB complexes to regulate Jasmonate-mediated anthocyanin accumulation and trichome initiation in *Arabidopsis thaliana*. *Plant Cell* **23**: 1795–1814.
- Qi, T., Huang, H., Song, S., and Xie, D.** (2015). Regulation of Jasmonate-Mediated Stamen Development and Seed Production by a bHLH-MYB Complex in *Arabidopsis*. *Plant Cell* **27**: 1620–33.
- Rakszegi, M., Kisgyorgy, B.N., Tearall, K., Shewry, P.R., Lang, L., Phillips, A.L., and Bedo, Z.** (2010). Diversity of agronomic and morphological traits in a mutant population of bread wheat studied in the Healthgrain program. *Euphytica* **174**: 409–421.
- Rasheed, A., Wen, W., Gao, F., Zhai, S., Jin, H., Liu, J., Guo, Q., Zhang, Y., Dreisigacker, S., Xia, X., and He, S.** (2016). Development and validation of KASP assays for genes underpinning key economic traits in bread wheat. *Theor. Appl. Genet.* **129**: 1843–1860.
- Ray, D.K.D., Mueller, N.D., West, P.C. and Foley, J.A.** (2013). Yield Trends Are Insufficient to Double Global Crop Production by 2050. *PLoS One* **8**: e66428.
- Rieu, I., Ruiz-Rivero, O., Fernandez-Garcia, N., Griffiths, J., Powers, S.J., Gong, F., Linhartova, T., Eriksson, S., Nilsson, O., Thomas, S.G., Phillips, A.L., and Hedden, P.** (2007). The gibberellin biosynthetic genes AtGA20ox1 and AtGA20ox2 act, partially redundantly, to promote growth and development throughout the *Arabidopsis* life cycle. *Plant J.* **53**: 488–504.
- Roberts, A. and Pachter, L.** (2012). Streaming fragment assignment for real-time analysis of sequencing experiments. *Nat. Methods* **10**: 71–73.
- Robinson, M.D., McCarthy, D.J., and Smyth, G.K.** (2010). edgeR: a Bioconductor package for differential expression analysis of digital gene expression data. *Bioinformatics* **26**: 139–40.

- Sadras, V.O. and Monzon, J.P.** (2006). Modelled wheat phenology captures rising temperature trends: Shortened time to flowering and maturity in Australia and Argentina. *F. Crop. Res.* **99**: 136–146.
- Sadras, V.O.** (2007). Evolutionary aspects of the trade-off between seed size and number in crops. *F. Crop. Res.* **100**: 125–138.
- Saini, H.S. and Aspinall, D.** (1982). Abnormal Sporogenesis in Wheat { *Triticum aestivum* L. } Induced by Short Periods of High Temperature. *Ann. Bot.* **49**: 835–846.
- Saini, H., Sedgley, M., and Aspinall, D.** (1983). Effect of heat stress during floral development on pollen tube growth and ovary anatomy in wheat (*Triticum aestivum* L.). *Aust. J. Plant Physiol.* **10**: 137–144.
- Saini, H.S., Sedgley, M., and Aspinall, D.** (1984). Developmental Anatomy in Wheat of Male Sterility Induced by Heat Stress, Water Deficit or Abscisic Acid. *Aust. J. Plant Physiol* **11**: 243–253.
- Sakata, T., Takahashi, H., Nishiyama, I., and Higashitani, A.** (2000). Effects of High Temperature on the Development of Pollen Mother Cells and Microspores in Barley *Hordeum vulgare* L. *J. Plant Res.* **113**: 395–402.
- Sakata, T. and Higashitani, A.** (2008). Male sterility accompanied with abnormal anther development in plants—genes and environmental stresses with special reference to high temperature injury. *Int. J. Plant Dev. Biol.* **2**: 42–51.
- Sakata, T., Oshino, T., Miura, S., Tomabechi, M., Tsunaga, Y., Higashitani, N., Miyazawa, Y., Takahashi, H., Watanabe, M., and Higashitani, A.** (2010). Auxins reverse plant male sterility caused by high temperatures. *Proc. Natl. Acad. Sci.* **107**: 8569–8574.
- Salamini, F., Ozkan, H., Brandolini, A., Schäfer-Pregl, R., and Martin, W.** (2002). Genetics and geography of wild cereal domestication in the near east. *Nat. Rev. Genet.* **3**: 429–41.
- Satake, T. and Hayase, H.** (1970). Male Sterility Caused by Cooling Treatment at the Young Microspore Stage in Rice Plants : V. Estimations of pollen developmental stage and the most sensitive stage to coolness. *Japanese J. Crop Sci.* **39**: 468–

473.

- Semenov, M.A. and Shewry, P.R.** (2011). Modelling predicts that heat stress, not drought, will increase vulnerability of wheat in Europe. *Sci Rep* **1**: 66.
- Semenov, M.A., Stratonovitch, P., Alghabari, F., and Gooding, M.J.** (2014). Adapting wheat in Europe for climate change. *J. Cereal Sci.* **59**: 245–256.
- Shewry, P.R.** (2009). Wheat. *J. Exp. Bot.* **60**: 1537–53.
- Shi, J., Cui, M., Yang, L., Kim, Y.-J., and Zhang, D.** (2015). Genetic and Biochemical Mechanisms of Pollen Wall Development. *Trends Plant Sci.* **20**: 741–53.
- Silverstone, A.L., Mak, P., Martinez, E.C., and Sun, T.** (1997). The New RGA Locus Encodes a Negative Regulator of Gibberellin Response in *Arabidopsis thaliana*. *Genetics* **146**: 1087–1099.
- Silverstone, A.L., Jung, H.S., Dill, A., Kawaide, H., Kamiya, Y., and Sun, T.P.** (2001). Repressing a repressor: gibberellin-induced rapid reduction of the RGA protein in *Arabidopsis*. *Plant Cell* **13**: 1555–1566.
- Simons, K.J., Fellers, J.P., Trick, H.N., Zhang, Z., Tai, Y.-S., Gill, B.S., and Faris, J.D.** (2006). Molecular characterization of the major wheat domestication gene Q. *Genetics* **172**: 547–55.
- Slade, A.J., Fuerstenberg, S.I., Loeffler, D., Steine, M.N., and Facciotti, D.** (2005). A reverse genetic, nontransgenic approach to wheat crop improvement by TILLING. *Nat. Biotechnol.* **23**: 75–81.
- Sloggett, C., Goonasekera, N., and Afgan, E.** (2013). BioBlend: automating pipeline analyses within Galaxy and CloudMan. *Bioinformatics* **29**: 1685–6.
- Small, I.** (2007). RNAi for revealing and engineering plant gene functions. *Curr. Opin. Biotechnol.* **18**: 148–153.
- Song, S., Qi, T., Wasternack, C., and Xie, D.** (2014). Jasmonate signaling and crosstalk with gibberellin and ethylene. *Curr. Opin. Plant Biol.* **21**: 112–119.
- Sparkes, D.L., Holme, S.J., and Gaju, O.** (2006). Does light quality initiate tiller death in wheat? *Eur. J. Agron.* **24**: 212–217.

- Sparks, C.A. and Jones, H.D.** (2009). Biolistics Transformation of Wheat. *Methods Mol. Biol.* **478**: 71–92.
- Stevenson, J.R., Villoria, N., Byerlee, D., Kelley, T., and Maredia, M.** (2013). Green Revolution research saved an estimated 18 to 27 million hectares from being brought into agricultural production. *Proc. Natl. Acad. Sci.* **110**: 8363–8368.
- De Storme, N. and Geelen, D.** (2014). The impact of environmental stress on male reproductive development in plants: biological processes and molecular mechanisms. *Plant. Cell Environ.* **37**: 1–18.
- Sun, T.P.** (2010). Gibberellin-GID1-DELLA: a pivotal regulatory module for plant growth and development. *Plant Physiol.* **154**: 567–70.
- Suresh, A. and Neethirajan, S.** (2015). Real-time 3D visualization and quantitative analysis of internal structure of wheat kernels. *J. Cereal Sci.* **63**: 81–87.
- Suwabe, K. et al.** (2008). Separated transcriptomes of male gametophyte and tapetum in rice: validity of a laser microdissection (LM) microarray. *Plant Cell Physiol.* **49**: 1407–1416.
- Tang, R.-S., Zheng, J.-C., Jin, Z.-Q., Zhang, D.-D., Huang, Y.-H., and Chen, L.-G.** (2007). Possible correlation between high temperature-induced floret sterility and endogenous levels of IAA, GAs and ABA in rice (*Oryza sativa* L.). *Plant Growth Regul.* **54**: 37–43.
- Taylor, A.A., Horsch, A., Rzepczyk, A., Hasenkampf, C.A., and Riggs, C.D.** (1997). Maturation and secretion of a serine proteinase is associated with events of late microsporogenesis. *Plant J.* **12**: 1261–1271.
- Tian, H., Qi, T., Li, Y., Wang, C., Ren, C., Song, S., and Huang, H.** (2016). Regulation of the WD-repeat/bHLH/MYB Complex by Gibberellin and Jasmonate. *Plant Signaling & Behavior*, **11**: 1118-1133..
- Trapnell, C., Williams, B.A., Pertea, G., Mortazavi, A., Kwan, G., van Baren, M.J., Salzberg, S.L., Wold, B.J., and Pachter, L.** (2010). Transcript assembly and quantification by RNA-Seq reveals unannotated transcripts and isoform switching during cell differentiation. *Nat. Biotechnol.* **28**: 511–5.
- Trapnell, C., Roberts, A., Goff, L., Pertea, G., Kim, D., Kelley, D.R., Pimentel, H.,**

- Salzberg, S.L., Rinn, J.L., and Pachter, L.** (2012). Differential gene and transcript expression analysis of RNA-seq experiments with TopHat and Cufflinks. *Nat. Protoc.* **7**: 562–578.
- Tsuji, H., Aya, K., Ueguchi-Tanaka, M., Shimada, Y., Nakazono, M., Watanabe, R., Nishizawa, N.K., Gomi, K., Shimada, A., Kitano, H., Ashikari, M., and Matsuoka, M.** (2006). GAMYB controls different sets of genes and is differentially regulated by microRNA in aleurone cells and anthers. *Plant J.* **47**: 427–444.
- Ueguchi-Tanaka, M., Ashikari, M., Nakajima, M., Itoh, H., Katoh, E., Kobayashi, M., Chow, T.Y., Hsing, Y.I., Kitano, H., Yamaguchi, I., and Matsuoka, M.** (2005). GIBBERELLIN INSENSITIVE DWARF1 encodes a soluble receptor for gibberellin. *Nature* **437**: 693–698.
- Varnier, A.-L., Mazeyrat-Gourbeyre, F., Sangwan, R.S., and Clément, C.** (2005). Programmed cell death progressively models the development of anther sporophytic tissues from the tapetum and is triggered in pollen grains during maturation. *J. Struct. Biol.* **152**: 118–128.
- De Vries, A.P.** (1971). Flowering Biology of Wheat, Particularly in View of Hybrid Seed Production -A Review. *Euphytica* **20**: 152–170.
- Wang, A., Xia, Q., Xie, W., Datla, R., and Selvaraj, G.** (2003). The classical Ubisch bodies carry a sporophytically produced structural protein (RAFTIN) that is essential for pollen development. *Proc. Natl. Acad. Sci.* **100**: 14487–14492.
- Wang, Y., Sun, F., Cao, H., Peng, H., Ni, Z., Sun, Q., and Yao, Y.** (2012). TamiR159 directed wheat TaGAMYB cleavage and its involvement in anther development and heat response. *PLoS One* **7**: e48445.
- Wang, Z., Gerstein, M., and Snyder, M.** (2009). The transcriptome is the complete set of transcripts in a cell, and their quantity. *Nat. Rev. Genet.* **10**: 57–63.
- Washio, K.** (2003). Functional dissections between GAMYB and Dof transcription factors suggest a role for protein-protein associations in the gibberellin-mediated expression of the RAmy1A gene in the rice aleurone. *Plant Physiol.* **133**: 850–863.
- Wen, C.-K. and Chang, C.** (2002). Arabidopsis RGL1 encodes a negative regulator of

gibberellin responses. *Plant Cell* **14**: 87–100.

Wilson, Z.A. and Zhang, D.B. (2009). From Arabidopsis to rice: pathways in pollen development. *J. Exp. Bot.* **60**: 1479–1492.

Woodger, F.J., Gubler, F., Pogson, B.J., and Jacobsen, J. V. (2003). A Mak-like kinase is a repressor of GAMYB in barley aleurone. *Plant J.* **33**: 707–717.

Wu, L., Taohua, Z., Gui, W., Xu, L., Li, J., and Ding, Y. (2015). Five pectinase gene expressions highly responding to heat stress in rice floral organs revealed by RNA-seq analysis. *Biochem. Biophys. Res. Comm.* **463**: 407-413.

Xie, H.-T., Wan, Z.-Y., Li, S., and Zhang, Y. (2014). Spatiotemporal Production of Reactive Oxygen Species by NADPH Oxidase Is Critical for Tapetal Programmed Cell Death and Pollen Development in Arabidopsis. *Plant Cell* **26**: 2007–2023.

Xu, F.-Q., Li, X.-R., and Ruan, Y.-L. (2008). RNAi-mediated suppression of hexokinase gene OsHXK10 in rice leads to non-dehiscent anther and reduction of pollen germination. *Plant Sci.* **175**: 674–684.

Xu, J., Yang, C., Yuan, Z., Zhang, D., Gondwe, M.Y., Ding, Z., Liang, W., Zhang, D., and Wilson, Z.A. (2010). The ABORTED MICROSPORES regulatory network is required for postmeiotic male reproductive development in Arabidopsis thaliana. *Plant Cell* **22**: 91–107.

Yamaguchi, I., Nakazawa, H., Nakagawa, R., Suzuki, Y., Kurogochi, S., Murofushi, N., Takahashi, N., and Weiler, E.W. (1990). Identification and Semi-Quantification of Gibberellins from the Pollen and Anthers of Zea mays by Immunoassay and GC/MS. *Plant Cell Physiol.* **31**: 1063–1069.

Yang, C., Vizcay-Barrena, G., Conner, K., and Wilson, Z.A. (2007). MALE STERILITY1 is required for tapetal development and pollen wall biosynthesis. *Plant Cell* **19**: 3530–3548.

Yi, J., Moon, S., Lee, Y.-S., Zhu, L., Liang, W., Zhang, D., Jung, K.-H., and An, G. (2016). Defective Tapetum Cell Death 1 (DTC1) Regulates ROS Levels by Binding to Metallothionein during Tapetum Degeneration. *Plant Physiol.* **170**: 1611–23.

Zadoks, J., Chang, T., and Konzak, C. (1974). A decimal code for the growth stages of cereals. *Weed Res.* **14**: 415-421.

- Zentella, R., Zhang, Z.L., Park, M., Thomas, S.G., Endo, A., Murase, K., Fleet, C.M., Jikumaru, Y., Nambara, E., Kamiya, Y., and Sun, T.P.** (2007). Global analysis of DELLA direct targets in early gibberellin signaling in *Arabidopsis*. *Plant Cell* **19**: 3037–3057.
- Zhang, D., Luo, X., and Zhu, L.** (2011). Cytological analysis and genetic control of rice anther development. *J. Genet. Genomics* **38**: 379–390.
- Zhang, D. and Yang, L.** (2014). Specification of tapetum and microsporocyte cells within the anther. *Curr. Opin. Plant Biol.* **17**: 49–55.
- Zhang, W., Sun, Y., Timofejeva, L., Chen, C., Grossniklaus, U., and Ma, H.** (2006). Regulation of *Arabidopsis* tapetum development and function by DYSFUNCTIONAL TAPETUM1 (DYT1) encoding a putative bHLH transcription factor. *Development* **133**: 3085–3095.

ANNEX I

Other *TaGAMYB* M₄ TILLING mutants available

| TARGET | POS | REF | ALT | CLASS | AA_CHANGE |
|-----------|------|-----|-----|-------------|-----------|
| TaGAMYb-A | 330 | G | A | upstream | N/A |
| TaGAMYb-A | 415 | G | A | synonymous | N/A |
| TaGAMYb-A | 496 | C | T | synonymous | N/A |
| TaGAMYb-A | 506 | G | A | missense | A49T |
| TaGAMYb-A | 571 | G | A | synonymous | N/A |
| TaGAMYb-A | 579 | C | T | missense | T73I |
| TaGAMYb-A | 589 | C | T | synonymous | N/A |
| TaGAMYb-A | 601 | G | A | synonymous | N/A |
| TaGAMYb-A | 611 | C | T | missense | L84F |
| TaGAMYb-A | 636 | C | T | missense | P92L |
| TaGAMYb-A | 641 | C | T | missense | L94F |
| TaGAMYb-A | 649 | G | A | synonymous | N/A |
| TaGAMYb-A | 651 | G | A | missense | G97E |
| TaGAMYb-A | 667 | G | A | synonymous | N/A |
| TaGAMYb-A | 689 | C | T | missense | L110F |
| TaGAMYb-A | 717 | C | T | missense | A119V |
| TaGAMYb-A | 717 | C | T | missense | A119V |
| TaGAMYb-A | 719 | C | T | missense | R120W |
| TaGAMYb-A | 746 | C | T | intron | N/A |
| TaGAMYb-A | 751 | C | T | intron | N/A |
| TaGAMYb-A | 759 | C | T | intron | N/A |
| TaGAMYb-A | 847 | C | T | intron | N/A |
| TaGAMYb-A | 922 | G | A | intron | N/A |
| TaGAMYb-A | 984 | C | T | intron | N/A |
| TaGAMYb-A | 1510 | C | T | intron | N/A |
| TaGAMYb-A | 1514 | C | T | intron | N/A |
| TaGAMYb-A | 1514 | C | T | intron | N/A |
| TaGAMYb-A | 1597 | G | A | stop_gained | W137* |
| TaGAMYb-A | 1612 | G | A | synonymous | N/A |
| TaGAMYb-A | 1692 | G | A | missense | S169N |
| TaGAMYb-A | 1692 | G | A | missense | S169N |
| TaGAMYb-A | 1821 | C | T | missense | A212V |
| TaGAMYb-A | 1856 | G | A | missense | A224T |
| TaGAMYb-A | 1891 | C | T | synonymous | N/A |
| TaGAMYb-A | 1899 | G | A | missense | G238E |
| TaGAMYb-A | 2002 | G | A | synonymous | N/A |
| TaGAMYb-A | 2009 | C | A | missense | L275M |
| TaGAMYb-A | 2009 | C | A | missense | L275M |
| TaGAMYb-A | 2012 | G | A | missense | G276S |
| TaGAMYb-A | 2067 | G | A | missense | G294E |
| TaGAMYb-A | 2121 | G | A | missense | R312K |
| TaGAMYb-A | 2181 | C | T | missense | P332L |
| TaGAMYb-A | 2218 | G | A | missense | M344I |

| TARGET | POS | REF | ALT | CLASS | AA_CHANGE |
|---------|------|-----|-----|-------------|-----------|
| TaGAMYb | 2142 | C | A | missense | A256E |
| TaGAMYb | 2198 | G | A | missense | G275S |
| TaGAMYb | 2419 | G | A | synonymous | N/A |
| TaGAMYb | 2428 | C | T | synonymous | N/A |
| TaGAMYb | 2441 | C | T | missense | P356S |
| TaGAMYb | 2472 | G | A | missense | C366Y |
| TaGAMYb | 2541 | G | A | missense | R389K |
| TaGAMYb | 2552 | C | T | missense | L393F |
| TaGAMYb | 2557 | C | T | synonymous | N/A |
| TaGAMYb | 2611 | C | T | synonymous | N/A |
| TaGAMYb | 2641 | G | A | stop_gained | W422* |
| TaGAMYb | 2641 | G | A | stop_gained | W422* |
| TaGAMYb | 2676 | G | A | missense | S434N |
| TaGAMYb | 2723 | C | T | missense | P450S |
| TaGAMYb | 2747 | C | T | missense | L458F |
| TaGAMYb | 2803 | G | A | intron | N/A |
| TaGAMYb | 2846 | C | T | missense | P463L |
| TaGAMYb | 2851 | C | T | synonymous | N/A |
| TaGAMYb | 2890 | C | T | missense | P478S |
| TaGAMYb | 2950 | G | A | missense | G498R |
| TaGAMYb | 3024 | C | T | synonymous | N/A |
| TaGAMYb | 3064 | C | T | missense | P536S |
| TaGAMYb | 3064 | C | T | missense | P536S |
| TaGAMYb | 3150 | C | T | downstream | N/A |
| TaGAMYb | 3160 | C | T | downstream | N/A |
| TaGAMYb | 3196 | G | A | downstream | N/A |
| TaGAMYb | 3221 | G | A | downstream | N/A |
| TaGAMYb | 3233 | C | T | downstream | N/A |
| TaGAMYb | 3270 | G | A | downstream | N/A |
| TaGAMYb | 3289 | C | T | downstream | N/A |
| TaGAMYb | 294 | C | T | upstream | N/A |
| TaGAMYb | 373 | G | A | missense | S8N |
| TaGAMYb | 401 | C | T | synonymous | N/A |
| TaGAMYb | 421 | G | A | missense | G24D |
| TaGAMYb | 476 | G | A | synonymous | N/A |
| TaGAMYb | 482 | G | A | synonymous | N/A |
| TaGAMYb | 527 | G | A | synonymous | N/A |
| TaGAMYb | 553 | C | T | missense | A68V |
| TaGAMYb | 580 | G | A | missense | R77H |
| TaGAMYb | 580 | G | A | missense | R77H |
| TaGAMYb | 585 | G | A | missense | G79S |
| TaGAMYb | 671 | C | T | synonymous | N/A |
| TaGAMYb | 681 | C | T | missense | H111Y |

| TARGET | POS | REF | ALT | CLASS | AA_CHANGE |
|-----------|------|-----|-----|-------------|-----------|
| TaGAMYb-A | 2305 | C | T | synonymous | N/A |
| TaGAMYb-A | 2370 | C | T | missense | S395F |
| TaGAMYb-A | 2402 | C | T | missense | P406S |
| TaGAMYb-A | 2420 | G | A | missense | V412I |
| TaGAMYb-A | 2429 | G | A | missense | E415K |
| TaGAMYb-A | 2508 | C | T | missense | S441F |
| TaGAMYb-A | 2531 | C | T | missense | P449S |
| TaGAMYb-A | 2534 | C | T | missense | P450S |
| TaGAMYb-A | 2624 | C | T | intron | N/A |
| TaGAMYb-A | 2684 | G | A | missense | A471T |
| TaGAMYb-A | 2697 | C | T | missense | A475V |
| TaGAMYb-A | 2727 | C | T | missense | S485F |
| TaGAMYb-A | 2810 | C | T | missense | L513F |
| TaGAMYb-A | 2836 | C | T | synonymous | N/A |
| TaGAMYb-A | 2851 | C | T | synonymous | N/A |
| TaGAMYb-A | 2886 | G | A | missense | S538N |
| TaGAMYb-A | 2917 | G | A | synonymous | N/A |
| TaGAMYb-A | 2917 | G | A | synonymous | N/A |
| TaGAMYb-A | 2940 | G | A | downstream | N/A |
| TaGAMYb-A | 2961 | G | A | downstream | N/A |
| TaGAMYb-A | 3000 | G | A | downstream | N/A |
| TaGAMYb-A | 3070 | G | A | downstream | N/A |
| TaGAMYb-A | 3081 | G | A | downstream | N/A |
| TaGAMYb-B | 659 | C | T | missense | P39S |
| TaGAMYb-B | 690 | C | T | missense | A49V |
| TaGAMYb-B | 727 | C | T | synonymous | N/A |
| TaGAMYb-B | 730 | C | T | synonymous | N/A |
| TaGAMYb-B | 733 | G | A | synonymous | N/A |
| TaGAMYb-B | 734 | G | A | missense | G64R |
| TaGAMYb-B | 734 | G | A | missense | G64R |
| TaGAMYb-B | 734 | G | A | missense | G64R |
| TaGAMYb-B | 751 | G | A | synonymous | N/A |
| TaGAMYb-B | 895 | G | A | synonymous | N/A |
| TaGAMYb-B | 1035 | G | A | intron | N/A |
| TaGAMYb-B | 1101 | C | T | intron | N/A |
| TaGAMYb-B | 1163 | G | A | intron | N/A |
| TaGAMYb-B | 1531 | A | A | intron | N/A |
| TaGAMYb-B | 1811 | C | T | stop_gained | R146* |
| TaGAMYb-B | 1991 | G | A | missense | A206T |
| TaGAMYb-B | 1994 | C | T | missense | P207S |
| TaGAMYb-B | 2081 | G | A | missense | A236T |
| TaGAMYb-B | 2084 | G | A | missense | G237R |
| TaGAMYb-B | 2084 | G | A | missense | G237R |

| TARGET | POS | REF | ALT | CLASS | AA_CHANGE |
|-----------|------|-----|-----|-------------|-----------|
| TaGAMYb-D | 694 | G | A | missense | G115D |
| TaGAMYb-D | 704 | G | A | stop_gained | W118* |
| TaGAMYb-D | 717 | G | A | missense | A123T |
| TaGAMYb-D | 823 | C | T | intron | N/A |
| TaGAMYb-D | 823 | C | T | intron | N/A |
| TaGAMYb-D | 1733 | C | T | synonymous | N/A |
| TaGAMYb-D | 1803 | C | T | missense | A212V |
| TaGAMYb-D | 1815 | G | A | missense | S216N |
| TaGAMYb-D | 1815 | G | A | missense | S216N |
| TaGAMYb-D | 1885 | G | A | missense | M239I |
| TaGAMYb-D | 1920 | G | A | missense | S251N |
| TaGAMYb-D | 1935 | G | A | missense | G256D |
| TaGAMYb-D | 1935 | G | A | missense | G256D |
| TaGAMYb-D | 1938 | C | T | missense | A257V |
| TaGAMYb-D | 2064 | G | A | missense | G299D |
| TaGAMYb-D | 2132 | C | T | missense | L322F |
| TaGAMYb-D | 2141 | C | T | missense | L325F |
| TaGAMYb-D | 2184 | C | T | missense | T339I |
| TaGAMYb-D | 2276 | C | T | missense | P370S |
| TaGAMYb-D | 2348 | C | T | missense | L394F |
| TaGAMYb-D | 2352 | C | T | missense | S395F |
| TaGAMYb-D | 2373 | C | T | missense | S402F |
| TaGAMYb-D | 2508 | C | T | missense | A447V |
| TaGAMYb-D | 2735 | C | T | missense | L495F |
| TaGAMYb-D | 2745 | G | A | missense | G498E |
| TaGAMYb-D | 2832 | G | A | missense | G527D |
| TaGAMYb-D | 2838 | G | A | missense | G529D |
| TaGAMYb-D | 3033 | G | A | downstream | N/A |
| TaGAMYb-D | 3062 | G | A | downstream | N/A |

ANNEX II

| Query | Hit Name |
|---------------|--|
| TaGA2ox-A4 | TRIAE_CS42_1AL_TGACv1_000229_AA0006730.1 |
| TaGA2ox-A8_1 | TRIAE_CS42_1AL_TGACv1_000738_AA0018190.1 |
| TaGID1-A | TRIAE_CS42_1AL_TGACv1_002026_AA0037970.1 |
| TaGA2ox-A8_2 | TRIAE_CS42_1AL_TGACv1_002643_AA0044170.1 |
| TaGA20ox-A4 | TRIAE_CS42_1AL_TGACv1_002876_AA0045790.1 |
| TaGA2ox-A1 | TRIAE_CS42_1AS_TGACv1_019368_AA0065660.1 |
| TaGA2ox-A10 | TRIAE_CS42_1AS_TGACv1_019522_AA0067640.1 |
| TaGA2ox-D8_1 | TRIAE_CS42_1BL_TGACv1_030297_AA0085860.1 |
| TaGID1-B | TRIAE_CS42_1BL_TGACv1_032368_AA0129000.1 |
| TaGA2ox-B8_2 | TRIAE_CS42_1BL_TGACv1_033092_AA0136980.1 |
| TaGA2ox-B4 | TRIAE_CS42_1BL_TGACv1_033362_AA0138950.1 |
| TaGA2ox-B10 | TRIAE_CS42_1BS_TGACv1_049430_AA0153290.1 |
| TaGA20ox-D4 | TRIAE_CS42_1DL_TGACv1_061442_AA0195410.1 |
| TaGA2ox-D4 | TRIAE_CS42_1DL_TGACv1_061847_AA0204240.1 |
| TaGID1-D | TRIAE_CS42_1DL_TGACv1_061931_AA0205760.1 |
| TaGA2ox-B8_1 | TRIAE_CS42_1DL_TGACv1_062649_AA0217700.1 |
| TaGA2ox-B1 | TRIAE_CS42_1DS_TGACv1_080296_AA0245530.1 |
| TaGA2ox-D1 | TRIAE_CS42_1DS_TGACv1_080296_AA0245530.1 |
| TaGA2ox-D10 | TRIAE_CS42_1DS_TGACv1_080501_AA0249160.2 |
| TaGA2ox-A6_1 | TRIAE_CS42_2AL_TGACv1_093213_AA0275220.1 |
| TaKS-A1 | TRIAE_CS42_2AL_TGACv1_095602_AA0312750.1 |
| TaGA3ox-A3 | TRIAE_CS42_2AL_TGACv1_096240_AA0318130.1 |
| TaGA13ox-A2 | TRIAE_CS42_2AS_TGACv1_112489_AA0339020.2 |
| TaGA2ox-B6_1 | TRIAE_CS42_2BL_TGACv1_129413_AA0382670.1 |
| TaKS-B1 | TRIAE_CS42_2BL_TGACv1_130687_AA0416140.2 |
| TaGA3ox-B3 | TRIAE_CS42_2BL_TGACv1_133400_AA0442410.1 |
| TaGA1ox-B1 | TRIAE_CS42_2BL_TGACv1_133400_AA0442430.1 |
| TaGA13ox-B2 | TRIAE_CS42_2BS_TGACv1_146629_AA0469690.1 |
| TaKS-D1 | TRIAE_CS42_2DL_TGACv1_158432_AA0518570.4 |
| TaGA2ox-D6_1 | TRIAE_CS42_2DL_TGACv1_159593_AA0540370.1 |
| TaGA13ox-D2 | TRIAE_CS42_2DS_TGACv1_177860_AA0586180.1 |
| TaGA20ox-A2 | TRIAE_CS42_3AL_TGACv1_194412_AA0632590.1 |
| TaGA20ox-A3 | TRIAE_CS42_3AL_TGACv1_194765_AA0639020.1 |
| TaGA20ox-D3_2 | TRIAE_CS42_3AL_TGACv1_194765_AA0639020.1 |
| TaGA2ox-A3 | TRIAE_CS42_3AL_TGACv1_195097_AA0644720.1 |
| TaGA3ox-A2 | TRIAE_CS42_3AS_TGACv1_211643_AA0692510.1 |
| TaGA2ox-A7 | TRIAE_CS42_3AS_TGACv1_212549_AA0701660.1 |
| TaGA3ox-B2 | TRIAE_CS42_3B_TGACv1_220696_AA0715770.1 |
| TaGID2-B2 | TRIAE_CS42_3B_TGACv1_220966_AA0725290.2 |

| | |
|---------------|--|
| TaGA20ox-B3 | TRIAE_CS42_3B_TGACv1_221467_AA0741640.1 |
| TaGA2ox-B3 | TRIAE_CS42_3B_TGACv1_222891_AA0772640.1 |
| TaGA2ox-B7 | TRIAE_CS42_3B_TGACv1_223452_AA0782440.1 |
| TaGA20ox-B2 | TRIAE_CS42_3B_TGACv1_223804_AA0787660.2 |
| TaGA20ox-D3_1 | TRIAE_CS42_3DL_TGACv1_249277_AA0843900.1 |
| TaGA20ox-D2 | TRIAE_CS42_3DL_TGACv1_249609_AA0852340.1 |
| TaGA2ox-D3 | TRIAE_CS42_3DL_TGACv1_250562_AA0870310.1 |
| TaGA3ox-D2 | TRIAE_CS42_3DS_TGACv1_271552_AA0902420.1 |
| TaGA2ox-D7 | TRIAE_CS42_3DS_TGACv1_273136_AA0928740.1 |
| TaGA20ox-A1 | TRIAE_CS42_4AL_TGACv1_288147_AA0938430.1 |
| TaKAO-A1 | TRIAE_CS42_4AL_TGACv1_291658_AA0995820.2 |
| TaGA2ox-A6_2 | TRIAE_CS42_4AS_TGACv1_306483_AA1008910.1 |
| TaGA2ox-B6_4 | TRIAE_CS42_4BL_TGACv1_320406_AA1038050.1 |
| TaGA2ox-B6_3 | TRIAE_CS42_4BL_TGACv1_320553_AA1042970.1 |
| TaGA13ox1-B1 | TRIAE_CS42_4BL_TGACv1_320864_AA1050510.1 |
| TaGA13ox1-D1 | TRIAE_CS42_4DL_TGACv1_342770_AA1121580.2 |
| TaGA13ox-A1 | TRIAE_CS42_4DL_TGACv1_342770_AA1121580.2 |
| TaGA2ox-D6_2 | TRIAE_CS42_4DL_TGACv1_343668_AA1137990.1 |
| TaGA20ox-B1 | TRIAE_CS42_5BL_TGACv1_404907_AA1314550.1 |
| TaGA20ox-D1 | TRIAE_CS42_5DL_TGACv1_433498_AA1414740.1 |
| TaGA2ox-B9 | TRIAE_CS42_6BL_TGACv1_500766_AA1609420.1 |
| TaGA2ox-A9 | TRIAE_CS42_6DL_TGACv1_526414_AA1682800.2 |
| TaGA2ox-D9 | TRIAE_CS42_6DL_TGACv1_526414_AA1682800.2 |
| TaCPS_A1 | TRIAE_CS42_7AL_TGACv1_556210_AA1758330.2 |
| TaKO-A1 | TRIAE_CS42_7AL_TGACv1_556473_AA1763880.1 |
| TaGA2ox-A2 | TRIAE_CS42_7AL_TGACv1_558723_AA1795690.1 |
| TaKAO-A2 | TRIAE_CS42_7AS_TGACv1_572167_AA1851630.1 |
| TaGA2ox-B2 | TRIAE_CS42_7BL_TGACv1_576990_AA1862150.1 |
| TaKO-B1 | TRIAE_CS42_7BL_TGACv1_577358_AA1873370.2 |
| TaCPS_B1 | TRIAE_CS42_7BL_TGACv1_577914_AA1885950.2 |
| TaCPS_D1 | TRIAE_CS42_7DL_TGACv1_602609_AA1962550.1 |
| TaGA2ox-D2 | TRIAE_CS42_7DL_TGACv1_603034_AA1974200.1 |
| TaKAO-D1 | TRIAE_CS42_7DS_TGACv1_623691_AA2055390.1 |
| TaGA20ox-B4 | TRIAE_CS42_U_TGACv1_641295_AA2091040.1 |
| TaGA2ox-B6_2 | TRIAE_CS42_U_TGACv1_641833_AA2105240.1 |
| TaKO-D1 | TRIAE_CS42_U_TGACv1_642210_AA2113450.1 |

Best hits for known GA-biosynthesis and signalling genes in TGACv1 reference genome (Developed by Dr. Andy Phillips).

ANNEX III

Complete Global hormone analysis

CYTOKININS

| Compound | tZ | | | tZR | | | tZ7G | | | tZ9G | | | tZOG | | | tZROG | | | |
|----------|--------|---------|----------|--------|---------|----------|--------|---------|----------|--------|----------|----------|--------|---------|----------|--------|---------|-------------|-------|
| sample | pmol/g | average | SD/SD(%) | pmol/g | average | SD/SD(%) | pmol/g | average | SD/SD(%) | pmol/g | average | SD/SD(%) | pmol/g | average | SD/SD(%) | pmol/g | average | SD/SD(%) | |
| 10C1 | 40.12 | 39.29 ± | 4.34 | 1.46 | 1.22 ± | 0.41 | | | | 315.29 | 279.35 ± | 29.93 | | | | <LOD | | 0.88 | |
| 10C2 | 33.60 | | 11.06 | 0.65 | | 33.36 | | | | 242.02 | | 10.71 | | | | <LOD | 0.88 | | |
| 10C3 | 44.14 | | | 1.56 | | | | | | 280.74 | | | | | | <LOD | | | |
| 10HT1 | 38.60 | 26.18 ± | 10.85 | 0.63 | 0.68 ± | 0.04 | | | | 397.90 | 211.94 ± | 137.92 | | | | <LOD | 1.82 | 1.37 ± | 0.44 |
| 10HT2 | 12.15 | | 41.47 | 0.70 | | 5.22 | | | | 68.01 | | 65.08 | | | | <LOD | 0.93 | | 32.30 |
| 10HT3 | 27.78 | | | 0.70 | | | | | | 169.90 | | | | | | | | | |
| 15C1 | 23.22 | 21.87 ± | 6.43 | 0.97 | 1.02 ± | 0.06 | | | | 162.49 | 135.67 ± | 45.87 | | | | <LOD | 2.19 | 5.12 ± | 2.29 |
| 15C2 | 13.41 | | 29.38 | 0.98 | | 5.93 | | | | 71.11 | | 33.81 | | | | <LOD | 5.38 | | 44.78 |
| 15C3 | 28.98 | | | 1.10 | | | | | | 173.43 | | | | | | | 7.79 | | |
| 15HT1 | 10.58 | 9.09 ± | 1.30 | 0.52 | 0.54 ± | 0.02 | | | | 55.62 | 48.58 ± | 7.64 | | | | <LOD | 1.55 | 1.49 ± | 0.06 |
| 15HT2 | 7.41 | | 14.29 | 0.56 | | 2.82 | | | | 37.96 | | 15.72 | | | | <LOD | 1.40 | | 4.34 |
| 15HT3 | 9.27 | | | 0.53 | | | | | | 52.16 | | | | | | | 1.52 | | |

| Compound | cZ | | | cZR | | | cZ9G | | | cZOG | | | cZROG | | | | | |
|----------|---------|-----------|----------|--------|----------|----------|---------|----------------|----------|---------|-----------|----------|--------|----------|----------|--------|---------|----------|
| sample | pmol/g | average | SD/SD(%) | pmol/g | average | SD/SD(%) | pmol/g | average | SD/SD(%) | pmol/g | average | SD/SD(%) | pmol/g | average | SD/SD(%) | pmol/g | average | SD/SD(%) |
| 10C1 | 68.95 | 154.08 ± | 74.59 | 189.33 | 212.71 ± | 21.47 | 9.38806 | 11.58 ± | 4.02 | 1093.84 | 1873.90 ± | 1080.97 | 296.93 | 237.51 ± | 42.28 | | | |
| 10C2 | 250.59 | | 48.41 | 241.18 | | 10.09 | 8.13 | | 34.73 | 3402.52 | | 57.69 | 213.56 | | 17.80 | | | |
| 10C3 | 142.71 | | | 207.62 | | | 17.21 | | | 1125.35 | | | 202.04 | | | | | |
| 10HT1 | 179.25 | 300.55 ± | 121.71 | 279.28 | 303.85 ± | 64.58 | 5.99 | 6.32 ± | 2.47 | 1771.88 | 1486.61 ± | 236.40 | 342.45 | 227.06 ± | 88.86 | | | |
| 10HT2 | 466.96 | | 40.50 | 392.31 | | 21.25 | 3.47 | | 39.14 | 1192.99 | | 15.90 | 212.46 | | 39.14 | | | |
| 10HT3 | 255.44 | | | 239.95 | | | 9.51 | | | 1494.97 | | | 126.26 | | | | | |
| 15C1 | 215.01 | 287.68 ± | 52.16 | 219.09 | 313.03 ± | 80.45 | 5.65 | 4.93 ± | 1.04 | 2006.70 | 1580.99 ± | 505.16 | 203.17 | 219.82 ± | 25.84 | | | |
| 15C2 | 334.99 | | 18.13 | 415.58 | | 25.70 | 3.45 | | 21.14 | 871.28 | | 31.95 | 256.32 | | 11.76 | | | |
| 15C3 | 313.05 | | | 304.41 | | | 5.68 | | | 1864.98 | | | 199.98 | | | | | |
| 15HT1 | 990.71 | 1082.90 ± | 70.44 | 306.00 | 350.12 ± | 31.42 | 2.63 | 2.51 ± | 0.17 | 755.31 | 872.46 ± | 118.53 | 273.99 | 223.62 ± | 37.12 | | | |
| 15HT2 | 1161.69 | | 6.50 | 367.64 | | 8.97 | 2.27 | | 6.68 | 827.22 | | 13.59 | 185.63 | | 16.60 | | | |
| 15HT3 | 1096.30 | | | 376.73 | | | 2.63 | | | 1034.87 | | | 211.24 | | | | | |

| Compound | DHZ | | | DHZR | | | DHZ7G | | | DHZ9G | | | DHZOG | | | DHZROG | | |
|----------|--------|---------|----------|--------|---------|----------|--------|---------|----------|--------|---------|----------|--------|---------|----------|--------|---------|----------|
| sample | pmol/g | average | SD/SD(%) | pmol/g | average | SD/SD(%) | pmol/g | average | SD/SD(%) | pmol/g | average | SD/SD(%) | pmol/g | average | SD/SD(%) | pmol/g | average | SD/SD(%) |
| 10C1 | | | | | | | | | | | | | | | | | | |
| 10C2 | | <LOD | | | <LOD | | | <LOD | | | <LOD | | | <LOD | | | <LOD | |
| 10C3 | | | | | | | | | | | | | | | | | | |
| 10HT1 | | | | | | | | | | | | | | | | | | |
| 10HT2 | | <LOD | | | <LOD | | | <LOD | | | <LOD | | | <LOD | | | <LOD | |
| 10HT3 | | | | | | | | | | | | | | | | | | |
| 15C1 | | | | | | | | | | | | | | | | | | |
| 15C2 | | <LOD | | | <LOD | | | <LOD | | | <LOD | | | <LOD | | | <LOD | |
| 15C3 | | | | | | | | | | | | | | | | | | |
| 15HT1 | | | | | | | | | | | | | | | | | | |
| 15HT2 | | <LOD | | | <LOD | | | <LOD | | | <LOD | | | <LOD | | | <LOD | |
| 15HT3 | | | | | | | | | | | | | | | | | | |

| Compound | IP | | | IPR | | | iP7G | | | iP9G | | |
|----------|---------|---------|----------|-------------|----------|----------|---------|---------|----------|--------|---------|----------|
| sample | pmol/g | average | SD/SD(%) | pmol/g | average | SD/SD(%) | pmol/g | average | SD/SD(%) | pmol/g | average | SD/SD(%) |
| 10C1 | 8.80 | 14.79 ± | 4.75 | 17.21 | 22.14 ± | 5.87 | 44.77 | 70.67 ± | 22.35 | | | |
| 10C2 | 20.41 | | 32.09 | 30.39 | | 26.49 | 99.31 | | 31.63 | | | <LOD |
| 10C3 | 15.16 | | | 18.83 | | | 67.92 | | | | | |
| 10HT1 | 14.30 | 19.93 ± | 6.43 | 17.10 | 63.06 ± | 50.92 | 70.69 | 68.03 ± | 4.24 | | | |
| 10HT2 | 28.93 | | 32.29 | 134.04 | | 80.74 | 62.05 | | 6.23 | | | <LOD |
| 10HT3 | 16.55 | | | 38.03 | | | 71.36 | | | | | |
| 15C1 | 26.65 | 26.26 ± | 1.32 | 47.71 | 73.03 ± | 24.75 | 78.17 | 80.35 ± | 9.31 | | | |
| 15C2 | 24.49 | | 5.01 | 106.63 | | 33.90 | 70.20 | | 11.59 | | | <LOD |
| 15C3 | 27.64 | | | 64.75 | | | 92.69 | | | | | |
| 15HT1 | 49.66 | 45.89 ± | 2.94 | 345.14 | 377.23 ± | 23.67 | 53.22 | 47.32 ± | 4.36 | | | |
| 15HT2 | 42.49 | | 6.40 | 385.04 | | 6.27 | 42.84 | | 9.21 | | | <LOD |
| 15HT3 | 45.52 | | | 401.51 | | | 45.89 | | | | | |
| Compound | 2MeScZR | | | 2MeScZ | | | 2MeSiPR | | | 2MeSiP | | |
| sample | pmol/g | average | SD/SD(%) | pmol/g | average | SD/SD(%) | pmol/g | average | SD/SD(%) | pmol/g | average | SD/SD(%) |
| 10C1 | 1.52 | 1.32 ± | 0.19 | 0.276775072 | 0.41 ± | 0.13 | 0.21 | 0.26 ± | 0.12 | 0.09 | 0.07 ± | 0.02 |
| 10C2 | <LOD | | 14.71 | <LOD | | 31.94 | 0.42 | | 47.21 | 0.05 | | 24.15 |
| 10C3 | 1.13 | | | 0.54 | | | 0.14 | | | 0.06 | | |
| 10HT1 | 0.63 | 1.96 ± | 1.33 | 0.30 | 0.84 ± | 0.54 | 0.14 | 0.83 ± | 0.72 | <LOD | 0.33 ± | 0.22 |
| 10HT2 | <LOD | | 67.88 | <LOD | | 64.58 | 1.82 | | 85.94 | 0.55 | | 66.78 |
| 10HT3 | 3.29 | | | 1.38 | | | 0.55 | | | 0.11 | | |
| 15C1 | 4.21 | 5.59 ± | 1.38 | 3.21 | 4.22 ± | 0.76 | 0.46 | 1.00 ± | 0.43 | 0.10 | 0.18 ± | 0.06 |
| 15C2 | <LOD | | 24.68 | 5.03 | | 17.97 | 1.52 | | 42.98 | 0.25 | | 35.56 |
| 15C3 | 6.97 | | | 4.42 | | | 1.03 | | | 0.19 | | |
| 15HT1 | 39.89 | 36.95 ± | 2.45 | 6.84 | 8.40 ± | 1.21 | 3.11 | 3.94 ± | 0.65 | 0.62 | 0.77 ± | 0.10 |
| 15HT2 | 37.07 | | 6.62 | 8.57 | | 14.38 | 4.69 | | 16.48 | 0.83 | | 13.55 |
| 15HT3 | 33.90 | | | 9.79 | | | 4.02 | | | 0.86 | | |

AUXINS

| Compound | TRA | | | TRP | | | ANT | | | IAM | | | | | |
|----------|---------|-----------|----------|------------|-------------|-----------|----------|------------|----------|---------|-----------|----------|--------|---------|----------|
| sample | pmol/g | average | SD/SD(%) | pmol/g | average | SD/SD(%) | pmol/g | average | SD/SD(%) | pmol/g | average | SD/SD(%) | | | |
| 10C1 | | | | 932597.93 | 801583.85 ± | 106402.21 | | | | 0.63 | 1.03 ± | 0.40 | | | |
| 10C2 | <LOD | | | 671978.23 | ± | 13.27 | <LOD | | | 1.43 | ± | 38.53 | | | |
| 10C3 | | | | 800175.41 | ± | | <LOD | | | | ± | | | | |
| 10HT1 | | | | 1194979.76 | 1262788.54 | 300039.30 | <LOD | | | <LOD | 30.94 ± | 27.03 | | | |
| 10HT2 | <LOD | | | 1659441.96 | ± | 23.76 | <LOD | | | 57.97 | ± | 87.36 | | | |
| 10HT3 | | | | 933943.91 | ± | | | | | 3.91 | ± | | | | |
| 15C1 | | | | 336031.47 | 775177.98 ± | 320734.96 | | | | 3.37 | 2.33 ± | 0.94 | | | |
| 15C2 | <LOD | | | 896419.50 | ± | 41.38 | <LOD | | | 1.09 | ± | 40.35 | | | |
| 15C3 | | | | 1093082.97 | ± | | | | | 2.53 | ± | | | | |
| 15HT1 | | | | 1002461.46 | 1182827.73 | 139460.03 | <LOD | | | 79.42 | 64.46 ± | 10.59 | | | |
| 15HT2 | <LOD | | | 1203911.95 | ± | 11.79 | <LOD | | | 56.26 | ± | 16.43 | | | |
| 15HT3 | | | | 1342109.77 | ± | | | | | 57.71 | ± | | | | |
| Compound | IAA | | | IAN | | | OxIAA | | | IEt | | | IBA | | |
| sample | pmol/g | average | SD/SD(%) | pmol/g | average | SD/SD(%) | pmol/g | average | SD/SD(%) | pmol/g | average | SD/SD(%) | pmol/g | average | SD/SD(%) |
| 10C1 | 518.81 | 399.03 ± | 98.13 | | | | 300.41 | 386.55 ± | 114.91 | | | | | | |
| 10C2 | 399.81 | ± | 24.59 | <LOD | | | 548.96 | ± | 29.73 | | | | <LOD | | <LOD |
| 10C3 | 278.45 | ± | | | | | 310.27 | ± | | | | | | | |
| 10HT1 | 464.05 | 520.67 ± | 320.87 | | | | 665.45 | 795.78 ± | 106.76 | | | | <LOD | | <LOD |
| 10HT2 | 938.90 | ± | 61.63 | <LOD | | | 926.95 | ± | 13.42 | | | | | | |
| 10HT3 | 159.06 | ± | | | | | 794.95 | ± | | | | | | | |
| 15C1 | 254.00 | 188.97 ± | 47.09 | | | | 563.54 | 450.88 ± | 93.44 | 158.13 | 296.65 ± | 101.25 | | | <LOD |
| 15C2 | 143.99 | ± | 24.92 | <LOD | | | 334.75 | ± | 20.72 | 397.31 | ± | 34.13 | | | |
| 15C3 | 168.93 | ± | | | | | 454.37 | ± | | 334.51 | ± | | | | |
| 15HT1 | 2420.72 | 3207.02 ± | 1095.53 | | | | 4641.39 | 21506.39 ± | 19253.81 | 754.39 | 1112.01 ± | 287.73 | | | <LOD |
| 15HT2 | 4756.28 | ± | 34.16 | <LOD | | | 48452.20 | ± | 89.53 | 1122.69 | ± | 25.87 | | | |
| 15HT3 | 2444.07 | ± | | | | | 11425.58 | ± | | 1458.94 | ± | | | | |
| Compound | IAAla | | | IALeu | | | IAVal | | | IAPhe | | | | | |
| sample | pmol/g | average | SD/SD(%) | pmol/g | average | SD/SD(%) | pmol/g | average | SD/SD(%) | pmol/g | average | SD/SD(%) | | | |
| 10C1 | | | | | | | | | | | | | | | |
| 10C2 | <LOD | | | <LOD | | | <LOD | | | <LOD | | | | | |
| 10C3 | | | | | | | | | | <LOD | | | | | |
| 10HT1 | | | | | | | | | | <LOD | 0.87 ± | 0.56 | | | |
| 10HT2 | <LOD | | | <LOD | | | <LOD | | | 1.43 | ± | 64.81 | | | |
| 10HT3 | | | | | | | | | | 0.31 | ± | | | | |
| 15C1 | | | | | | | | | | | | | | | |
| 15C2 | <LOD | | | <LOD | | | <LOD | | | <LOD | | | | | |
| 15C3 | | | | | | | | | | <LOD | | | | | |
| 15HT1 | | | | | | | | | | 6.79 | 15.78 ± | 8.18 | | | |
| 15HT2 | <LOD | | | <LOD | | | <LOD | | | 26.58 | ± | 51.83 | | | |
| 15HT3 | | | | | | | | | | 13.98 | ± | | | | |
| Compound | IAAsp | | | IAGlu | | | IAGly | | | | | | | | |
| sample | pmol/g | average | SD/SD(%) | pmol/g | average | SD/SD(%) | pmol/g | average | SD/SD(%) | | | | | | |
| 10C1 | | | | | | | | | | | | | | | |
| 10C2 | <LOD | | | <LOD | | | <LOD | | | | | | | | |
| 10C3 | | | | | | | | | | | | | | | |
| 10HT1 | | | | | | | | | | | | | | | |
| 10HT2 | <LOD | | | <LOD | | | <LOD | | | | | | | | |
| 10HT3 | | | | | | | | | | | | | | | |

| | | m full epp. [mg] | m empty epp. [mg] | m sample [mg] |
|----|---------------|------------------|-------------------|---------------|
| 1 | | 1108.77 | 1107.99 | 0.78 |
| 2 | 10 cm CONTROL | 1102.73 | 1100.73 | 2 |
| 3 | | 1104.78 | 1103.94 | 0.84 |
| 4 | | 1104.65 | 1104.25 | 0.4 |
| 5 | 10 cm HT | 1106.4 | 1103.57 | 2.83 |
| 6 | | 1104.35 | 1102.98 | 1.37 |
| 7 | | 1110.5 | 1108.11 | 2.39 |
| 8 | 15 cm CONTROL | 1102.47 | 1098.12 | 4.35 |
| 9 | | 1099.47 | 1097.01 | 2.46 |
| 10 | | 1110.26 | 1104.01 | 6.25 |
| 11 | 15 cm HT | 1101.62 | 1096.6 | 5.02 |
| 12 | | 1106.34 | 1101.91 | 4.43 |

| | | | | | | | |
|----------|---------|-----------|----------|------|------|------|------|
| 15HT1 | 416.16 | 1251.61 ± | 786.02 | | | | |
| 15HT2 | 2304.37 | | 62.80 | <LOD | <LOD | <LOD | <LOD |
| 15HT3 | 1034.29 | | | | | | |
| Compound | OPC-6 | | | | | | |
| sample | pmol/g | average | SD/SD(%) | | | | |
| 10C1 | | | | | | | |
| 10C2 | | | | | | | |
| 10C3 | | | | | | | |
| 10HT1 | | | | | | | |
| 10HT2 | | | | | | | |
| 10HT3 | | | | | | | |
| 15C1 | | | | | | | |
| 15C2 | | | | | | | |
| 15C3 | | | | | | | |
| 15HT1 | | | | | | | |
| 15HT2 | | | | | | | |
| 15HT3 | | | | | | | |

Gibberellins

| Compound | GA 15 | | | GA 24 | | | GA 4 | | | GA 51 | | | GA 34 | | |
|----------|--------|---------|----------|--------|---------|----------|--------|---------|----------|--------|---------|----------|--------|---------|----------|
| sample | pmol/g | average | SD/SD(%) | pmol/g | average | SD/SD(%) | pmol/g | average | SD/SD(%) | pmol/g | average | SD/SD(%) | pmol/g | average | SD/SD(%) |
| 10C1 | <LOD | | | <LOD | | | <LOD | | | <LOD | | | 0.14 | 0.26 ± | 0.12 |
| 10C2 | | | | | | | | | | | | | 0.38 | | 45.22 |
| 10C3 | | | | | | | | | | | | | <LOD | | |
| 10HT1 | <LOD | | | <LOD | | | <LOD | | | <LOD | | | <LOD | 0.88 ± | 0.62 |
| 10HT2 | | | | | | | | | | | | | 1.50 | | 70.22 |
| 10HT3 | | | | | | | | | | | | | 0.26 | | |
| 15C1 | <LOD | | | <LOD | | | <LOD | | | <LOD | | | 0.50 | 0.43 ± | 0.32 |
| 15C2 | | | | | | | | | | | | | 0.78 | | 73.55 |
| 15C3 | | | | | | | | | | | | | 0.01 | | |
| 15HT1 | <LOD | | | <LOD | | | <LOD | | | <LOD | | | 3.00 | 1.43 ± | 1.18 |
| 15HT2 | | | | | | | | | | | | | 0.18 | | 82.23 |
| 15HT3 | | | | | | | | | | | | | | | 1.11 |

| Compound | GA 53 | | | GA 44 | | | GA 19 | | | GA 1 | | | GA 8 | | |
|----------|--------|----------|----------|--------|----------|----------|--------|----------|----------|--------|---------|----------|--------|---------|----------|
| sample | pmol/g | average | SD/SD(%) | pmol/g | average | SD/SD(%) | pmol/g | average | SD/SD(%) | pmol/g | average | SD/SD(%) | pmol/g | average | SD/SD(%) |
| 10C1 | <LOD | 374.87 ± | 314.19 | 32.15 | 136.72 ± | 97.69 | 105.14 | 449.40 ± | 271.97 | <LOD | | | 27.33 | 41.29 ± | 10.28 |
| 10C2 | | 60.68 | 83.81 | 110.81 | | 71.45 | 770.09 | | 60.52 | | | | 44.74 | | 24.90 |
| 10C3 | | 689.06 | | 267.19 | | | 472.95 | | | | | | 51.79 | | |
| 10HT1 | 392.13 | 198.19 ± | 153.03 | 104.75 | 90.29 ± | 22.33 | 555.71 | 577.23 ± | 273.72 | <LOD | | | 35.61 | 66.54 ± | 49.52 |
| 10HT2 | 184.38 | | 77.21 | 58.74 | | 24.73 | 253.27 | | 47.42 | | | | 136.42 | | 74.41 |
| 10HT3 | | 18.06 | | 107.38 | | | 922.72 | | | | | | 27.60 | | |

| | | | | | | | | | | | | | | | |
|-------|---------|----------|--------|-------|---------|-------|--------|----------|--------|--------|----------|-------|---------|-----------|--------|
| 15C1 | 16.25 | 48.20 ± | 35.83 | 80.98 | 69.15 ± | 13.83 | 535.08 | 326.96 ± | 165.11 | <LOD | 98.86 ± | 40.57 | 51.51 | 83.29 ± | 41.79 |
| 15C2 | 98.24 | | 74.34 | 49.74 | | 20.00 | 131.20 | | 50.50 | 139.43 | | 41.04 | 142.33 | | 50.17 |
| 15C3 | 30.11 | | | 76.74 | | | 314.61 | | | 58.29 | | | 56.05 | | |
| 15HT1 | 652.57 | 936.60 ± | 260.07 | <LOD | | | 208.93 | 120.67 ± | 62.57 | 139.02 | 133.89 ± | 10.69 | 1412.22 | 1617.99 ± | 175.42 |
| 15HT2 | 1280.97 | | 27.77 | | | | 70.98 | | 51.86 | 143.65 | | 7.98 | 1840.87 | | 10.84 |
| 15HT3 | 876.26 | | | | | | 82.10 | | | 119.01 | | | 1600.87 | | |

Brassinosteroids

| Compound | GA 29 | | | GA 6 | | | GA 5 | | | GA 3 | | |
|----------|--------|---------|----------|----------|---------|----------|--------|---------|----------|----------|---------|----------|
| sample | pmol/g | average | SD/SD(%) | pmol/g | average | SD/SD(%) | pmol/g | average | SD/SD(%) | pmol/g | average | SD/SD(%) |
| 10C1 | <LOD | | | <LOD | | | <LOD | | | 2.83 | 4.41 ± | 1.59 |
| 10C2 | | | | | | | | | | <LOD | | 35.94 |
| 10C3 | | | | | | | | | | 6.00 | | |
| 10HT1 | <LOD | | | <LOD | | | <LOD | | | <LOD | | |
| 10HT2 | | | | | | | | | | | | |
| 10HT3 | | | | | | | | | | | | |
| 15C1 | <LOD | | | <LOD | | | <LOD | | | 2.67 | 3.56 ± | 1.22 |
| 15C2 | | | | | | | | | | 5.29 | | 34.29 |
| 15C3 | | | | | | | | | | 2.73 | | |
| 15HT1 | <LOD | | | <LOD | | | <LOD | | | <LOD | | |
| 15HT2 | | | | | | | | | | | | |
| 15HT3 | | | | | | | | | | | | |
| Compound | BL | | | 24-epiBL | | | CS | | | 24-epiCS | | |
| sample | pmol/g | average | SD/SD(%) | pmol/g | average | SD/SD(%) | pmol/g | average | SD/SD(%) | pmol/g | average | SD/SD(%) |
| 10C1 | <LOD | | | <LOD | | | <LOD | | | <LOD | | |
| 10C2 | | | | | | | | | | | | |
| 10C3 | | | | | | | | | | | | |
| 10HT1 | <LOD | | | <LOD | | | <LOD | | | <LOD | | |
| 10HT2 | | | | | | | | | | | | |
| 10HT3 | | | | | | | | | | | | |
| 15C1 | <LOD | | | <LOD | | | <LOD | | | <LOD | | |
| 15C2 | | | | | | | | | | | | |
| 15C3 | | | | | | | | | | | | |
| 15HT1 | <LOD | | | <LOD | | | <LOD | | | <LOD | | |
| 15HT2 | | | | | | | | | | | | |
| 15HT3 | | | | | | | | | | | | |